Faculty of Science and Engineering
Department of Chemical Engineering

Modelling and Optimization of Combined Wastewater Treatment and CO_2 Bio-fixation in a Batch Algal Photobioreactor

Ahmed Majeed Daife Al Ketife

This thesis is presented for the degree of

Doctor of Philosophy

of
Curtin University

May 2017

Declaration

I declare that, this thesis contains no material previously published any other person expect where due acknowledgment has been made.

This thesis contains no material which has been accepted for the award of any other degree or diploma in any university.

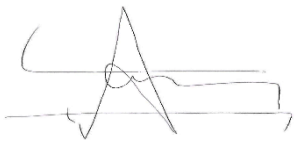

Signature

Date: 03 / 05 / 2017

Acknowledgements

I express my sincere thanks to my major supervisor, Dr. Hussein Znad who supported from very beginning and for his advice, patience and substantial supports during my PhD. I am also, thankful for co-supervisor A/Prof. Hari Vuthaluru for his support. I would like to extend my great thankful to Prof Moses Tade for his entourage and support. I would like to express about my warms thanks and appreciations to Prof. Simon Judd for his continuous support during my PhD research work.

I would like to offer my special thanks to all Chemical Engineering Department technical staffs, Ms Karen Haynes, Mr. Jason Wright, Mr. Xiao Hua, Mr. Araya Abera, Dr. Roshanak Doroushi, Dr. Guanliang Zho, Ms Ann Carroll, Ms Ania Werner for their help and technical support in the lab. My special thanks for Mr. Andrew Chan and Mrs Melina Miralles for their extreme effort for helping students in the lab either technically or emotionally.

I would like to thank my friends and family for their continuous support and encouragement.

Finally, special thanks to Qatar foundation / Qatar National Research Fund (QNRF) I gratefully acknowledge the National Priorities Research Programme (NPRP) for their partial support financially during my Ph.D. study in the frame of the project NPRP - 6 - 1436 - 2-581.

Dedication

To my God, Allah

To my Mother

To my Family

Abstract

Algal photobioreactors (PBRs) have attracted considerable attention as a biological method for combined removal of nutrients (nitrogen N and phosphorus P) from wastewaters and CO_2 fixation from flue gases. PBRs offer a more sustainable cost effective alternative method to the established biological nutrient removal (BNR) process that demands more energy. However, optimization of PBR cultivation conditions, to enhance the CO_2 fixation, biomass production and nutrient removal, is critical for economic viability since the latter is dependent on generating a usable biofuel product at the lowest possible cost. There is thus a practical significance and potential economic benefit of combined nutrient abatement and CO_2.

The current aims to quantify the impact of the key process variables of CO_2 concentration (C_{cg}), light intensity (I) and temperature (T), along with feed water (total) nitrogen ((T)N), (total) phosphorus ((T)P) and total carbon (TC) on the key performance parameters of biomass concentration (X), specific growth rate (μ), CO_2 fixation rate (R_C), nutrient removal efficiency (RE) and lipid productivity (P_{lipids}). Different wastewater qualities (namely primary (P_{WW}), secondary (S_{WW}) and petroleum effluents (P_E)) mixed with different volumetric ratios of standard medium (MLA) were used to cultivate the microalgae *Chlorella vulgaris* (*C. vulgaris*) for nutrient *RE* and biomass production. Box Behnken design (BBD) was used to identify the optimum cultivation condition, based on nutrient *RE* from wastewater with R_C in a single practical experimental study. A mathematical model was developed for predicting the rate of algal biomass accumulation, nutrient *RE* and light intensity profile (I_{av}) against a range of nutrient concentrations, I and C_{cg}. Finally, microalgae cell cultivation for irradiation at different light wavelength (λ_{max}) and I values was assessed, applying different coloured tape light filter (CT), namely, blue (CT_B), green (CT_G), red (CT_R), yellow (CT_Y), and white (CT_W), compared to unfiltered light.

In the initial study, P_{WW}, S_{WW} and P_E media were found to provide an appropriate nutrient concentration and balance for significantly promoting more rapid algal growth than MLA. The highest growth rate was attained for P_{WW} alone, with both growth rate and TN removal decreasing with the P_{WW}:MLA blends. Although P was almost quantitatively removed throughout under the test conditions employed, the lowest recorded μ and *RE* values related to P_E. The results indicate municipal wastewater to be a more effective medium for promoting algal growth and nutrient removal than the MLA growth medium, and these properties vary between different wastewater types.

Nutrient removal was investigated at different concentrations of *TN* (0-56 mg/L) and *TP* (0-19 mg/L), equating to N/P ratios of 0.31-58, to establish any synergistic effects between N and

P with reference to *C. vulgaris* growth. The N/P ratio at which both the growth rate and nutrient removal were found to be greatest was within the range of 7-10. At N/P = 10, complete P and N removal was obtained at the end of the cultivation period. μ decreased by more than 75% when the medium *TN* content was below 2.5 mg L^{-1}. Application of the BBD experimental programming combined with response surface methodology (RSM) was successful in identifying the optimum conditions, based on μ and nutrient *RE*, for the nutrient balance.

Further investigation was conducted into the key influential process parameters of $C_{c,g}$, *I*, *T* and nutrient concentration on the μ, R_c and nutrient *RE* using based on the same BBD method. Results revealed the highest *I* and $C_{c,g}$ to suppress biomass growth by up to an order of magnitude. BBD analysis revealed optimum values of 5% CO_2, 100 µE and 22°C, to achieve the highest growth rate of 1.53 d^{-1}, and 100% nutrient *RE*. Regression analysis indicated a good fit between experimental and statistical model data, and the statistically-derived outcomes were validated by further experimentation under the identified optimum condition. This further indicates the applicability of BBD for identifying the optimum condition, as well as permitting a wider range of determinants to be encompassed than those normally considered in similar published experimental MCT studies.

A comprehensive mathematical model has been developed to evaluate the effects of nutrient concentration within the boundary conditions employed in the experimental studies. The model encompassed gas-to-liquid mass transfer, algal uptake of carbon dioxide (C_d), nutrient *RE*, and the growth biokinetics of *C. vulgaris*. The model was validated using experimental data on the *C. vulgaris* species growth in an externally illuminated photobioreactor (PBR). The fitted parameters of the model were found to be in good agreement with experimental data obtained over the range of cultivation conditions explored, and the model accurately reproduced the dynamic profiles of the algal biomass and nutrient (*TN* and *TP*) concentrations, and light attenuation at different input $C_{c,g}$ values. Whilst limited by semi-empiricism, the model nonetheless represents an advance on the state of the art by providing a basis for predictive dynamic performance of the PBR based on the key process inputs.

Finally, CT-filtered light spectrum was characterized based on λ_{max} and *I*, with respect to μ, nutrient *RE*, and R_C. The maximum growth rate, algal cell lipid content and nutrient *RE* values were recorded for CT_W. By comparison, the normalised algal growth and P_{lipids} parameters against *I* for unfiltered light were all lower - by up to 75% - than those for CT_W with CT_B yielding the lowest performance. Results suggest that optimizing both light intensity and wavelength by this simple process modification can enhance algal growth, with up to a 50% and an associated improvement in nutrient removal efficiency.

Publications

Journal Papers

1. Znad, H. T., A. Alketife, S. Judd, F. AlMomani, and H. Vuthaluru. 2018. "Bioremediation and nutrient removal from wastewater by Chlorella vulgaris." *ECOLOGICAL ENGINEERING* 110: 1-7.

2. Al Ketife, A., S. Judd, and H. Znad. 2017. "Synergistic effects and optimization of nitrogen and phosphorus concentrations on the growth and nutrient uptake of a freshwater *Chlorella vulgaris"*. ***Environmental technology*** 38: 94-102.

3. AL KETIFE, A., JUDD, S. & ZNAD, H. 2017. Optimization of cultivation conditions for combined nutrient removal and CO_2 fixation in a batch photobioreactor. ***Journal of Chemical Technology and Biotechnology***. 92(5): 1085-1093.

4. AL KETIFE, A. M., JUDD, S. & ZNAD, H. 2016. A mathematical model for carbon fixation and nutrient removal by an algal photobioreactor. ***Chemical Engineering Science***, 153, 354-362.

International Conference papers

1. A. Alketife, H. Znad, H. Vuthaluru, Effects and optimization of nitrogen and phosphorus concentrations on the growth and nutrient uptake of a freshwater microalga Chlorella vulgaris. ***5th International Conference on Algal Biomass, Biofuels and Bioproducts***. San Diego, USA June 7-10, 2015.

Table of Contents

Declaration ii
Acknowledgements iii
Dedication iv
Abstract v
Publications vii
Journal Papers vii
International Conference papers vii
Table of Contents viii
List of Figures xiii
List of Tables xvi
List of Symbols and Abbreviations xvii
Chapter 1 Introduction 1
1.1 Background and Motivation 2
1.2 Scope and Objectives 4
1.3 Research significance 5
1.4 Thesis Structure 6
Chapter 2 Background and literature review 9
2.1 Introduction 10
2.2 Mechanism of photosynthesis 12
2.2.1 Photosynthesis in microalgae 13
2.3 Algal cultivation conditions 15
2.3.1 Photoautotrophic cultivation 15
2.3.2 Heterotrophic cultivation 15
2.3.3 Mixotrophic cultivation 15
2.3.4 Photoheterotrophic cultivation 16
2.4 Algal cultivation systems 16
2.5 Photobioreactors (PBRs) 17
2.5.1 Bubble column PBRs 17
2.5.2 Airlift PBRs 18
2.5.3 Flat plate PBRs 18
2.5.4 Tubular PBRs 18
2.6 Factors effecting microalgae cultivation process 18
2.6.1 Light Intensity 18

2.6.2 Light wavelength, λ_{max} 19
2.6.3 Macro and micro-nutrients 21
2.7 pH 24
2.8 Temperature 25
2.9 Environmental application of microalgae 25
2.9.1 Carbon dioxide fixation 26
2.9.2 Wastewater Treatment (WWT) 29
2.9.2.1 Wastewater resources 30
2.9.2.1.1 Municipal wastewater 30
2.9.2.1.2 Industrial wastewater 31
2.9.2.2 Bioremediation of wastewater using microalgae 32
2.9.2.3 Nitrogen and phosphorus nutrients removal 32
2.10 Mathematical modeling 35
2.10.1 Algal photobioreactor key system facets 35
2.11 Optimization of cultivation conditions 35
2.12 Summary 36

Chapter 3 Research Methodology and Analytical Techniques 38
3.1 Introduction 39
3.2 Materials 39
3.2.1 Cultivation media 39
3.2.2 Wastewater 40
3.2.3 Microalgae 40
3.2.4 Bubble column photo-bioreactors 40
3.3 Methods 42
3.3.1 Typical cultivation and sampling procedures 42
3.3.2 Gas mixture 42
3.3.3 Illumination system 43
3.4 Analysis, algal cells 43
3.4.1 Optical density measurement 43
3.4.2 Algal dry weight determination 44
3.4.3 Cell number 45
3.4.4 Microalgae carbon content analysis 45
3.4.5 Dry method lipids content analysis 45
3.5 Analysis, wastewater 46
3.5.1 *TN* and *TP* 46
3.5.2 Chemical oxygen demand (COD) 47
3.5.3 TOC 47

3.5.4 Macro and micro nutrients 47
3.6 Coloured tape (CT) light filter 48
3.7 Experimental design and data processing 48
3.7.1 Background 48
3.7.2 Statistical experimental programme 49
3.7.3 Regression analysis 50

Chapter 4 Influence of the wastewater quality on the performance of *Chlorella Vulgaris* 51
4.1 Introduction 52
4.2 Material and methods 55
4.2.1 Generic materials and methods 55
4.2.2 Experimental design 55
4.2.3 Wastewater origin and characterization 56
4.3 Results and discussion 56
4.3.1 Wastewater nutrient characterization 56
4.3.2 Influence of wastewater quality on growth and macronutrient removal 57
4.3.3 Influence of organic carbon on *Cv* metabolism 61
4.3.4 Macro and micro nutrient removal 62
4.4 Summary 64

Chapter 5 Synergistic effects and optimization of nitrogen and phosphorus concentrations on the growth and nutrient uptake of a freshwater *chlorella vulgaris* 66
5.1 Introduction 67
5.2 Material and methods 68
5.2.1 Practical measurement 68
5.3 Experimental design and regression analysis 68
5.4 Results and Discussion 70
5.4.1 Influence of initial *TN* and *TP* 70
5.4.2 Multiple regression analyses 73
5.4.3 Analysis of variance (ANOVA) 76
5.4.4 Desirability and optimum conditions 78
5.5 Summary 79

Chapter 6 Optimization of cultivation conditions for combined nutrient removal and CO_2 fixation in a batch photobioreactor 81
6.1 Introduction 82
6.2 Material and Methods 84
6.2.1 Algae preparation and determination 84
6.2.2 Experimental design and regression analysis 85

6.3 Results and discussion 86
6.3.1 Scoping trials: Growth as a function of CO_2 concentration 86
6.3.2 Scoping trials: Growth and nutrient removal 87
6.3.3 Multiple regression analysis and analysis of variance 88
6.3.4 BBD analysis and optimization 91
6.4 Summary 94

Chapter 7 Modelling algal photobioreactors for CO_2 bio-fixation and nutrient removal 96
7.1 Introduction 97
7.1.1 Algal photobioreactor key system facets 97
7.1.2 Previous mathematical model studies 98
7.2 Materials and methods 99
7.2.1 Modelling equations 100
7.2.2 Gases dynamics in liquid phase of PBRs 102
7.2.3 Biomass growth rate 103
7.3 Results and discussion 106
7.3.1 Mass transfer coefficient 106
7.3.2 Model calibration 106
7.3.3 Model validation 108
7.3.4 Sensitivity and regression analysis 110
7.3.5 Nutrient removal 111
7.3.6 Light attenuation profile 113
7.4 Summary 114

Chapter 8 Enhancement of CO_2 biofixation and lipids productivity by *chlorella vulgaris* using coloured polypropylene film for light spectral conversion 115
8.1 Introduction 116
8.2 Material and methods 118
8.2.1 Coloured tape light filter (CT) 118
8.3 Results and discussion 119
8.3.1 Influence of I and λ_{max} on *Chlorella vulgaris* growth 119
8.3.2 Nutrients removal under different λ_{max} 121
8.3.3 λ_{max} and I impacts on lipids production of *Chlorella vulgaris* 122
8.3.4 Growth and productivity normalisation 123
8.4 Summary 124

Chapter 9 Conclusions and Recommendations 126
9.1 Conclusions 127

9.2 Recommendations 130
References 132
Appendix A Articles copyright 151

List of Figures

Figure 1.1 Thesis structure 8

Figure 2.1 Summary of research articles in key subject area according to *SCOPUS*, based on the search of term algae (a) including microalgae, *Chlorella vulgaris* and wastewater, *Chlorella vulgaris* and CO_2, (b) *Chlorella vulgaris* and subjected area. 12

Figure 2.2 Schematic mechanisms of photosynthesis and bio-photolysis of photoautotrophic microbes[42] 13

Figure 2.3 Photosynthesis in algal cell [39] 14

Figure 2.4 Algal PBRs system configuration 17

Figure 2.5 Biofuel from microalgae culture technology (MCT), schematic. *OC* Organic carbon, CHP combined heat and power (adapted from [142]) 26

Figure 2.6 Block diagram of typical wastewater treatment. 29

Figure 2.7 Schematic of BNR process, including anaerobic zone for P removal. 30

Figure 4.1 Schematic diagram of a single cylindrical photobireactor (PBR). 56

Figure 4.2 Growth of *Cv* in standard medium (MLA) with different ratios of P_{WW}: (a) X transient, and (b) μ_{max} and nutrient removal as a function of % P_{ww} (0% reprenset those results using only standared medium (MLA)). 58

Figure 4.3 Effect of the initial *TP* and *TN* concentrations on the growth of *Chlorella vulgaris* in; P_{WW}, S_{WW} and P_E. 60

Figure 4.4 Effect of initial organic carbon concentration (*OC*) on the growth of *Chlorella vulgaris* in P_{WW}, S_{WW}, P_E and standard medium (MLA). 61

Figure 4.5 Algal growth trends in the undiluted effluent (100% P_{WW}, S_{WW}, P_E) and standard medium (MLA). 62

Figure 5.1 Effect of the initial *TP* concentrations on the growth of *Chlorella vulgaris* in MLA growth medium. 70

Figure 5.2 Influence of the TP concentration (at TN=70 mg/l) on the growth rate, removal efficiencies of both TN and TP. 71

Figure 5.3 Effect of the initial TN concentrations on the growth of Chlorella vulgaris in MLA growth medium 72

Figure 5.4 Influence of the *TN* concentration (at *TP*=8 mg/l) on the growth rate, removal efficiencies of both *TN* and *TP*. 73

Figure 5.5 Comparison between experimental and predicated values of *TN* and *TP* removal, and specific growth rate μ, (•) Experimental points, (⋯) Confidence bands>(95%), (-) Fit line, Eqs.5.6-5.8 , (⋯)Mean of the Y Leverage Residuals 75

Figure 5.6 Contour lines and 3D response surface for μ (a-b), *TN* removal (c-d) and *TP* removal (e-f) 78

Figure 5.7 (3D) Cube desirability plots for *TN*, TP and *TC*. 79

Figure 6.1 Algal growth trends with feed gas CO_2 concentration: (a) X, (b) P_x, (c) R_c', and (d) R_c."Control" refer to the sample aerated with only air (0.03%), (I=200 μmol m^{-2} s^{-1}, T=24 °C) 86

Figure 6.2 X_{max} and % nutrient removal, 13 days cultivation, at different initial nutrient concentrations (TN_{init} and TP_{init}): normalised initial nutrient concentration = initial nutrient concentration / maximum initial nutrient concentration ($TN_{init,max}$ and $TP_{init,max}$ = 56 and 19 mg L^{-1} respectively). 88

Figure 6.3 Specific growth rate and nutrient removal efficiencies after 13 days of cultivation and a function of N/P concentration ratio. 88

Figure 6.4 Comparison between experimental data and predicated values of R_c, *TN* and *TP* removal, and μ. The dotted curved lines indicate the >95% confidence bands; horizontal dotted lines represent the mean of the Y leverage residuals (i.e. the measure of agreement with the model). 90

Figure 6.5 3D response surface and contour map for CO_2 fixation rate (a ,b) and μ (c ,d), at the optimum temperature of 22 ^oC..... 93

Figure 6.6 3D response surface and contour map for CO_2 fixation rate (a ,b) and μ (c ,d), at the optimum temperature of 22 ^oC..... 94

Figure 7.1 Modelling strategy 101

Figure 7.2 A schematic drawing of the photobioreactor and the elements included in the model. 105

Figure 7.3 Model calibration and fitting for different cultivation conditions (a) *TP*=6 mg L^{-1}, *TN*=28 mg L^{-1}, CO_2=2.5 % , *I*= 250 µE m^{-2} s^{-1} and (b) *TP*=6 mg L^{-1}, *TN*=28 mg L^{-1}, CO_2=0.03 % , *I*= 250 µE m^{-2} s^{-1}..... 107

Figure 7.4 Model verification applying different cultivation conditions (a) *TN* = 28-207 and *TP* = 6-8 mg L^{-1} for an air feed ($C_{c,g}$ = 0.03% CO_2); and (b) *TN* = 28 and *TP* = 6 mg L^{-1} for CO_2-supplemented gas feed ($C_{c,g}$ = 0.03-5% CO_2) for experimental (data points) and model (continuous trend) data. ... 109

Figure 7.5 Predicted mean algal biomass concentration profile and its variation based on ±20% variation in (a) μ_X, and (b) K_d, based on four runs. 110

Figure 7.6 Regression analysis of fit between predicted and experimental biomass concentration R^2 = 0.94, P = 0.0001 and p>F = <0.0001 (i.e. significant). Dotted curved lines indicate >95% confidence bands; horizontal dotted lines represent mean of the Y leverage residuals (i.e. the measure of agreement with the model). 111

Figure 7.7 Evolution of total nutrient concentration under different conditions of initial aqueous nutrient concentration (a, c: $C_{c,g}$ = 0.03%,) and feed gas CO_2 concentration (b, d: TP_{init} and TN_{init} = 6 and 28 mg L^{-1} respectively)..... 112

Figure 7.8 Average irradiance I_{av} profile during experiment period of 10 days in dished line and the predicated response in solid line. 113

Figure 8.1 Light intensity (*I*) variation at different wavelength (λmax) CT of various colours: white (CT_W), blue (CT_B), green (CT_G), yellow (CT_Y), and red (CT_R) at fixed extrneal light intesity (I_E) of 250 µE. 118

Figure 8.2 Cultivation of *C. vulgaris* in MLA under different λ_{max} and fixed *I of 250* $\mu E\ m^{-2}\ s^{-1}$: (a) *X* profiles, and (b) μ and C_d as function of λ_{max}. 120

Figure 8.3 TP, TN removal efficiencies under different λ_{max}. 121

Figure 8.4 CO_2 fixation and lipids production rate at different wavelength. 122

Figure 8.5 Normalised growth parameters and lipids productivity against light wavelength; normalised parameters = Vlaues of selected parameter (R_C, μ, X_{max} and P_{lipids}) / filtered light intensity (I_f). 123

List of Tables

Table 2.1 Comparison between open and closed cultivation systems [56, 57]. 16

Table 2.2 Reported CO_2 fixation rates for various algae species, light intesity batch systems unless otherwise stated. 20

Table 2.3 Reported light wavelength influence on microalgae growth 21

Table 2.4 Reported macro – nutrient influence on algal growth 23

Table 2.5 Reported micro – nutrient influence on algal growth 24

Table 2.6 Comparison between different recent methods for carbon dioxide fixation strategies. 27

Table 2.7 Reported CO_2 fixation data, 2010 onwards. 28

Table 2.8 Variation of the TP and TN removal efficiencies with the optimum N/P ratio. 34

Table 4.1 Reported *Chlorella vulgaris* algal growth parameters with nutrient removal efficiency for various wastewaters 53

Table 4.2 Reported *Chlorella vulgaris* algal growth parameters with Macro and Micro nutrient removal efficiency for various wastewaters. 54

Table 4.3 Wastewater and MLA composition 57

Table 4.4 Macro/micro nutrient concentrations and RE values in P_{WW}, S_{WW}, P_E and standard MLA medium 63

Table 5.1 Input and output values for BBD analysis 69

Table 5.2 Analyses of variance results for the fitted models of *RE* (%) for *TN*, *TP*, and μ (d^{-1}) as influenced by different intitial concentration (mg L^{-1}) of *TN*, *TP*, and *TC* in the cultivation media 74

Table 5.3 Analysis of variance (ANOVA) from BBD 76

Table 5.4 Comparison between the predicted and the experimental optimum conditions. 79

Table 6.1 Parameter values 85

Table 6.2 BBD matrix, experimental outputs 88

Table 6.3 Analyses of variance results for the fitted models of *RE* (%) for *TN*, *TP*, μ (d^{-1}), and R_C (mg L^{-1}) as influenced by different cultivation paramters of *I*(µE), $C_{,cg}$ (%), and *T*(℃) 91

Table 6.4 Comparison between predicted and experimental optimum conditions 94

Table 7.1 Parameter values assumed in recently-published PBR mathematical models, batch processes 99

Table 7.2 Summary of base parameters values 108

Table 7.3 Set of experiments used for model validation 108

Table 8.1 Light filter and LED based algal growth studies reported in the literature for *Chlorella vulgaris* (*C. vulgaris*) 117

Table 8.2 CT film characterization, 48 mm width, tape 119

List of Symbols and Abbreviations

Symbol	*Description and Units*
$C_{c,g}$	CO_2 concentration in the inlet gas, %
I	Light incident, light quantity, µE $m^{-2}s^{-1}$
P_x	Biomass productivity, g L^{-1} d^{-1}
R_c	CO_2 uptake rate, g L^{-1} d^{-1}
Rc'	Biomass–normalised CO_2 fixation rate, g CO_2 g $biomass^{-1}$ d^{-1}
T	Temperature, °C
TC	Total carbon, mg L^{-1}
TN	Total Nitrogen concentration, mg L^{-1}
TP	Total Phosphorus concentration, mg L^{-1}
OC	Organic carbon, mg L^{-1}
COD	Chemical Oxygen Demand, mg L^{-1}
DOC	Dissolved organic carbon, mg L^{-1}
X	Biomass concentration, g L^{-1}
Cd	Cells density, cells mL^{-1}
RE	Removal efficiency, %
C	Dissolved carbon concentration, mg L^{-1}
C_s	Saturated concentration of CO_2, mg L^{-1}
M_{CO2}	Molecular weight of carbon dioxide, g mol^{-1}
M_C	Molecular weight of carbon, g mol^{-1}
D_C, *Do*	Diffusivity of of CO_2, oxygen, $m^2.s^{-1}$
$H_{C,O}$	Henry constant for O_2 or CO_2
K	Light extinction coefficient, g m^{-2}
K_c	Chlorophyll-base light extinction coefficient of algae, cm^2 (mg Chl-a).

k_C, k_O	Mass transfer coefficient of CO_2, oxygen, d^{-1}
HRT	Hydraulic residence time, d
K_d	Biomass loss (death) rate, d^{-1}
K_i	Carbon dissociation constant of species *i*, mol L^{-1}
K_N	Half saturation constants for N
K_P	Half saturation constants for P
K_{TC}	Half saturation constant for total carbon
L_{av}	Photosynthetically active radiation (PAR), µE $m^{-2}s^{-1}$
K_L	PAR half saturation constants, µE $m^{-2}s^{-1}$
MW_i	Molecular weight of species *i*, g mol^{-1}
n	Shape factor
p	Pressure, bar
r	Photobioreactor radius, m
R	Universal gas constant, L^3 bar^{-1} k^{-1} mol^{-1}
S_i	Concentration of selected nutrient, mg L^{-1}
V	Volume, L
y	Mole fraction of CO_2 in gas phase
Y_{CTOT}	Yield coefficient for total carbon, (g_c g_x^{-1})
Y_i	*i* nutrient yield coefficient, (g_i $g_{biomass}^{-1}$)
Y_{O2}	Oxygen yield coefficient, (g_{O2} $g_{biomass}^{-1}$)
λ_{max}	wavelength number, nm^{-1}
P_{lipids}	Lipid productivity, mg L^{-1} d^{-1}

Greek characters

μ	Specific growth rate, d^{-1}
ε	Gas holdup volume, L
$\gamma_{w,i}$	Half saturation constant for *i* nutrient
μ_{max}	Maximum specific growth rate, d^{-1}

θ	Angle of incident light, (º)

Subscripts

i, init	Initial value
f, fin	Final value
max	Maximum
g	Gas phase
l	Liquid phase
tot	Total concentration
R	Reactor
atm	Atmospheric
feed	Feed

Abbreviations

Cv	Microalgae, *Chlorella vulgaris*
ANOVA	Analysis of variance
P_{WW}	Primary wastewater
S_{ww}	Secondary wastewater
P_E	Petroleum effluent
BBD	Box Behnken Design
RSM	response surface methodology
BNR	Biological nutrient removal
DDF	Derringer's desired function
df	degree of freedom
MLA	Marine labs American society of microbiology-derived medium
PBR	Photobioreactor
GHGs	Greenhouses gases
PBRs	Photobioreactors
Fd	Oxidized ferredoxin

NADP+	Nicotinamide adenine dinucleotide phosphate
ATP	Adensine triphosphate
MCT	Microalgae cultivation technology
CCMs	Carbon concentration mechanisms
EBPR	Enhanced biological phosphorus removal
LF	Solar light filter
SD	Standard deviation
WwT	Wastewater treatment
CT	coloured tape solar filter
CT_B	Blue coloured tape solar filter
CT_G	Green coloured tape solar filter
CT_R	Red coloured tape solar filter
CT_W	white coloured tape solar filter
CT_Y	Yellow coloured tape solar filter
U	Unfiltered solar light

Chapter 1

Introduction

1.1 Background and Motivation

Climate change and global warming are two major global challenges in the fields of environmental science and technology, and international economics and politics. Global warming is induced by a rapid increase of CO_2 emissions of greenhouse gases (GHGs) in the atmosphere. Carbon dioxide (CO_2) is one of the major constituents (68%) of the total GHG emissions [1]. The rapid increase in population and associated anthropogenic activities have further contributed to the freshwater scarcity partly through the discharge of excessive amounts of wastewater (with significant nutrient content, nitrogen N and phosphorus P) into the water bodies. Nutrient discharge produces eutrophication, the depletion of oxygen through algal growth, which is has been an pollution issue since the middle of the last century [2]. There has thus been increasing focus on energy-neutral and waste-free wastewater treatment.

Various methods have been undertaken to mitigate GHG emissions through chemical, physical, geological and biological methods [3]. Chemical and physical methods are widely used in large-scale industrial processes. Whilst effective in mitigating atmospheric pollution, they are very costly and generate undesirable by-product that demand further treatment and management prior to their disposal. A potentially more sustainable approach is to biochemically convert CO_2 into useful products. In this regard, carbon can potentially be captured by microalgae cells and used in the photosynthetic process to generate useful biomass [4].

Discharged wastewater contains a substantial amount of organic matter, nutrients (macro and micro), toxins and heavy metals. Nitrogen arises as ammonia, urea or organic nitrogen, and phosphorus as phosphate or organic phosphorus. Biological nutrient removal (BNR) is used to remove nutrients from wastewater, but the process demands energy for aeration and the pumping of sludge between various tanks in the treatment scheme [5, 6]. In this process half of total energy demanded is used to supply oxygen to the bacteria consortium so as to oxidise the organic carbon and nitrogen to CO_2 and nitrate, with the latter subsequently being converted to N_2 by denitrification [7]. The gases are then released to the atmosphere [8].

The use of microalgae for biological treatment has been proposed as being a promising method for both nutrient and heavy metals removal for various wastewater sources [9]. The majority of the essential materials required to support algal growth are in the wastewater, although the composition varies according to the wastewater source [10]. Algae based treatment can potentially achieve cost effective and low-energy nutrient removal compared to the conventional BNR treatment [11], since the biomass aeration is obviated.

Algae are fast-growing, higher photosynthetic organisms that can effectively transform the inorganic nutrients, carbon dioxide, water and other substances into biomass in the presence of light through the photosynthesis process. Microalgae produce approximately half of the atmospheric oxygen on earth, while consuming significant amounts of the greenhouse gas (GHG) carbon dioxide [12] along with the bulk nutrients (N and P). The microalgae biomass generated has been extensively studied as a source for the production of different products, such as animal feeds, health products, pharmaceuticals and biofuel [13].

Microalgae are considered as one of the most promising alternative sources for renewable energy production [14]. However, algal biofuel production is still economically unfeasible, with higher production costs calculated as exceeding 10 €/kg in some studies [15, 16] if based on commercial sources of the raw materials: approximately 200 t of CO_2, 5 t of N and 1 t of P are required to produce 100 t of microalgae biomass [17]. To offset biomass production costs fresh water and nutrient costs microalgae biofuel production can be coupled with wastewater treatment [18-20]. Further cost reduction may be possible from utilizing the flue gas as the CO_2 source [15]. Microalgae, configured as photobioreactors (PBRs), have thus received considerable attention as the basis of combined biological method for removal of nutrients (nitrogen N and phosphorus P) from wastewaters and CO_2 fixation from flue gases [21].

In this regards, *chlorella* species are considered as promising candidates for CO_2 fixation, with reported fixation rates between 0.73 and 1.79 g L^{-1} d^{-1} [22]. This species appears to be fairly robust, and has been shown to be largely unaffected by the volatile compounds present in the wasdte gas streams [23]. The microalgae *Chlorella vulgaris* (*Cv*) in particular has been extensively studied for CO_2 mitigation under a range of operating conditions, including gas CO_2 concentration [24-28], light intensity [29, 30] and temperature [30, 31].

Environmental factors such as temperature, nutrient load and especially light irradiation have a direct impact on PBR performance. Effective and efficient microalgae cultivation in monocultures relies on a number of fundamental system properties which include (i) distribution of light throughout the biomass, (ii) enhanced CO_2 mass transfer from the gas to liquid phase, and (iii) enhanced CO_2 assimilation by the algal biomass (largely achieved through (i) [13]). Light intensity, light wavelength and photoperiod cycle (i.e. the relative durations of the light and dark periods) are crucial factors in determining algal growth rate, especially for photoautotrophic cultures [32]. Inefficiencies arise when microalgae are exposed to light intensities above the saturation limits, as a result of photo-inhibition or overheating. Against this, at high algal cell densities commensurately higher light intensities are required to ensure light penetration through the bulk of the culture [33].

Whilst algal microalgae culture technology (MCT) would appear to offer a viable alternative to non-renewable fossil fuels, the challenges associated with the requirement for effective light distribution and appropriate conditions for both nutrient and carbon dioxide assimilation effectively limit its economic viability. An examination of factors which may mitigate against such constraints is thus of obvious interest.

1.2 Scope and Objectives

The scope of the work encompasses the experimental examination and modelling of combined wastewater treatment with CO_2 bio-fixation by algal biomass. The impact of nutrient and carbon load on biomass production is examined using a series of batch bubble column PBRs under various cultivation conditions. Other system facets examined include light intensity and wavelength, as well as feedwater quality. The detailed objectives of this study are to:

1. Investigate the influence of wastewater quality, based on both synthetic and real municipal and industrial wastewaters, on the nutrient removal (P, N, and macro/micro nutrients) and CO_2 fixation of algal biomass;

2. Investigate and quantify the synergistic effects of different initial N and P relative concentrations on the nutrient removal and algal growth;

3. Investigate and quantify the impacts of the key operating parameters of light, CO_2 gas concentration, and temperature on the algal growth rate, CO_2 bio-fixation rate, and nutrient removal;

4. Establish a comprehensive mathematical model to quantify the influence of nutrient concentration, light intensity, and feed CO_2 gas concentration on the algal biokinetic parameters, CO_2 uptake rate and nutrient removal;

5. Investigate PBR performance, with reference to biomass growth rate, CO2 bio-fixation rate, nutrient removal and lipids production, using a simple, low-cost method to modify and filter a light source to attenuate the light intensity and adjust the wavelength range.

The work has all been based on batch experiments conducted at the bench scale using a bubble column configuration for the PBR and a *Cv* algal species; one of the most extensively studied and widely applied algal species in MCT system.

1.3 Research significance

The work addresses a number of research needs in the area:

1. Wastewater quality is an important factor affecting PBR performance for CO_2 fixation, nutrients removal (macro and micro), and biomass production. Most existing studies investigating the influence of individual macro-and micro nutrients have not considered their synergistic impacts, and the nutrient balance (N:P) specifically, for a single water source. In the current study statistical experimental programming has been conducted to address this, both for analogue waters (Chapters 5-6) and real wastewaters (Chapter 4).

2. The use of statistical experimental programming generally, and Box Behken design (BBD) specifically, has been very limited in the MCT research space despite its generally increased use across the environmental technology research area generally. The work conducted has sought to validate the BBD method both with respect to nutrient removal (Chaoter 5) and MCT process optimisation with reference to the key process variables of light intensity, gas CO_2 concentration, and temperature (Chapter 6). The use of BBD results in the generation of empirically-derived algorithms quantifying the impact of the various process operating parameters and feedwater quality on process performance according to the output from a limited set of experiments conducted under controlled conditions. BBD greatly reduced the number of tests, as well as providing the synergistic relationships, compared with classic testing based on n-factorial experimental planning.

3. All three of the key process performance determinant attributes most germane to combined CO_2 and nutrient mitigation, these being of algal growth rate, CO_2 fixation, and nutrient removal, have been encompassed in the study. This has not necessarily been the case in all studies conducted within this research space, which have tended to be exclusive to either algal growth (predominantly for biofuel production) or nutrient removal from wastewater rather than these two objectives combined.

4. Despite of the large number of mathematical method that have been published in the literature within the MCT area, no models have been focused on the combined influences of CO_2 gas concentration, medium composition, and light intensity with reference to both biomass production and nutrient removal from wastewater as with the current work (Chapter 7).

5. Whilst one or two other studies have been focused on the impact of light wavelength on algal growth, the use of a practical, low-cost method for modifying the light source for improving algal growth and fatty acid production – this being an essential precursor for

biofuel, has not previously been considered. The current work includes the application of coloured tape for light attenuation and wavelength modification (Chapter 8).

1.4 Thesis Structure

The thesis comprises nine chapters (Fig. 1.1), linked with the stated objectives:

- **Chapter 1** provides an introduction and background to the thesis.

- **Chapter 2** presents and appraises the recent literature on microalgae applications to wastewater treatment, CO_2 bio-fixation, and nutrient removal. The key parameters defining and influencing the algal cultivation process are outlined, and mathematical modelling studies for describing the algal growth parameters identified. This section includes a consideration of the influence of light intensity and wavelength on the algal growth, nutrient removal and lipids production.

- **Chapter 3** provides an overview on the methodology employed, including a detailed description on the sample preparation, experimental setup and analytical methods involved.

- **Chapter 4** reports the results of the characterization and influence of wastewater quality (primary wastewater (P_{WW}), secondary wastewater (S_{WW}), and petroleum effluent (P_E) - both as discrete streams and mixed at different volumetric ratios with the standard medium MLA) blended with different ratios of standard medium (MLA) on the algal growth, nitrogen N and phosphorus P nutrients removal.

- **Chapter 5** reports the results of the study of the effects of different initial nutrient concentrations and ratios on algal growth and nutrient removal efficiency, using statistical experimental design.

- **Chapter 6** reports the results of the study of the impact of light intensity, feed gas CO_2 and temperature on the algal growth parameters, N, P removal efficiencies and CO_2 fixation rate, again using statistical experimental design.

- **Chapter 7** offers a comprehensive mathematical model to simulate the algal growth, nutrient removal, and light profile under different cultivation conditions of light intensity, CO_2 gas concentration and initial nutrient concentration in a batch or semi-batch system.

- **Chapter 8** reports the results of the study of the influence on the algal growth parameters, nutrients removal efficiencies and lipids productivity using light filtering to modify the light intensity and wavelength.

- **Chapter 9** provides conclusions and recommendations for tfuture work based on the outcomes of the study.

Chapters 1, 2, and 3 have all been published in peer journals (see page *vii* of publication section). Sections of Chapters 1, 2, and 3 have been drawn from the same portfolio of published work by the author, and the pertinent papers have been cited accordingly in the text [335-338].

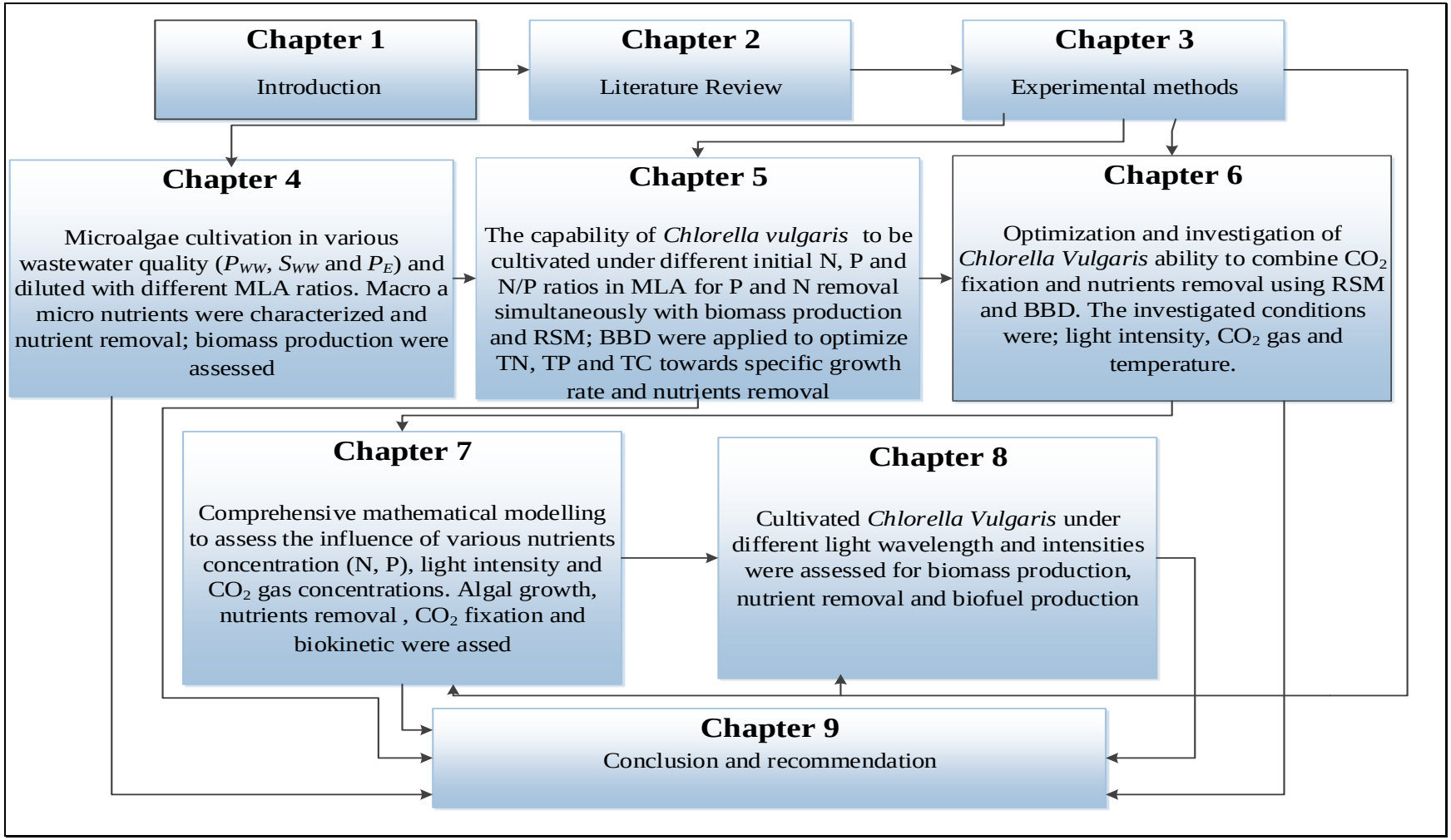

Figure 1.1 Thesis structure

Chapter 2

Background and literature review

2.1 Introduction

The worldwide energy demand is estimated to increase by 49% between 2007-2035 roughly in accordance with the expanding world population and associated industrialisation and human activity and consumption [34]. The associated global petroleum consumption increased by 6.3 % from 2009 to 2013, according to United States Energy Information Administration (EIA). Partly as a result, the associated average atmospheric CO_2 concentration has risen from 400 to 407.7 mg L^{-1} [35]. Several strategies have been suggested for reversing the trend by either fixing CO_2 gas or limiting its release, including the development of biofuels to displace mineral fuel sources, the expansion of nuclear power and the capturing and fixing of the emitted CO_2 [36]. The signing of the Kyoto Protocol in December 1997 was a historic step forward in attempting to reverse the trend in CO_2 emissions, the first regulation implemented to control atmospheric pollutant, targeting a 5% reduction in emissions against the 1990 level [37].

Also associated with human activity is the inexorable increase in the volumes of wastewater generated from freshwater sources, estimated to be 3908 billion m^3 in 2009 [38]. Wastewater requires treatment prior to discharge, since excessive concentrations of nutrients (nitrogen (N) and phosphorus (P)) in the wastewater cause problems of eutrophication affecting the balance of the ecosystem. Nutrients must therefore be removed to acceptable limits (N average concentration of 8 to 10 mg L^{-1} and P of 1 to 3 mg L^{-1}) before discharge to the waterbody [39].

Microalgae have been identified as a promising alternative for CO_2 bio-fixation and wastewater treatment due to their high photosynthetic efficiency, high biomass production rate, high levels of useful organic product (lipids and carbohydrates) accumulated, tolerance to diverse environmental conditions, and high resistance to contaminents [34, 40, 41], compare with territorial plant. However, commercialization of the algal cultivation process remains challenging because the cost of the extracted useful products generated remains relatively high.

Microalgae are single-celled (unicellular), highly diverse microorganisms which can survive individually or in chains or clusters [42], and are highly diverse in size and appearance. They are found in freshwater of all kinds, barks, soil, rocks and marine habitats group of photosynthetic organisms. The first use of microalgae by humans dates back 2000 years to the Chinese, who used the strain Nostoc as a food source during a famine [12]. There are estimated to be 200,000-800,000 species in total, of which only about 35,000 species have been identified and described [42]. Microalgae species exist in both suspended and attached forms, the latter adhere to a submerged surface. Microalgae produce approximately half of the atmospheric oxygen on earth, while consuming significant amounts of carbon dioxide [12].

An indication of the relative scientific importance of microalgae can be attained through the use of search engines for examining scientific publication database, such as *SCOPUS*. Searches of keywords appearing in the databases for search terms based on algae/microalgae, and either wastewater with *Chlorella vulgaris/Cv* (wastewater ∩ *Chlorella vulgaris*/*Cv*), and carbon dioxide with *Chlorella vulgaris/Cv* (carbon dioxide ∩ *Chlorella vulgaris*) can be used to specify the number of publications directly relevant to the use of *Chlorella vulgaris* for wastewater treatment and carbon dioxide fixation. A consideration of all research papers dating back to the mid-1970s reveals research articles encompassing wastewater and *Chlorella vulgaris*/*Cv* to be about 1.37-fold higher those based on carbon dioxide and *Chlorella vulgaris* (Fig. 2.1 a).

The application of *Chlorella vulgaris* for carbon capture appears to be a relatively recent area of study with considerable increase research effort only evident from 2006 onwards. Against this, the number of research articles whose keywords encompass all topics in algae is significantly higher compared to those for the combined topics sets, with the rate rapidly increasing. On this evidence, *Chlorella vulgaris* presents itself as a good candidate for simultaneous nutrient removal and CO_2 fixation, in that has been extensively studied recently is a number of different fields within environmental science (Fig. 2.1 b). This is it because it meets most of the recognized criteria for MCT, these being [43]:

(i) high CO_2 fixation ability,
(ii) (high algal growth rate,
(iii) low operational cost,
(iv) low contamination risk,
(v) ease of harvesting,
(vi) rich in valuable product (including lipids content),
(vii) toleration of high light intensity,
(viii) adjustment to the natural light/dark cycle, and
(ix) appropriate for outdoor cultivation.

The lipid content of *Cv* has reported to be as high as 58% [14] and tolerant to CO_2 concentrations as high as 15% and temperatures of 30℃ or more [301], and can grow under both heterotrophic and mixotrophic as well as the typical autotrophic conditions. These properties underpin the widespread study of this species as well as its application to pilot/full-scale installations.

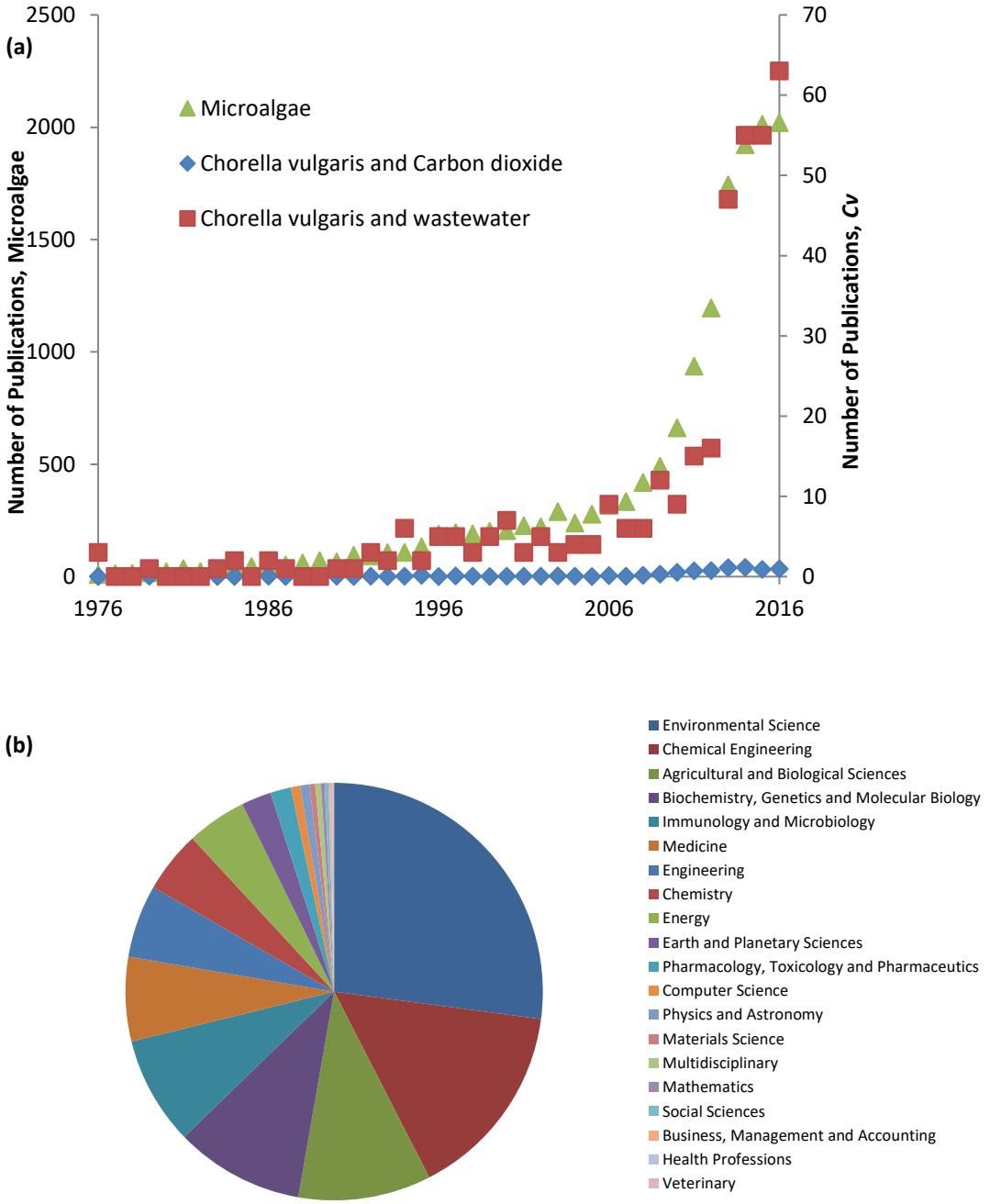

Figure 2.1 Summary of research articles in key subject area according to *SCOPUS*, based on the search of term algae (a) including microalgae, *Chlorella vulgaris* and wastewater, *Chlorella vulgaris* and CO_2, (b) *Chlorella vulgaris* and subjected area.

2.2 Mechanism of photosynthesis

Photoautotrophic microorganisms such as eukaryotic green microalgae, process chlorophyll and other pigments to fix sunlight energy and utilize photosynthetic systems (PSII and PSI) to implement plant-like oxygenic photosynthesis [43]. The pigments in PSII (P680) absorb the

photons with a wavelength shorter than 680 nm, generating strong oxidant capable of splitting water into protons ($\mathbf{H}^+$), electrons ($\boldsymbol{e}^-$) and O_2 (Fig.2.2).

The electrons or reducing equivalents are transferred through a series of electron carriers and cytochrome complexes to PSI. The pigments in PSI (P700) adsorb the photons at a wavelength under 700 nm causing an increase in the energy level of the electrons which then convert ferredoxin (Fd) and nicotinamide adenine dinucleotide phosphate (NADP+) to their reduced forms. The proton gradient formed across the cellular (or thylakoid) membrane drives adensine triphosphate (ATP) production via ATP synthase. CO_2 is reduced with ATP and NADPH via a reductive pentose phosphate pathway or Calvin cycle to create cell growth. The excess reduced carbon is stored inside the cells as carbohydrate and/or lipids. The types of carbohydrate product produced rely on the type of strain being used. The reducing power (Fd) may also be directed to hydrogenase (Hase) for hydrogen evolution [42].

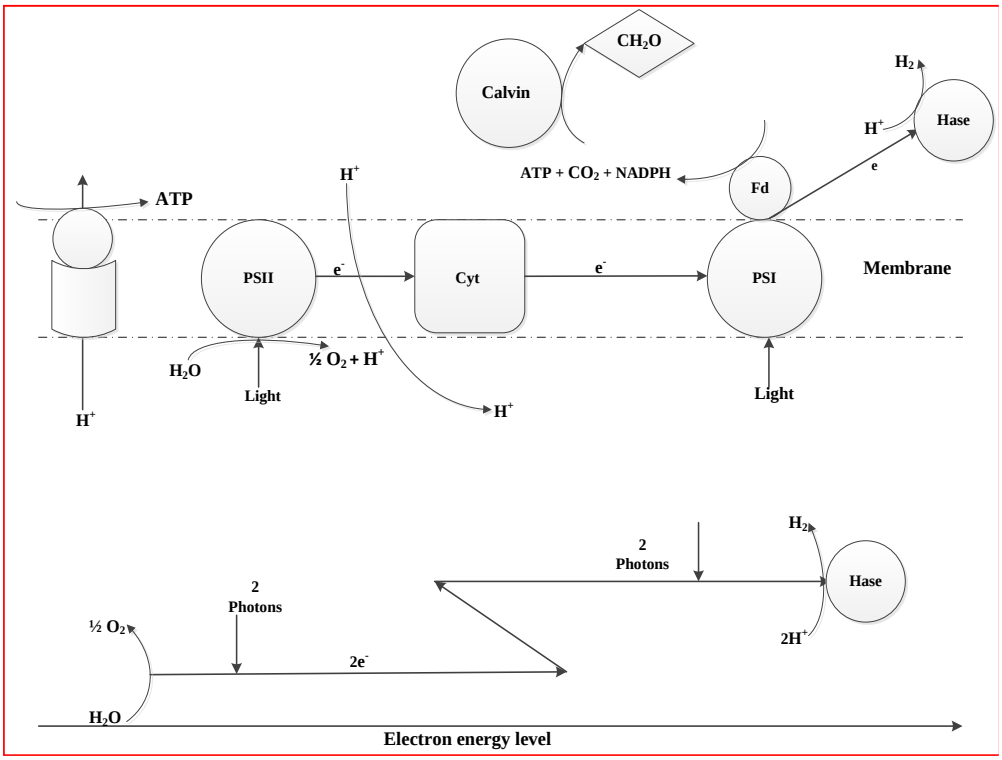

Figure 2.2 Schematic mechanisms of photosynthesis and bio-photolysis of photoautotrophic microbes[42]

2.2.1 Photosynthesis in microalgae

Microalgae can assimilate dissolved CO_2 gas in the form of inorganic carbon as substrates, resulting in CO_2 fixation [44], through carbon concentration mechanisms (CCMs). The carbon is utilized by microalgae cells is passively diffused across the cytoplasmic membrane. It is subsequently actively transported through the plasma membrane and chloroplast envelope via

carrier proteins [44]. In order to complete the formation of carbohydrate (CH_2O) from the photosynthesis process, light (as energy and electron source) and water are needed [45]:

$$nCO_2 + nH_2O + Light \xrightarrow{Chlorophyll} (CH_2O)_n + O_2 \quad \textbf{2.1)}$$

In the presence of microalgae cells, light oxdizes the water and O_2 produced simultaneously with the formation of adenine dinucleotide phosphate reduced form (NADPH), Adenosine Triphosphate (AT) and nicotinamide (Fig. 2.3). CCMs ultilization of the energy depends on active inorganic carbon transport to increase the intracellular CO_2 concentration at the site of ribulose 1,5-bisphosphate carboxylase/oxygenase (Rubisco), the key enzyme in the net carbon assimilation, to facilitate photosynthetic CO_2 fixation rates even at low inorganic concentrations [46] in Calvin Cycle. Practically, ATP and NADPH must be consumed before the actual carbon fixation is implemented in the Calvin Cycle. Interchange between various dissolved carbon forms occurs in the periplasmic space, catalyzed by carbonic anhydrase (CA) [44] through the supply of CO_2 to Rubisco by dehydration of accumulated bicarbonate [47].

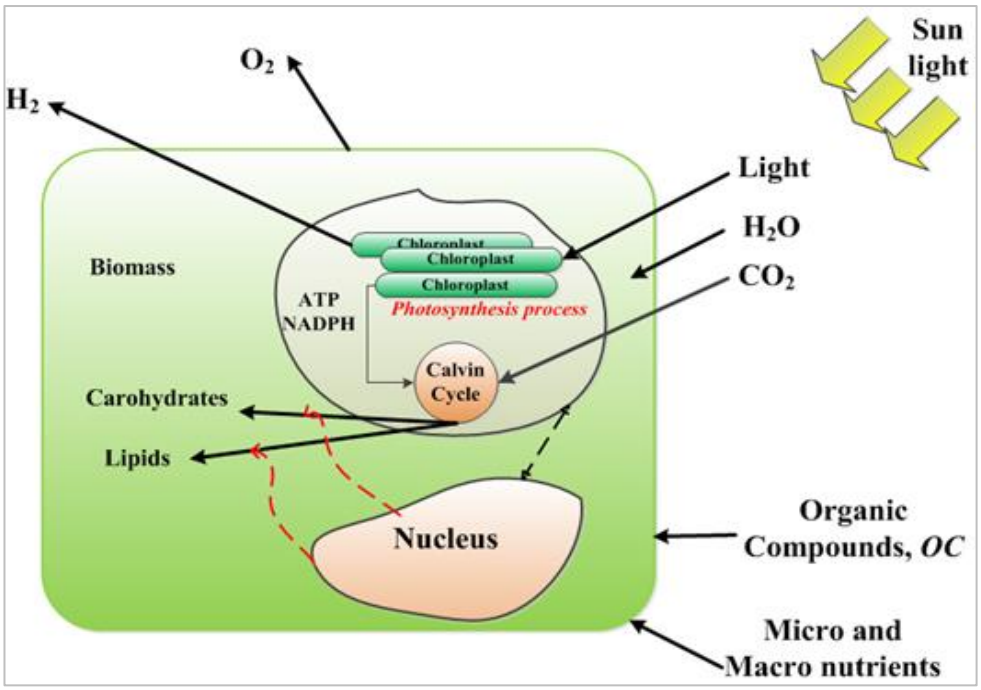

Figure 2.3 Photosynthesis in algal cell [39]

The CO_2 uptake rate depends on many different parameters, such algal strain, medium pH, light availability, temperature and CO_2 gas concertation. Photosynthesis converts approximately 27% of solar energy into chemical energy, producing 467 kJ of energy per mole of carbohydrate (CH_2O), whilst 1744 kJ $mole^{-1}$ energy is required to complete the photosynthesis process [45].

2.3 Algal cultivation conditions

Algal cells may be cultivated with different sources of energy and carbon which then influence the growth characteristics and algal cells composition [48]. They can grow under a number of different conditions relating to energy and food sources, specifically photoautotrophic, heterotrophic, mixotrophic, and photoheterotrophic cultivation.

2.3.1 Photoautotrophic cultivation

Photoautotrophic cultivation implies that light is the only the energy source for algal cell generation from inorganic carbon (e.g. carbon dioxide), and is converted to chemical energy via photosynthesis reactions. Autotrophic cultivation is associated with high algal growth rates, lipids productivity and nutrients removal. Moreover, it is economically feasible, environmentally sustainable and can be used for outdoor cultivation systems. However, the amounts of biomass and lipids vary widely - between 1% to 70% for lipids content according to the algal species [14, 49-51].

2.3.2 Heterotrophic cultivation

Heterotrophic cultivation employs organic carbon e.g. acetate, glucose and glycerol) for food and energy, similar to bacteria. This implies that light limitation does not constrain growth, as with photoautotrophic cultivation, and cultivation thus occurs under the full dark cycle. A high lipids content can be obtained and accumulation faster than for photoautotrophic conditions. For instance, *Chorella protothecoides* has been shown to generate a 40% higher lipids content when cultivation conditions changed from phototrophic to heterotrophic [52]. However, heterotrophic conditions create a higher risk of contamination, increased expense, and reduced nutrient removal and growth rate [52-54].

2.3.3 Mixotrophic cultivation

For mixotrophic conditions organic compounds and CO_2 can both be used as an energy source for algal growth through photosynthesis. This means the algal cells can survive under either heterotrophic or phototrophic cultivation or both. The CO_2 generated from the organic compounds consumption during respiration can be reused in phototrophic cultivation. Slightly lower growth rate and higher biomass accumulation can be obtained compared to the phototrophic process [14].

2.3.4 Photoheterotrophic cultivation

Photoheterotrophic cultivation can also be termed photoorganotrophic, photoassimilation or photometabolism cultivation. Algal cells require light to use organic compounds as a carbon source. Hence, this cultivation condition demands both light and an organic compound. This technique is rarely used for biodiesel production [55].

2.4 Algal cultivation systems

The microalgae culturing systems can be classified into open system (open or raceway ponds RW) and closed system (photobioreactor, PBR) (Table 2.1), with various configurations of the latter (Fig. 2.4). A comparison between open and close systems (Table. 2.1) indicates open systems as being cost effective, particularly at large scale process and low land costs, and simple in implementation. Against this, these system incur a higher contamination risk, lower CO_2 fixation and concomitantly a lower biomass productivity. PBRs offer a higher biomass productivity, CO_2 fixation, lower contamination risks and are fully controllable system, but are most costly and complicated in design. They are thus most suited to small-scale applications.

Table 2.1 Comparison between open and closed cultivation systems [56, 57].

Parameter	Raceway systems, RW	Closed systems, PBR
Contamination risk	High	Low
Space required	High	Low
Water losses	High	Almost none
CO_2- losses	High	Almost none
CO_2 bio-fixation	Lower	Higher
Temperature variation	High	controlled
Oxygen inhibition	High	Almost none
Maintenance requirements	Low	High
Produced Biomass	Low, approx. 0.1 – 0.2 g L^{-1}	High, approx. 0.82 – 6 g L^{-1}
Control ability	Poor	Higher
Autoclaving and Sterilization	Not necessary	Required
Nutrients removal	Lower	High
Harvesting efficiency	Low	High
Design complexity	Simple	Complex
Capital investment	Small	High
Process descriptions	Industrial scale, continuous	Lab and pilot scales, batch, semi continuous
HRT	Lower	Higher

HRT= hydrodynamic retention time.

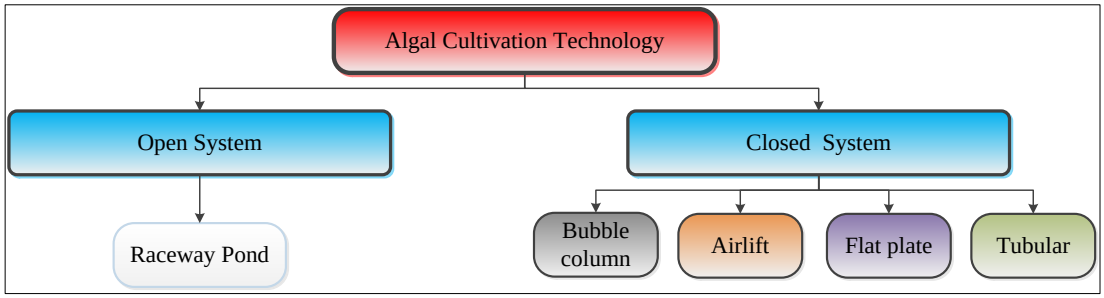

Figure 2.4 Algal PBRs system configuration

2.5 Photobioreactors (PBRs)

A photobioreactor (PBR) can be defined as an enclosed, illuminated culture vessel designed to control biomass production through adjustment of the operating parameters. The PBRs may tbe operated in either batch or continuous mode, with retained algal biomass providing a useful final product. Various types of PBRs have been designed and developed for algal biomass production. The reactor can be configured with tubular or flat plate geometry either as vertical bubble or air-lift columns or as a serpentine horizontal path, and may either use sedimentation or membrane separation for retaining the algal biomass [58]. The key system parameters governing microalgae growth, nutrient removal efficiency, and CO_2 capture are: light penetration and distribution within the PBR, CO_2 loading level, control of the photo-synthetically-produced oxygen, gas transfer, mixing, temperature, pH and nutrient availability, cultivation media compositions [59] and hydrodynamic residence time (HRT). No single configuration can provide the optimum conditions for all these parameters. The literature suggests that airlift and bubble column photo-bioreactors are among the most used reactors used for algal cultivation because of the advantages offered, which include good mixing, well-defined fluid flow pattern, relatively high gas liquid mass transfer rate and relatively low operating costs [60].

2.5.1 Bubble column PBRs

Bubble column bioreactors are vertical columns either cylindrical or rectangular shape through which gas is bubbled through sparger fixed at the column base. They offer minimum shear stress for the mixing attained with lower associated energy consumption and higher mass transfer and gas hold up rate. They are also relatively low in cost, simple to operate, have lower photoinhibition and photo-oxidation risks and are effective for immobilization of algae. This system is thus preferred to other PBR cultivation systems [61, 62]. However, the illumination area offered by this configuration is relatively small [63].

2.5.2 Airlift PBRs

Airlift PBRs consist of interconnected zones using baffles or draft tubes. Gas is bubbled through one side of the partition causing a fluid current pattern to develop with air bubbles rising in the "riser" and fluid falling in "downcomer" [64]. The airlift PBR offers similar advantages to the bubble column PBR. It can achieve high biomass concentrations, and provides low shear stress and good mixing with relatively low associated energy consumption. It is also easily sterilized and achieves effective immobilization of algae with reduced photoinhibition risk. As with the bubble column, the illumination surface area is small and which significantly decreases with scale up[64].

2.5.3 Flat plate PBRs

Flat pate reactors are characterized by higher illumination surface area with an associated high photosynthesis efficiency and subsequent biomass productivity compared with the bubble column and air-lift configurations. However, the parallel flow channel is more expensive in construction and more difficult to control with respect to the temperature, and incurs higher hydrodynamic stress [65].

2.5.4 Tubular PBRs

The tubular PBR consists of an array of horizontal transparent tubes which are interconnected to form a long serpentine path. The arrangement permits a large illumination surface area and high biomass productivity. However, the tubes are more prone to fouling than the vertical configurations of the bubble column and air lift reactors, and the required area for cultivation to achieve the illumination depends on tube arrangement. They are also subject to poor mass transfer and high O_2 accumulation, with an associated photoinhibition risk, with reduced temperature control and a high hydrodynamics stress [66].

2.6 Factors effecting microalgae cultivation process

As already stated, algal cultivation in PBRs depends on several critical operating conditions, such as CO_2 loading, pH, light intensity and wavelength, medium composition and contamination by other microorganisms [67].

2.6.1 Light Intensity

Generally, light intensity decreases exponentially with the distance from the reactor wall due to the increase of the algal cells concentration:

$$\frac{I_L}{I_O} = \exp(-XL) \quad \textbf{(2.2)}$$

where I_L represents the light intensity at distance L, I_o is the incident light intensity, and X is algal cells concentration. The light intensity tends to rapidly decrease due to the light shading from the algal cells [68]. However, at short light path lengths and at an appropriate light intensity sufficient light penetration into the algal culture can be achieved giving a high light utilization efficiency. Against this, at excessive light intensities a considerable amount of heat may be generated causing algal cell growth inhibition. The interaction between light intensity and other factors, such as temperature, and feed CO_2 gas concentration, is critical in optimising the microalgae production rate (along with CO_2 fixation and nutrient assimilation) and lipids content [69]. In addition to light intensity, the light-dark cycle has to found also significantly influence microalgae growth [70]. Continuous illumination is employed in many studies, although for some microalgae species this is not the favoured mode for promoting growth [70].

PBR performance is thus limited by light availability for microalgae cells to perform the photosynthesis process. Light availability depends on the cell concentration, which is inversely proportional to light penetration distance inside the PBR. The selection or development of the different PBR configurations has in part been based on improving light penetration within the reactor PBR to enhance algal growth [71-73].

CO_2 fixation as a function of I appears to follow no recognisable pattern across either different species or different investigations for the same species [21] (Table 2.2). Against this, for individual studies subject to the same standardized conditions fixation and biomass productivity both these parameters increase with I as expected to some maximum governed by light saturation [25, 74, 75]. Batch experiments on four different algal species (*C. vulgaris*, *P. subcapitata*, *S. salina*, and *M. aeruginosa*) indicate that an approximate trebling of light intensity (from 36 μmol m^{-2} s^{-1}) yields a 70-90% and 35-45% increase in biomass productivity and CO_2 uptake respectively [76]. Further increases in I may then inhibit and diminish R_c and μ [77].

2.6.2 Light wavelength, λ_{max}

Light is crucial in microalgae cultivation systems and can significantly enhance or inhibit algal growth. The two light components of light intensity (I) and wavelength number (λ_{max}) are known to significantly influence the cell growth rate [78-80]. Generally, limited light intensity can inhibit the algal growth whereas excessive light can lead to photo-oxidative and damage the algal cells, since the photosynthetic rate is directly affected by both I and λ_{max}.

Table 2.2 Reported CO_2 fixation rates for various algae species, light intesity batch systems unless otherwise stated.

Light intensity, µmol m^{-2} s^{-1}	*CO_2 fixn. rate, R_c g $L^{-1}d^{-1}$*	*HRT, d*	*Max. biomass concn, X_{max}, g L^{-1}*	*Inlet CO_2 $C_{c,g}$, %v/v*	*Flow rate Q_g, vvm*	*R_c', g CO_2 g biomas s^{-1} d^{-1}*	*Specific growth rate µ, d^{-1}*	*Refs*
Botryococcus braunii								
62.5	0.496	53	3.11	5	--	0.15	0.24	
87.5-538	0.089	2.5	1.9	0.03[a]	--	0.047	--	[82]
570	0.024	1[b]	0.92	1	--	0.026	0.052	[83]
Scenedesmus obliquus								
107	0.097	0.8-0.2	1.39	0.03[a] -35	2.1-8.3	0.06	0.64	[27]
180	0.28	--	1.84	0.03[a] -50	0.25	0.15	0.94	[84]
135-200[s]	--	1	--	0.03[a]	--	--	0.28	[85]
60	0.549	--	3.5	10	0.003	0.15	1.19	[22]
40-50	0.08[**]	33	0.3	15	2	0.26	1.14	[86]
40	0.049[**]	--	0.53	0.03[a]	--	0.098	--	[87]
Anabaena sp.								
900	1.45	2-3[b]	3	0.03[a]	0.2	0.48	--	[88]
0-460	0.43	3.3[b]	0.76	10.6	~3 x 10^{-4}	0.56	--	[17]
250	0.65-0.8	5	0.58-1.2	5-15, 10	0.04	0.66-1.12	--	[25]
650	0.16-0.58	0.7-6[b]	0.35-0.95	0.03[a]	0.13-0.75	0.45-0.61	--	[74]
975	0.25-0.65	0.7-6[b]	0.45-1.35	0.03[a]	0.13-0.75	0.55-0.48	--	
1625	0.36-1	0.7-6[b]	0.5-2	0.03[a]	0.13-0.75	0.72-0.5	--	
Chlorella vulgaris								
180	0.47	100	1.34	0.03[a]	--	0.35	1.19	[75]
62.5	0.25	53	1.94	5	--	0.12	0.29	[81]
126	0.30	--	0.821	0.03[a]	--	0.36	0.73	[76]
(60-70)	0.162	--	0.75	(0.03[a]-5)	--	0.21	0.28	[26]
(40-50)	0.062[**]	33	0.29	15	2	0.21	1.37	[86]
40	0.046[**]	--	0.49	0.03[a]	--	0.094	--	[87]
142	0.12[**]	2[b]	1.37	4	0.014	0.09	--	[89]

[a]Atmospheric level; HRT = hydraulic residence time; vvm = volume gas per volume liquid per minute.
[b]Continuous system otherwise Batch system and [s] for semi continuous.
[**]R_c estimated from Chisti ratio: $CO_{0.48}H_{1.83}N_{0.11}P_{0.01}$; $R_c = 1.88 \times P_{overall}$, $P_{overall} = \Delta X/\Delta t$.

At low light intensity, microalgae can achieve up to 80% of the theoretical maximum photosynthesis efficiency (PE) of 0.125 mol CO_2 fixed per mol photos absorbed [90-93]. Therefore, a steep light gradient may be expected to proceed at a high *I* level applied to the cultivation medium, since it is practically impossible to obtain the maximum photosynthetic efficiency (PE) at higher *I*. In a high cell density culture, most of the light energy is absorbed in small volume fraction of the photobioreactor (PBR) at the side exposed to light. In this case algal cells are subject to more light energy than the amount that can be converted to biochemical energy by photosynthesis. This causes oversaturation, which is consequently dissipated as heat [94] resulting in a lower PE than that attainable at low *I*. Therefore, optimising the physiological state of cells by manipulating the light conditions, through providing a better balance between light capture and the photochemical process [95-97], can significantly enhance the photosynthesis efficiency. There are various studies investigating the influence of λ_{max} or different LED transmitters on algal growth efficiency (Table 2.3).

Table 2.3 Reported light wavelength influence on microalgae growth

LF Source	Microalgae species	Wavelength λ, nm	X_{max} , g L^{-1}	$C_{d,}$ Cells mL^{-1}	μ, d^{-1}	*Refs.*
		λ_B	nr	nr	0.64	
		λ_W	nr	nr	0.66	
	Nannochloropsis	λ_G	nr	nr	0.54	
LED	*Sp.*	λ_R	nr	nr	0.51	[98]
		$\lambda_{B,\ 457}$	nr	1.45×10^7	1.64	
	Nannochloropsis	$\lambda_{R,\ 660}$	nr	1.11×10^7	1.61	
	Sp.	λ_W	nr	0.93×10^7	1.59	
		$\lambda_{B,\ 457}$	nr	0.25×10^7	1.47	
		$\lambda_{R,\ 660}$	nr	0.20×10^7	1.43	
LED	*Teraselmis*	λ_W	nr	0.24×10^7	1.44	[99]
		λ_R,	1.7	nr	nr	
		λ_B,	1.45	nr	nr	
		λ_G	1	nr	nr	
Fluorescent Paint	*Chorella sp.*	λ_Y	1	nr	nr	[100]

λ= wavelength number, B=blue, R= Red, G= green, O=Orange, V= violate, Y= Yellow, W= white, LED= light emitting diode, nr= not reported, LF= light filter.

2.6.3 Macro and micro-nutrients

Microalgae have attracted much attention in wastewater treatment for N and P removal as the primary nutrients, simultaneously with CO_2 fixation during the cultivation process, with other macronutrients such as sulphur, potassium, calcium and magnesium also receiving attention [101]. Oxygen is consequently generated by photosynthesis as the algal biomass develops, providing a potential source of renewable energy for biofuel production [102]. Approximate

of 3726 kg water, 0.33 kg nitrogen and 0.71 kg phosphate are need to produce 1 kg of microalgae cells, when using the freshwater without recycling[103]. The influence of macro-nutrients on a single algal cells growth has been extensively studied in the literature (Table 2.4). However, micro-nutrients are also needed to support the algal growth in smaller amounts, and these include manganese, molybdenum, copper, iron, zinc, boron, chloride and nickel. In addition, some other elements can be essential for certain algal species, like sodium, silicon, cobalt, iodine, vanadine and selenium. To prevent growth limitation by micro-nutrient, these are often added to commercial algal cultures together with a chelating agent such as EDTA [104].

Low concentrations of essential micronutrients results in very efficient uptake in microalgae. Studies on micro-nutrients have focused on the roles of essential and other elemental nutrients. Some micronutrients may be absorbed at levels exceeding the biostoichimetrically-determined concentrations, or else may be absorbed by microalgae but not required for growth [105]. For instance, the most important micronutrients in the microalgae are those in redox reactions (e.g. Fe^{3+}, Mn^{2+}, Cu^{2+}), and acid-base catalysis (e.g. Zn^{2+}, Ni^{2+}). It is evident, from various published studies [110-119], that these micro-nutrients exert an influence on microalgae cell physiology which might then be expected to be reflected in the biomass production and CO_2 fixation rates (Table 2.5).

Whilst nutrient removal from wastewater using microalgae cultivation technology has been widely investigated, few until recently have addressed the coupling macro and micro-nutrients and the possible impact of different wastewater sources on biomass production in this regard [85, 87, 89, 106-113]. A variety of microalgae species (*Ourococcus multisporus*, *Nitzschia cf pusilla*, *Chlamydomonas mexicana*, *Scenedesmus obliquus*, *Chlorella vulgaris* and *Micractinium resseri*) have been examined using municipal, agricultural, and industrial wastewater sources [22], providing a range of nutrient concentrations. *Chlorella vulgaris* has been cultivated in different wastewaters, including artificial, piggery, domestic and secondary wastewater sources [111, 112]. However, these studies have largely focused on the influence of N and P, ignoring other macro and micro-nutrients.

Table 2.4 Reported macro – nutrient influence on algal growth

Macro – nutrient	Ion used by cells	Type of reaction	Biological function	Limitation influence	Location in cells structure	Nutrient Importance	Refs
Sulphur	Sulphide, S^{2-} Sulfate, SO_4^{-2}	Redox, oxidized	Maintain cells viability functions for transport proteins and enzymes	Reduction in sulphate uptake	Membrane sulfolipids cells walls, vacuoles Chloroplasts and plastids	High	[114]
Sodium	Na^+	Osmotic	Control of nitrate reductase through protein factor(s) Constitutes ~70% of total positive charge on major osmotic solute	Nitrite toxicity, chlorophyll loss chlorosis, Increase the enzyme nitrate reductase	Cytoplasm, and vesicles	High	[115]
Potassium,	K^+	Osmotic	See Sodium	Changes in protein level reduce the algal growth	Cytoplasm, and vesicles	High	[116]
Magnesium,	Mg^{2+}	Photosynthetic	Critical component of chlorophyll Increase the cells division rate Effects on RNA synthesis andincrease the protein. Increase the cell size	decrease the cells volume Inhibited growth Inhibited the cells division Chlorotic cells	Ground cytoplasm, and Vesicles	High	[117]
Calcium	Ca^{2+}	Alkalinity	Active ATPase. Quantity of pectic substances produced in cells walls Reduction of medium alkalinity	Reduce the rate of photosynthesis Endoplasmic drops Low algal rate	Ground cytoplasm Vesicles	High	[118, 119]

Table 2.5 Reported micro – nutrient influence on algal growth.

Macro – nutrient	***Influence on algal cells***	***Refs***
Mn^{2+}	Mn^{2+} deficiency in the cultivation medium can cause chlorotic microalgae which effects directly on the *chlorophyll* formation of microalgae and PSII.	[120]
Zn^{2+}	Essential micronutrient element exist in the nucleic apparatuses such as, eoxyribonucleic acid (DNA) and ribonucleic Acid (RNA), finding the RNA content was low in Zn^{2+} deficiency, involved in CO_2 supply to Ribulose -1,5-bisphosphate carboxylase/oxygenase (RUBISCO) for CO_2 fixation in photosynthesis process algal cells.	[121] [122]
Cu^{2+}	Play a role in the photosynthetic electron transport chain of microalgae that use metallo – protein plastocyanin, in PSI activity and respiratory electron transport chain, in addition to the Cu^{2+}-Zn^{2+} from superoxide dismutase, and in the transmembrane uptake of Fe^{3+}.	[123, 124]
Ni^{2+}	Ni^{2+} scarcity limits urea utilization in the marine environment as a result of organic complexation and slow uptake kinetics	[125]
Se^{2-}	Necessary for synthesis of selenium containing proteins, called selenoproteins, which are believed to be physiologically active and functional molecular from of Se^{2-} in cells.	[126].
Fe^{3+}	Iron is particularly important in oxygenic photosynthesis and it is present in the two photosynthetic reaction centers (photosynthetic I and II, which contain respectively 12 and 2-3 iron atoms each) and the cytochrome complex which is involved in adenosine and three phosphate (ATP) synthesis.	[127].
Pb^{2+}	Approved was not inhibitory metals below this concentration of (700 µg L^{-1}).	[128]
As^{3+}	Higher concertation of As^{3+} caused inhibition for algal growth.	[129].

2.7 pH

According to the microalgae carbon concentration mechanisms (CCMs), the most important forms of dissolved inorganic carbon (CO_2 and HCO_3^-) are closely related to the pH value of the algal medium [130, 131] (see Sections 2.2.1). The variation of pH value in the cultivation medium depends on the hydrolysis of CO_2 and the chemical properties of the cultivation medium. The influence of pH on the algal carbon fixation and biomass production is mainly related to the CO_2 gas concentration.

There is no significant change in pH value of the cultivation medium when aerated with atmospheric CO_2. The pH range is about 7.9-8.3 for marine algae and between 6 and 8 for freshwater algae. Algal cells assimilate the carbon, escalating the pH value to 9-10 with an extremely low (0.038%) associated CO_2 concentration. Against this, a high CO_2 concentration

(10-20%) can cause sharp decline in the pH value to about 5.5, which has been reported to inhibit the Rubisco activity in CCMs and thereby algal growth. Most microalgae species can tolerate a wide range of pH change, although they normally have an optimum range or value (for instance, synechococcus PCC7942 at pH 6.8 [132]) or in are inhibited at other pH ranges (for instance *Chlorella Sp. KR-1* is inhibited at pH 4 [133]).

2.8 Temperature

Temperature can also significantly influence algal biomass production and CO_2 bio-fixation. Physicochemical reactions during microalgae photosynthesis are naturally temperature dependent. Generally, lower temperatures are not favoured due to the reduced Rubisco activity which then commensurately reduces photosynthesis efficiency and so CO_2 fixation. On the other hand, higher temperatures inhibit algal embolic growth and respiration intensity [134], and also decrease the CO_2 solubility in cultivation medium in accordance with Henry's Law. Therefore there is an optimum temperature or range depending on microalgae species and culture medium composition that should be indicated. Previous work have indicated most common microalgae species can survive between 15 and 26℃ [135]. Room temperature (18-20 ℃) is often recommended for algal growth. Generally, temperatures lower than 16 can retard algal growth, whilst the temperatures above 35℃ have been shown to inactivate a number of microalgae species [133, 136, 137].

2.9 Environmental application of microalgae

Coupling wastewater treatment and CO_2 bio-fixation using microalgae cultivation technology (MCT) has received some attention in recent studies. MCT can successfully remove significant amounts of the polluting nutrient species (as NH_4^+, NO_3^-, PO_4^{-3}, etc) required for microalgae growth [138], as well as capturing CO_2, fixing 183 tons per every 100 tons of biomass produced. Biodiesel from microalgae is thus one of the very few biofuels with negative CO_2 emissions [139]. Morever, the extracted algal residue can be used for biomass production [138] (Fig. 2.5), allowing further energy recovery and so further reducing the environmental footprint. Despite this, MCT scale up remains challenging by process unreliability and high cost for large scale processes, which remain economically unfeasible [140]. However, there remains a need for alternative and sustainable sources of fuel. Given the environmental attractiveness of combined fixation of CO_2 from flue gases and pollutant removal from wastewater combined with generation of a renewable fuel source, the currently existing economic feasibility limitations have to some extent been set aside in pursuit of an optimum configuration and/or scenatio for the application [141].

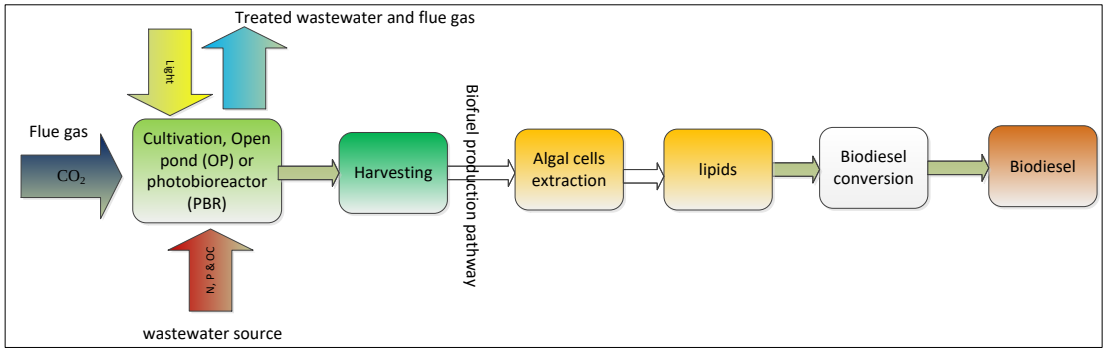

Figure 2.5 Biofuel from microalgae culture technology (MCT), schematic. *OC* Organic carbon, CHP combined heat and power (adapted from [142])

2.9.1 Carbon dioxide fixation

Various methods have been implemented for CO_2 fixation (Table 2.6). However, these methods are expensive; generate considerable amounts of by-products, require large pieces of equipment, incur a relatively high energy demand. They are nonetheless widely used in industry out of necessity.

Algae consume the dissolved carbon in a cultivation medium, which includes dissolved inorganic carbon (IC). When CO_2 gas dissolves in water it generates a weak acid/base buffer system comprising carboxylic acid (H_2CO_3), bicarbonate (HCO_3^-) and carbonate (CO_3^{2-}). These species exist a different concentrations at different pH ranges. The CO_2 - bicarbonate - carbonate equilibrium is the most essential chemical buffer system found in the natural water, and permits fixation of the carbon by algal species.

In the last 50 years a number of different algal species have been examined for CO_2 fixation [37, 143-147]. In particular *Chlorella vulgaris* has been widely studied for CO_2 fixation under a range of operating conditions of CO_2 concentration, [24-28] light intensity [29, 30] and temperature. Both atmospheric and industrial [148] sources of CO_2 can be harnessed, with algal growth from atmospheric sources being constrained by the low CO_2 concentration (0.036%) [138]. Whilst algal growth is promoted at higher CO_2 concentrations [149], this may be mitigated to some extent at higher temperatures due to the decreased CO_2 solubility [150].

Table 2.6 Comparison between different recent methods for carbon dioxide fixation strategies.

CO_2 fixation method	Advantages	Disadvantages	Ref.
MEA Scrubbing; A chemical absorption process used with a mono ethanol amine (MEA)	Carbon dioxide captured can be used for industrial processes or to supply the needs of a photo-bioreactor system	Expensive required large equipment sizes and high regeneration energy requirement	[151] [152]
Membrane Technology; The principle behind membrane technology could be used to assist the carbon dioxide capture	*Reducing the installation and operating costs by 30–40%. *Increase the mass transfer area in a given volume, and to avoid the problems associated with vapour–liquid contact surfaces	In most membrane types, the amine either destroyed or wetted the surface, causing blockage except Pdytetrafluoroethylene (PTFE) membrane type was successful.	[152] [153] [154]
Desiccant Adsorption; Pressure and temperature swing adsorption (PTSA), using zeolite as desiccant	* Carbone dioxide can be regenerated under depressurization. * Regenerative capacity and power reductions can be achieved. * Target removal efficiencies of 90–99% purity of CO_2.	The reaction of the desiccant with SOX in the flue gas.	[155]
Molecular Sieve; Sieve that separates molecules based on their molecular weight or molecular size	*Produce minimal waste, *High separation efficiency.	Very high cost effective.	[156] [157]
Enhanced oil recovery(EOR); Carbon dioxide is injected into an oil reservoir	EOR projects depend on the price of oil and pure carbon dioxide.	*Economically unfeasible *High cost of the CO_2 removal. *requires large amounts of energy.	[158] [159]
Coal Seams; Geologic injection, Carbon dioxide diffuses through the pore structure of coal.	Coal beds often contain large amounts of methane	The process need to be optimised	[159]
Oceanic Injection Direct injection into the ocean.	Most viable method due to technological and economic reasons.	*Decreases the pH level of surrounding area. * Around 15-20 % of the injected carbon dioxide will be leached back to the atmosphere.	[159] [3]

The retention of carbon dioxide in a PBR generally depends on CO_2 transfer from the gas to liquid phase and CO_2 uptake by algal cells. Either one or both of these factors may be a function of the light intensity, CO_2 gas concentration, biomass concentration in a PBR, hydrodynamic retention time, algal specie and cultivation medium physically properties (pH and temperature). Individual experimental studies have rarely encompassed all the relevant variables.

Generally, CO_2 uptake as a proportion of the supplied CO_2 is largely dependent on the gas retention time (or hold up). Table 2.7 indicates that biomass production is generally in the range 0.01-1.03 g L^{-1} d^{-1} for moderate to higher (0.03 -5 %) feed gas CO_2 concentration. CO_2 fixation can be enhanced by increasing the light intensity, within the optimum limits, enhancing the mass transfer coefficient and adjusting the macro and micro nutrients (and N and P specifically) in the cultivation medium.

Table 2.7 Reported CO_2 fixation data, 2010 onwards.

Algal Species	***Cultivation medium***	***TP_{in}, mg L^{-1}***	***TN_{in} mg L^{-1}***	***Light intensity, $\mu mol\ m^{-2}\ s^{-1}$***	***Inlet CO_2, %v/v***	***P_A, g biomass^{-1} $L^{-1}d^{-1}$***	***CO_2, fixed,g L^{-1} d^{-1}***	***Refs***
C.v	TS	1.2	19	132	0.03*	0.04	0.07**	[160]
	TS					0.01	0.01**	
Ps. Sub.	nr	140	39	800	nr	1.02	1.83**	[161]
	C	126-158	14-18			1.03	1.85**	
Na. gad.	AM	7	25	300		0.27	0.48**	
	AM			500		0.36	0.64**	
	40% C	5	149	300	5	0.27	0.48**	[162]
	50% C	8	258	300		0.31	0.55**	
	40% C	5	149	500		0.38	0.68**	
	50% C	8	258	500		0.44	0.79**	
Sc. acutus	Ww	2.5	22	610	nr	0.073	0.13**	[163]
	Ww	41	3		nr	0.079	0.14**	

MLA = Marine labs American Society of microbiology-derived medium; TS treated sewage; C centrate; Ww municipal wastewater; *Sc. Acutus=Scenedesmus acutus* , *Nannochloropsis gaditana= Na. gad, Pseudokirchneriella subcapitata= Ps. Sub.*, nr not reported; *atmospheric air,**%CO_2 fixed estimated from Chisti ratio: CO0.48H1.83N0.11P0.01; Rc = 1.88 × Poverall, Poverall = $\Delta X/\Delta t$.

2.9.2 Wastewater Treatment (WWT)

Typical WWT operations (Fig. 2.6) are generally denoted primary, secondary and tertiary treatment. In the initial primary treatment stage large solids that easily settle out are removed by sedimentation [164]. The remaining clarified liquid is then subjected to secondary treatment, in which bacteria ingest the organic material in wastewater to provide up to 90% of removal of the dissolved and suspended organic matter. Secondary treatment requires a further solid-liquid separation process to remove the microorganisms from the treated water prior to discharge or tertiary treatment [165, 166]. In most modern municipal WWT operations the nutrients N and P must be removed, and in some cases other materials such heavy metals. The process used for biological nitrogen removal is well developed and involves a simple adaptation of the classical secondary treatment process (the activated sludge process, ASP) through the introduction of an anoxic zone before the aerobic zone. However, removal of residual phosphorus demands further adaptation.

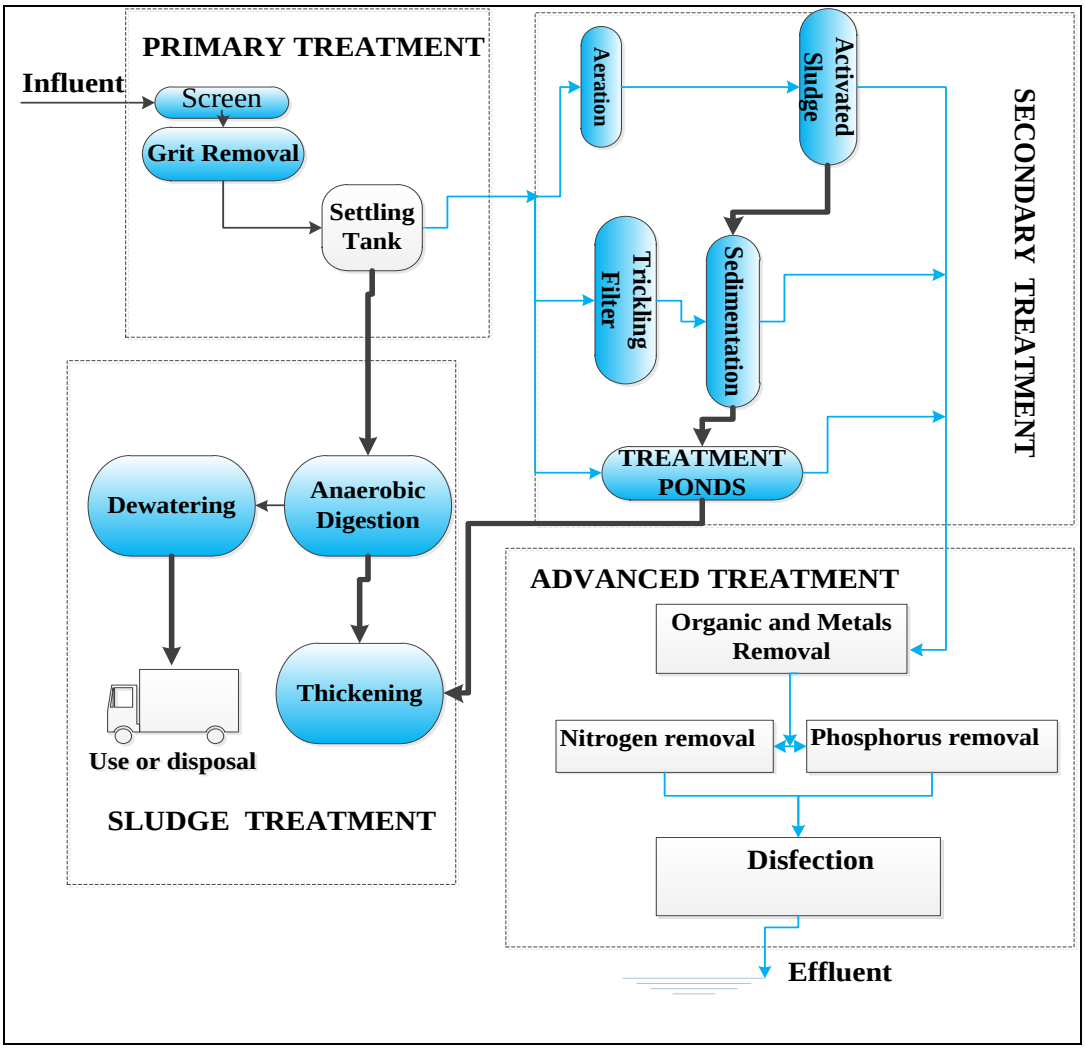

Figure 2.6 Block diagram of typical wastewater treatment.

Whilst adbanced BNR processes can satisfactory removal N and P, to as low as 3 mgL^{-1} *TN* and *TP* to 0.3 mgL^{-1} TP if fully optimised [39], the process relies on the existing ASP being in place. BNR also demands the pumping of sludge between various tanks in the treatment scheme [5, 6] (Fig. 2.7). In future, zero-energy wastewater treatment schemes are envisaged using anaerobic treatment. Anaerobic wastewater treatment provides effective organic carbon removal but provides no N or P removal. MCT thus provides an option for low-energy nutrient removal under such circumstances.

Algae have been used to recover N and P from municipal wastewater, potentially integrating with the existing installation wastewater treatment and utilizing the effluent as a source of both the macro and micro nutrients. The efficient growth of microalgae in wastewater depends on water quality determinants, such as pH and nutrient concentration (including organic carbon), the availability of solar light and CO_2. These variables will obviously depend on the wastewater source, as well as the algae strain itself.

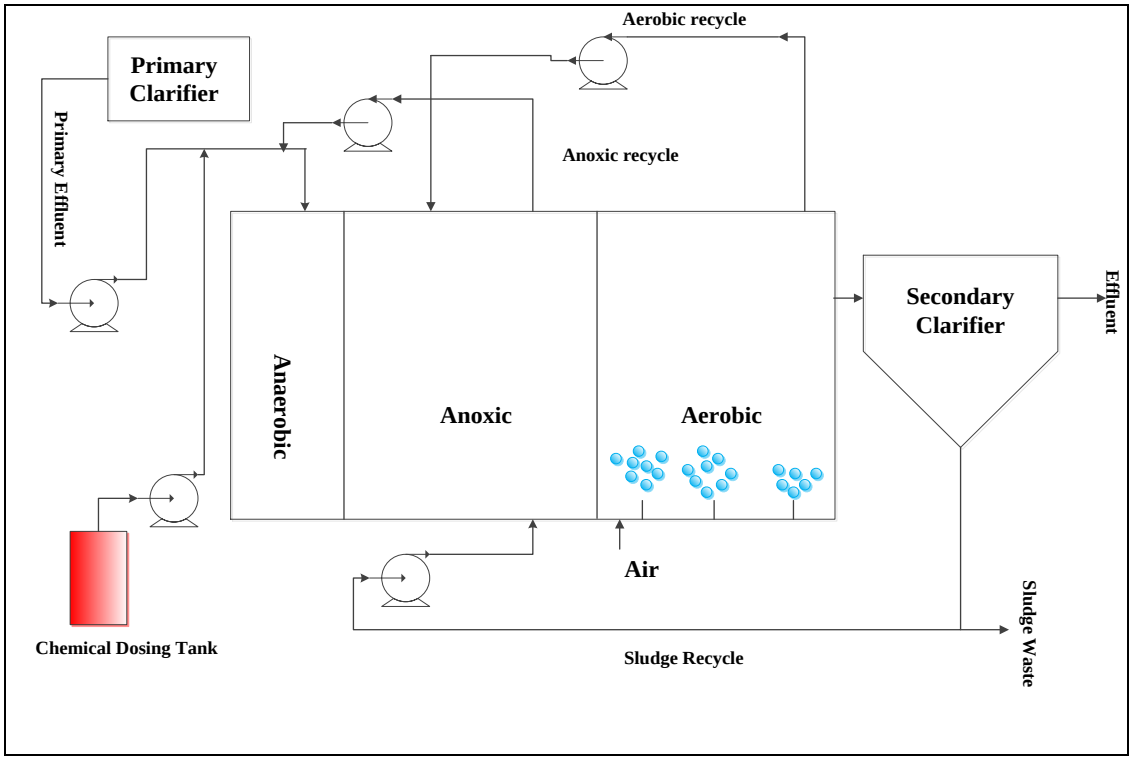

Figure 2.7 Schematic of BNR process, including anaerobic zone for P removal.

2.9.2.1 Wastewater resources

2.9.2.1.1 Municipal wastewater

Municipal wastewater is generated by domestic use of water, deriving from sanitary sewers and storm drains. It generally ostensibly soluble and insoluble organic matter, microbes, and trace quantities of heavy metals, such as lead, zinc and copper, and organic chemicals of

concern such as halogenated organics. It is also odorous, arising from various volatile organic compounds along with hydrogen sulphide. Industrial wastewaters tend to have higher organic concentrations as well as high nutrient levels (e.g. 110 and 52 mg L^{-1} N and P respectively in winery wastewater [167]), compared with municipal wastewater of 15-90 and 5-20 mg L^{-1} respectively [168]. Within a wastewater treatment plant (WwTP) there may be stream from the sludge processing plant containing, for example the centrate from the centrifugal separation process, which contains very high nutrient and organic carbon levels, making it a more effective source for microalgae cultivation [169] than the tertiary wastewater stream, which nonetheless is a suitable feedstock for MCT [170].

2.9.2.1.2 Industrial wastewater

Industrial wastewater can be high in heavy metal content, including cadmium, chromium, zinc from industries such as tanning and heavy industries, and high in organic content, for example from food and beverages from food and beverage processing and production, and possibly toxic organic matter, such as from refineries, paper mills or pharmaceutical wastewaters. Tolerance of the algal species to high levels and/or shock loads of toxic materials is therefore of some importance for treating such effluents using MCT. Thus far, few algal species have been studied for their heavy metal sorption ability [18]. Industrial wastewaters may require dilution or blending with other streams to mitigate against toxicity and algal growth inhibition [18, 171, 172]. Microalgae have been cultivated in various industrial wastewaters with a view to removing heavy metal pollutants and organic chemical toxins [59, 173-175], where a fraction of the pollutant (organics or heavy metals) may incur toxic effects on the aquatic ecosystem [176-178]. However, the tolerance of algae species varies between species: *Chorella Vulgaris*, for example, has been reported to be sensitive microalgae to hydrocarbons, biocides and surfactants [179].

Untreated petroleum effluent (P_E) usually contains approximately the same amount of nutrients as municipal wastewaters, but often contains oil and grease, hydrocarbons, phenols, sulphides and heavy metals. The presence of these materials is known to be responsible for toxicity of discharged petrochemical wastewater streams [180]. P_E generally has a high organic content, with the organic constituents exerting a different toxicities susceptibilities to anaerobic and aerobic degradation [180]. Various studies have reported nutrient content in P_E ranging from 9.9 to 16.2 and 0.08 to 28.7 mg L^{-1} for N and P respectively [180].

2.9.2.2 Bioremediation of wastewater using microalgae

The application of microalgae to municipal wastewater treatment was originally investigated in the 1950s [181], and for nutrient removal from the mid-1970s onwards [182, 183] as an effective means of mitigating eutrophication [184, 185]. A number of benchmark reviews of the subject have been published [186], along with a seminal close-out report for the Aquatic Species Program (ASP), which ran from 1978 to 1996 [187].

Microalgae have been proven to be efficient in removing N and P and toxic metals from a wide variety of wastewaters [9, 188, 189]. There have been extensive studies of algae growth in municipal [190, 191], agricultural [192], and industrial wastewaters [18, 67] which have indicated substantial nutrient removal and concomitant algae biomass production. Microalgae either assimilate the nutrients or render them innocuous, such that the treated water can potentially be reused or discharge to the ecosystem [193]; phosphorus removal is mainly through assimilation absorption of chemical precipitation. The microalgae biomass contains a significant nitrogen and phosphorus, approximately 10 and 11%, respectively on a dry weight basis [194].

The use of photobioreactors (PBRs) for N and P removal from wastewaters has received considerable attention [195, 196] [197] [198] [199]. PBRs offer a more sustainable alternative to the established biological nutrient removal (BNR) process, which demands energy for aeration and the pumping of sludge between various tanks in the treatment scheme, as well as supplementary chemical dosing with coagulants to obtain the required P removal [7]. However, whilst offering a potentially sustainable solution for combined nutrient and CO_2 abatement, the process footprint can be up to two orders of magnitude greater than that of the BNR process [21].

2.9.2.3 Nitrogen and phosphorus nutrients removal

Nitrogen in wastewater exists in the form of nitrate, nitrite, ammonia, and urea (or mixtures of them) [200]. Whereas the ammonium ion is directly assimilated by the algae, nitrate is removed via reduction to amino acids before being assimilated [200]. Whilst algae are apparently able to assimilate most of the nitrogen species in wastewater, there is a greater risk of contamination from real wastewaters than from bespoke cultivation media [201].

Control of nutrient loads has been shown to provide beneficial effects. Nitrogen limitation has been observed to lead to increased lipid content in some *chlorella* strains such as *C.emersonii* (63%), *C. minutissima* (56%), *C. vulgaris* (57.9%), *C. luteoviridis* (28.8%), *C. capsulata* (11.4%), and *C. pyrenoidosa* (29.2%) [202]. It has also been observed [203] that triglyceride

accumulation in *Nannochloris sp.* cells could be 2.2 times greater than that in the cells in nitrogen sufficient cultures. The intracellular triglyceride content can be improved by prolonging the cultivation period during the stationary phase after nitrogen depletion. However, the creation of high-lipid and high caloric cells in stress states, such as nutrient deficiency, is associated with reduced cell division [204]. Therefore, there is an important balance between producing high caloric value cells and maintaining high biomass productivity through optimizing nitrogen in algal cultivation medium.

Phosphorus is usually available in the wastewater as inorganic anions species such as $H_2PO_4^-$ and HPO_4^{2-} [205]. As with all nutrients, phosphorus is important for microalgae metabolism and growth, through adenosine triphosphate (ATP), which is essential to the cellular processes related to energy transfer. Phosphorus can be removed from wastewater through chemical precipitation, physical processes (using filtration and membrane), or by enhanced biological phosphorus removal (EBPR, an extension of the BNR process). Chemical precipitation is commonly referred to as chemical addition or flocculation, which can be achieved through addition of alum, lime, or iron salts to the wastewater which cause aggregation of particles to allow them to more readily be removed by sedimentation. This process can reduce the overall P concentration by more than 95%, depending on the extent of optimisation of chemical dosing. Chemical dosing increases the inorganic content of the waste sludge, and thus the cost of its disposal [206]. It is thus preferable to use wholly biochemical methods, i.e. EBPR, since these involve no chemicals and produce less sludge [205]. EBPR typically involves modifies the BNR process modification (alternating aerobic and anaerobic and anoxic conditions) that allows for a high degree of P assimilation and potentially very low residual P levels (<0.1 mg/L), especially if combined with chemical dosing [205].

In the case of photosynthesis for algal production, large amounts of proteins (notably Rubisco) are generated through phosphorus rich ribosomes [207]. Since phosphorus-containing ATP/adenosine diphosphates are essential for photophosphorylation, limitation of growth by phosphate starvation may influence microalgal metabolism, and specifically lipid accumulation. Phosphorus is preferentially assimilated as inorganic phosphates in the form of $H_2PO_4^{2-}$ and HPO_4^{3-} [208, 209]. It has been postulated that phosphates may form complexes or precipitates with some metal ions, and that not all the added P is bioavailable [183] such that supplementation may be required for optimal operation.

Algal growth and nutrient (N and P) removal efficiencies depend on a large number of variables, including medium composition and environmental conditions such as the initial nutrient concentration, light intensity, the N/P ratio, the light/dark cycle and algal species [210] (Table 2.8). Whilst there have been a large number of recent studies of nutrient abatement

using PBRs based on a number of system variables [89, 211] few have actually focused on the key aspect of nutrient balancing in a wholly consistent way.

Table 2.8 Variation of the TP and TN removal efficiencies with the optimum N/P ratio.

Cultivation wastewater	*Strain*	*Optimum N/P ratio*	*TP % removal*	*TN% removal*	P_X *(mg L^{-1} d^{-1})*	*Ref*
Domestic	Mixed	14	92.4	77	--	[212]
Domestic	*C. vulgaris*	192.6	84.2	44	--	[213]
Domestic	*C. vulgaris*	1-10	89	78	2.75	[214]
		11-20	81	84	2.3	
		21-30	59	83	1.18	
		61-70	24	73	0.41	
Synthetic	*C. vulgaris*	8	--	93	--	[215]
Domestic	*C. vulgaris*	2.85	97.8	67.2	234	[107]
Synthetic	*C. vulgaris*	18.8	85.9	82.5	72	[89]
Domestic	*C. vulgaris*	7	70	86	--	[216]
Municipal	*C. vulgaris*	21	100	70	54	[217]
	Co-culture[1]		100	80	65	
Synthetic	*C. vulgaris*	5	96	97	230-212	[218]

[1]*C. vulgaris & Planktothrix*

Xin et al. [219] cultivated *Scenedesmus sp.LX1* in a photobioreactor under different concentrations of initial TN (2.5, 5, 10, 15, 25 mg L^{-1}) and TP (0.1, 0.2, 0.5, 1, 2 mg L^{-1}). The authors reported the maximum removal of 99% for both N and P for initial TN and TP concentrations of 10 and 2 mg/L respectively, i.e. for an N/P mass ratio of 5. Feng et al. [218] reported a maximum of 97% NH_4^+ and 96% TP removal using *Cv* cultivated in artificial wastewater at initial TN and TP of 20 and 4 mg L^{-1} respectively, i.e. at the same N/P ratio. Aslan and Kapdan [220] investigated the capability of *Cv* for nutrient removal at different N and P concentrations and reported NH_4^+-N to be completely removed from the media at initial concentrations of 13-21 mg L^{-1}, while only 78% of the PO_4^{3-}-P was removed at a inital concentration of 7.7 mg/L. Lau et al. [221] demonstrated immobilized *Cv* cells to provide higher N and P removal efficiency (over 95% within 3 days) from primary settled wastewater than the free cells due to the higher metabolic activities of the immobilized cells as well as the interaction between the polysaccharide matrices and the nutrient ions in the wastewater. However, in all cases nutrient removal by algal processes is hindered by the long residence times of 2-5 days required [222].

2.10 Mathematical modeling

2.10.1 Algal photobioreactor key system facets

Key system properties affecting the microalgae cultivation process include (i) distribution of light dose throughout the biomass, (ii) CO_2 mass transfer from the gas to liquid phase, (iii) CO_2 assimilation by the algal biomass (largely achieved through (i)), (iv) nutrient load or concentration, and (v) removal of O_2 generated during the photosynthetic process which may otherwise inhibit the algal growth [13]. Carbon dioxide functions as the carbon source for most algae, with the assimilated carbon contributing about 50% of the algal biomass. The local carbon dioxide concentration at any point of a bubble column PBR should be above the minimum threshold to sustain photosynthesis to avoid carbon limitation [42]. Nutrient limitation can be employed to enhance lipids production [223] leading to protein synthesis, the excess photosynthesized carbon being stored as triacylglycerides or starch [224].

Light intensity and photoperiod cycle (i.e. the relative durations of the light and dark periods) are crucial factors in determining algal growth rate, especially for photoautotrophic cultures [32, 225]. Inefficiencies arise when microalgae are exposed to light intensities above the saturation limits, as a result of photo-inhibition or overheating. Against this, at high algal cell densities commensurately higher light intensities are required to ensure light penetration through the bulk of the culture [33].

Microalgal PBR processes are thus more complex than classical biological treatment processes and present a number of challenges for control and optimization. Mathematical models are thus needed which are capable of quantifying the impact of practical system parameters such as bioreactor configuration, CO_2 mass transfer, carbon and nutrient uptake and water quality (pH, temperature, etc) on microalgal growth. The mass transfer coefficient is primarily a function of the hydrodynamic properties of the system [77, 226]. Whilst, CO_2 uptake is known to increase with increase mass transfer coefficient [227], it is not obvious as to whether mass transfer – which informs the optimum CO_2-liquid contact time, reported to be up to 23 hours for a column PBR [226] – provides the primary limitation in a large scale process.

2.11 Optimization of cultivation conditions

The complexity of the MCT process demands extensive experimentation to allow quantification of the impacts of all the key parameters. An alternative to the classical factorial-based approach is the use of statistical experimental design both to reduce the number of tests in identifying synergistic relationships and optimum conditions. For instance, to optimise the system for just five of the key variables for a single algal species and reactor configuration,

based on just three parameter values and a classical n-factorial approach, would demand 243 (i.e. 3^5) individual experiments.

Box Behnken Design (BBD), while developed in the early 1960s [228], has only recently been employed for algal bioreactor optimisation specifically [229] and MCT generally, in particular relating to lipid or biofuel generation [230, 231]. BBD combined with response surface methodology (RSM) permits a significant reduction in the number of experiments, whilst still enabling synergies between the different parameters to be identified along with the optimum set of conditions [232]. It is therefore provides an elegant and efficient approach for elucidating inter-relationships for complex, multi-parameter systems, such as PBRs, and has also been successfully demonstrated for various engineering applications [6, 233], including the optimization of water treatment processes [234, 235].

2.12 Summary

The recent literature related to the application of microalgae culture technology (MCT) to both prospective CO_2 biofixation and nutrient from wastewater has been summarized with reference to (a) photosynthesis process principles and algal cultivation conditions, (b) carbon dioxide sequestration strategies, and (c) wastewater treatment. The influence of the key system parameters on the algal PBR performance with reference to both CO_2 fixation and macro and micro nutrient has been appraised using photobioreactor (PBR) configuration, wastewater characteristics, and general process operating conditions. Factors such as light intensity and distribution, CO_2 mass transfer and nutrient balancing have been discussed in detail. The MCT process has been compared with the main alternative methods used for nutrient removal from wastewater.

Most of the published nutrient optimization studies have focused on algal growth rate. None appear to have combined algal growth optimisation with that of nutrient removal from the wastewater, nor considered the impacts of influent gas CO_2 concentration, light intensity and temperature on the algal growth parameters. Notwithstanding the ostensibly scientific studies in the MCT research area, the main constraint to more widespread implementation of the technology remains a substantially economic one – as recognised in the most recent review of this aspect [317]. The economic viability is potentially driven by the combined gaseous CO_2 and aqueous nutrient abatement/assimilation in a single process technology where added value is provided by the stream which would usually be considered a waste in a conventional wastewater treatment process. It is this aspect that has precipitated the research, the objectives and the related prospective research outputs significance as outlined in Sections 1.2 and 1.3 respectively. Further advancement of the technology demands more rigorous process

optimisation expedited by appropriate statistical experimental programme design methods and encompassing all process parameters germane to the dual CO_2/nutrient abatement process objective.

Chapter 3

Research Methodology and Analytical Techniques

3.1 Introduction

This chapter provides the comprehensive research methodology employed for the study, including the experimental setup and analytical techniques used. This includes:

- the medium preparation, pre-culture process and algal stock culture preparation;
- the design of the bench-scale photobioreactors (PBRs), including the gas supply providing the CO_2;
- the origin and sampling of the wastewaters used as feedstock for some of the studies;
- the software used for the Box Behnken Design of the experimental programme and the processing of the data produced from the experimental test programme.

3.2 Materials

3.2.1 Cultivation media

The standard growth medium (MLA, *Marine labs American society of microbiology-derived medium*) used for inoculation and cultivation is substantially modified from ASM-1 medium [236]. The MLA medium consists of the following components (in mg L^{-1}): $MgSO_4 \cdot 7H_2O$ 49.4; $NaNO_3$ 170; K_2HPO_4 34.8; H_3BO3 2.47; vitamin B_{12} 0.05×10^{-3}, thiamine HCl 0.1; biotin 0.05×10^{-3}; Na_2EDTA 4.56; $FeCl_3 \cdot 6H_2O$ 1.58; $MnCl_2.4H_2O$ 0.36;$CuSO_4 \cdot 5H2O$ 0.01; $ZnSO_4 \cdot 7H_2O$ 22×10^{-3}; $CoCl_2 \cdot 6H_2O$ 0.01; $NaMoO_4 \cdot 2H_2O$ 0.006; $NaHCO_3$ 16.9; $CaCl_2 \cdot {}_2H_2O$ 29.4. The concentrations of both $NaNO_3$ and K_2HPO_4 in the standard medium were varied to accommodate different concentrations of *TN* (0-56 mg L^{-1}) and *TP* (0-19 mg L^{-1}).

All the analytical grade chemicals used to prepare the MLA were purchased from (Sigma-Aldrich Pty Ltd, Australia) and (Chem-supply, South Australia). A variety of fully sterilized glassware items (e.g., bakers, Erlenmeyer flasks, cylinders, spatulas, funnels, filter holders and burets) were used in preparing the cultivation media (Chemical Engineering laboratories, Curtin University, Australia). The laminar fume-hood (HWS Series, CLYDE-APAC, Australia) used to house the equipment was regularly cleaned using 70% ethanol. Stock solutions and cultivation media were contained in autoclaved Schott bottles (1.2 L) and stored at 5 ℃ until used.

3.2.2 Wastewater

Three different wastewater qualities were used for microalgae cultivation. Primary wastewater (P_{WW}) and secondary wastewater (S_{WW}) were collected from Beenyup municipal wastewater treatment plant (WWTP), Western Australia. P_{WW} samples were taken from the outlet of the Primary Clarifier. S_{WW} samples were withdrawn from the outlet of the secondary clarifier before the disinfection unit. Petroleum effluent (P_E) was collected from BP Kwinana Refinery in Western Australia. P_E samples were taken from the outlet of the dissolved air flotation (DAF) unit and before the biological treatment unit (BTU). The wastewater effluent samples were immediately filtered using 0.2 µm nylon microfilters and were then autoclaved at 120°C for 15 minutes (Floor Autoclave, LABEC, Australia). Samples were then characterized before conducting the experiments to obtain the chemical and physical properties (Table.3.1). Finally, the prepared samples were placed in fully sterilized Schott bottles and stored at 5 ℃ for further experimentation.

3.2.3 Microalgae

The green algae *Chlorella vulgaris* (strain: CCAP 211/11B, CS-42) was supplied by Australian National Algae Culture Collection/CSIRO Microalgae Research and cultivated in Curtin University, Department of Chemical Engineering.

The *Chlorella vulgaris* sample was inoculated in a 250 mL Erlenmeyer flask contained 150 mL of autoclaved MLA medium at 10% concentration. The microalgae cells were cultivated in a shaker incubator (Bench Top Orbital Shaker, LABEC, Australia) at 200 rpm and 20℃ under continuous illumination of white fluorescent light at 50 μE for three weeks inside incubator refrigerator (Temperature Cycling Chamber, LABEC, Australia), and periodically shaken by hand to prevent the microalgae adhering to the inside surface of the glass.

Sub-culturing, inoculation, sampling and medium transfer were carried out in Laminar Flow Workstation (HWS Series, CLYDE-APAC, Australia) supplied with UV-light sterilization and surfaces were cleaned with 70% ethanol. Algal media and flasks were all sterilized at 120°C for 15 minutes.

3.2.4 Bubble column photo-bioreactors

A set of five cylindrical glass columns photo-bioreactors (PBR), each with a total volume of 350 mL (ID = 4 cm) for a single PBR used for algal cells cultivation (Fig. 3.1). The PBR constructed material is Gallium Lanthanum Sulphide Glass (GLS 80) [237], which is widely used in manufacturing the laboratory SCHOTT bottles, as high transparency material, resist

for chemical, temperature and pressure. Quick – release autoclavable polypropylene screw cap allows the PBRs to be easily opened and closed. The 40 mm wide neck facilitates easy and safe changing and removal of liquid and algal culture. The wide neck also makes cleaning the PBR particularly easy. The working volume of the reactor was 250 mL and the volume ratio illuminated surface/ volume (S/V) was designed to be equal to 100 m^{-1}.

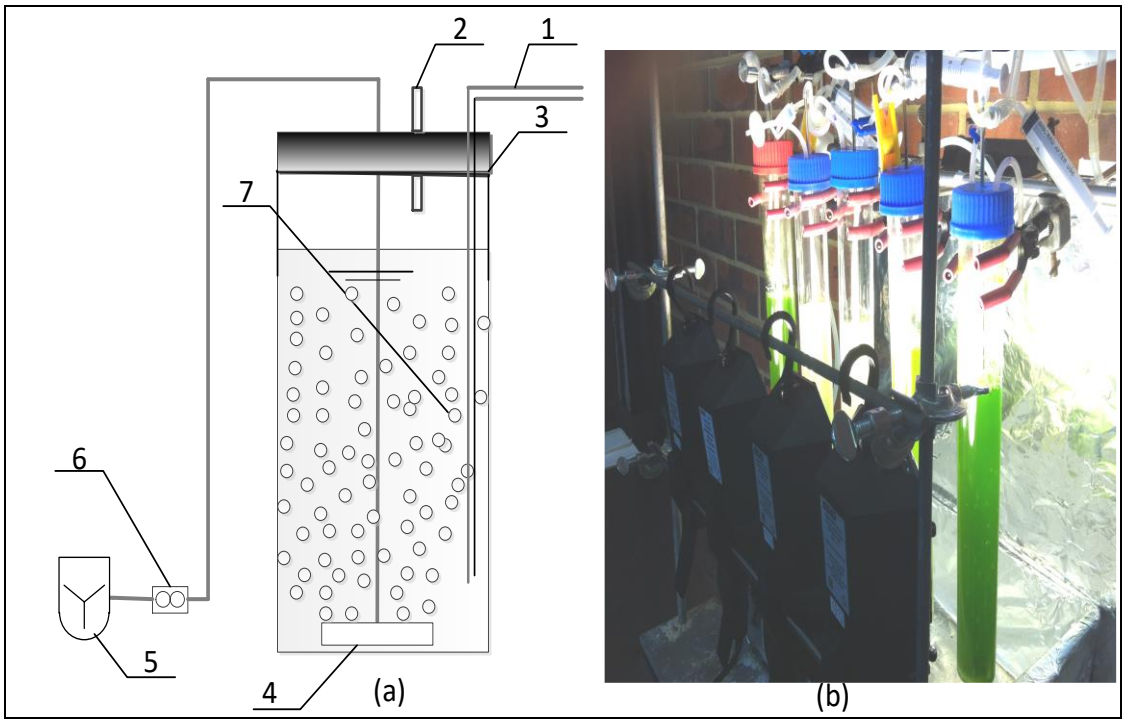

Figure 3.1 (a) Schematic diagram of a single bubble column photobioreactor: ((1) sampling port, (2) gas outlet, (3) polypropylene screw cap, (4) gas sparger, (5) Ari-CO_2 mixtrue system, (6) flowmeter, (7) gas bubble, and (b) photo of the experimental set-up.

The PBR was equipped with an aeration system comprising an air-CO_2 mixture fed to a gas inlet port. The gas was injected into the bottom of the PBR through a ring sparger (a silicon tube) placed horizontally in the bottom centre of the reactor to ensure culture was bubbled continuously with filtered air (PTFE, Merckmilipore, Germany). Ports in the head of screw cap provided access for sampling tubes, air spargers, and exhaust gases. The PBRs were affixed vertically to ensure efficient light penetration through reactors.

3.3 Methods

3.3.1 Typical cultivation and sampling procedures

To perform culturing in fully aseptic conditions, fresh medium were added to the PBR and then sterilised for 15 minutes at 121℃ in a steam pressure autoclave (Floor Autoclave, LABEC, Australia). Following autoclaving, the PBR was allowed to cool in the autoclave overnight so as to minimise the amount of precipitate that could from from the presence of sodium bicarbonate in the cultivation medium. The PBR was then connected to the aeration system and inlet gas tube, humidifier, and rotameters were all connected. Prior to every experimental run, a sub culture of inoculum was prepared. Inoculation was performed by aseptically transferring the stock culture to the bioreactor according to a 1:10 standard ratio of culture to inoculum. Samples were taken for further analysis directly after inoculation and subsequently daily. A sample of the stock culture was also taken and analysed to measure the biomass concentration (i.e. cell density). Temperature, pH, aeration rate and CO_2 concentration in the inlet and outlet streams were monitored regularly.

3.3.2 Gas mixture

The culture were aerated continuously with filtered air (0.03 % CO_2) using a set of high performance output pump of 125 L h^{-1} (Marina 300 pump, Hagen, Canada). The air follow rate was continuously calibrated (MINI - Buck CALIBRATOR, A.PBUCK, incorporated Orlando, Florida, USA) and controlled by air-flow meter (InFulx, DUFF and M MACINTOSH, Australia). Pure CO_2 was supplied by BOC (British Oxygen Company, Ltd.) at a purity of >99 %, <50 ppm moisture, <20 pmm hydrocarbons (as methane), <20 pmm oxygen, 0.5 pmm sulphur compounds, and <0.5 pmm nitrogen oxide. Air enriched with different CO_2 concentrations (0.03-22%) were adjusted by digital mass flow controllers (MC-100SCM, Cole-Parmer, USA). The corresponding air-CO_2 flowrates was compressed though a coil of PVC rigged pipe to ensure sufficent time for homogenous mixing. The gas mixture was then passed through a humidifier before entering the PBR to prevent water evaporation from the microalgae culture (Fig. 3.2).

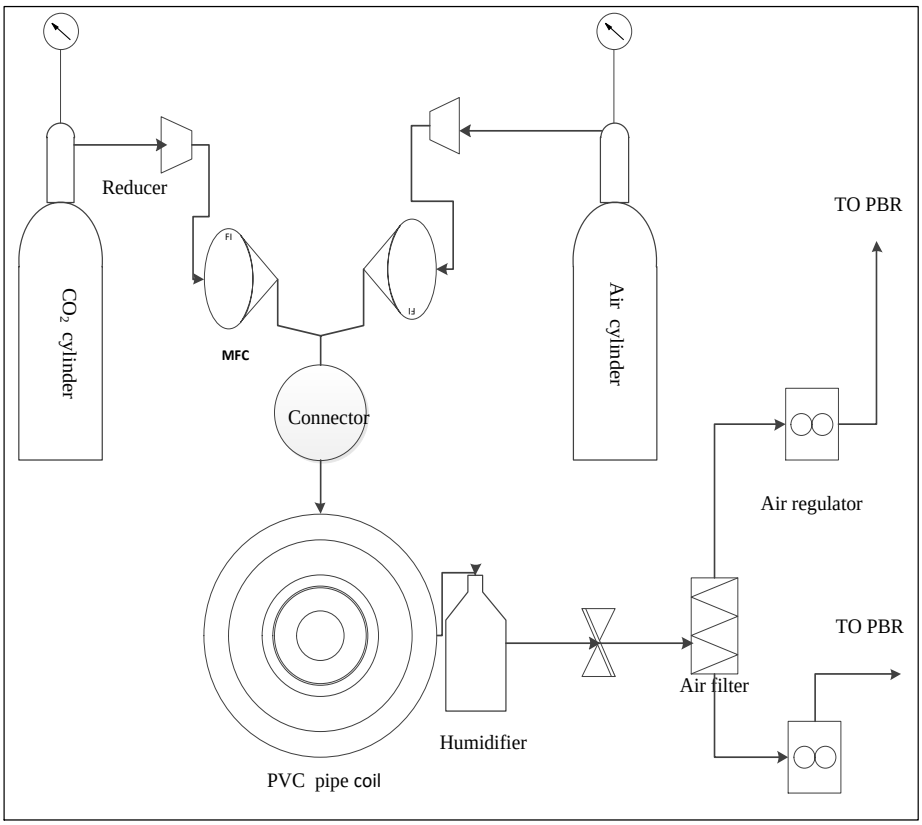

Figure 3.2 Air – CO_2 mixture system.

3.3.3 Illumination system

The cultivation temperature was thermostatically maintained at 24 ± 2 ℃ (Thermal Anemometer, Testo, USA). Continous illumination at a light intensity between 180 and 400 µE m^{-2} s^{-1} was provided by eight LED lamps each rated at 10W. The light intensity was measured using a light meter (LI-250A, LI-COR, US & Canada) which could be connected either to a Quantum Sensor (LI-192SA, LI-Core Inc., US& Canada) or spherical underwater sensor (US-SQS, WALZ, Germany). Both number of LEDs and the distance from the surface of PBR were adjustable, to permit a range of various light intensities to the PBR.

3.4 Analysis, algal cells

3.4.1 Optical density measurement

The optical density (OD) of the extracted samples was measured using a UV-Vis spectrophotometer (Jasco *V-670*). The maximum absorbance was observed at 680 nm over the spectral range of 400-700 nm measured. All cell concentrations were thus determined in terms

of the OD at this wavelength (Fig. 3.3). Culture samples were diluted with distilled water prior to OD measurements to ensure the spectrophotometer measurements were between 0.1-0.9, and all measurements carried out in triplicate.

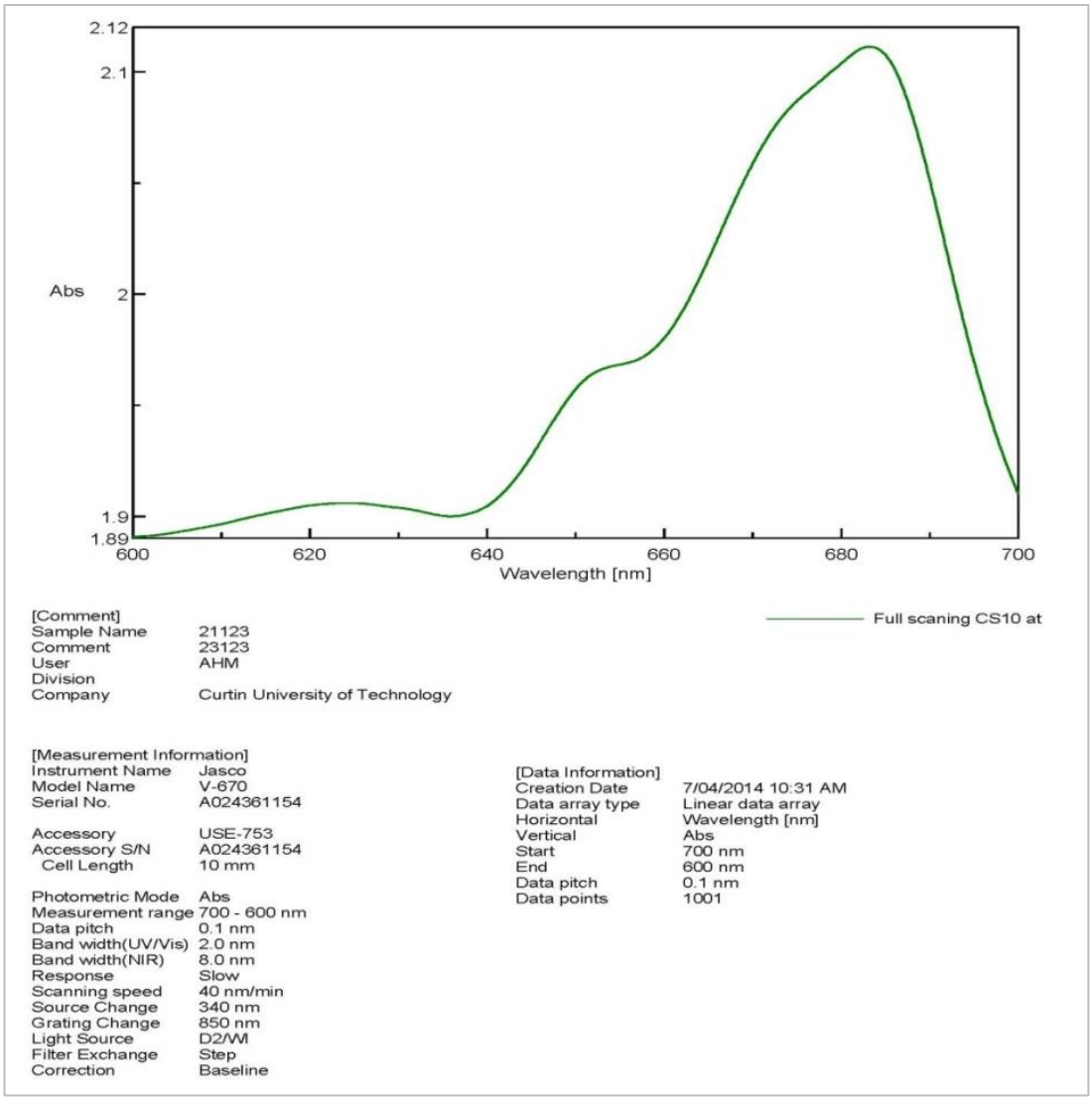

Figure 3.3 Biomass absorbance.

3.4.2 Algal dry weight determination

10 mL of the microalgae samples were filtered using pre-weighted glass filter then oven-dried at 80 ℃ for 12 hours before being stored in a vacuum desiccator and re-weighted for calculating the dry weight of biomass. Calibration revealed the correlation between the biomass concentration X in g L^{-1} and OD at 680 nm (OD_{680}) to be given by:

$$X\ (g\ L^{-1}) = 0.35\ OD_{680} - 0.002\ (R^2 = 0.99) \quad \textbf{(3.1)}$$

The specific growth rate μ was then calculated from the initial (X_0) and final biomass concentration (X_t). according to:

$$\text{Specific growth rate}, \mu\ (d^{-1}) = \ln(X_t - X_o)/(t - t_o) \quad \textbf{3.2)}$$

Biomass productivity, P_X was calculated using the equation:

$$\text{Biomass productivity}, P_X\ (g\ L^{-1}d^{-1}) = \frac{X_t - X_0}{t} \quad \textbf{3.3)}$$

3.4.3 Cell number

Microalgal cells were enumerated by placing a 10 µL sample in a Marienfeld Thoma counting chamber, the chamber then being placed under light microscope at ×40 magnification (ACHRO 40X/0.65, Saxon, New Zealand). The number of cells was counted in 9 large squares of Thoma chamber, each measuring 16 × 0.0025 mm^2 with total area of 0.04 mm^2. An average number of cells was counted per small square. This value was substituted into the formula $D = a \times [1/(0.1 \times 0.2 \times 0.2 \times 1000)] \times 2500$ where D is the number of cells in 1 ml, a the cells counted. The ideal number of cells are between 30 to 70, since algal cells need to be sufficiently dispersed to ensure the cells distribute uniformly and can be counted accurately.

3.4.4 Microalgae carbon content analysis

Algal cells were harvested by centrifugation at 5000 rpm for 15 min (C-28A, BOECO, and Germany) and the supernatant decanted. The cell pellets were washed with distilled water and then freeze-dried at -50 ℃ for 15 hrs (Alpha 2-4 LDplus Laboratory Freeze Dryer, Christ, and Germany). The carbon percentage (%C) in samples was measured using elemental analyser (CHNS/O analyser, PerkinElmer, USA), and the CO_2 bio-fixation rate R_C in g L^{-1} d^{-1} determined from:

$$R_C\ (\text{g L}^{-1}\text{d}^{-1}) = \%\text{C} \times P_x \times M_{CO2}/M_C \quad \textbf{(3.4)}$$

where, P_X, M_{CO2} and M_C are the biomass product molecular weight of CO_2 and Carbon respectively.

3.4.5 Dry method lipids content analysis

The total lipids were extracted from freeze-dried algal biomass using a method modified from that of Blight and Dyer [238]. Appropriate solvents were selected for extraction of lipids from the samples, and the solvents evaporated and the retained material measured as lipids content

[239]. 50 mg of lyophilized algal biomass was placed in a 15 mL test tube and mixed with a 2:1 chloroform-methanol solvent. The mixture was then ultrasonically treated at 0.4 W mL^{-1}, with a pulse of 55/5 and an amplitude of 90%, at 20°C for 10 minutes (Vibra cell, Sonic Materials, USA). The chloroform-methanol phase containing the extracted lipids was then centrifuged (C-28 A, BOECO, Germany) to separate liquid mixture and cells debris, then separated and the solvent removed using a vacuum rotary evaporator (R-201, Rose Scientific Ltd, Canada) at 5 psi pressure and temperature of 70°C.

The lipids productivity (P_{lipid}) was calculated from [240]:

$$Lipids\ productivity, P_{lipid}\ (\mathrm{mg\ L^{-1}\ d^{-1}}) = \frac{X_{\max} \times Y(\%)}{V \times t} \quad \textbf{3.5)}$$

where X_{max} is the cumulative microalgae biomass produced (g), V the working volume (L) and t the cultivation period. Y, the %lipids content, was obtained quantitatively from lipids density and algal biomass according to the following equation [241]:

$$Y(\%) = \frac{\text{Weight of extracted lipid}}{\text{Weight of biomass}} \times 100 \quad \textbf{3.6)}$$

3.5 Analysis, wastewater

All wastewater analyses were generally carried out according to standard methods [242].

3.5.1 *TN* and *TP*

Total Nitrogen (*TN*) and Total Phosphorus (*TP*) concentrations in the liquid samples were determined colorimetrically using HACH test kits (DR/890 Colorimeter, HACH, USA). The sample was 0.45 μm-filtered to separate the algal cells using. For *TN* identification, alkaline persulfate digestion was used to convert all nitrogen to nitrate. Sodium metabisulfite was then added after digestion to eliminate halogen oxide interference. The nitrate was then reacted with chromotropic acid (under strongly acidic conditions to from a yellow complex with an absorbance peak near 420 nm, measureable colorimetrically. For *TP* analysis, phosphates present in organic and condensed inorganic forms (meta-, pyro- or ortho) were converted to reactive orthophosphate prior to analysis. The sample was then pre-treated with heated acidified persulfate so as to provide the conditions for hydrolysis of the condensed inorganic forms, organic phosphates being converted to orthophosphate [243]. Methods for both N and

P were adopted from standard methods, code #10072 and 10127 respectively in the analytical procedure of the DR/800 instrument.

3.5.2 Chemical oxygen demand (COD)

A DR/890 HACH spectrophotometer was used to measure COD following the standard procedure of sample digestion (Method #8000). The COD in mg L^{-1} is defined as the mg of O_2 consumed per litre of sample under prevailing oxidation conditions, comprising heating for two hours in potassium dichromate. Oxidizable organic compounds react, reducing the dichromate ion ($Cr^2O_7^{2-}$) to green chromic ion (Cr^{3+}) and the Cr^{3+} produced is determined. Mercury ions are added to complex with chloride in the sample to limit its interference with the analysis.

3.5.3 TOC

Total organic carbon (TOC) and Total carbon (TC) were both determined using a Shimadzu TOC analyser (TOC-VCPH, Shimadzu, Japan) equipped with an inorganic carbon (IC) reaction vessel. Prior to sample injection, the 5 mL sample (5 mL) was filtered using a 0.45 µm PTFE membrane filter to separate the algal cells. The IC concentration was calculated by subtraction of total carbon from total organic carbon in the sample.

3.5.4 Macro and micro nutrients

Inductively coupled plasma optical emission spectrometry (ICP – OES) and inductively coupled plasma mass spectrometry (ICP – MS) (PerkinElmer, USA) were both used to determine the initial and final concentrations of micro nutrients (Ca^{2+}, S^{2-}, Mg^{+2}, K^{+1}) and macronutrients (As^{3+}, Ni^{2+}, Co^{2+}, Pb^{2+}, Zn^{2+}, Cu^{2+}, Mn^{2+}, Fe^{3+}, Cd^{2+} and Se^{2-}) in P_{WW}, S_{WW}, P_E and MLA liquid samples. For ICP – OES the respective emission wavelengths for each element were Ca 317.933 nm, S 181.975 nm, Mg 285.213 nm, and K 766.490 nm. An internal litium standard added to all samples and standards was used to account for non–spectral inferences. 5 ml samples were taken from each PBR at the beginning and end of each experiment and then 0.45 µm-and acidified with 1% nitric acid prior too measurement to assist nebulizing. All reagents and standards were used of "HIGH- PURITY STANDARDS". Higher concentrations standard of (Ca, S, Mg, K, As, Ni, Co, Pb, Zn, Cu, Mn, Fe, Cd, Se) (1000 µg mL^{-1}, initially diluted in 0.02 HNO_3) was diluted to the required concentrations using high purity deionized water. All results obtained in triplicate, then averaged.

3.6 Coloured tape (CT) light filter

CT of different colours (blue, white, green, yellow, and red) was used to filter the light (Fig 3.8, a- e). CT spectral characteristics were obtained from spectra analysis software (Jasco V-670, JASCO Corporation, Japan), to produce illumination with corresponding wavelength mainly in the visible range. This implies an associated reduction in energy (i.e. longer wavelengths) from that of the incident white light. The filtered light intensities inside the PBRs were then measured using light meter equipped with spherical sensor. The CTs were subsequently directly wrapped around the PBRs to select the appropriate irradiated light wavelength range (Fig. 3.4).

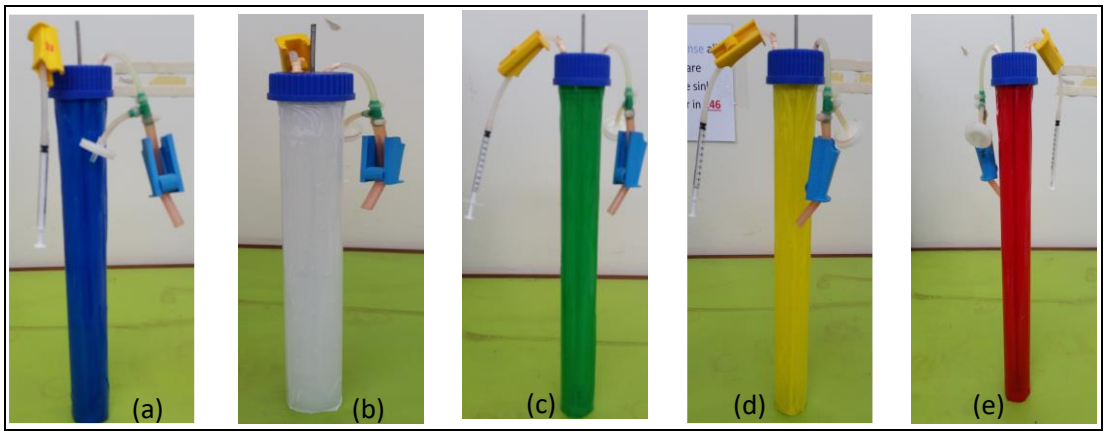

Figure 3.4 Wrapped PBRs with different colored tape: (a) blue (CT_B), (b) white (CT_W), (c) green (CT_G), (d) yellow (CT_Y) and (e) red (CT_R)

3.7 Experimental design and data processing

3.7.1 Background

Response surface methodology (RSM) provides a useful and increasingly employed tool for reducing the number of experimental tests required to achieve a result. The key objective of RSM is to optimize the response (or measured impacted parameter or dependent output variable) surface influenced by several independent input parameters. RSM also identifies the relationship between the controllable input parameters and the response variable. The statistical method calculates the influence of changes in the selected parameter and their mutual interactions on the process through a specific experimental design. The three systematic steps used in the statistical experimental design and optimisation are (i) statistical design of experiments, (ii) estimation of coefficient of a mathematical model using experimental data and (iii) analysis of model applicability and mathematical optimisation which verified by experimental data.

A common method used to design experiments is Box Behnken Design. BBD employs a matrix of tests based on a number of parameters. The impact of each parameter is evaluated by selecting three or more values (or "levels") of these parameters and then conducting tests which encompass every combination of each parameter value. The results of the experiments in terms of the response parameter(s) can then be evaluated through a statistical model [232]. In the case of a three-level, three-parameter system, which would demand 27 individual tests for an experimental programme based on classical factorial experimental design, the number of tests required is 15. This was the case in the current study, where two such BBD matrices were created to examine the synergistic relationships between these sets of three parameters within specific limits. The output of the statistical model is second order polynomial featuring terms – 10 in all - in all the parameters and their combinations [235]. The response values from the 15 experiments determine the 10 coefficient values in the polynomial.

3.7.2 Statistical experimental programme

In this study, Box Behnken Design (BBD) was employed to optimize the cultivation process and investigate the interactive effects of initial concentration of total nitrogen (TN), total phosphorus (*TP*), total carbon (*TC*), CO_2 gas concentration ($C_{c,g}$), light intensity (I) , and temperature (T) on the system performance. A multi-level, three-parameter matrix was employed to examine the synergistic relationships between the input parameters as follows:

(a) μ in d^{-1}, biomass productivity P_X in g (dry weight) biomass L^{-1} d^{-1}, CO_2 capture (R_C), as a function of feed $C_{c,g}$ (X_1) , I(X_2) , and T (X_3), and,

(b) Nutrient removal (% *RE TN* and *TP*), as a function of feedwater composition with reference to *TN* (X_1), *TP* (X_2) and total carbon ((*TC*), X_3).

The 15 experimental runs were randomly sequenced in duplicate to reduce the effect of the temporal-related errors. *JMP* statistical discovery software (SAS v11.2.1) was used to complete the regression analysis and generate the graphical relationships. The variability of the factors was expressed as coefficient of determination (R^2) values. The model equation was then used to identify the interaction between the variables within the specified experimental boundary conditions. To identify the maximum conditions of the selected responses were through maximising the desirability function in Derringer's desired function (DDF) methodology [244].

3.7.3 Regression analysis

The experimental results were fitted with the quadratic model by multiple regression analysis for predicting the optimum values were derived according to the following equation:

$$Y=\beta_o + \sum_{i-1}^{k} \beta ii x_i^2 + \sum_{i-1}^{k-1} \sum_{j-i+1}^{k} \beta Xi + \varepsilon \quad \textbf{(3.7)}$$

where Y is the response variable; i and j are the index number for the patterns; β_o is the constant coefficient; β_i , β_{ii} and β_{ij} are the coefficient for linear, quadratic, and interaction influence, respectively; x_i and x_j are the variables to be studied, the coded variables are defined as:

$$x_i = \frac{Xi - Xo}{\Delta Xi} \quad \textbf{(3.8)}$$

where x_i is the coded value of the independent variables, X_i is the actual value of the independent variable, X_o is the actual value of the factor at the centre point, and ΔX_i is the step change value.

All error bars on graphs were determine as standard deviation.

Chapter 4

Influence of the wastewater quality on the performance of *Chlorella Vulgaris*

4.1 Introduction

Municipal and industrial wastewaters require treatment for removal of organic carbon and nutrients (nitrogen, N and phosphorus, P) prior to discharge. Photobioreactors (PBRs) using microalgae present a potentially economically viable alternative to conventional aerobic biological methods for wastewater treatment [245], since they offer the potential of alternative resource recovery and recycling options which can offset some of the operational costs [140]. Microalgae have attracted considerable attention for this duty, with reference to their capability for bulk nutrient (N and P) removal (Table 4.1), combined with simultaneous CO_2 capture [101]. As well as these bulk nutrients, other macro nutrients and micro nutrients, the latter commonly regarded as micropollutants, are also assimilated during algal growth (Table 4.2). These include calcium (Ca^{2+}), magnesium (Mg^{2+}), potassium (K^{+}), sodium (Na^{+}), sulphur (as SO_4^{2-}), the heavy metals manganese (Mn^{2+}), molybdenum (Mo^{2+}), copper (Cu^{2+}), iron (Fe^{2+}), zinc (Zn^{2+}), and nickel (Ni^{2+}), and – for some algal species – boron (as B, borate), silicon (Si, as silicate), cobalt (Co^{2+}), iodine, vanadium and selenium (Se^{2-}) [4]. Some micro-nutrients may be added to commercial algal cultures together with a chelating agents such as EDTA [104, 246] to sustain algal growth. Algal biofilm reactor was also suggested as an integrated system for rural wastewater treatment with simultaneous biomethane, biomass and bio fertilizer production [247]. The study confirmed that the biomass productivity achieved was 4 g m^{-2} d^{-1} using livestock wastewater. Choudhary et al. [248] investigated 9 native microalgae consortia for biomass production and nutrient removal from rural wastewaters for bioenergy applications. all the investigated consortia showed 80–100% reduction in nutrient from the tested wastewaters under controlled conditions, and the maximum biomass concentration of 1.93 g/l was achieved in livestock wastewater which was higher than that produced in the standard medium (BG11) (1.17 g/l). Prajapati et al. [249] pointed out that *Chroococcus sp.1* cultivated in neat livestock wastewater is the best for biomass production under controlled (2.13 g L^{-1}) and outdoor conditions (4.44 g L^{-1}) with >80% of nutrients removal.

Whilst bulk nutrient removal capability of PBRs has received attention (Table 4.1), attaining consistent removal efficiency (% *RE*) values so as to meet the increasingly wastewater discharge standards remains a challenge. Moreover, the capability of PBRs for micro-nutrient removal has received little attention (Table 4.2), despite the increasing focus on the fate of micropollutants and their abatement in wastewater treatment processes.

Table 4.1 Reported *Chlorella vulgaris* algal growth parameters with nutrient removal efficiency for various wastewaters

PBR = Photobioreactor; PBR_C Continuous system, PBR_s semi continuous, otherwise batch system; ww =wastewater; SAnMB = effluent of a submerged anaerobic membrane PBR; MPBR = membrane PBR; $BMPBR_C$

WW	*System*	X_{max}, *g* L^{-1}	C_d, *cells* mL^{-1}	*Inlet* CO_2 $C_{c,g}$, %v/v	P_x, *g* L^{-1} d^{-1}	CO_2 *fixn. rate,* R_c *g* $L^{-1}d^{-1}$	μ, d^{-1}	TP_{in}, *mg* L^{-1}	TN_{in} *mg* L^{-1}	COD_{in}, *mg* L^{-1}	*N/P, ratio*	RE *TP, (%)*	RE *TN, (%)*	RE *COD, (%)*	*pH, value*	*HRT,* d^{-1}	*Refs*
Artificial	PBR_B	1.98 ±0.1	nr	2	0.32±0.1	0.56	0.13	nr	nr	nr	nr	nr	nr	nr	4.5	nr	[106]
Piggery	PBR_B	0.49 ±0.2	nr	nr	0.02	0.04	nr	13.5±0.6	56±2	nr	4.1:1	18	49	nr	nr	nr	[87]
Artificial	PBR_s	nr	6.4×10^6	nr	nr	nr	0.377	~0.57	~23		46:1	70.2	74.3	nr	7.2	nr	[85]
Sww		nr	5.3×10^6	nr	nr	nr	0.186	~0.57	~22	nr	46:1	80.3	60.1	nr	nr	nr	
SAnMBR	PBRs	0.595	nr	nr	0.23	0.41	0.66± 0.1	5.1-10.5	52.3	nr	5:10	97.8	67.2	nr	7.2	2	[107]
Synthetic	PBR_B	0.2	nr	0.03[a]	0.03	0.05	0.59	1.69-2.17	7.48-22.1	nr	9.7:12.9	>95	>95	nr	nr	5	[108]
Aq_{WW}	$MPBR_C$	0.04	nr	0.03[a]	0.04	0.07	0.17	0.42	6.81	nr	16.2:1	82.7	86.1	nr	nr	1	[109]
Domestic	MPBR	0.2-0.75	nr	0.03[a]	0.06	0.1	0.17	1.69-2.17	7.48-22.1	nr	15.5:22					2 - 5	
Sww	MPBR	0.95	nr	4	0.04	0.08	nr	0.8	15	5	18.75:1	85 ± 3	64 ± 6	nr	6.8-7.5	2	[89]
	$BMPBR_C$	1.37	nr	4	0.07	0.12	nr					86 ± 2	83 ± 4				
Mww	VFPPBR	nr	6.3×10^6	0.03[a]	nr	nr	1.39	1.8	12	nr	6.6:1	>99	>99	nr	nr	60	[110]
Sww	PBR	0.64	nr	5	0.03	0.06	0.11	0.64	10.04	nr	15:1	53.8	49.6	nr	7.2±0.2	nr	[111]
Pww	EF	2.71	nr	0.03[a]	0.09	0.17	0.61	10	40.8± 0.4	242±2	4.1:1	35.2	60.2	40	7.86	nr	[112]
Sww		1.86	nr	0.03[a]	0.06	0.11	0.52	26	44±0.2	59±0.5	2.4:1	11.9	55.9	30	7.53		
Cww		2.37	nr	0.03[a]	0.08	0.14	0.25	200	130±2	601±4	0.7:1	25.9	33.6	61	4.86		
Artificial	CYPBR	0.62	nr	nr	0.15	0.27	0.69	nr	90	100	nr	nr	nr	15.2	nr	nr	[113]
Urban		0.36	nr	nr	0.09	0.15	0.33	nr	90		nr	nr	nr	77.6	nr		

= Biofilm membrane PBR; OMPBR = Osmotic membrane PBR; VFP= Vertical flat-plate PBR; C_{ww}= Centrate wastewater; EF= Erlenmeyer flask; *Mww*= Municipal wastewater; CYPBR= Cylindrical PBRs; Aq_{WW} Aquaculture wastewater; HRT = hydraulic residence time, [a]Atmospheric level, *Rc* = CO_2 fixation rate which estimated from Chisti ratio: $CO_{0.48}H_{1.831}N_{0.11}P_{0.01}$; $Rc = 1.88 \times P_x$, P_x = biomass productivity which estimated from $\Delta X/\Delta t$, Not reported= nr.

Table 4.2 Reported *Chlorella vulgaris* algal growth parameters with Macro and Micro nutrient removal efficiency for various wastewaters.

Macro, Micro Nut.	***WW***	***System***	***X_{max}, g L^{-1}***	***C_d, cells mL^{-1}***	***Inlet CO_2 $C_{c,g}$, %v/v***	***P_x, g L^{-1} d^{-1}***	***CO_2 fixn. rate, R_c g $L^{-1}d^{-1}$***	***μ, d^{-1}***	***TP_{in}, mg L^{-1}***	***TN_{in} mg L^{-1}***	***N/P, ratio***	***COD_{in}, mg L^{-1}***	***Mac_{init} (mg L^{-1}), Mic_{init} (μg L^{-1})***	**RE *TP, (%)***	**RE *TN, (%)***	**RE *COD, (%)***	**RE *Mac, Mic (%)***	***pH, value***	***HRT, d^{-1}***	***Refs***
Macro nutrient																				
Ca^{2+}	*Mww*	VFPPBR	nr	6.3×10^6	0.03[a]	nr	nr	1.39	1.8	12	6.6:1	nr	35.3	>99	>99	nr	19.6	nr	60	[110]
S^{2-}	*STWW*	BCPBR	0.8	1.6×10^7	nr	0.2	0.35	nr	17.2	10	1.72	nr	66.6	100	100	nr	nr	8	3.3-3	[250]
Mg^{+2}	*MBM*	SF	1.8	nr	0.7-2.1	0.18	0.31	nr	53.1	41.2	0.77	nr	7.4	nr	nr	nr	70	nr	10-50	[251]
K^{+1}	*PLA*	GBCPBR	1.3	nr	0.03[a]	0.11	0.13	nr	5.32	75	14	nr	13.3	40	100	nr	13	7	nr	[252]
Micro nutrient																				
As^{3+}	*SWW*	EF	nr	8.3×10^5	nr	nr	nr	nr	0.36	7.08	19.4	nr	2.65±0.1	82.2	92.3	nr	<50	nr	nr	[253]
Ni^{2+}	*SWW*	EF	nr	8.3×10^5	nr	nr	nr	nr	0.36	7.08	19.4	nr	6.21±0.2	82.2	92.3	nr	<50	nr	nr	
Co^{2+}	*SWW*	EF	nr	8.3×10^5	nr	nr	nr	nr	0.36	7.08	19.4	nr	0.82±0.0	82.2	92.3	nr	<50	nr	nr	
Pb^{2+}	*SWW*	EF	nr	8.3×10^5	nr	nr	nr	nr	0.36	7.08	19.4	nr	1.03±0.13	82.2	92.3	nr	<50	nr	nr	
Zn^{2+}	*Mww*	VFPPBR	nr	6.3×10^6	0.03[a]	nr	nr	1.39	1.8	12	6.6:1	nr	130	>99	>99	nr	100	nr	60	[110]
Cu^{2+}	*Dse*	$MPBR_c$	1.72	nr	4	0.05	0.089	nr	14.1±0.9	0.78 ±0.1	18.2	39.9±5	19	76.6	87.7	0	64.7	7.8	2	[254]
Mn^{2+}	*Dse*	$MPBR_c$	1.72	nr	4	0.05	0.089	nr	14.1±0.9	0.78 ±0.1	18.2	39.9±5	17	76.6	87.7	0	100	7.8	2	
Fe^{3+}	*Dse*	$MPBR_c$	1.72	nr	4	0.05	0.089	nr	14.1±0.9	0.78 ±0.1	18.2	39.9±5	153	76.6	87.7	0	100	7.8	2	[255]
Cd^{2+}	*C medium*	EF	nr	nr	nr	nr	nr	nr	nr	nr	nr	nr	0-152	nr	nr	nr	32.5-13.1	7.5	1.5	
Se^{2-}	*SW*	VPBRs	nr	nr	nr	nr	nr	nr	0.56-4.48	0.155	3.6-29	nr	695	nr	nr	nr	98±2	nr	2 to 1	[256]

Mac_{init}, Mic_{init}= Macro or Micro nutrients initial concentrations; SF = Shake flask; *MBM*= Modified 3N-Bristol medium; GBCPBR= glass bubble column PBR; *PLA*= Poultry litter Ash; *DSE*= Domestic secondary effluent; VPBR= Vessel PBR; *SW*= Seawater; TF= Triangular falsk; BG= Bristol's medium; *STWW*= Secondary -treated wastewater; BCPBR= 12 bubble -column type reactors with spherical bases; *C. medium*= Culture medium; *SWW*= Raw wastewater.

This study aims to address this knowledge gap with reference to one of the most commonly studied algal species (*Chlorella vulgaris*, *Cv*) along with the N and P in combination with a range of macro and micro-nutrients. Specifically, the influence of different wastewater quality on the growth rate and nutrient (macro and micro) removal capability of *Chlorella vulgaris* will be investigated.

The study encompassed both a standard growth medium (MLA) in combination with three wastewater sources (primary wastewater, P_{WW}, secondary wastewater, S_{WW}, and petroleum effluent, P_E), with impacts focused on algal growth and nutrient removal for batch operation.

4.2 Material and methods

4.2.1 Generic materials and methods

The algae strain and cultivation method is detailed in Sections 3.2.1, 3.2.3 and 3.3.1, and the sampling and analysis of the algal biomass given in Section 3.4.1-3.4.3. Details of the PBR bubble column design and the associated apparatus are provided in Section 3.2.4 and the operation in Sections 3.3.1-3.3.3. Wastewater characterisation methods are all detailed in Section 3.5 and comprised nitrogen and phosphorus spot tests (Section 3.5.1), COD (Section 3.5.2), TOC (Section 3.5.3) and spectroscopic methods for macro/micro nutrients (Section 3.5.4). Statistical analysis of data for significance was carried out using JMP statistical discovery software (SAS v11.2.1) based on one-way ANOVA, and results reported as mean ± SD.

4.2.2 Experimental design

Experiments were conducted in batch mode using four (350 mL) cylindrical glass columns of 4 cm internal diameter and a 250 mL working volume. 250 ml batches of sterilized media containing 100%, 75%, 50%, 25% V/V wastewater (P_{WW}, S_{ww} or P_E) to MLA were inoculated with 1 vol% pre-cultured *Chlorella vulgaris* to maintain an initial optical density (OD) of 0.06 at 680 nm. The culture was continuously fed with a flow of 50 mL min^{-1} filtered air, adjusted by digital mass flow controllers (MC-100SCM, Cole-Parmer, USA) at an ambient temperature of 24°C (Fig. 4.1). Unidirectional continuous illumination at a light intensity (I) of 180 µE was provided by adjusting the number of 4W LED lights, the intensity being measured by a light meter (LI-250A, LI-COR, US & Canada). A 5 mL sample was extracted daily for analysis, equating to a hydraulic and solids residence time of 50 days, and all runs lasted 10-13 days.

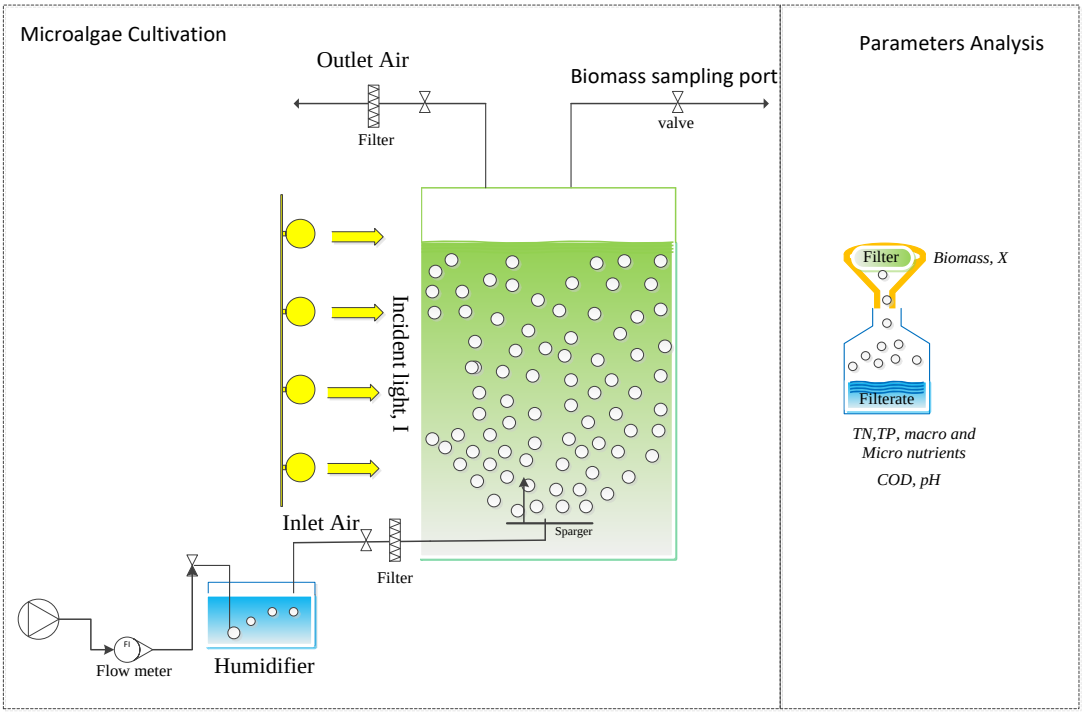

Figure 4.1 Schematic diagram of a single cylindrical photobireactor (PBR).

4.2.3 Wastewater origin and characterization

Primary wastewater (P_{WW}) and secondary wastewater (S_{ww}**)** were collected from Beenyup municipal wastewater treatment plant, Western Australia. Petroleum effluent (P_E) was collected from the BP Kwinana Refinery in Western Australia. P_{WW} samples were taken from the outlet of the primary clarifier, and S_{WW} samples from the outlet of secondary clarifier. P_E samples were taken from the outlet of the Dissolved Air Flotation (DAF) unit prior to the Biological Treatment Unit (BTU). The samples were immediately filtered using 0.2 µm nylon microfilters and autoclaved at 120°C for 15 minutes to ensure sterile conditions before analysis for the various constituents. Similarly, the cultivation media formed from mixing different volumetric ratios of P_{WW}, S_{WW} and MLA (0:100%, 25%: 75%, 50%: 50%, and 75%: 25%) of total 250 mL were characterized before and after each batch test for bulk, macro and micro nutrients, along with organic carbon and COD (Table 4.3).

4.3 Results and discussion

4.3.1 Wastewater nutrient characterization

The C:N:P ratio in the P_{WW} was found to be 110:4.6:1, somewhat higher in nutrient than previously reported figures [257]. In the case of S_{WW} the recorded ratio was ~8:2.1:1, indicating an unusually low OC content, and for the P_E sample it was 121:12:1, very close to a reported ratio of 78:11:1 [86]. Since reported *TN* and *TP* consumption rates have varied according to

the culture medium composition and initial nutrient concentrations (Table 4.2), nutrient balancing would appear to be as important in PBRs as in conventional wastewater treatment. An optimum N:P ratio of 8:1 has been proposed for *Cv* [220] .

Table 4.3 Wastewater and MLA composition

Nutrient	*MLA*	$P_{WWinit.}$ (%)				S_{WWinit} (%)				P_{Einit}
***Macro*, µg L^{-1}**		**100**	**75**	**50**	**25**	**100**	**75**	**50**	**25**	
Ca^{2+}	4.6	23	n.d	n.d	n.d	27	n.d	n.d	n.d	24
***S2*-**	6.5	21	n.d	n.d	n.d	17	n.d	n.d	n.d	42
Mg^{+2}	5.0	10	n.d	n.d	n.d	10	n.d	n.d	n.d	25
K^{+1}	16	26	n.d	n.d	n.d	26	n.d	n.d	n.d	21
***Micro*, mg L^{-1}**										
As^{3+}	0.0	1.1	n.d	n.d	n.d	0.7	n.d	n.d	n.d	17
Ni^{2+}	0.0	2.3	n.d	n.d	n.d	0.9	n.d	n.d	n.d	4.5
Co^{2+}	2.4	0.4	n.d	n.d	n.d	0.2	n.d	n.d	n.d	1.4
Pb^{2+}	0.0	1.1	n.d	n.d	n.d	0.3	n.d	n.d	n.d	0.0
Zn^{2+}	4.8	26	n.d	n.d	n.d	20	n.d	n.d	n.d	0.0
Cu^{2+}	2.5	38	n.d	n.d	n.d	4.8	n.d	n.d	n.d	0.4
Mn^{2+}	84	8.2	n.d	n.d	n.d	6.3	n.d	n.d	n.d	4.0
Fe^{3+}	370	57	n.d	n.d	n.d	10	n.d	n.d	n.d	5.7
Cd^{2+}	0.0	0.1	n.d	n.d	n.d	0.03	n.d	n.d	n.d	0.0
Se^{2-}	0.8	39	n.d	n.d	n.d	40	n.d	n.d	n.d	102
Nutrients, mg L^{-1}										
TN	28	30.6	29	29	25	11.8	15.9	20	24.7	23
TP	6	6.6	5	5.1	5.8	5.6	5.7	5.8	5.9	1.9
COD	3	373	280	188	95.5	32	24.75	17.5	10.2	505
TOC	1.45	109.6	100.1	47	30.8	7.8	7.27	6.25	3.4	120.8
pH	6.9	9.3	9.4	9.5	9.5	8.9	9	9	8.9	9.3

n.d: not detected

4.3.2 Influence of wastewater quality on growth and macronutrient removal

Cultivation in MLA containing 25%, 50%, 75% and 100% P_{WW} revealed the growth rate to increase with increasing P_{WW} fraction with reference to the maximum biomass (X_{max}) and cell density (C_d) and specific growth rate (μ) (Fig. 4.2a). This would seem to reflect the considerably higher total carbon (*TC*) level of 137 mg L^{-1} in the P_{WW} compared with only 2.4 mg L^{-1} in MLA. COD removal efficiency values decreased from 33-34% down to 22% on decreasing the P_{WW} content from 75% down to 25%. The lowering of carbon removal is a consequence of the commensurate decrease in the organic carbon concentration, and reflects the energetic preference for dissolved carbon assimilation compared with CO_2 fixation by mixotrophic cultures [258], the latter being dictated by photo-limitation [170]. Microalgae cells achieve higher growth rate when organic carbon, nitrogen and other nutrients are provided in the growth media [259], since the cells simultaneously photosynthesize inorganic carbon and assimilate organic material under mixtotrophic conditions [260, 261].

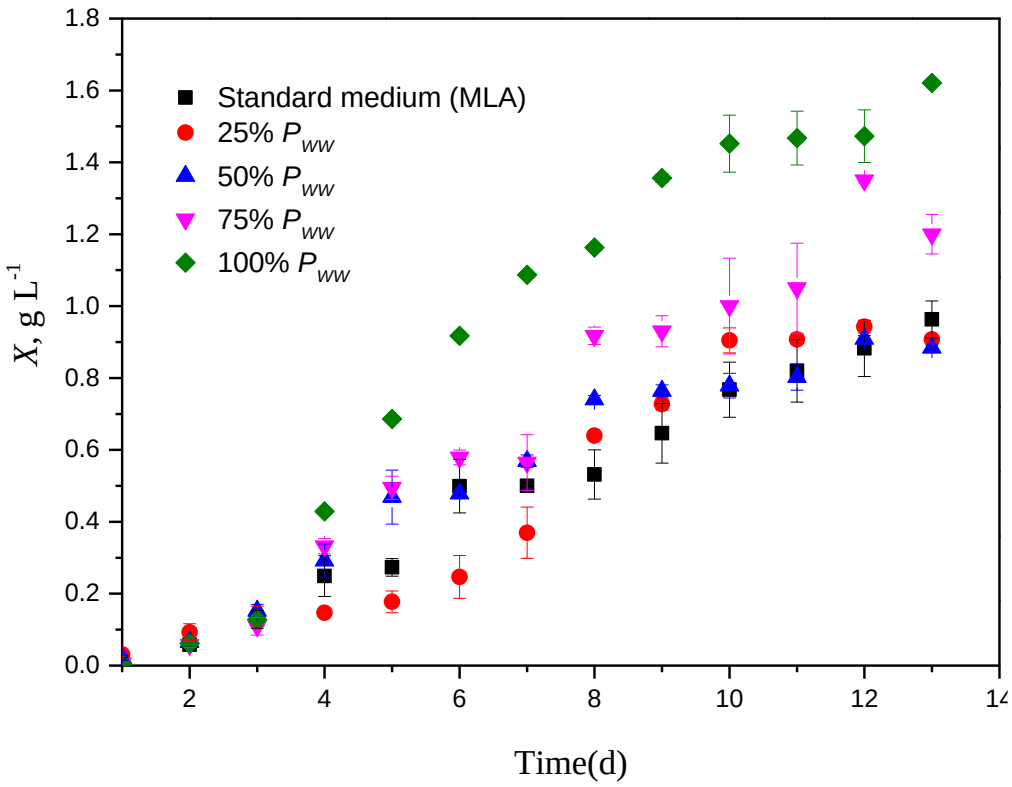

(a)

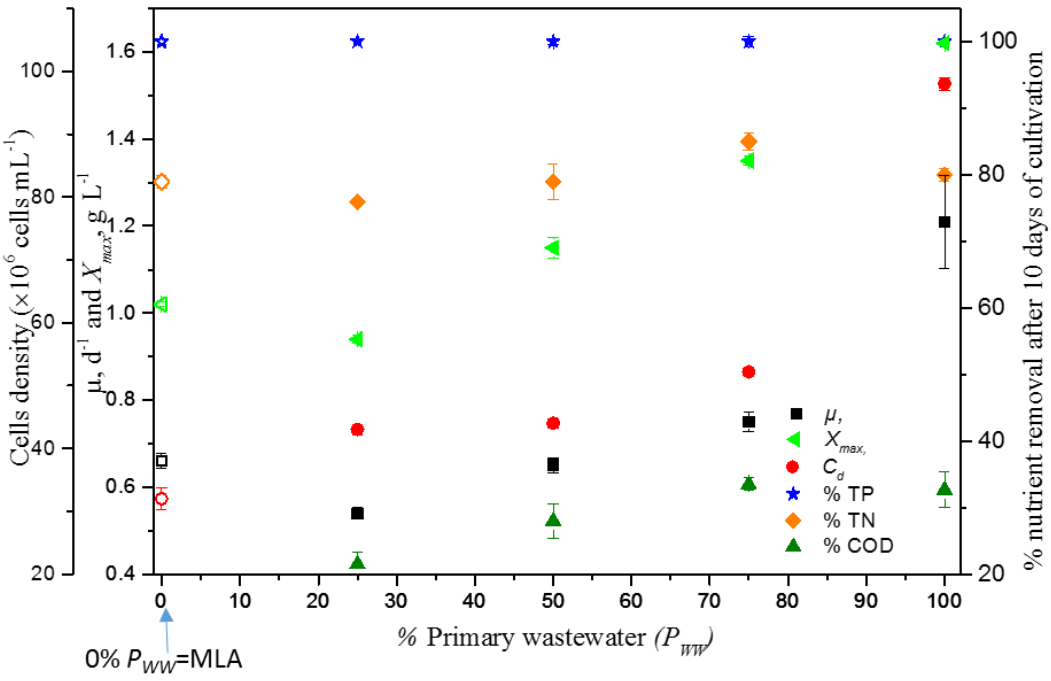

(b)

Figure 4.2 Growth of *Cv* in standard medium (MLA) with different ratios of P_{WW}: (a) *X* transient, and (b) μ_{max} and nutrient removal as a function of % P_{ww} (0% reprenset those results using only standared medium (MLA)).

In the absence of assimilable OC and for 100% MLA growth media, autotrophic growth from a CO_2 food source (from aeration) is evidently up to 55% slower than growth using an organic carbon source (Fig. 4.2b). N and P limitation after ~10 days meant that growth halted at this juncture. For a 100% P_{WW} feed the maximum specific growth rate of 1.2 d^{-1} was recorded, with corresponding *TN* and *TP* removal efficiencies of 80%, and 100% respectively and X_{max} and C_d values of 1.62 g L^{-1} and 98 $\times 10^6$ cells mL^{-1} respectively. This reflects the readily assimilable nature of the organic carbon in the P_{WW} sample. Lower values have been reported for a synthetic wastewater [108], for which the X_{max} and μ values were 0.2-0.75 g L^{-1} and 0.17 d^{-1} respectively. This compares with 2.13 g L^{-1} of biomass produced with >80% nutrient removal reported for *Chroococcus sp.1* cultivated in neat livestock wastewater [249].

100% *TP* removal efficiency was achieved for other cultures in the MLA:P_{WW} blends (25, 50, 75%) after 13 days of cultivation (Fig 4.2.b). This reflects both the low P:N and P:C ratios and the adaptability of the algal biomass in assimilating P. Phosphorus forms various structural and functional components required for growth and development of microalgae [40], and literature suggests that algae can be supported at N:P molar ratios varying from 5:1 when P is available in excessive concentrations up to 100:1 when it is depleted [87].

The trend in COD removal indicates increasing growth and nutrient uptake coupled with a lowering of COD removal on increasing the proportion of the wastewater from 50 to 100% (Fig. 4.2). This can be attributed to the organic carbon to biomass (or food to microorganism, F:M ratio) exceeding the optimum value for effective removal, such that the organic carbon concentration exceeds that which the biomass can assimilate at the maximum growth rate. N uptake follows the same pattern, increasing between 0 to 50% wastewater but decreasing thereafter. Thus, at some point between 50 and 100% P_{WW} the algal biomass reached its capacity to assimilate C and N, but not P.

Corresponding trends in *X* for S_{WW} were similar to those of P_{WW}, but with insignificant impact on μ, measured as 0.62 and 0.66 d^{-1} respectively, between S_{WW} and MLA (Fig. 4.3). These recorded growth rates were comparable with other studies reporting a μ of 0.64 [111] and 0.52 d^{-1} [112]. The maximum C_d reached was of 69×10^6 and 32×10^6 cells mL^{-1} respectively for S_{WW} and MLA, somewhat lower than for P_{WW} for which the corresponding value was 98×10^6 cells mL^{-1}. The corresponding COD removals in 25-100% S_{WW} were ~100%, based on a much lower COD_{init} for S_{WW} of 32 mg L^{-1} compared with that for P_{WW} for which the COD concentration was an order of magnitude higher. 100% *TP* removal efficiency was achieved for all cultures in the MLA:S_{WW} blends after 13 days of cultivation.

Removal efficiencies for TN were in the range of 79-83% across all three wastewater samples (Fig. 4.3), including the S_{WW} sample where growth would appear to be OC limited (Table 4.3). This can only reasonably be explained by the form of the TN. In the primary effluent the N is predominantly as TKN (including ammoniacal nitrogen) and is readily co-assimilated with OC by the biomass through mixotropic growth. This is to be distinguished from the assimilation of nitrogen in the nitrate form, as arsing in the secondary effluent following aerobic treatment. Since OC is deficient in S_{WW}, growth proceeds via the slower autotrophic path. The N is nonetheless removed to roughly the same extent when predominantly as nitrate as it is as TKN, but results in slower growth. TN removal therefore changes little from 0 to 100% S_{WW}:MLA, since growth proceeds photoautotrophically regardless of the ratio.

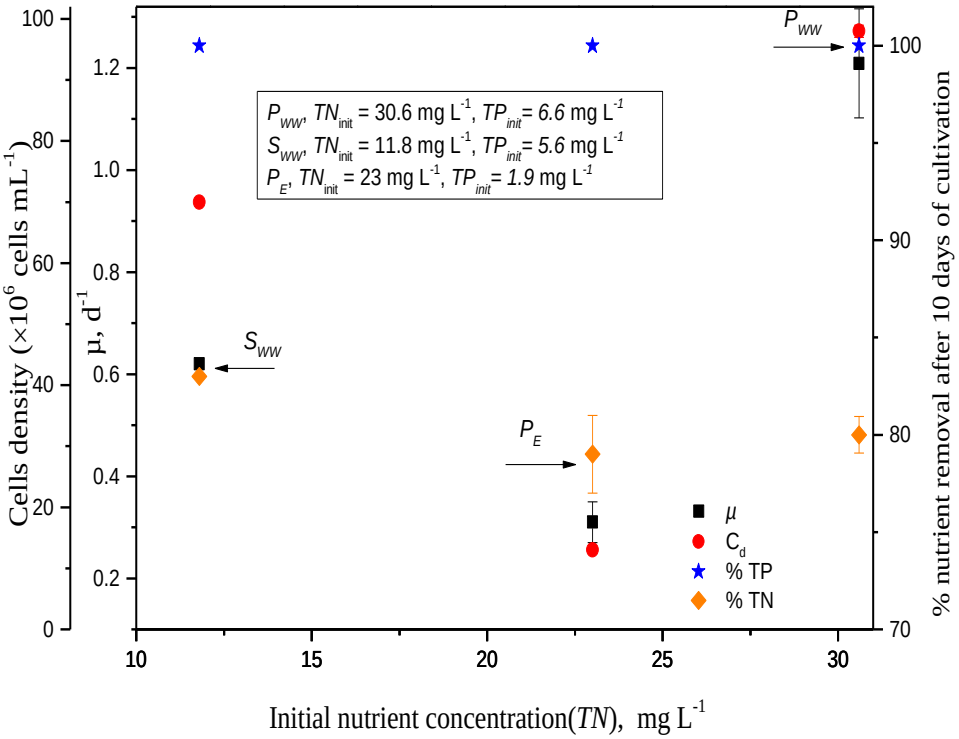

Figure 4.3 Effect of the initial *TP* and *TN* concentrations on the growth of *Chlorella vulgaris* in; P_{WW}, S_{WW} and P_E.

In the case of the P_E growth was faster in MLA than in the effluent (0.66 and 0.31 d^{-1} respectively) with corresponding biomass concentration of 0.69 g L^{-1} and 1.02 g L^{-1} respectively. However, notwithstanding the higher COD concentration (Tale 4.3), growth was slower for this wastewater, reflecting the nature of the organic carbon (Section 4.3.3). 100% *TP* removal was achieved after 13 days from both P_E and MLA, at initial concentrations of 1.9 mg L^{-1} and 6 mg L^{-1} respectively. *TN* was reduced by 79% and 70 % from 23 and 28 to 8.4 mg L^{-1} respectively for P_E and MLA, further removal possibly being inhibited by phosphorus limitation in P_E.

4.3.3 Influence of organic carbon on *Cv* metabolism

The presence of carbon in the organic form has a significant influence on algal growth in P_{WW}, S_{WW}, P_E and MLA (Figs. 4.4 and 4.5), with X_{max} and μ values of 1.62 g L^{-1} and 1.2 d^{-1} respectively measured in 100% P_{WW}. *Cv* growth declined dramatically on blending P_{WW} with the MLA growth medium to an μ and X_{max} of 0.54 d^{-1} and 0.94 g L^{-1} respectively in 25% P_{WW}. The general trend of algal growth observed in S_{WW} was the same as for P_{WW} when blended with standard medium (MLA), although the initial *OC* concentrations measured for S_{WW} were significantly lower at 3.4-8 mg L^{-1} such that the decline was less pronounced (Figs. 4.4 and 4.5). The X_{max} and μ values obtained in 100% and 25% S_{WW} were 0.62 d^{-1} and 1.16 g L^{-1}, and 0.52 d^{-1} and 0.9 g L^{-1} respectively. The trends can be explained by the substrate source: mixotrophic growth takes place when an *OC* substrate is present [48], whereas photoautotrophic growth proceeds when CO_2 is the main carbon source for algal growth.

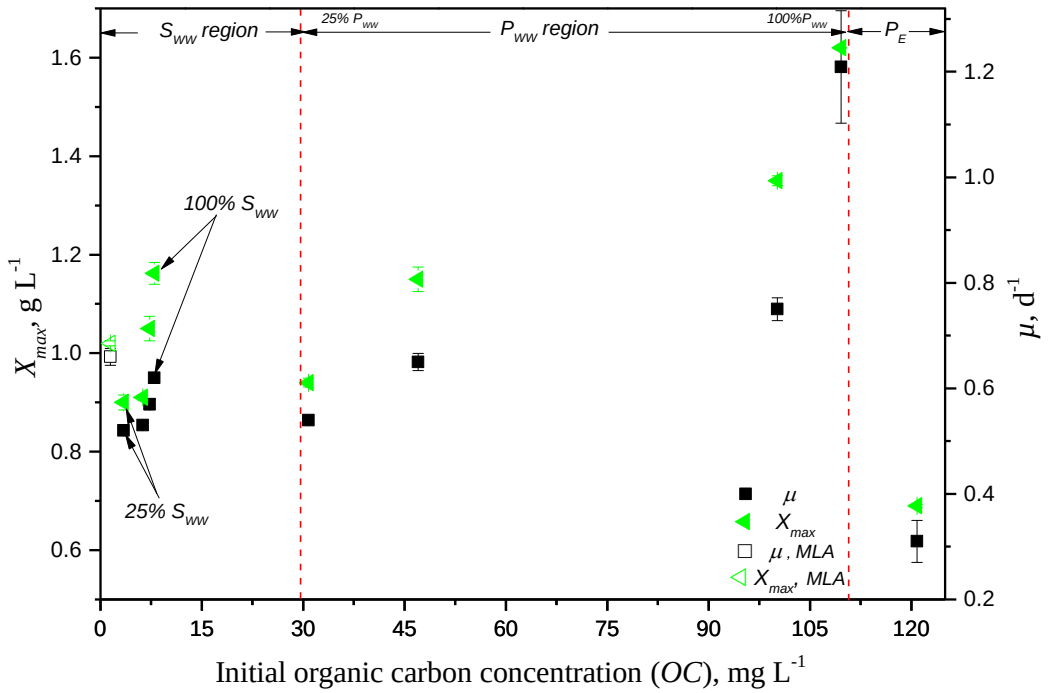

Figure 4.4 Effect of initial organic carbon concentration (*OC*) on the growth of *Chlorella vulgaris* in P_{WW}, S_{WW}, P_E and standard medium (MLA).

Generally in photoautotrophic metabolism (i.e. based on a CO_2 food source) alkalization proceeds when the pH value increases - from 6.9 to 8.5 for MLA in the current study. For S_{WW}, on the other hand, the recorded pH range of 8.9-8.1 was little changed over the growth period due to mixotrophic growth provided by the OC food source (Fig. 4.5) having negligible impact on pH. Similar trends in comparative mixotrophic and autotrophic growth have been reported for synthetic wastewater vs. real urban wastewaters [113], the respective μ values being 0.33

cf. 0.69 d^{-1} with corresponding OC removals of 15% and 78%. However, the highest organic carbon in P_E of ~121 mg L^{-1} had an inhibitory influence on algal growth (Fig. 4.5). μ decreased by almost 75% from 1.2 d^{-1} on increasing the organic carbon concentrations from 109 in the P_{WW} to 121 mg L^{-1} in the P_E. This would appear to reflect on either the toxicity of the industrial effluent at the highest concentrations [176-178], or the biorefractory nature of the OC. It is well known [262] that industrial effluents are more biorefractory than municipal ones, such that sample P_E is likely to have contained potentially inhibitive chemicals such as free and emulsified oil, phenols, cyanide, sulphides, and mercaptans [263]. Thus, for P_E, both the growth rates (Fig. 4.3-4.5) and the corresponding removal values are lower than for the municipal effluent samples primarily because the organic carbon is less assimilable: the residual COD decreased from 504 to only 144 mg L^{-1} over 13 days.

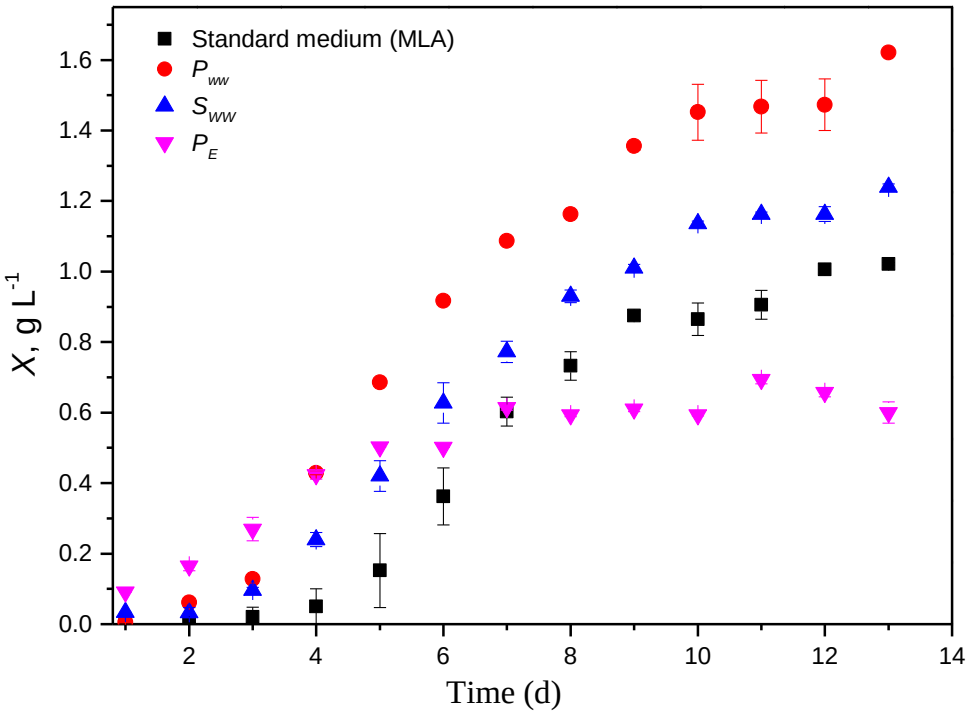

Figure 4.5 Algal growth trends in the undiluted effluent (100% P_{WW}, S_{WW}, P_E) and standard medium (MLA).

4.3.4 Macro and micro nutrient removal

>95% removal of all micronutrients arises for the two municipal wastewaters, whereas their removal is generally lower for the P_E sample (Table 4.4). The trends in previously reported individual macro and micro nutrients in different PBR systems and using different effluents are summarised in Tables 4.1-4.2.

Table 4.4 Macro/micro nutrient concentrations and RE values in P_{WW}, S_{WW}, P_E and standard MLA medium

Nutrient	***MLA***	P_{WWinit}	P_{WWf}	***%RE***	S_{WWinit}	S_{WWf}	***%RE***	P_{Einit}	P_{Ef}	***% RE***
Macro, mg L^{-1}										
Ca^{2+}	4.6	23	0.0	**100**	27	9.1	**66**	24	6.4	**73**
S^{2-}	6.5	21	6.3	**70**	17	12	**29**	42	22	**48**
Mg^{+2}	5.0	10	1.8	**82**	10	3.7	**63**	25	5.0	**80**
K^{+1}	16	26	12	**54**	26	18	**30**	21	7.2	**66**
Micro, µg L^{-1}										
As^{3+}	0.0	1.1	0.0	**98**	0.7	0.0	**100**	17	5.4	**68**
Ni^{2+}	0.0	2.3	0.0	**100**	0.9	0.0	**100**	4.5	0.8	**83**
Co^{2+}	2.4	0.4	0.0	**100**	0.2	0.0	**100**	1.4	0.4	**71**
Pb^{2+}	0.0	1.1	0.0	**100**	0.3	0.0	**100**	0.0	0.0	**nd**
Zn^{2+}	4.8	26	0.0	**100**	20	0.0	**100**	0.0	0.0	**nd**
Cu^{2+}	2.5	38	0.0	**100**	4.8	0.0	**100**	0.4	0.3	**13**
Mn^{2+}	84	8.2	0.4	**95**	6.3	0.3	**95**	4.0	0.6	**84**
Fe^{3+}	370	57	3.0	**95**	10	2.7	**73**	5.7	2.4	**57**
Cd^{2+}	0.0	0.1	0.0	**100**	0.03	0.0	**100**	0.0	0.0	**nd**
Se^{2-}	0.8	39	0.0	**100**	40	0.0	**100**	102	50	**51**

nd: not detected.

Calcium (Ca^{2+}) reduction of 100%, 66% and 73% was obtained in P_{WW}, S_{WW} and P_E respectively. These trends do not appear to relate to the initial concentration in either case. 82 and 80 % of Magnesium (Mg^{+2}) ions were removed in both P_E and P_{WW} compare with 63% only in S_{WW} with corresponding initial concentrations of 10, 25 and 10 mg L^{-1} respectively. It has been reported that higher Mg^{+2} ions >8.9 mg L^{-1}, saturates the algal biomass with Mg^{+2} ions such that they are adsorbed on the cell surface rather than incorporated in its cytoplasm [251]. 54%, 30 % and 66% were obtained for potassium (K^+) removal from P_{WW}, S_{WW} and P_E respectively. Complete K^+ removal was recorded in poultry litter wastewater with corresponding 40 mg L^{-1} > $K^+ \leq$ 20 mg L^{-1} using $NaNO_3$ as a nitrogen source, whereas there wasn't a significant difference in % *RE* for ammonia [247]. This may explain the reason for higher *RE* in P_E compared with S_{WW}, and relates to the form of N [252] (Table 4.5). The obtained results are comparable to ones that have been reported in the literature (Table 4.1).

70% sulphur removal (as S^{2-}) was measured for P_{WW}, while its removal in both S_{WW} and P_E was lower at 29% and 48% with corresponding initial concentrations of 21, 17, and 42 mg L^{-1} respectively. This trend may reflect OC and N availability: it has been reported that in mixotrophic cultivation and in the presence of high viable organic carbon concentration, microalgae cells assimilate more nutrients than one in cultivated at lower OC concentration [264]. This is related to the interconnection of sulphur assimilation to nitrogen and carbon, as well as the role of the pathway for stress response [114].

The *RE* values recorded for the different micro-nutrients varied across the three wastewaters tested. *RE* values between 73 and 100 % were recorded for P_{WW} and S_{WW} for As, Ni, Co, Pb, Zn, Cu, Mn, Fe, Cd, and Se. Removal efficiencies were more variable for P_E, ranging from 83-84% for Ni and Mn down to 13% for Cu, due to the low feed concentration of the latter in the P_E (Table 4.4). Results are broadly comparable to those reported from other studies (Table 4.2). It is likely that removal was physicochemical (absorption/adsorption) rather than physiological (i.e. assimilation) when present at concentrations beyond those which the algae can use for growth (Table 2.5). Micro-nutrients are nonetheless essential for microalgal growth, linked to many cellular enzymes and involved in various metabolic photosynthetic pathways and energy storage [265] and sometimes acting synergistically. For instance, it has been reported that increased Se^{2-} assimilation arises when algal cells are cultivated at a moderate N concentration of 80 µM with EDTA-Fe(III) instead of $Fe(OH)_3$ as an iron source (Table 4.4) [256].

4.4 Summary

The capability of the microalgae *Chlorella vulgaris (Cv)* for biomass production and nutrients removal under different wastewater quality has been studied. *Cv* was cultivated in a standard medium (*Marine labs American society of microbiology-derived medium*, MLA) blended with primary wastewater (P_{WW}), secondary wastewater (S_{WW}) and petroleum effluent (P_E) in different volume ratios. Macro and micro nutrients were characterized in each solution, and the impact on the rate of biomass growth (specific growth rate, μ) and removal efficiency (RE) determined for the bulk nutrients (total nitrogen *TN* and total phosphorus *TP*) along with a range of macro- and micro-nutrients.

P_{WW}, S_{WW} and P_E media were found to provide an appropriate quantity and balance of nutrients to promote significantly more rapid algal growth than the standard medium MLA, with ~80% nutrient removal achieved at the end of cultivation period, notwithstanding the low OC concentration for S_{WW}. Over a 13-day period the highest biomass concentration X_{max} of 1.6 g L^{-1} was attained for P_{WW} with corresponding values of 1.2 d^{-1}, 80 % and 100 % for μ, and *TN* and *TP* RE respectively. μ decreased to 0.75 d^{-1} for a 75%:25% blend of P_{WW} with MLA and to 0.54 d^{-1} on further decreasing the blend ratio to 25:75 P_{WW}:MLA, with corresponding *TN* removal efficiencies of 85% and 76% respectively; 100% removal of *TP* was obtained throughout. There was a slight increase in X_{max}, μ and *TN* removal of 1.16 g L^{-1}, 0.62 d^{-1} and 83% respectively for S_{WW}. The lowest X_{max} of 0.64 g L^{-1} in P_E was recorded was associated with values of 0.31 d^{-1}, 79% and 100% for μ, and removal efficiencies of *TN* and *TP* respectively.

Whilst the outcomes are promising, a number of facets of the experiments need to be considered further:

The study was based on a batch test with a cultivation time of around 10 days. Adapting to more appropriate conditions of shorter HRTs (of 2-5 days) whilst retaining or extending the biomass retention demands sedimentation or rejection (by membrane perm-selectivity) of the biomass, as with a conventional biological treatment process.

However, the most critical parameter with reference to combined CO_2 mitigation and nutrient removal is the relative assimilation rates of the CO_2 and the organic carbon. The outcomes of the current study indicate that high OC levels favour OC removal with concomitant rapid heterotrophic growth at the expense of CO_2 fixation. The benefit of increased biomass generation, and the associated value from biofuel production, must therefore be balanced against the mitigation of CO_2 and their associated environmental impacts.

Chapter 5

Synergistic effects and optimization of nitrogen and phosphorus concentrations on the growth and nutrient uptake of a freshwater *chlorella vulgaris*

5.1 Introduction

Discharging excess nutrients (N and P) from wastewater to the water bodies has been identified as one of the major pollution point source leading to eutrophication [221].The application of microalgae to municipal wastewater treatment was originally investigated in the 1950s [181], with their use for mitigation of the nutrients phosphate, nitrate and ammonia in wastewater treatment studied from the mid-1970s onwards [182, 183]. Established biological methods for removing nitrogen and phosphorus (N and P) from wastewater, biological nutrient removal (BNR), demand energy for aeration and the pumping of sludge between various tanks in the treatment scheme [5, 6]. Aluminium-based coagulants have also been used to remove phosphorus from wastewater [266]. The use of photobioreactors (PBRs) for nutrient removal provides an economical and environmentally sustainable alternative, combined with bioenergy and bio-products production and CO_2 mitigation [36, 190, 267].

Algal growth and nutrient (N and P) removal efficiencies depend on a large number of variables, including medium composition and environmental conditions such as the initial nutrient concentration, light intensity, the N/P ratio, the light/dark cycle and algal species [210]. Whilst, there have been a large number of recent studies of nutrient abatement using PBRs based on a number of system variables [89, 211] few have actually focused on the key aspect of nutrient balancing in a completely consistent way so as to maximise algal growth with minimum residual nutrient levels following cultivation.

Xin et al.[219] cultivated *Scenedesmus sp.LX1* in a photobioreactor under different concentrations of initial *TN* (2.5, 5, 10, 15, 25 mg L^{-1}) and *TP* (0.1, 0.2, 0.5, 1, 2 mg L^{-}). A maximum removal of 99% was recorded for both N and P with initial *TN* and *TP* concentrations of 10 and 2 mg L^{-1} respectively, i.e for an N/P ratio of 5. Feng et al. [218] reported a maximum of 97% (NH_4^+) and 96% (TP) removal using *C. vulgaris* cultivated in artificial wastewater at initial *TN* and *TP* of 20 and 4 mg L^{-1} respectively (N/P ratio = 5). Aslan and Kapdan [220] investigated the capability of *C. vulgaris* for nutrient removal at different N and P concentrations and reported that (NH_4^+-N) was completely removed from the media when the intital cocentration was in the range of 13.2 - 21.2 mg L^{-1}, while only 78% of the (PO_4^{3-}-P) was removed when the (PO_4^{3-}-P) initial concentration was 7.7 mg L^{-1}. Lau et al. [221] demonstrated that the immobilized *C. vulgaris* cells provide higher nutrient (N and P) removal efficiency (over 95% within 3 days) from primary settled wastewater than the free cells, due to the higher metabolic activities of the immobilized cells as well as the interaction between the polysaccharide matrices and the nutrient ions in the wastewater. However, employing the immobilizing *C. vulgaris* for N and P removal from wastewater is not feasible for extended treatment periods (more than 3 days).

It is important to optimise the cultivation parameters (such as medium composition) to improve microalgae growth combined with high nutrient uptake. The statistical experimental design, based on Box Behnken Design (BBD) [228, 268] combined with response surface methodology (RSM) for identifying synergistic trends and optimum operating conditions for the cultivation process has also been successfully demonstrated for various engineering applications [6, 233], optimising water treatment processes [234, 235], and for optimising the cultivation parameters.

Most of the previous studies have focused on optimum medium or nutrient (P and N) concentrations for enhancing growth. In the current investigation, the optimum nutrient concentrations (P, N and C) were identified not for only enhancing the growth rate but also for both high *TN* and *TP* removal efficiencies which are very crucial when using wastewater effluent as a medium. Therefore, the current study aims to investigate and systematically optimise the influence of the initial N and P concentrations on the nutrient removal efficiency, growth rate and biomass accumulation.

5.2 Material and methods

5.2.1 Practical measurement

Details related to experimental settings, procedures and analysis are given in Chapter 3, specifically regarding cultivation, measurement and characterisation of the algae, wastewater analysis and the general experimental set-up. Statistical analysis of data for significance was carried out using JMP statistical discovery software (SAS v11.2.1) based on one-way ANOVA, and results reported as mean ± SD.

Sterilized 250 ml medium with different concentrations of total nitrogen (0-56 mg L^{-1}), total phosphorous (0-19 mg L^{-1}), and total carbon (0-20 mg L^{-1}) was inoculated with 1 vol% pre-cultured *C. vulgaris*. The culture was bubbled continuously with filtered air (0.04% CO_2) at a flowrate of 50 mL min^{-1}. The cultivation temperature was maintained at 24±2°C. Continuous illumination of 180 µE was provided by 4x10 W LED lights, as measured by a light meter (LI-250A). A 5 mL sample was extracted daily for analysis, equating to a hydraulic and solids residence time of 50 days, and all runs lasted for 10-13 days.

5.3 Experimental design and regression analysis

Box Behnken Design (BBD) was employed to optimise the cultivation process and investigate the interactive effects of initial concentration of total nitrogen (*TN*), total phosphorus (*TP*), and total carbon (*TC*) on the system performance. A multi-level, three-parameter matrix was

employed to examine the synergistic relationships between the three parameters using the data set shown in Table 5.1. Three response (i.e. impacted) parameters were used; the specific growth rate (μ), and removal efficiencies of *TN* and *TP*.

Table 5.1 Input and output values for BBD analysis

Run	Factors			Response values, %removal				Response values, μ d^{-1}	
	X1[c]	*X2*[c]	*X3*[c]	Exp. TN	Pred. TN	Exp. TP	Pred. TP	Exp.	Pred. μ
1	56	12	10	100	100	98	100	1.163	1.29
2	56	6	0	81	74	100	85	0.803	0.73
3	56	0	10	0	0	0	0	0	0
4	0	12	10	0	0	0	0	0	0
5	56	6	20	90	80	100	90	0.98	0.9
6	28	0	0	0	0	0	0	0	0
7	0	6	0	0	0	0	0	0	0
8	0	0	10	0	0	0	0	0	0
9	28	12	0	91	80	64	60	0.734	0.67
10	28	0	20	0	0	0	0	0	0
11	0	6	20	0	0	0	0	0	0
12	28	12	20	86	78	82	74	0.855	0.8
13	28	6	10	69	69	100	100	0.69	0.69
14	28	6	10	70	69	100	100	0.69	0.69
15	28	6	10	69	69	100	100	0.7	0.69

X1= TN, *X2 = TP*; *X3 = TC*, c= coded, Exp.= Experimental, Pred.= Predicated,

Appropriate combinations of the selected variables enables the construction of a model for determining the complex response function [6]. The quadratic model for predicting the optimum values was derived according to the following equation:

$$Y = \beta_0 + \sum_{i-1}^{k} \beta ii X_i^2 + \sum_{i-1}^{k-1} \sum_{j-1}^{k} \beta Xi + \varepsilon \qquad \textbf{(5.1)}$$

Where *Y* is the response variable; i and j are the index number for the patterns; β_o is the constant coefficient; β_i , β_{ii} and β_{ij} are the coefficient for linear, quadratic, and interaction influence, respectively; x_i and x_j are the variables to be studied, the coded variables are defined as:

$$xi = \frac{Xi - Xo}{\Delta Xi} \qquad \textbf{(5.2)}$$

where x_i is the coded value of the independent variables, X_i is the actual value of the independent variable, X_o is the actual value of the factor at the centre point, and ΔX_i is the step change value. The multi-level experimental design (minimum and maximum) employed

ranges of variables of 0-56 mg L^{-1} *TN*, 0-12 mg L^{-1} *TP* and 0-20 mg L^{-1} *TC*, the range of these concentrations encompasses the values given in Table 3.1.

A total of 15 experimental runs, randomly conducted in duplicate to reduce the effect of the temporal-related errors, were conducted to determine the 10 coefficients of the second order polynomial generated from Eq. (5.4). JMP statistical discovery software (SAS version 11.2.1) was used for completing the regression analysis and plot the contour and 3D graphs. The variability of the factors was expressed as the multiple coefficients of determination (R^2) values, and the model equation used to predict the optimum value and identify the interaction between the variables within the specified experimental boundary conditions.

5.4 Results and Discussion

5.4.1 Influence of initial *TN* and *TP*

Increasing the initial *TP* (0, 1.2, 2.7, 7 and 19 mg L^{-1}) at constant *TN* (70 mg L^{-1}) produced a predictable increase in biomass growth rate (Fig. 5.1) but with a less consistent trend in removal efficiency (Fig. 5.2). The control sample condition (*TP* = 6 mg L^{-1} and *TN* = 28 mg L^{-1}) presented in Fig 5.1, represent the *TP* and *TN* concentrations in the standard medium (MLA) as recommended by the microalgae supplier, and was applied only for comparison.

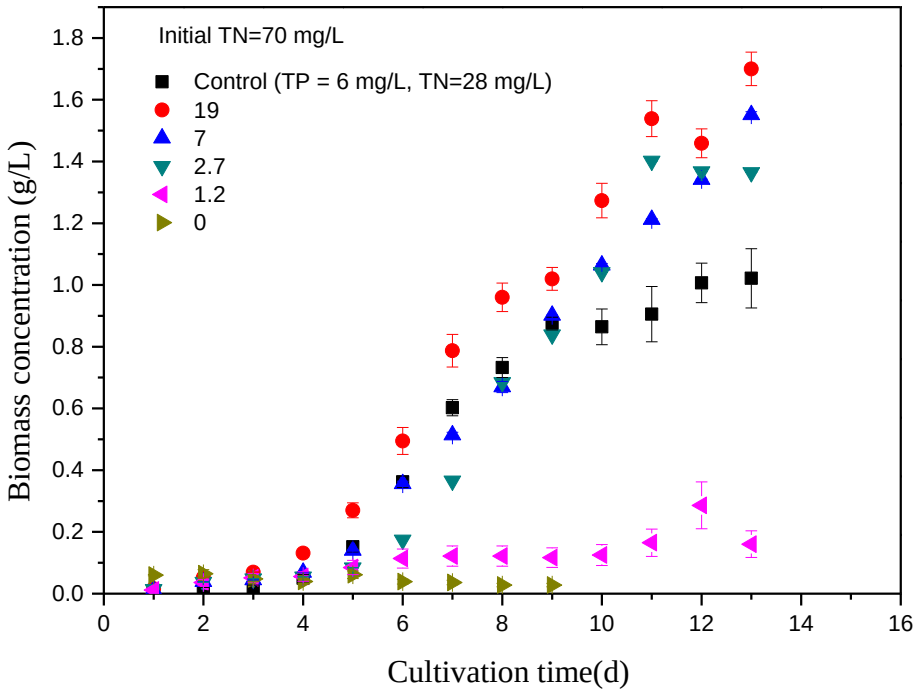

Figure 5.1 Effect of the initial *TP* concentrations on the growth of *Chlorella vulgaris* in MLA growth medium.

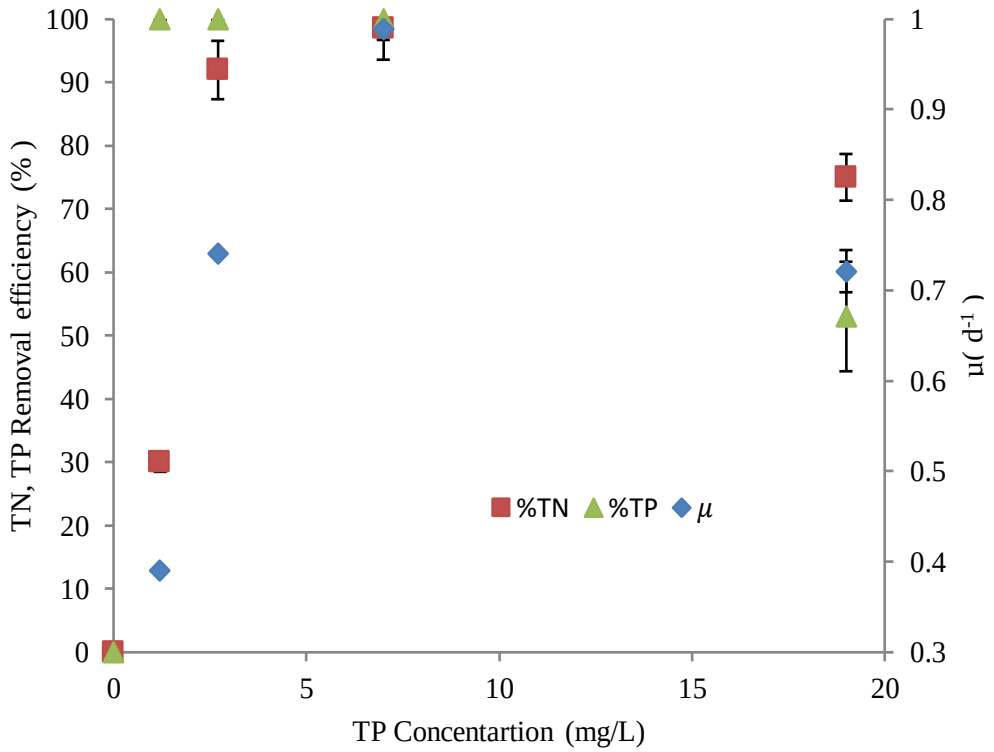

Figure 5.2 Influence of the TP concentration (at TN=70 mg/l) on the growth rate, removal efficiencies of both TN and TP.

Initial *TP* concentration apparently has a significant impact on algal growth rate and *TN* uptake for *Chlorella vulgaris*, with only 30% N removal at the lowest *TP* concentration (1.2 mg L^{-1}) and no uptake at zero initial *TP* levels due to phosphorus limitation. Against this, 100% *TP* removal was attained within the *TP* range of 2.7-7 mg L^{-1}, which was enough to provide adequate nutrients removal [85], whilst the *TN* and *TP* removal efficiencies respectively decreased to 75% and 53% at the highest initial *TP* concentration of 19 mg L^{-1} (N/P ratio=3.7). A possible reason for lower removal efficiency at high P concentrations is the unbalanced N/P ratio (low N/P ratio), notwithstanding the apparent excess of P for sustaining growth.

However, the growth rate appears to reach a maximum at around 7 mg L^{-1} with nutrient removal declining at the highest concentration applied, implying that nutrient P limitation ceases between 7 and 19 mg L^{-1}. The initial N/P ratio directly influences both microalgae growth and the removal capacities of N and P. It was evident from Figs. 5.1 and 5.2, the optimum N/P ratio for maximum specific growth rate (1 d^{-1}) and 100% removal of both *TP* and *TN* was equivalent to 10 (*TN*=70 and *TP*=7 mg L^{-1}).

A similar pattern is evident regarding the impact of the initial *TN* concentration up to 56 mg L^{-1} (Fig. 5.3). However, in this instance both nitrogen and phosphorous removal, 98% and 90% respectively, are sustained at the highest initial *TN* concentration Fig. 5.4. Furthermore, the maximum specific growth rate (1.04 d^{-1}) was achieved at *TN* of 56 mg L^{-1} (N/P ratio equal

to 7). Thus, increasing the *TN* concentration does not inhibit the microalgae growth, at least within the investigated range.

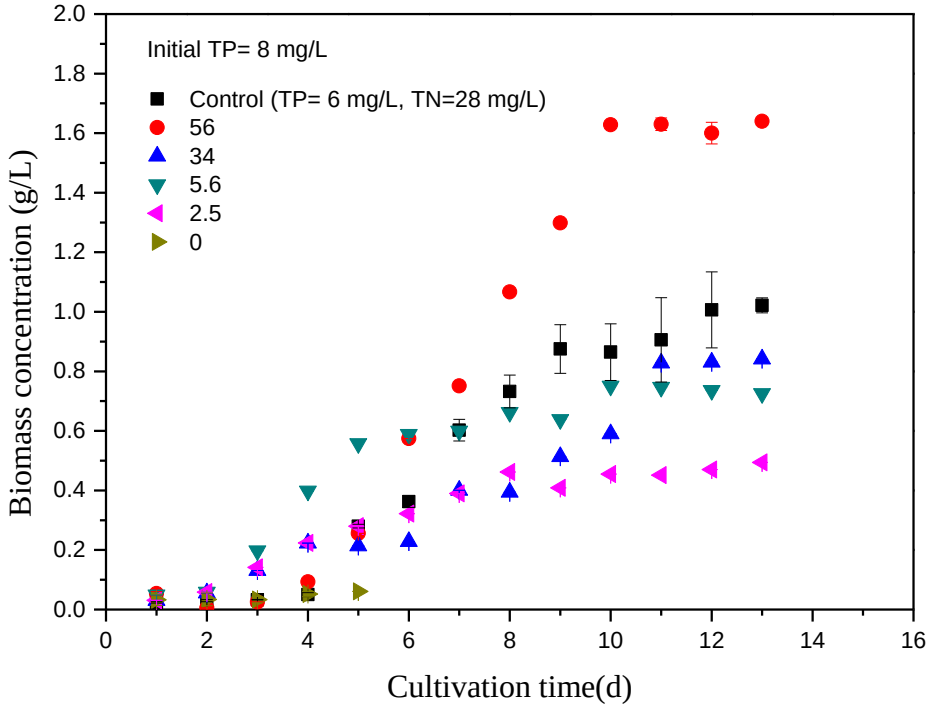

Figure 5.3 Effect of the initial TN concentrations on the growth of Chlorella vulgaris in MLA growth medium

When the nitrogen content of the medium was zero or not sufficient (<2.5 mg/l) the specific growth rate was significantly reduced from 1.04 d^{-1} (at *TN*=56 mg L^{-1}) to 0.23 d^{-1} (at *TN*=2.5 mg L^{-1}) and the maximum biomass produced was dropped 3.4- fold to 0.50 g L^{-1}. The reason may be that some metabolic pathways in *C. vulgaris* are probably modified by N deprivation, which resulted in low protein content and chlorophyll [269] along with increased lipids fraction. Also the results revealed that though low N content reduced the growth rate it enhanced the nutrient (N and P) removal efficiencies (Fig. 5.4). It was noticed in this study that high N/P ratios (higher than 26) suggest P limitation, while low ratio (less than 3.7) suggest N limitation. Under these conditions both the *TN* removal and specific growth rate reduced significantly to 27% and 0.4 d^{-1} respectively. Thus, under both N & P limitation the TN removal and specific growth rate reduced significantly to 27% and 0.4 d^{-1} respectively.

The optimal N/P ratio achieved for highest biomass growth and nutrients (N and P) removal varies between 7 and 10. Table 2.8 shows that different authors reported different N/P ratio. Aslan and Kapdan [220] reported that N/P ratio had a crucial effect on the nutrient removal, and found the optimum N/P ratio was 8, which is very similar to the ratio obtained in this study.

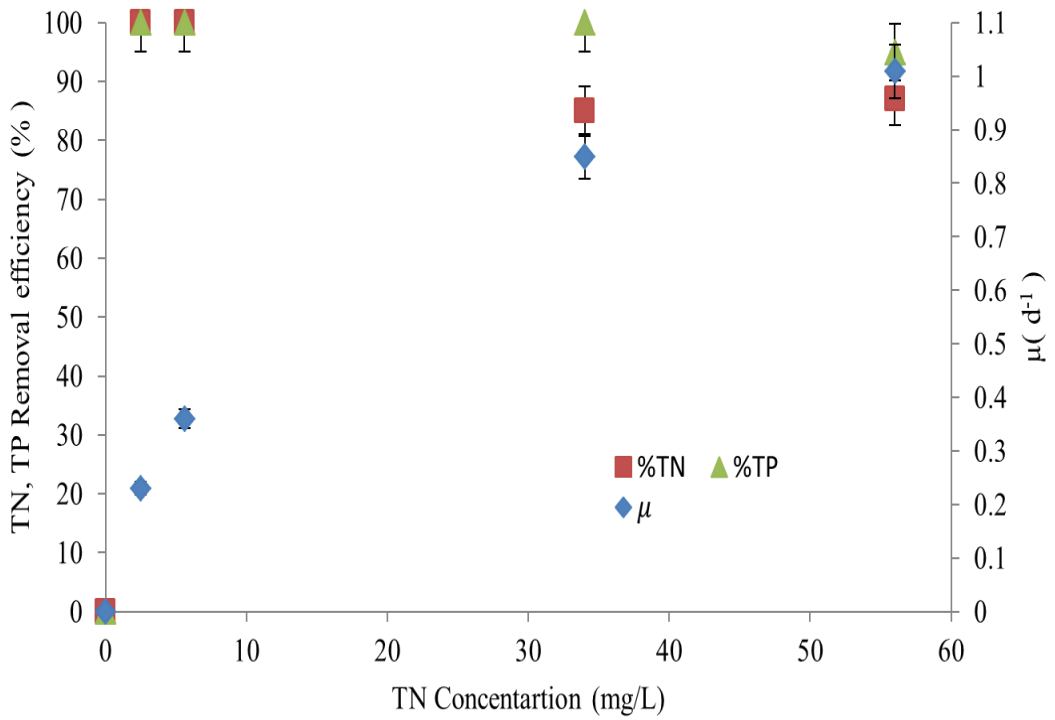

Figure 5.4 Influence of the *TN* concentration (at *TP*=8 mg/l) on the growth rate, removal efficiencies of both *TN* and *TP*.

5.4.2 Multiple regression analyses

Multiple regression analysis for determining the relationships between the three response parameters of N and P removal efficiency and specific growth rate (μ) with respect to *TN*, *TP* and *TC* concentration generated second-order polynomial equations based on the BBD matrix of actual data (Table 5.1):

$$\textit{Specific growth rate} = -0.16062 + 0.0135x_1 + 0.0756x_2 + 0.0057x_3 + 0.00173065x_1x_2 + 0.000158036x_1x_3 + 0.0000625x_2x_3 - 0.00022146x_1^2 - 0.00543403x_2^2 - 0.00040625x_3^2 \quad (5.3)$$

$$\textit{TN removal efficiency} = -21.65 + 1.916x_1 + 9.154x_2 + 0.18x3 + 0.133x_1x_2 + 0.00803x_1x_3 - 0.0208x_2x_3 - 0.0292x_1^2 - 0.559x_2^2 - 0.0115x_3^2 \quad (5.4)$$

$$\textit{TP removal efficiency} = -36.5 + 2.776x_1 + 15.583x_2 + 3.375x_3 + 0.133x_1x_2 + 1.90\times10^{-17}x_1x_3 - 0.0753x_2x_3 - 0.0408x_1^2 - 1.26389x_2^2 - 0.18x_3^2 \quad (5.5)$$

Where x_1, x_2 and x_3 are the coded values of the initial *TN*, *TP* and *TC* respectively calculated based on Eq. (5.5) (Table 5.1). The coefficient of determination (R^2) of the regression equations for the specific growth rate, *TN* and *TP* removal efficiencies were 0.92, 0.95 and 0.95 respectively, indicating that the quadratic equations can adequately describe the

relationship between the factors and responses, with values predicted from Eqs.(5.6-5.8) in reasonable agreement with those determined experimentally Fig. 5.5.

Table 5.2 Analyses of variance results for the fitted models of *RE* (%) for *TN*, *TP*, and μ (d^{-1}) as influenced by different intitial concentration (mg L^{-1}) of *TN*, *TP*, and *TC* in the cultivation media

Source of variance	*Degree of freedom*	*Sum of square*	*Mean square*	*F-ratio*	*p-value, (prob<F)*
Generated models					
Specific growth rate, μ (d^{-1})					
Model	3	2.68	3×10^{-1}	21	0.01
Residual	5	7.1×10^{-2}	1×10^{-2}	--	--
Lack of fit	3	7.1×10^{-2}	2.4×10^{-2}	--	--
Pure error	2	6.6×10^{-5}	3.3×10^{-5}	--	--
Total	14	2.75	--	--	--
Removal efficiency TN (%)					
Model	9	2.47×10^{4}	2.74×10^{3}	10	0.001
Residual	5	1.4×10^{3}	2.79×10^{2}	--	--
Lack of fit	3	1.4×10^{3}	4.65×10^{2}	--	--
Pure error	2	6.67×10^{-1}	3.30×10^{-1}	--	--
Total	5	2.61×10^{4}	1.40×10^{1}	--	--
Removal efficiency TP (%)					
Model	9	3.19×10^{4}	3.54×10^{3}	11	0.003
Residual	5	1.63×10^{3}	3.26×10^{2}	--	--
Lack of fit	3	1.63×10^{3}	5.43×10^{2}	--	--
Pure error	2	0.00	0.00	--	--
Total	5	3.35×10^{4}	1.40×10^{1}	--	--

The statistical significance of the current experimental designs was determined by the F-test for ANOVA (Table 5.2). The p-values obtained for the specific growth rate, *TN* and *TP* removal efficiencies models were 0.01, 0.001, and 0.003 respectively. This outcome reflects the statistical relation between the responses and selected factors at high confidence level of 95% (Table 5.1), and thus shows that the regression analysis is statistically significant.

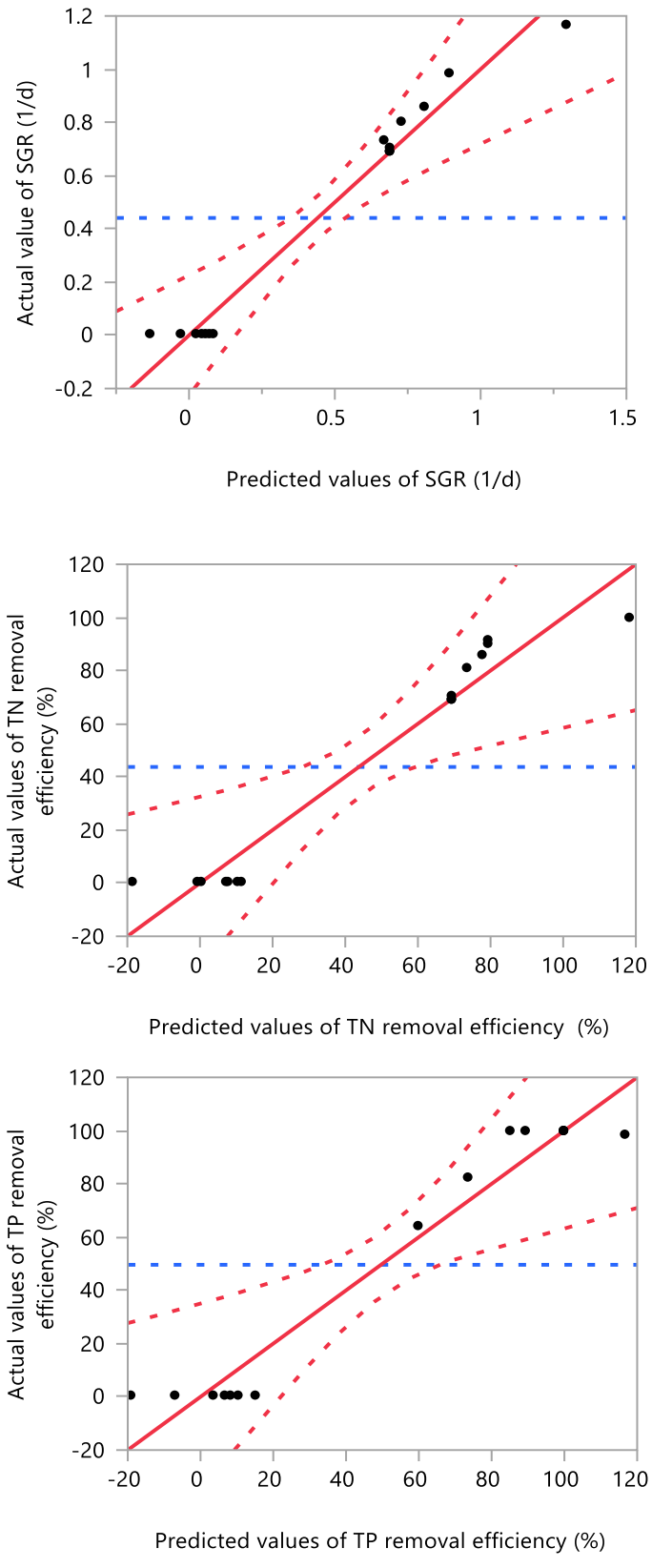

Figure 5.5 Comparison between experimental and predicated values of *TN* and *TP* removal, and specific growth rate μ, (•) Experimental points, (⋯) Confidence bands>(95%), (−) Fit line, Eqs.5.6-5.8 , (⋯)Mean of the Y Leverage Residuals

5.4.3 Analysis of variance (ANOVA)

ANOVA was applied to generate the sum of squares, degree of freedom (df), mean squares, f-values and *p*-values by fitting the experimental results to the second-order polynomial equations (Eqs. 5.6 – 5.8). Model terms are considered significant when the corresponding *p*-value is less than 0.05.

Table 5.3 Analysis of variance (ANOVA) from BBD

Source	*Coefficient (β)*	*Standard error*	*f-value*	*p-value* [a]
μ				
Intercept	0.69	0.06	---	---
$x_{1(0,56)}$	0.36	0.04	76.19	0.0003*
$x_{2(0,12)}$	0.34	0.04	66.48	0.0005*
$x_{3(0,20)}$	0.037	0.04	0.77	0.4177
$x_1\ x_2$	0.29	0.05	23.74	0.0046*
$x_1\ x_3$	0.04	0.05	0.55	0.4916
$x_2\ x_3$	0.03	0.05	0.25	0.6337
x_1^2	-0.17	0.06	8.12	0.0358*
x_2^2	-0.22	0.06	13.19	0.0150*
x_3^2	-0.07	0.06	1.29	0.3075
TN				
Intercept	69.33	9.64	----	----
$x_{1(0,56)}$	33.87	5.90	32.87	0.0023*
$x_{2(0,12)}$	34.62	5.90	34.34	0.0021*
$x_{3(0,20)}$	0.5	5.90	0.0072	0.9358
$x_1\ x_2$	25	8.35	8.95	0.0304*
$x_1\ x_3$	2.25	8.35	0.072	0.7985
$x_2\ x_3$	-1.25	8.35	0.022	0.88
x_1^2	-22.91	8.69	6.94	0.04*
x_2^2	-21.41	8.69	6.06	0.05
x_3^2	-3.66	8.69	0.17	0.69
TP				
Intercept	100	10.42	-----	-----
$x_{1(0,56)}$	37.25	6.38	34.07	0.0021*
$x_{2(0,12)}$	30.5	6.38	22.84	0.0050*
$x_{3(0,20)}$	2.25	6.38	0.12	0.73
$x_1\ x_2$	24.5	9.02	7.36	0.0420*
$x_1\ x_3$	0	9.02	0.00	1.0000
$x_2\ x_3$	4.5	9.02	0.24	0.63
x_1^2	-31	9.39	10.89	0.0215*
x_2^2	-44.5	9.39	22.44	0.0052*
x_3^2	-19	9.39	4.091	0.09

* *P*-values indicate the results statistically significant <0.05.

As shown in Table 5.3, x_1 and x_2, that represent *TN* and *TP* concentrations respectively, significantly influenced the specific growth rate (μ), *TN* and *TP* removal efficiencies (p-value < 0.05). While the effect of *TC* (x_3) concentration is less significant in the examined range, where *p*-values was greater than 0.1. The x_1x_3, x_2x_3 and x_3 interaction was less significant within the experimental data range (Table 5.2). *TN* removal efficiency was significantly influenced

by the initial concentration values x_1x_2, whereas the interaction between (x_2x_3) was less significant. The negative terms in the generated models indicate inferable effect on the μ, *TN* and *TP* removal efficiencies, whereas the positive terms showed favourable effects.

Fig. 5.6 depicts the outputs of the analysis as contour and 3D plots, similar topography for both the specific growth rate μ (Fig. 5.6 b) and phosphorus removal (Fig. 5.6f) surfaces are evident.

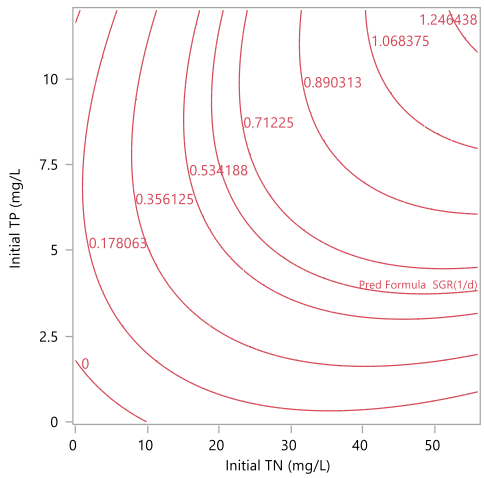

(a)

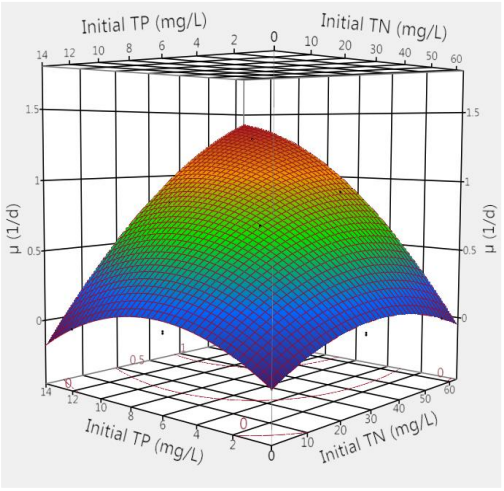

(b)

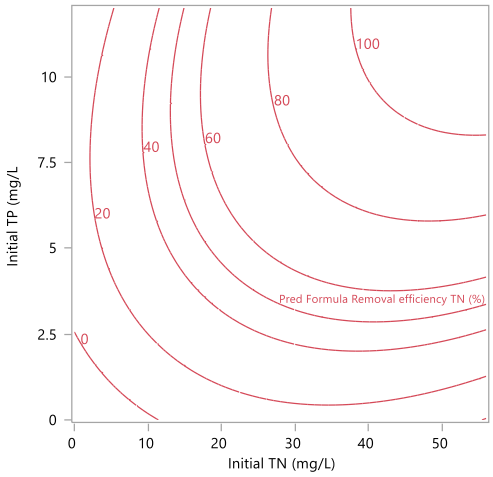

(c)

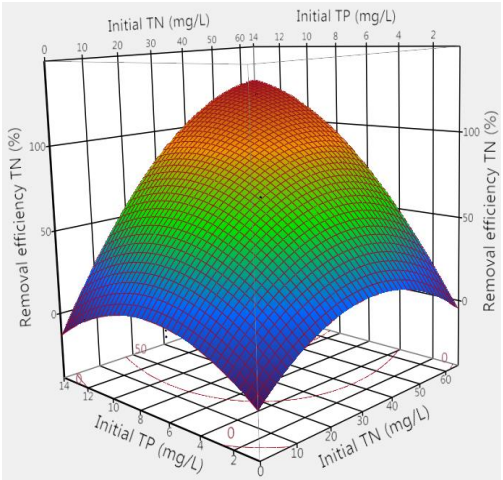

(d)

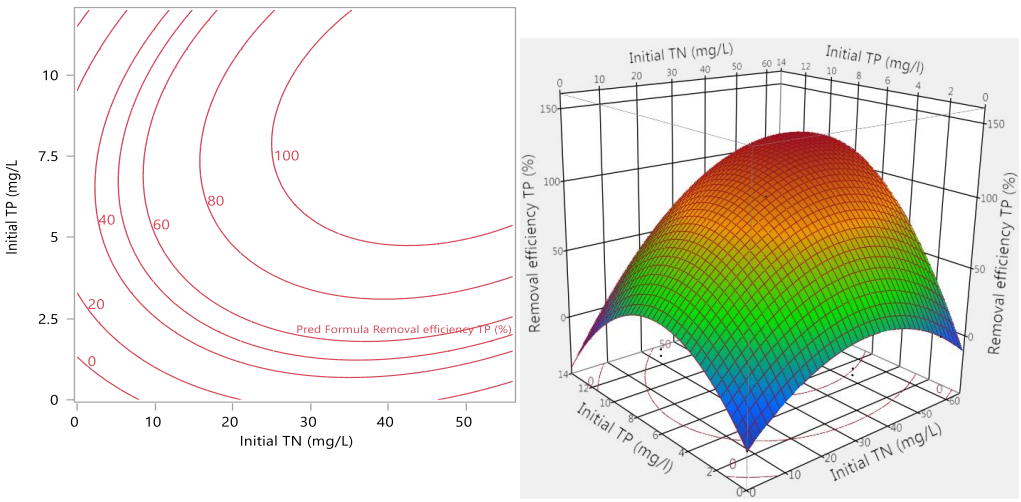

(e) **(f)**

Figure 5.6 Contour lines and 3D response surface for μ (a-b), *TN* removal (c-d) and *TP* removal (e-f)

Significant interaction was indicated between the *TN* and *TP* concentrations, as expected intuitively in the case of μ. Under optimum conditions cell growth is concomitant with nutrient uptake (i.e. *TN* and *TP*); no algal growth was evident when either initial *TN* or *TP* were zero. The maximum removal efficiency of ~100 % could be achieved at initial *TN* concentrations between 50 and 60 mg L^{-1} and initial *TP* concentrations of 6-12 mg L^{-1} while *TC* was maintained constant at its central point of 10 mg L^{-1}.

5.4.4 Desirability and optimum conditions

The scale of desirability function ranges between (*d=0*) for an unacceptable response value and (*d=1*) for a totally desirable one. Fig.5.7 shows higher desirability factor (*d*=0.94) supporting the obtained model. The optimzed *TP*, *TN* and *TC* concentrations in the medium that support 100% removal efficiencies of both P and N, and specific growth rate of 0.95 d^{-1} were 7 mg L^{-1}, 54.84 mg $L^{-1}$and 10 mg L^{-1}respectively, which is also resulted in a balanced N/P ratio of 7.85.

To validate the current optimization, a separate experiment was carried out at *TP*= 7 mg L^{-1}, *TN*= 55 mg $L^{-1}$and *TC*= 10 mg L^{-1}, the obtained results, Table 5.3, confirm the validity of the model equations (Eqs. 5.6-5.8) well and with an acceptable errors.

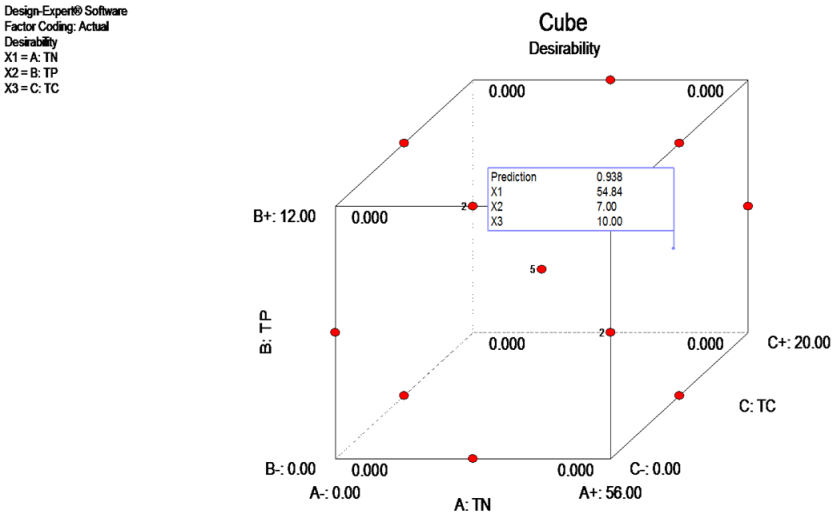

Figure 5.7 (3D) Cube desirability plots for *TN*, TP and *TC*.

Table 5.4 Comparison between the predicted and the experimental optimum conditions.

Factors (mg L^{-1})	Response	Experimental	Predicted (Eqs. 6-8)	% error
TN = 55	*TN RE* (%)	89.5	100	10.5
TP = 7	*TP RE* (%)	100	100	0
TC = 10	SGR (d^{-1})	0.98	0.95	3.15

5.5 Summary

The synergistic effects and optimization of nitrogen (N) and phosphorus (P) concentrations on the growth of *Chlorella vulgaris* (CCAP 211/11B, CS-42) and nutrient removal have been investigated under different concentrations of N (0 - 56 mg L^{-1}) and P (0 - 19 mg L^{-1}) or N/P ratios of 0.31 - 58. The study showed that the N/P ratio has a crucial effect on the biomass growth and nutrient removal. The balanced N/P ratio at which both the growth rate and nutrient (N, P) removal at the highest was within the range of 7-10. When the N/P=10, a complete P and N removal was achieved at the end of cultivation with specific growth rate (SGR) of 1 d^{-1} and maximum biomass concentration of 1.58 g L^{-1}.

It was also observed that when the N content of the medium less than 2.5 mg L^{-1}, the SGR significantly reduced from 1.04 d^{-1} to 0.23 d^{-1} and the maximum biomass produced was decreased more than three-fold to 0.5 g L^{-1}. Box-Behnken experimental design (BBD) and

response surface method (RSM) were used to study the effects of the initial concentrations (P, N and C) on cell growth and P and N removal efficiencies. The optimised P, N and C concentrations in the medium supporting 100% removal of both P and N at a specific growth rate of 0.95 were 7, 55 and 10 mg L^{-1} respectively, with desirability value of 0.94. The results and analysis obtained could be very useful when applying the microalgae for efficient wastewater treatment and nutrient removal.

Chapter 6

Optimization of cultivation conditions for combined nutrient removal and CO_2 fixation in a batch photobioreactor

6.1 Introduction

Microalgae, configured as photobioreactors (PBRs), have attracted considerable attention as the basis of combined biological method for removal of nutrients (nitrogen N and phosphorus P) from wastewaters and CO_2 fixation from flue gases [21]. The microalgae *Chlorella vulgaris* has been extensively studied for CO_2 mitigation under a range of operating conditions, including gas CO_2 concentration, [24-28], light intensity [29, 30] and temperature [30, 31]. These parameters, along with the dissolved inorganic carbon (DIC) associated with CO_2 dissolution, liquid CO_2 residence time, pH, biomass cultivation mode (which influence the biomass growth phase), nutrient concentration, mixing and algal species, all impact on the PBR process efficacy.

Nutrient removal using microalgae PBRs has been studied since the mid-1970s [182]. PBRs offer a more sustainable alternative to classical biological nutrient removal (BNR), since the latter requires energy for aeration and the pumping of sludge between various tanks in the treatment process as well as supplementary coagulant dosing with to obtain the required P removal [7]. However, whilst offering a potentially sustainable solution for combined nutrient and CO_2 abatement, the process footprint can be up to two orders of magnitude greater than that of the BNR process [21]. Optimization of microalgae cultivation process, so as to enhance the CO_2 fixation (and so biomass growth) and nutrient assimilation, is thus critical.

Reported figures for the biomass–normalised CO_2 fixation rate, R_c' (Table 2.2) for a single species (*Anabaena sp.*) vary between 0.5 and 1.2 g CO_2 g biomass^{-1} d^{-1} for a gas stream containing different CO_2 concentrations range from 0.03% to 15% [74], the precise R_c' value being dependent on CO_2 concentration $C_{c,g}$ [25] light intensity I [74], and other operating conditions such as hydraulic residence time (HRT) and gas flow rate. Corresponding figures for *B. braunii* indicate somewhat lower rates of 0.15 g CO_2 g biomass^{-1} d^{-1} but a higher maximum attainable algal biomass concentration (X_{max}), while reported data for *C. vulgaris* and *Scenedesmus obliquus* indicate moderate CO_2 fixation rates of 0.09-0.35 and 0.098-0.26 g CO_2 g biomass^{-1} d^{-1} respectively with corresponding maximum specific growth rates (μ_{max}) of 1.37 d^{-1} and 1.19 d^{-1}.

Reported data for CO_2 fixation as a function of I for different algal species appears to follow no recognisable pattern across either different species within a single study, or different studies for the same species (e.g. *Chlorella vulgaris* or *Anabaena sp.*) (Table 2.2) [21]. Against this, for individual studies subject to the same controlled conditions fixation and biomass productivity both increase with I as expected to some maximum limit associated with light saturation [25, 74, 75]. Batch experiments on four different algal species (*C. vulgaris*, *P.*

subcapitata, *S. salina*, and *M. aeruginosa*) indicate that an approximate trebling of light intensity (from 36 µmol photons m^{-2} s^{-1}) yields a 70-90% and 35-45% increase in biomass productivity and CO_2 uptake respectively [76]. Further increases in I may then inhibit and diminish R_c and μ [77]. In the case of nutrient removal, a wide range of removal and biomass productivity (P_X) values for *C. vulgaris* have been reported (Table 2.8).

The hydraulic retention time (HRT) is a key processes parameter determining the required nutrient load and the water quality of the discharged effluent. Extended HRTs are required to provide a cultivation period ensure high removal efficiency [211]. A maximum uptake rate of 4-5 mg $L^{-1}d^{-1}$ N and 0.4-0.6 mg $L^{-1}d^{-1}$ P has been reported for both a classical stirred tank PBR and a membrane PBR operating at a 2-5 d HRT [108]. Nutrient removal for continuous processes of 2-3 d HRT are generally below 85% for both N and P, compared to 75-88% N and 80-99% P for the BNR process [21]. This reduced robustness compared with BNR arises primarily from the combined impact of the lower X_{max} (generally <1.5 g/L, cf. >3 gL^{-1} for BNR) and slower algal biokinetics compared with that of bacteria.

Whilst various studies have reported trends in key parameters such as X and R_c, optimisation is complicated by the large number of variables, including light intensity, CO_2 gas or organic carbon (*OC*) liquid load, biomass concentration and volume, biomass retention time, algal species, biomass physico-chemistry (specifically pH and temperature) and feedwater nutrient load. To optimise the system for just five of the key variables for a single algal species and reactor configuration, based on just three parameter values and a classical n-factorial approach, would demand 243 (i.e. 3^5) individual experiments.

An alternative to the classical factorial-based approach is the use of statistical experimental design to reduce the number of tests, and identify synergistic relationships and optimum conditions. This includes Box Behnken Design (BBD) which, while developed in the early 1960s [228], has only recently been employed for algal bioreactor optimisation [229], in particular relating to lipid or biofuel generation [230, 231]. BBD permits a significant reduction in the number of experiments whilst still enabling synergies between the different parameters to be identified along with the optimum set of conditions [232]. It therefore provides an elegant and efficient approach for elucidating inter-relationships for complex, multi-parameter systems, such as PBRs.

Given the practical significance and potential economic benefit of combined nutrient abatement and CO_2 fixation [21], it is of obvious interest to evaluate this specific application more extensively. The current study appraises the influence of the most important process variables of influent gas CO_2 concentration, light intensity and temperature, along with feed

water *TN*, *TP* and *TC*, on the key performance determinants of biomass accumulation, CO_2 fixation rate, and nutrient removal. The study uniquely both (a) employs Box Behnken statistical experimental design to identify the optimum condition, and (b) combines nutrient abatement from wastewater with CO_2 fixation, potentially from flue gases, in a single practical experimental study. The use of BBD for this dual function enables the optimum conditions to be identified.

6.2 Material and Methods

More details related to experimental settings, procedures and analysis are provided in Chapter 3. Statistical analysis of data for significance was carried out using JMP statistical discovery software (SAS v11.2.1) based on one-way ANOVA, and results reported as mean ± SD.

6.2.1 Algae preparation and determination

The concentrations of both $NaNO_3$ and K_2HPO_4 in the standard medium were varied to accommodate different concentrations of *TN* (0-56 mg L^{-1}) and *TP* (0-19 mg L^{-1}). 250 ml batches of sterilized medium with different concentrations of *TN* (0-56 mg L^{-1}), *TP* (0-19 mg L^{-1}), and *TC* (0-20 mg L^{-1}) were inoculated by 1 vol% pre-cultured *C. vulgaris* with initial cells concentration of 0.7×10^6 cells mL^{-1}. The initial pH value of the cultivation medium was set to 7, according to the MLA preparation method [270]; there is no significant change in pH value of the cultivation medium when aerated with atmospheric CO_2. The culture was continuously fed with a flow of 50-52 mL min^{-1} filtered air enriched with 0.03-22% CO_2, adjusted by digital mass flow controllers (MC-100SCM, Cole-Parmer, USA); inlet and outlet gas concentration ($C_{c,g}$) was measured using a CO_2 probable meter (G110, Geotech, UK). The control sample was aerated with air only (0.03 % CO_2). The cultivation temperature (*T*) was varied from ambient 30°C down to 20°C using an incubator refrigerator (Temperature Cycling Chamber, LABEC, Australia). Continuous illumination at a light intensity (*I*) between 180 and 400 µE, provided by adjusting the number of 8W LED lights between 4 and 8, was measured by a light meter (LI-250A, LI-COR, US). All experiments were conducted in batch mode with 5 mL samples extracted daily for analysis, equating to a hydraulic and solids residence time of 50 days, and all runs lasted for 10-13 days.

For all nutrient tests the control sample contained 6 mg L^{-1} TP and 28 mg L^{-1} TN, based on the typical medium MLA composition stipulated by the supplier.

6.2.2 Experimental design and regression analysis

Box Behnken Design (BBD) was employed to e the process based on algal growth, expressed as μ in d^{-1}, biomass productivity P_X in g (dry weight) biomass L^{-1} d^{-1}, and:

- CO_2 capture (R_C), as a function of feed $C_{c,g}$, I, and T, and
- Nutrient removal, as a function of feedwater composition with reference to *TN*, *TP* and total carbon (*TC*).

R_C is given by $C\ P_X\ M_{CO2}/M_C$, where C is the dried cells % carbon content, measured by an element analyser (CHNS/O analyser, PerkinElmer, USA), P_X the biomass productivity, and M_{CO2} and M_C are the respective molar weights of CO_2 and carbon.

BBD experimental design employs a matrix of tests based on a number of parameters, in this case three. The impact of each parameter is evaluated by selecting three or more values (or "levels") of these parameters and then conducting tests which encompass every combination of each parameter value. The results of the experiments in terms of the impacting (or "response") parameters can then be evaluated through a statistical model [232]. Two such multi-level, three-parameter BBD matrices were created to examine the synergistic relationships between these sets of three parameters within specific limits (Table 6.1). A total of 15 experimental runs, randomly sequenced in duplicate to reduce the effect of the temporal-related errors, were conducted to determine the 10 coefficients of the second order polynomial generated from the statistical model [235]. *JMP* statistical discovery software (SAS v11.2.1) was used to complete the regression analysis and generate the graphical relationships. The variability of the factors was expressed as coefficient of determination (R^2) values. The model equation was then used to identify the interaction between the variables within the specified experimental boundary conditions. Subsequent optimisation to identify the conditions for maximising μ, R_C and nutrient removal was through maximising the desirability function using Derringer's desired function (DDF) methodology.[244]

Table 6.1 Parameter values

Parameters	*Range of values*	
CAMPAIGN 1	*Min*	*Max*
$\%CO_2$ $C_{c,g}$, v/v	0.04	5
Light intensity I, μE	100	400
Temperature T, ℃	20	30
CAMPAIGN 2		
TC, mg L^{-1}	0	20
TN, mg L^{-1}	0	56
TP, mg L^{-1}	0	12

6.3 Results and discussion

6.3.1 Scoping trials: Growth as a function of CO_2 concentration

The specific growth rate μ at a fixed T of 24°C and I of 200 µE over a 10-day cultivation period increased from 0.64 d^{-1} (R_c = 0.328 g L^{-1} d^{-1}) for $C_{c,g}$ = 0.03% to 1.17 d^{-1} at 5%, with a corresponding X_{max} of 2.94 g L^{-1} (R_c = 0.744 g L^{-1} d^{-1}) at the higher $C_{c,g}$ (Fig. 6.1 a-d) Increasing $C_{c,g}$ further to 22% resulted in a decreased growth rate (μ = 0.097 d^{-1}, X_{max} = 1.11 g L^{-1}, R_c = 0.28 g L^{-1} d^{-1}).

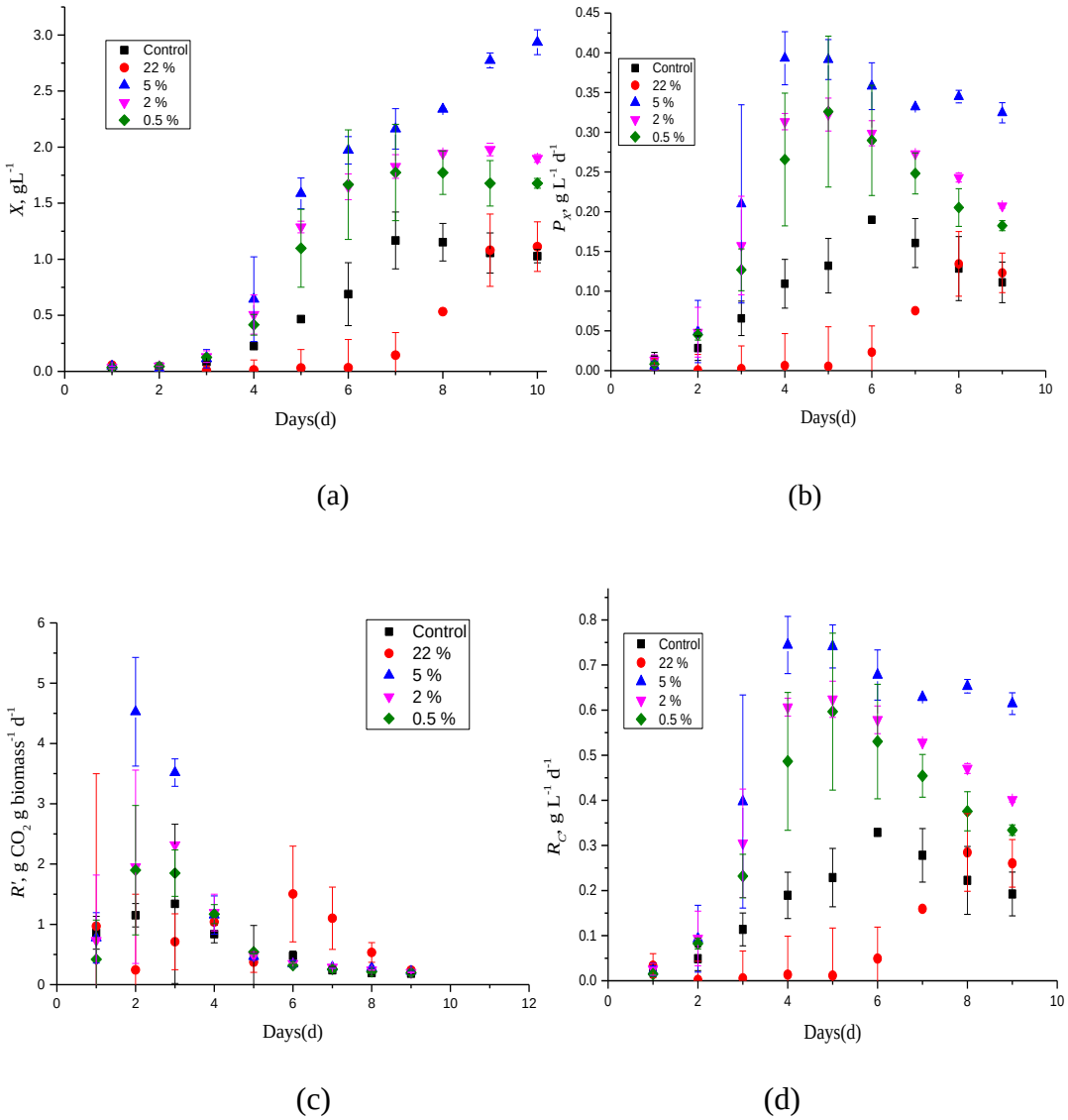

Figure 6.1 Algal growth trends with feed gas CO_2 concentration: (a) X, (b) P_x, (c) R_c', and (d) R_c."Control" refer to the sample aerated with only air (0.03%), (I=200 µmol m^{-2} s^{-1}, T=24 °C).

The reduced biomass production at the highest $C_{c,g}$ of 22% is likely to be due to the inhibitive impact of the associated low pH on growth and CO_2 mass transfer, the latter pertaining to the

relatively slow rate of hydrolysis of CO_2 to H_2CO_3 [21], and the associated suppression of photosynthesis [271, 272]. Low-intermediate $C_{c,g}$ concentrations (0.03-5%), on the other hand, caused insignificant inhibition: these levels were associated with pH values in the optimum range of 7-7.5. A 25% increases in μ (from 0.52 to 0.65 d^{-1}) has been previously reported as increasing $C_{c,g}$ from ambient levels to 15%, whilst other reports [24, 107, 214, 273] have indicated that increasing $C_{c,g}$ from 2.5% to 9.5% has little influence on growth. The pathway/mechanism through which CO_2 affects the biomass growth is photosynthesis, which is outlined in Section 2.2.1.

6.3.2 Scoping trials: Growth and nutrient removal

Increasing the initial *TN* concentration (TN_{init} = 0-56 mg L^{-1}) at a constant *TP* of 8 mg L^{-1} produced the expected increase in *C. vulgaris* biomass growth (Fig. 6.2) and with close to 100% *TP* removal within the TP_{init} range of 2.7-7 mg L^{-1}. Against this, the initial *TP* concentration apparently has a significant impact on algal growth and *TN* uptake, with only 30% N removal at the lowest TP_{init} concentration (1.2 mg L^{-1}). *TN* removal also declined from >90% to 75% removal at the highest TP_{init} concentration of 19 mg L^{-1}, where the corresponding *TP* removal also declined to 53%. The low removal efficiency (*RE*) can be largely attributed to the excessive nutrient load and/or its unbalanced N/P ratio (Fig. 6.3), along with the impairment of light transmission by the high biomass concentration. Whilst high *TP* concentrations generally favour biomass productivity [214], studies conducted at a number of different N/P ratios (Table 2.8) have demonstrated that the ratio is crucial for effective nutrient removal. An optimum value of 8 has been reported [215] – within the range of 7-10 found for the current study (Fig. 6.3) – associated with a maximum specific growth rate of 1.04 d^{-1}.

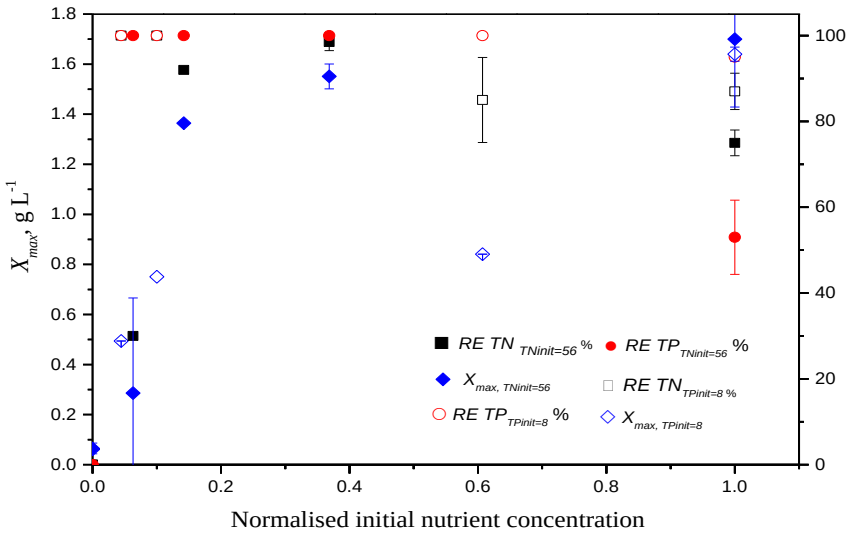

Figure 6.2 X_{max} and % nutrient removal, 13 days cultivation, at different initial nutrient concentrations (TN_{init} and TP_{init}): normalised initial nutrient concentration = initial nutrient concentration / maximum initial nutrient concentration ($TN_{init,max}$ and $TP_{init,max}$ = 56 and 19 mg L^{-1} respectively).

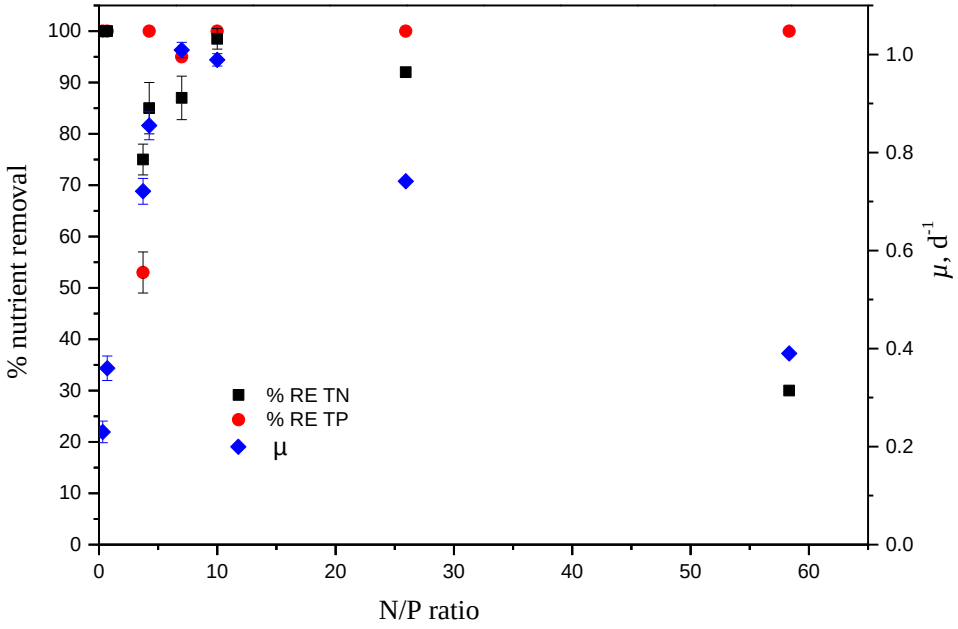

Figure 6.3 Specific growth rate and nutrient removal efficiencies after 13 days of cultivation and a function of N/P concentration ratio.

6.3.3 Multiple regression analysis and analysis of variance

Multiple regression analysis conducted to determine the relationships between the three response parameters of R_C, *TN* and *TP RE*, and μ with respect to $C_{c,g}$, *I* and *T* generated the second-order polynomial equations from the BBD matrix of experimental data (Table 6.2):

Table 6.2 BBD matrix, experimental outputs

Run	C_{cg}, %	*I*, μE m^{-2} s^{-1}	*T*, C°	*TN RE*, %	*TP RE*, %	μ, d^{-1}	R_C, mg L^{-1} d^{-1}
1	5	250	20	98	100	1.30	958
2	2.5	250	25	92	100	0.89	386
3	0.04	250	30	74	76	0.64	358
4	2.5	400	30	67	86	0.56	357
5	2.5	400	20	72	90	0.61	363
6	0.04	250	20	75	85	0.67	363
7	0.04	100	25	80	100	0.72	377
8	2.5	250	25	92	100	0.89	386
9	5	400	25	80	100	0.9	539
10	2.5	250	25	92	100	0.9	386
11	2.5	100	30	100	100	1.35	899
12	5	175	25	100	100	1.47	72
13	5	250	30	95	100	1.25	525
14	0.04	400	25	60	50	0.42	112
15	2.5	100	20	100	100	1.32	900

$$R_C, \text{mg L}^{-1}\text{d}^{-1} = 4710 + 298\,C_{c,g} - 2.93\,I - 331\,T + 0.0128\,C_{c,g}\,I - 8.63\,C_{c,g}\,T - 1.56 \times 10^{-3}\,I\,T - 0.965\,C_{c,g}^{2} + 3.23 \times 10^{-3}\,I^{2} + 6.83\,T^{2} \quad \textbf{(6.1)}$$

$$\mu, \text{d}^{-1} = 2.02 + 0.216\,C_{c,g} - 1.27 \times 10^{-4}\,I - 0.090\,T - 3.60 \times 10^{-4}\,C_{c,g}\,I - 5.24 \times 10^{-4}\,C_{c,g}\,T - 2.36 \times 10^{-5}\,I\,T + 4.26 \times 10^{-3}\,C_{c,g}^{2} + 1.18 \times 10^{-5}\,I^{2} + 1.90 \times 10^{-3}\,T^{2} \quad \textbf{(6.2)}$$

$$TN\ RE\ (\%) = 41.2 + 9.33\,C_{c,g} + 0.067\,I + 3.00\,T - 2.03 \times 10^{-17}\,C_{c,g}\,I - 0.040\,C_{c,g}\,T + 1.42 \times 10^{-017}\,I\,T - 0.812\,C_{c,g}^{2} - 3.11 \times 10^{-4}\,I^{2} - 0.060\,T^{2} \quad \textbf{(6.3)}$$

$$TP\ RE\ (\%) = -32.2 - 1.71\,C_{c,g} - 0.049\,I + 11.5\,T + 0.012\,C_{c,g}\,I + 0.181\,C_{c,g}\,T - 9.47 \times 10^{-18}\,I\,T - 0.589\,C_{c,g}^{2} - 3.88 \times 10^{-5}\,I^{2} - 0.245\,T^{2} \quad \textbf{(6.4)}$$

The coefficient of determination (R^2) of the regression equations for the correlations for R_c, μ, and the *RE* values for *TN* and *TP* were 0.94, 0.98, 0.98 and 0.94 respectively (Fig. 6.4). The above quadratic expressions thus adequately describe the relationship between the factors and responses.

Analysis of variance (ANOVA) was applied to generate the sum of squares, degree of freedom (df), mean squares, f-values and p-values by fitting the experimental results to the second-order polynomials Eqs. (6.1-6.4). *P*-values below 0.05, i.e. representing a significant correlation, were generated for $C_{c,g}$ and *I* for μ, R_c, and *TN* and *TP* removal. The impact of *T* was found to be less significant (p-values > 0.1) within the range examined. Whilst the linear terms (i.e. terms in $C_{c,g}$ and *I*) were found to significantly influence μ (p-value<0.05), the combined terms (i.e. $C_{c,g}T$ and *IT*) were less significant. *N* and *P* removals were both significantly influenced by the individual and combined initial terms $C_{c,g}$ and *I*, whereas the influence of the $C_{c,g}T$ and *IT* terms was less significant. Similarly, for R_C there was better interaction between $C_{c,g}$ and *T*, but *T* itself remained insignificant in comparison with the other parameters. The satisfactory agreement found between the experimental and model data (Fig. 6.4), justified the use of the equations for generating the response surface correlations.

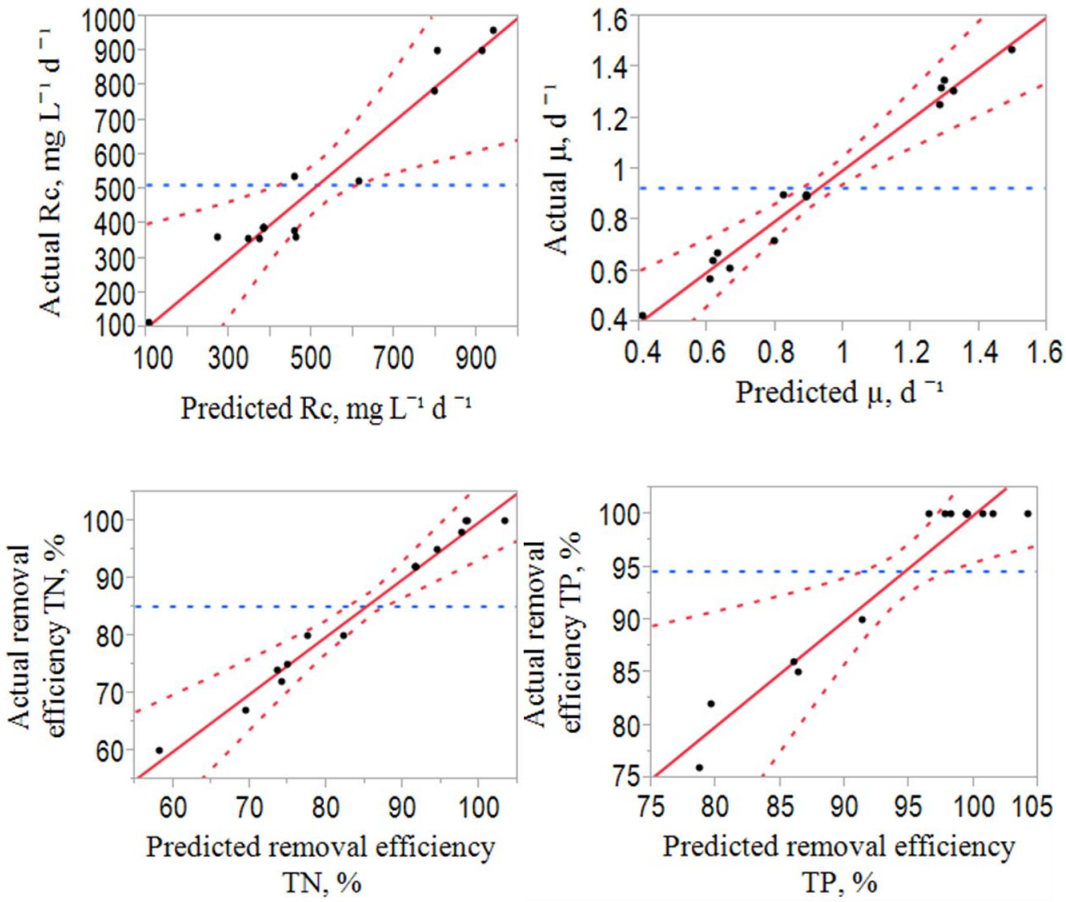

Figure 6.4 Comparison between experimental data and predicated values of R_c, *TN* and *TP* removal, and μ. The dotted curved lines indicate the >95% confidence bands; horizontal dotted lines represent the mean of the Y leverage residuals (i.e. the measure of agreement with the model).

The statistical significance of the design was assessed according to an F-test for analysis of variance (ANOVA) (Table 6.3). The ANOVA analysis indicates that the quadratic polynomial Equations (6.1 – 6.4) significantly represent a definite relationship between the response and variables with p-values for R_c, μ, and the *RE* values for *TN* and *TP* of 0.01, 0.0006, 0.01 and 0.0001 respectively. The model terms are significant when the p-values are less than 0.05.

Table 6.3 Analyses of variance results for the fitted models of *RE* (%) for *TN*, *TP*, μ (d^{-1}), and R_C (mg L^{-1}) as influenced by different cultivation paramters of *I*(μE), $C_{,cg}$ (%), and *T*(℃)

Source of variance	*Degree of freedom*	*Sum of square*	*Mean square*	*F-ratio*	*p-value, (prob<F)*
Generated models					
CO_2 capture (R_C) (mg L^{-1})					
Model	9	8.4×10^5	9.3×10^4	9.4	0.01
Residual	--	--	--	--	--
Lack of fit	3	4.93×10^4	1.64×10^4	--	--
Pure error	2	0.00	0.00	--	--
Total	5	4.93×10^4	--	--	--
Specific growth rate, μ (d^{-1})					
Model	9	1.5	0.16	33	0.0006
Residual	--	--	--	--	--
Lack of fit	3	2.4×10^{-2}	8×10^{-3}	2.5×10^2	0.004
Pure error	2	6.6×10^{-5}	3.3×10^{-5}	--	--
Total	14	2.7	--	--	--
Removal efficiency TP (%)					
Model	9	9.26×10^2	1.02×10^2	9	0.01
Residual	1629	5	3.25×10^2	--	--
Lack of fit	57.1	19.3	--	--	--
Pure error	0.00	2	0.00	--	--
Total	5	57.1	--	--	--
Removal efficiency TN (%)					
Model	9	2.44×10^3	270	32	0.0001
Residual	--	--	--	--	--
Lack of fit	3	42.2	--	--	--
Pure error	2	0.00	0.00	--	--
Total	5	42.2	--	--	--

6.3.4 BBD analysis and optimization

3D response surface and 2D contour plots (Figs 6.5 - 6.6) were generated from Eqs.(6.1-6.4) for two factors ($C_{c,g}$, *I*), the third (*T*) being kept constant. The discrete data points refer to actual experimental response data values, added to demonstrate the fit with the model-generated response surface.

R_c increases with increasing $C_{c,g}$, between 0.03 and 5%, and also with *I* up to 100 μE (Fig. 6.5 a-b), corroborating previous studies [274] reporting similar trends. However, growth decreased with beyond 100 μE $m^{-2}s^{-1}$. Microalgal cells exposed to high light irradiance may undergo damage of the photosynthetic units, making them non-functional and causing photo-inhibition. Whilst this can take place at all irradiance levels, non-photochemical quenching (NPQ) processes become evident if the rate of photo-inhibition exceeds the rate of repair resulting in large proportions of the captured light being dissipated [96]. Conversely, as light irradiance decreases the level of photosynthesis-active radiation decreases to low levels which significantly reduce photosynthesis activity, as reflected in the CO_2 fixation rates (see also Section 2.8).

Generally, growth and metabolic rates are enhanced by increasing the temperature until an optimum value is reached for a species; further temperature increases may then reduce cell growth through cell damage or death [275]. It has been reported that microalgae can grow in the temperature range between 20-35°C [276], whereas some other species have been reported as being temperature tolerant at 60°C [277, 278] (see also Section 2.8). For the current study the temperature range of 20-30°C selected was insufficiently broad to generate a significant change in R_c through either microbial or gas solubility impacts. The results recorded were nonetheless consistent with those previously reported [279], and were reflected in the related parameter μ which demonstrated similar trends (Fig. 6.5 c-d).

TN RE followed a similar trend of increasing removal with increasing $C_{c,g}$ and decreasing I over the ranges studied (Fig. 6.6 a-b), with ~100% removal attained at a relatively low irradiance (50-200 μE) and 3-5% $C_{c,g}$. *TP* trends indicated a flatter response with irradiation at the maximum $C_{c,g}$ of 5% (Fig. 6.5 c-d). *TN* uptake appears to be reduced at low CO_2 concentrations [280]. Conversely, high CO_2 concentrations activate N reductase, enhancing N assimilation [24] as well as increasing the HCO_3^- concentration through reaction of CO_2 with protons generated from N and P uptake by microalgae cells [281]. Viable algae thus maintain a neutral pH value, providing more favourable conditions for algal growth which are reported to lie between a pH of 5 to 8 [282] for *chlorella vulgaris*. A pH value of ~11, on the other hand, has been reported to negatively influence algal growth [283].

TP was 100% removed at all irradiance levels studied at the highest $C_{c,g}$ of 5%, only demonstrating irradiance dependency at lower $C_{c,g}$ levels. Light stress associated with high light intensities arises when the energy imparted cannot be dissipated as fluorescence and heat. This can impair photosynthesis [284], potentially breaching the light saturation limit of the algae and negatively impacting on P removed. Consumption of *TP* was accompanied by photosynthesis uptake of dissolved inorganic carbon. However, P removal is impacted more than N removal by pH via abiotic precipitation, though assimilation by algae remains the primary P removal mechanism [285]. P removal close to 100% has been previously reported [86].

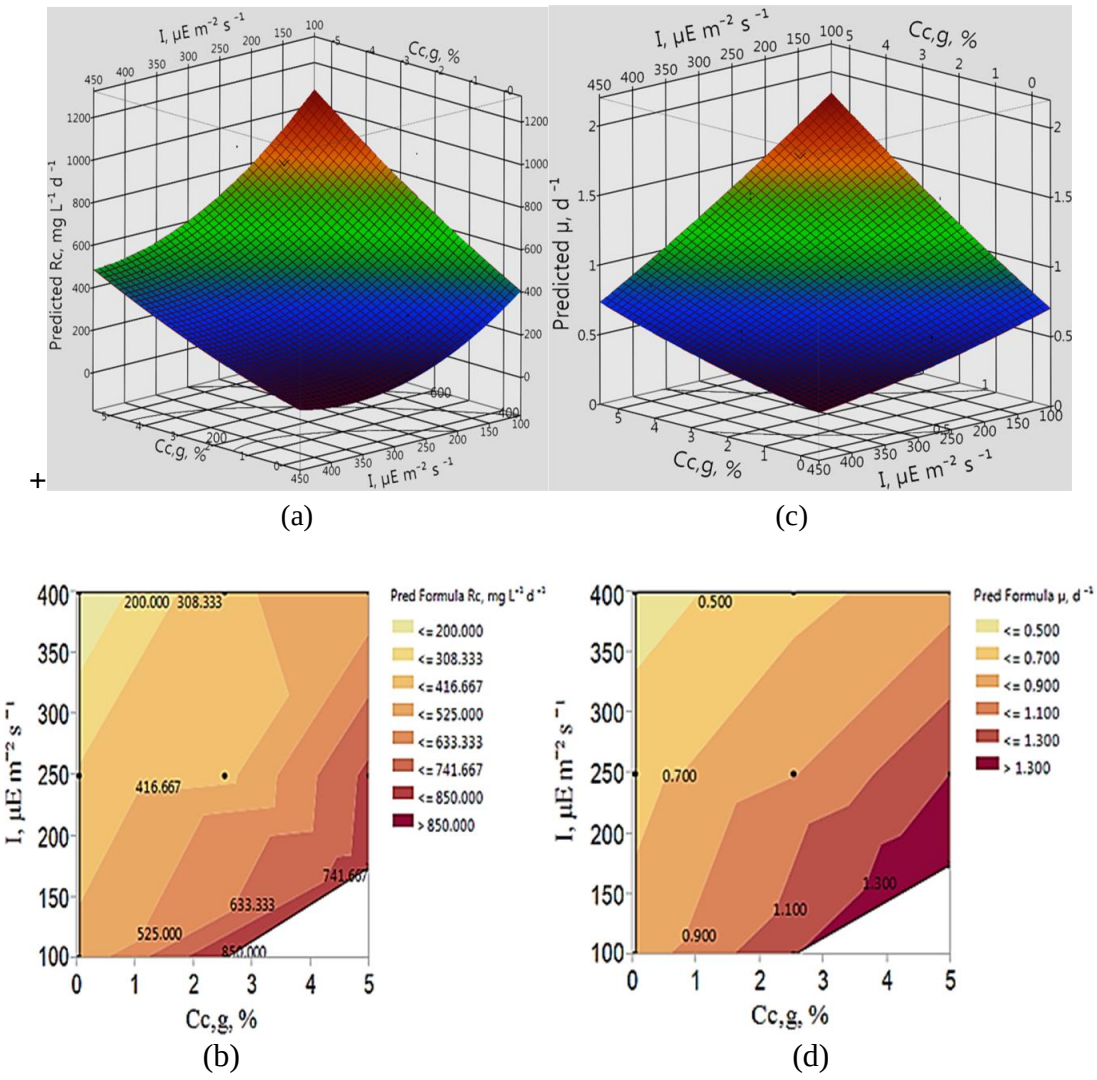

Figure 6.5 3D response surface and contour map for CO_2 fixation rate (a ,b) and μ (c ,d), at the optimum temperature of 22 ^{o}C.

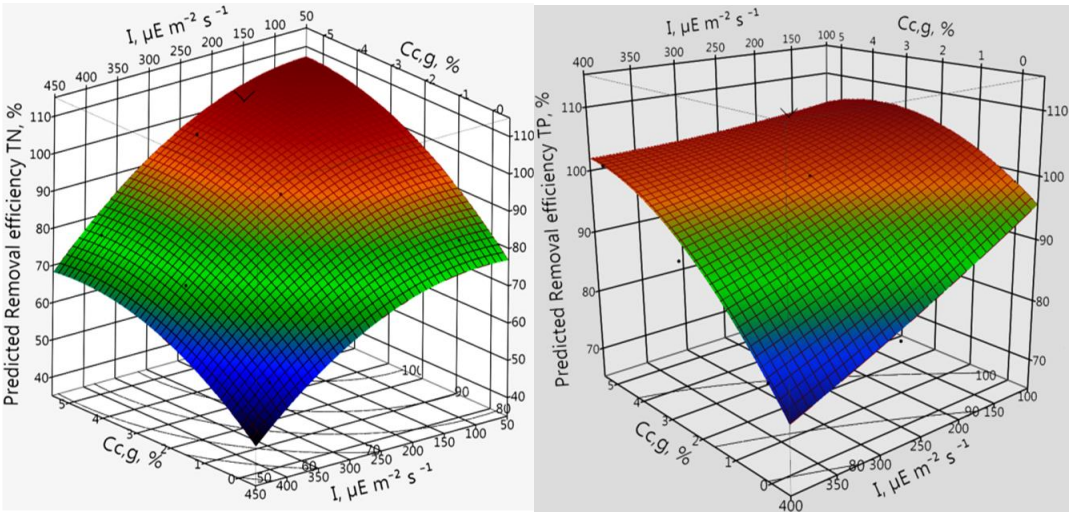

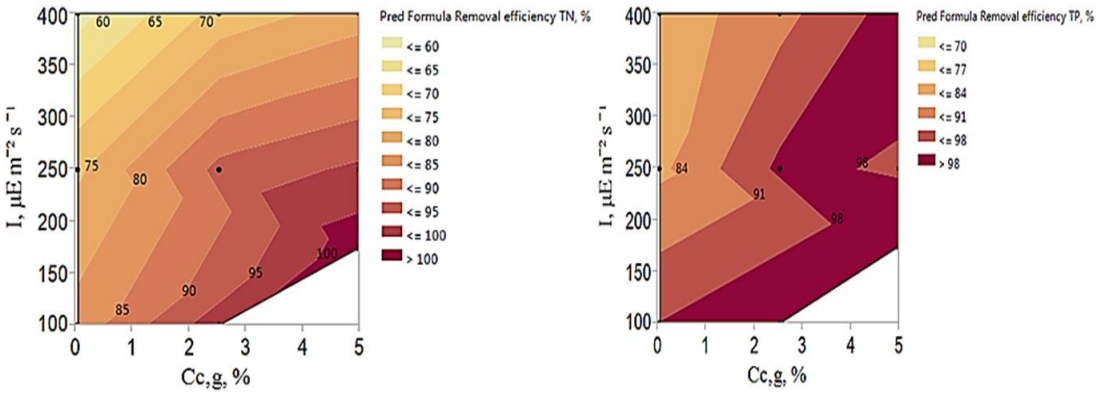

(b) (d)

Figure 6.6 3D response surface and contour map for CO_2 fixation rate (a ,b) and μ (c ,d), at the optimum temperature of 22 ^{o}C.

According to the BBD results, the optimal conditions for maximizing R_c, μ, and the *TN* and *TP* removal efficiencies based on Derringer's desired function (DDF) methodology were found to be at $C_{c,g}$ = 5%, I = 100 µE m^{-2} s^{-1} and T = 22 ^{o}C. Under these conditions, the predicted R_c, μ and *TN*, *TP* removal efficiencies were found to be 1000 mg L^{-1} d^{-1}, 1.53 d^{-1} and 100% *RE* for both N and P respectively (Table 6.3).

Table 6.4 Comparison between predicted and experimental optimum conditions

Factors	***Response***	***Experimental***	***Predicted***	***% error***
$C_{c,g}$ = 5 %	R_C g L^{-1}.d^{-1}	1032	1000	3.4
I = 100 μE	μ, d^{-1}	1.51	1.53	1.4
T = 22℃	RE TN, %	96	100	4.0
	RE TP, %	100	100	0.0

6.4 Summary

The application of the microalgae *Chlorella vulgaris* to combined CO_2 capture and nutrient removal has been optimised using response surface methodology based on Box Behnken statistical experimental design (BBD). Experimental conditions employed comprised feed gas concentrations ($C_{c,g}$) of 0.03-22% CO_2, irradiation intensities (I) of 100-400 µE, temperatures of 20-30°C and nutrient concentrations of 0-56 and 0-19 mg L^{-1} nitrogen (N) and phosphorus (P) respectively, the response parameters being specific growth rate μ, CO_2 uptake rate R_c and %nutrient removal. Over a 10-day period the biomass concentration X reached almost 3 g L^{-1} for a $C_{c,g}$ of 5% CO_2, with corresponding values of 0.74 g L^{-1} d^{-1} and 1.17 day^{-1} for R_c and μ respectively and 100% N and P removal. At the highest CO_2 gas concentration of 22% the rates of both carbon fixation and biomass growth decreased by around an order of magnitude,

and nutrient removal also decreased to 79% and 50% for N and P respectively, indicating impairment of the photosynthesis process at these high irradiation levels. Response surface methodology (RSM) and Box-Behnken experimental design (BBD) were used to identify the optimum values of the three key parameters of $C_{c,g}$, I and temperature (T), based on the impact on μ, R_c, and nutrient removal. Optimum values 5% CO_2, 100 µE and 22°C were identified for $C_{c,g}$, I and T respectively, with μ and R_c reaching 1.53 day^{-1} and 1000 mg L^{-1} d^{-1} respectively along with associated nutrient removal of 100%. Regression analysis indicated a good fit between experimental and model data.

The current study demonstrates optimization of microalgae cultivation conditions using BBD-RSM as offering a useful means for simultaneously improving CO_2 fixation and nutrient removal in a single experimental campaign. In the case of real wastewaters the impact of organic carbon would need to be considered, as discussed in Chapter 4.

Chapter 7

Modelling algal photobioreactors for CO_2 bio-fixation and nutrient removal

7.1 Introduction

7.1.1 Algal photobioreactor key system facets

Environmental and operational factors, nutrient load and light irradiation have a direct influence on biomass productivity in an algal photobioreactor (PBR). Effective and efficient microalgae cultivation relies on a number of fundamental system properties which include (i) distribution of light dose throughout the biomass, (ii) enhanced CO_2 mass transfer from the gas to liquid phase, (iii) enhanced CO_2 assimilation by the algal biomass (largely achieved through (i)), and (iv) effective removal of O_2 generated during the photosynthetic process which may otherwise inhibit the algal growth [13]. Carbon dioxide functions as the carbon source for most algae, with the assimilated carbon contributing about 50% of the algal biomass. The local carbon dioxide concentration at any point of a bubble column PBR should be above the minimum threshold to sustain photosynthesis to avoid carbon limitation based on the cultivation conditions [42]. It has reported that a CO_2 gas concentration of at least 1% needs to be provided to sustain the algal biomass [286], such that atmospheric CO_2 levels (0.03%) are insufficient for supporting a high algal growth rate and biomass productivity in large scale process [287]. However, it is the CO_2 load and transfer which represents the limiting factor, rather than the concentration, and sustainable PBR operation also depends on control of dissolved oxygen accumulation [288, 289].

As with all microorganisms, algal species demand various nutrients to support growth, of which nitrogen (N) and phosphorus (P) are the most important. The total N and P concentrations (*TN* and *TP*), relative to that of the algal biomass, may thus determine both algal growth and the corresponding nutrient depletion rate through their bio-assimilation, as sustained by the light irradiation and the availability of dissolved CO_2 [139]. Nitrogen starvation conditions have been extensively applied for maintaining metabolic fluxes to lipids [223] leading to protein synthesis, the excess photosynthesized carbon being stored as triacylglycerides or starch [224].

Light intensity and photoperiod cycle (i.e. the relative durations of the light and dark periods) are crucial factors in determining algal growth rate, especially for photoautotrophic cultures [32, 225]. Inefficiencies arise when microalgae are exposed to light intensities above the saturation limits, as a result of photo-inhibition or overheating. Against this, at high algal cell densities commensurately higher light intensities are required to ensure light penetration through the bulk of the culture [33].

Microalgal PBR processes thus present a number of challenges for control and optimization. Mathematical models are thus needed which are capable of quantifying the impact of practical

system parameters such as bioreactor configuration, CO_2 mass transfer, carbon and nutrient uptake and water quality (pH, temperature, etc) on microalgal growth.

7.1.2 Previous mathematical model studies

Many different studies have been undertaken to establish a mathematical model to successfully predict algal growth in batch system. These have included:

- the fitting of experimental data to a biokinetic model for a batch PBR [290];
- the representation of the impact of light intensity (attenuated by culture media depth) and temperature on the photoautotrophic growth of *Cyanothece* [291] (and subsequent scale-up to pilot scale for biomass production [292, 293];
- the optimisation of nutrient removal by microlagae, calibrated and validated with both repirometric and titrimetric data [292];
- the construction and experimental validation of a model of microlagae biomass and lipids accumulation in a PBR using initial *TN*, light intensity and temperature as the primary inputs [293]
- a simple model to predict biomass values, using kinetic growth parameters, as a function of HRT to maximise biomass productivity in a continuous PBR [294].

Despite the large number of mathematical models presented in the literature to simulate PBRs, no models have been proposed which comprehensively incorporate all phenomena relevant to combined biomass growth and nutrient removal from wastewater. Most of the published models, including the most recent [292], do not address the effects of the initial nutrient concentration on both the treated wastewater quality and algal growth. Whilst the classic mathematical dynamic model of microalgae growth proposed by Droop [295, 296] accounts for the dilution rate and effects of inorganic nitrogen concentration, the impact of all other parameters (including CO_2 gas concentration $C_{c,g}$, light irradiation intensity I, and the nutrient uptake rate) is neglected. Models have otherwise been developed for lipid synthesis as it relates to algal growth rate and N uptake [297], and luxury uptake of phosphorus as polyphosphate as a function of the available P, light intensity and temperature so as to provide P removal efficiency[298]. Thus, whilst a wide range of base parameter values that have been employed in these models (Table 7.1), these have not led to the same sort of treated effluent nutrient concentration profile outputs as provided by classical biological nutrient removal (BNR) models [5].

There is an evident need for a numerical mathematical model capable of simulating algal growth rates as a function of initial *TP*, *TN* including the influence of $C_{c,g}$ and *I*. Such a model could then be employed to estimate nutrient removal and predicated dynamic behavior of a batch system.

Table 7.1 Parameter values assumed in recently-published PBR mathematical models, batch processes

μ_{max} maximum specific growth rate; k_d biomass loss rates; Q_g gas flow rate; vvm = volume gas per volume liquid

PBR configuration	μ_{max} (d^{-1})	k_d (d^{-1})	$C_{c,g}$ (%v/v)	Q_g (vvm)	*HRT* (d^{-1})	$K_{l,C}$ (d^{-1})	*TP*, (mg L^{-1})	*TN*, (mg L^{-1})	*TC*, (mg L^{-1})	*T*, (C^o)	*I*, ($\mu E\ m^{-2}\ s^{-1}$)	*Ref.*
Classical PBR	0.1-0.52	--	0.03[a]	0.5	3.3[s]	--	12.7	54.58	384[c]	20±3	90	[290]
Tubular PBR	1.75	--	10	0.028	1.36[b]	--	--	--	--	25-37	275-23	[291]
Flat plate PBR	0.156	--	--	--	1-10[b]	--	--	--	--	23	150	[299]
Bubbled PBR	--	--	0.03[a]	--	280	--	1.12	12	--	25	250-30	[300]
Breeding reactor	0.1-2	--	0.03[a]	--	--	5-10	4	6	--	26	130-90	[292]
Combine algal unit	0.1-11	--	2	2.5	--	0.3-19	--	--	--	20	90	[301]
Solix PBR	0.6	0.01	2.5		65	--	1.12	12	--	21-24	200	[293]
Helical PBR	1.77	--	4	0.047	15-2.5[b]	--	5	260	5	24-33	156	[302]
BIOSTAT PBR	0.52	--	10	16	2.5	--	--	--	--	25	--	[303]
Flat panel PBR	0.94	--	5	0.63	3.4-1.1[b]	1.63	31	--	--	20	250	[294]

per minute; HRT hydraulic residence time; $K_{l,C}$ CO_2 mass transfer rate; TP total phosphorus; TN total nitrogen; TC total carbon; I irradiation intensity, T temperature; [a]Atmospheric level; [b]Continuous or [s]semi continuous system; [c] COD.

7.2 Materials and methods

More details related to experimental settings, procedures and analysis have been mentioned in Chapter 3. The model was initially parameterized using values and ranges taken from literature, modified according to the values used in the current study for *N*, *P*, *C* and light intensity. The range of values selected were 6-8 mg L^{-1} for P, 28-270 mg L^{-1} for N, 0.03-5% for CO_2 and 180-250 µE for *I*. These ranges of values were considered appropriate for examining the model applicability to a real life scenario for combined CO_2 fixation and wastewater treatment in a full-scale installation.

The initial pH value was maintained within the range 6-8 using 0.1 M HCl and 0.1 M NaOH [270], and through control of the CO_2 gas concentration injected into the cultivation media.

7.2.1 Modelling equations

The model development proceeded through the steps indicated in Figure 7.1. The mathematical model used to simulate the experimental data in this study was based on the classical homogenous model for a bubble column PBR operated in batch mode [302]. The model was developed as a set of parameterized nonlinear first order differential equations defined by fundamental physical and/or chemical mechanisms and base experimental data. Biological, gas and liquid phases considered in the PBR and mass balance equations were derived according to the following assumptions:

- All cultivation conditions factors affecting *Chlorella vulgaris* growth were encompassed, including gas flow rate, light intensity, temperature, feed water quality.

- The Henry constant (H) was considered to be unaffected by the gas pressure: values were taken at 25°C and atmospheric pressure for both CO_2 and O_2.

- Microalgal cells were assumed to be able to fix dissolved inorganic carbon regardless of its form (i.e. CO_2, HCO_3^- and CO_3^{2-}).

- The light intensity was sufficient to ensure growth without being impaired by dissipation by the biomass concentration but not so excessive so as to cause light limitation, with the threshold biomass concentration assumed to be 1 g L^{-1} [42].

- Light inhibition (due to excessive irradiation levels of 500-2500 µE m^{-2} s^{-1} [304, 305] was ignored; a range of 100-250 µE m^{-2} s^{-1} light irradiation range was employed.

- Operation was assumed not to be limited by the nutrient or carbon concentration. The culture media were continuously aerated with air and CO_2 gas during cultivation to provide adequate carbon for the algal cells. A cultivation period of 10 days was selected to prevent N and P nutrient limitation.

Some simplifying assumptions were made in developing the model to reduce the complexity of the model parameters:

- The gas flow rate was considered to remain constant with time and culture depth: the gas was assumed to be uniformly distributed in the cultivation medium.

- Spatial analysis was assumed to be negligible due to the small batch photobioreactor used (250 ml).

- Oxygen inhibition was ignored, since it was removed to low levels in the experimental tests.

- A batch growth culture was considered, although the model could be readily adapted to a semi-batch or fed-batch reactor.

- Only autotrophic growth from light irradiation was considered: other possible growth mechanisms were ignored.

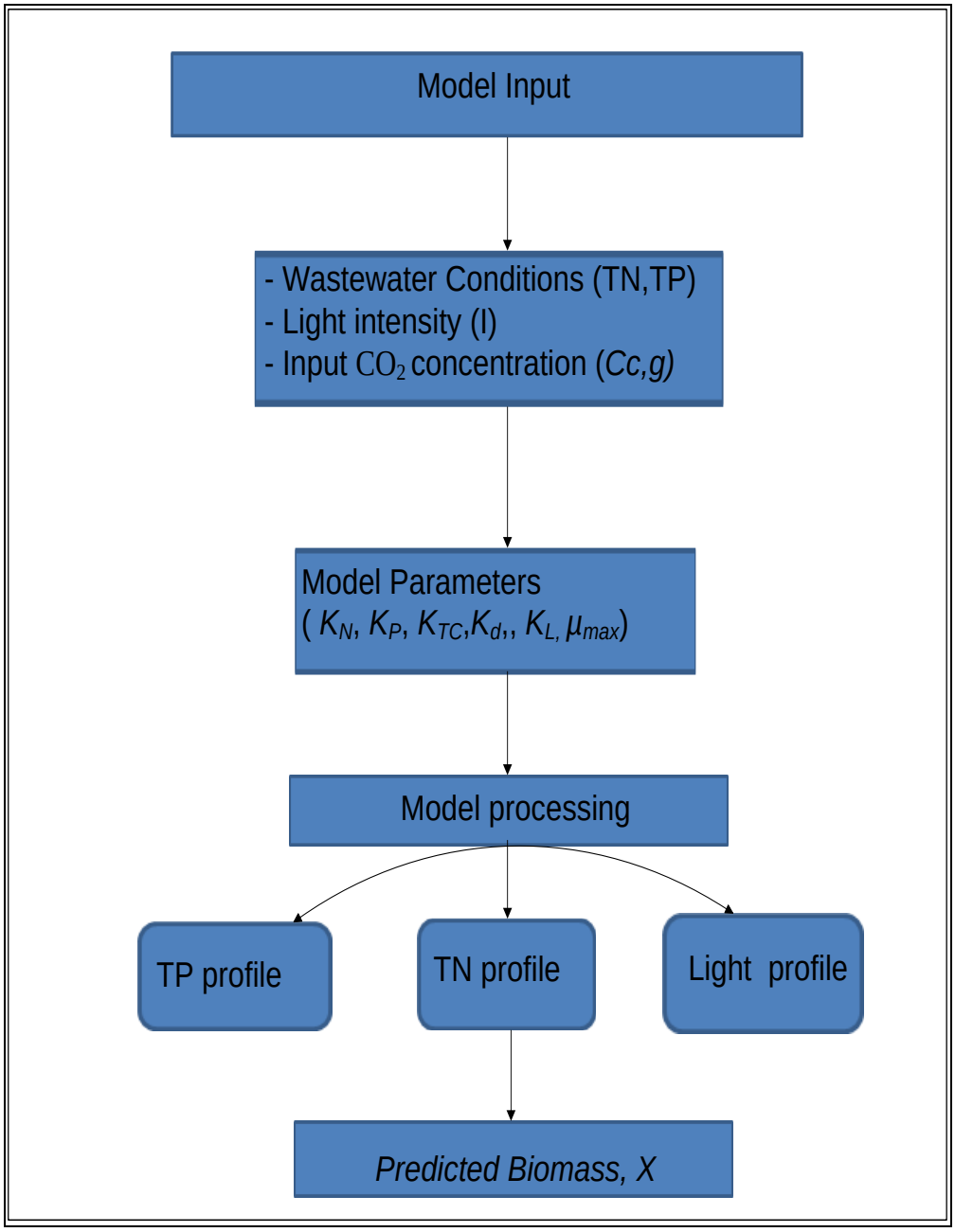

Figure 7.1 Modelling strategy

7.2.2 Gases dynamics in liquid phase of PBRs

The rate of CO_2 transferred from the gas to liquid phase is represented by dual-film theory [306]:

$$R_C = k_C (C_s - C) V (1-\varepsilon) \quad \textbf{(7.1)}$$

Where k_C is the mass transfer coefficient for the transfer of CO_2 from the gas phase to bulk culture phase, C_s is the saturated concentration of CO_2, C is the concentration of inorganic carbon, V the reactor volume and ε the gas hold up. According to Henry's law, C_s can be evaluated using Eqs.(7.2).

$$C_s = \frac{p\,y}{RTH} \mathrm{MW}_{\mathrm{HCO3}} 1000 \quad \textbf{(7.2)}$$

where p is the pressure, y is the gas phase CO_2 fraction, R is the gas constant, T is the temperature, H is the Henry's Law constant and $\mathrm{MW}_{\mathrm{HCO3}}$ is the molar mass of bicarbonate, 1000 is a conversion factor to convert (g L^{-1}) into (mg L^{-1}). k_C can be estimated from correlations available [307] for the transfer coefficient for oxygen k_O using the aqueous phase diffusivities of CO_2 and O_2 (D_C and D_O respectively):

$$k_C = k_O \sqrt{\frac{D_C}{D_O}} \quad \textbf{(7.3)}$$

ε was estimated by volumetric expansion as proposed by Chisti [58] based on the gassed and un-gassed height of fluid (h_G and h_L respectively) in each part of the PBR:

$$\varepsilon = \frac{h_G - h_L}{h_G} \quad \textbf{(7.4)}$$

The uptake rate of carbon (dC/dt) by the algal culture can be expressed as a function of biomass concentration (X), the yield coefficient (total carbon consumed per algal biomass produced $Y_{C,tot}$) and μ_X, the algal specific growth rate:

$$\frac{dC}{dt} = -1000 Y_{C,tot}\, \mu_X X \quad \textbf{(7.5)}$$

The total carbon dissolved in the algal culture can be obtained from subtract equations (7.1) and (7.5).

$$\frac{dC_{total}}{dt} = k_C\,(C_s - C)\,V\,(1-\varepsilon) - 1000\,Y_{C,tot}\mu_X X \qquad \textbf{(7.6)}$$

With appropriate initial conditions of:

$$\left[C_{total}\right] = \left[C_{init,total}\right] \text{ at t=0} \qquad \textbf{(7.7)}$$

The first term on the right hand side of Eq. (7.6) takes into account mass transfer phenomena from the gas to liquid phase and the second term is the CO_2 consumption and concomitant liquid phase microalgae production process.

The mass balance for total dissolved nutrients (N and P) not involved in the gas liquid mass transfer phenomena can be expressed as follows:

$$\frac{dC_{N,P}}{dt} = -1000 Y_{N,P}\,\mu_X\,X \qquad \textbf{(7.8)}$$

With appropriate initial conditions:

$$\left[N,P\right] = \left[N_{init}, P_{init}\right] \qquad \textbf{(7.9)}$$

7.2.3 Biomass growth rate

The final growth rate of algal biomass, *dX/dt*, can be written as:

$$\frac{dX}{dt} = \mu_X\,X - K_d X \qquad \textbf{(7.10)}$$

Where K_d is the biomass loss rate. According to Monod model [308] the nutrient-limited algal growth rate μ_X can be expressed as

$$\mu_X = \mu_{\max}\left[\frac{S_i}{K_i + S_i}\right] \qquad \textbf{(7.11)}$$

where S_i is the nutrient (*N* or *P*) concentration, K_i the nutrient half saturation constant and μ_{max}, the maximum specific growth rate.

The following integrated Monod model considering the effect of multiple factors (*N*, *P*, *C* and light intensity) on the specific growth rate of the algae was proposed by extending Equation (7.11):

$$\mu_X = \mu_{max}\left[\frac{S_N}{K_N + S_N}\right]\left[\frac{S_P}{K_P + S_P}\right]\left[\frac{TC_c}{K_{TC} + TC_c}\right]\left[\frac{I_{av}{}^n}{K_L{}^n + I_{av}{}^n}\right] \quad \textbf{(7.12)}$$

where S_N, S_P, TC_c are the respective N, P and total carbon concentrations in the culture and K_N, K_P , K_{TC} , K_L are the corresponding half saturation constants for nitrogen, phosphorus, total carbon and light respectively. The average light intensity I_{av} within the culture in cylindrical bubble PBR illuminated by a unidirectional parallel flux can be expressed by:

$$I_{av} = \frac{2I}{r\,K\,X\,\pi}\left[1 - \int_0^{\pi/2}\cos(\theta)\exp(-2rKX\cos(\theta))d\theta\right] \quad \textbf{(7.13)}$$

Where *r* represents the PBR radius. *K* is the overall light extinction coefficient, given by:

$$K = K_c\,C_{chl} + K_w \quad \textbf{(7.14)}$$

where K_c is the chlorophyll-based light extinction coefficient of algae, C_{chl} is the chlorophyll concentration, which is a function of biomass concentration and is determined experimentally, and K_w is the light extinction coefficient of pure water.

A schematic drawing of a completely mixed photobioreactor and the elements included in the model is shown in Fig 7.2.

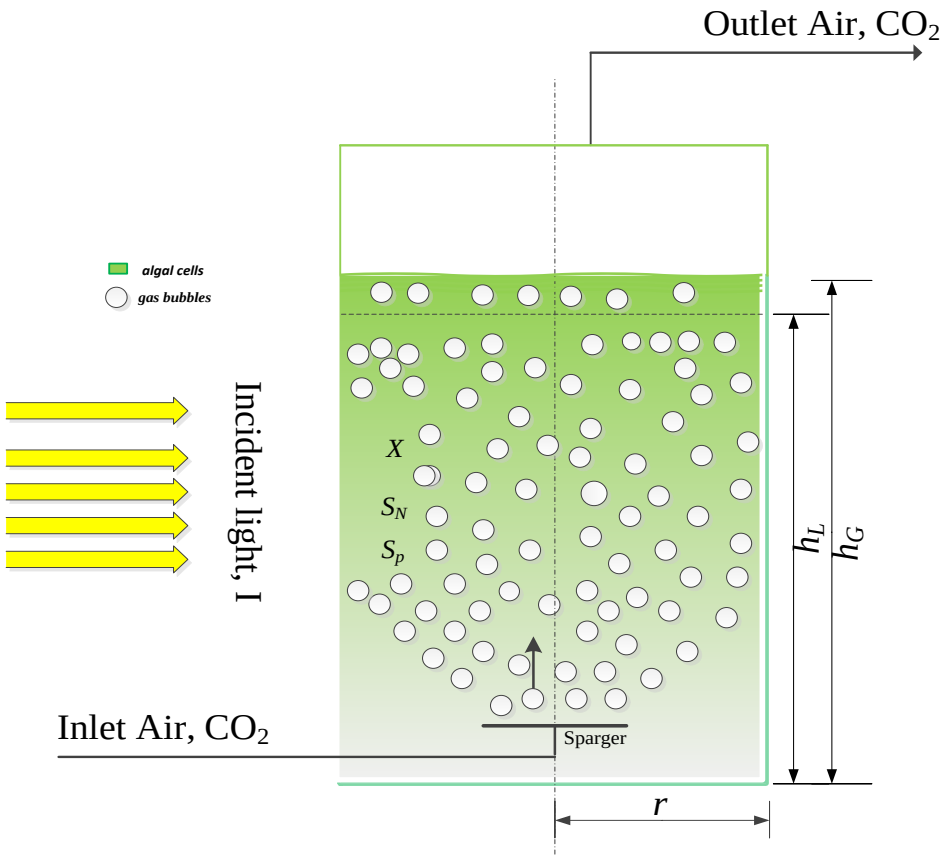

Figure 7.2 A schematic drawing of the photobioreactor and the elements included in the model.

The combined set of ordinary differential equations (*ODEs*) were coded in MATLAB to combine the time-dependent algal biomass concentration X (g L^{-1}) and algal nutrient uptake functions with light intensity, and the simulations validated with the experimentally-determined *Cv* growth data. A sensitivity analysis of a parameter P_j was conducted with respect to X to assess the response of biomass concentration to changes in each model parameter to assess the validity of the simplifying assumptions (Section 7.2.1):

$$\sigma_x = \frac{\Delta X}{\Delta P_j}\frac{P_{jnom}}{X_{nom}} \qquad \textbf{(7.15)}$$

where P_{jnom} is the parameter nominal value and X_{nom} the model response when nominal parameters are used. A ±20% variation in ΔP_j was applied to obtain the test values to determine ΔX. Four biomass profiles were used in calculating the mean profile with the standard deviation estimated from the four runs. The sensitivity coefficient for each parameter was calculated from the average spread according to the method of Bernard et al. [309].

An F–test was performed to determine the variance between the predicted and measured values using *Jmp* statistical discovery software (*SAS version 11.2.1*).

7.3 Results and discussion

7.3.1 Mass transfer coefficient

k_C was estimated from k_O data using Equation 7.3. A previous reported correlation for bubble columns [203, 310] was used to calculate k_C in terms of ε measured at the corresponding gas flowrate. This procedure produced a k_C of 5.8×10^{-6} s^{-1} at a gas flowrate of 50 mL min^{-1}, towards the low end of the range of values reported in the literature of 3.8×10^{-6} s^{-1} [301] for different PBR configurations.

7.3.2 Model calibration

The influence of the parameters TN_{init}, TP_{init}, I and $C_{c,g}$ on the kinetics of Cv was determined through mathematical simulation, and the reliability of the model data assessed using validatory experimental test data. Further experiments were carried out to evaluate the influence of the initial concentrations of dissolved inorganic carbon, N and P on algal growth by varying respectively the concentrations of sodium bicarbonate, sodium nitrate and potassium bisphosphate in the MLA cultivation medium. The feed gas $C_{c,g}$ was also varied at a constant Q_g of 50 mL min^{-1}. A pH 6-8 was maintained throughout.

The proposed model (combining growth and light profile) was fitted to experimental data conducted under different conditions (TP=6 mg L^{-1}, TN=28 mg L^{-1}, CO_2=2.5 % , I= 250 µE m^{-2} s^{-1} and TP=6 mg L^{-1}, TN=28 mg L^{-1}, CO_2=0.03 % , I= 250 µE m^{-2} s^{-1}). Calibration was through determination of μ_{max} from Equations 7.8 – 7.13 tuned through a nonlinear fitting procedure, with the parameters estimation based on non-linear least square fitting of the model-predicted data to that derived from experiments conducted at different conditions, the relative error obtained by the fitting procedure was around 1%. These parameters (K_L, $K_{TC,}$ K_N, K_P, K_d, K_C, K_w, n) were then numerically ed to obtain a best fit of the model to experiment data (Fig. 7.3) using the simplex search algorithm of MATLAB [311].

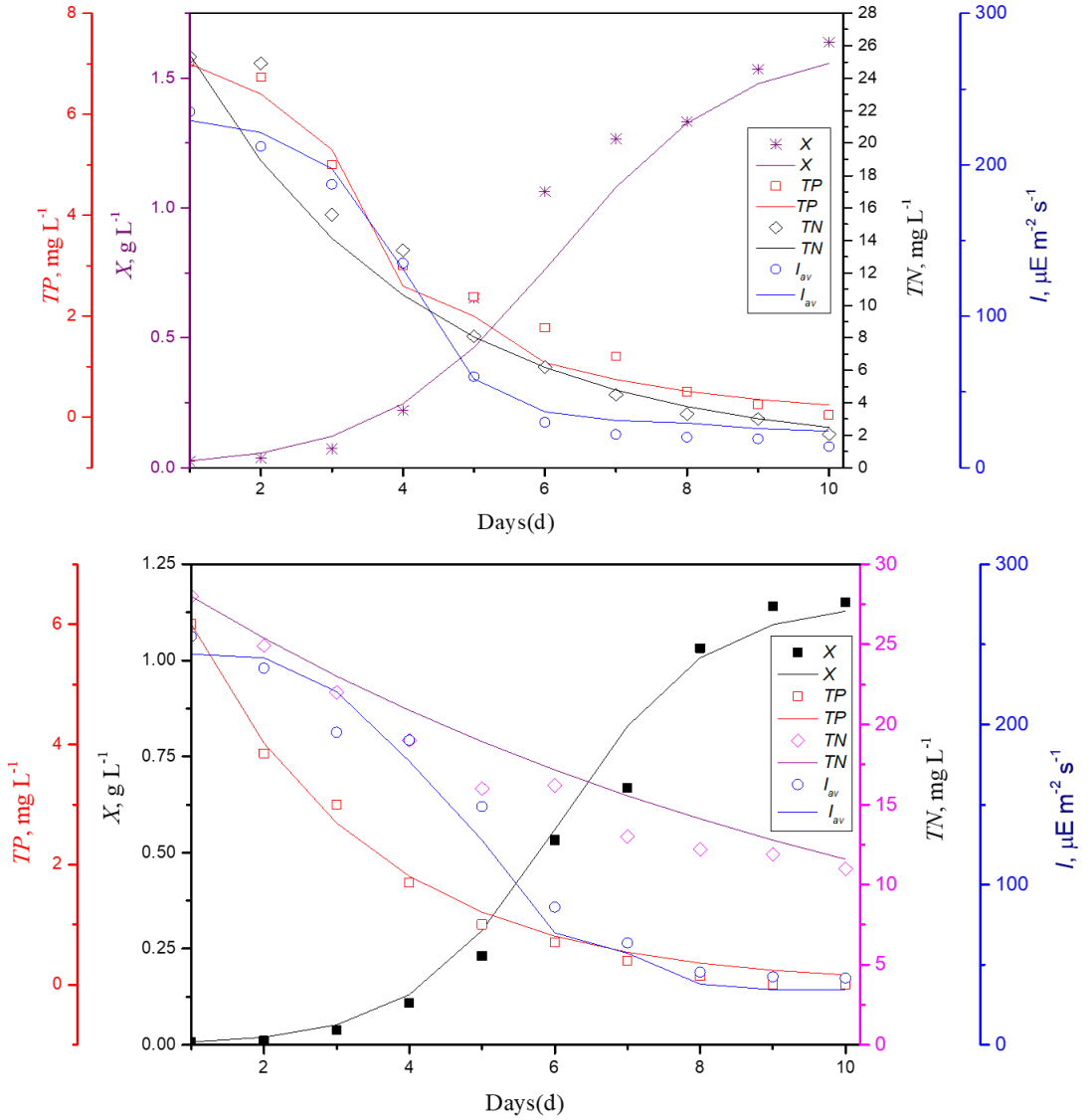

Figure 7.3 Model calibration and fitting for different cultivation conditions (a) *TP*=6 mg L^{-1}, *TN*=28 mg L^{-1}, CO_2=2.5 % , *I*= 250 µE m^{-2} s^{-1} and (b) *TP*=6 mg L^{-1}, *TN*=28 mg L^{-1}, CO_2=0.03 % , *I*= 250 µE m^{-2} s^{-1}.

Best-fit values generated by simulation during the calibration process for estimated parameters are shown in Table 7.2.

Values for the shape factor parameter *n*, accounting for light limitation caused by the biomass density, were adjusted according to the assumptions presented in Section 7.2.1. The best fit value obtained for *n* was 1.4, this value being slightly outside the range of 1.49-2.2 reported in previous studied [302, 312, 313].

Table 7.2 Summary of base parameters values

Symbol	*Unit*	*Parameter value*	*Notes*
μ_{max}	d^{-1}	1.400	Current study, estimated
K_d	d^{-1}	0.198	Current study, estimated
K_L	µE m^{-2} s^{-1}	16	Current study, estimated
K	m^2 g^{-1}	2.5×10^{-1}	Current study, estimated
K_p	g L^{-1}	4×10^{-2}	Current study, estimated
K_N	g L^{-1}	3.7×10^{-1}	Current study, estimated
K_{TC}	g L^{-1}	5×10^{-1}	Current study, estimated
N	-	1.42	Current study, estimated
$H_{e,C}$	-	8.32×10^{-1}	[314]
$H_{e,O}$	-	3.2×10^{-2}	[314]
Y_{ctot}	g_c $g_{biomass}^{-1}$	5×10^{-1}	Current Study, calculated
Y_p	g_P $g_{biomass}^{-1}$	2.4×10^{-2}	Current Study, calculated
Y_N	g_N $g_{biomass}^{-1}$	2×10^{-1}	Current Study, calculated
Y_O	g_{O2} $g_{biomass}^{-1}$	0.534	[315, 316]
d_B	m	1×10^{-6}	Current Study, calculated
D_C	m^2 s^{-1}	14.7×10^{-9}	[275]
D_O	m^2 s^{-1}	8.0×10^{-9}	[275]
$K_{La,C}$	d^{-1}	0.499	Current Study, calculated
K_w	cm^{-1}	0.0018	[317]

$Y_i = (S_o\text{-}S)/(X\text{-}X_o)$, where $i=c_{tot}, p, N$

7.3.3 Model validation

The model was validated by comparing the experimentally-determined biomass concentration profiles for five sets of experimental conditions (Table 7.3) with model predications using the parameter values determined by the calibration process.

Table 7.3 Set of experiments used for model validation

Parameters	**Exp-1**	**Exp-2**	**Exp-3**	**Exp-4**	**Exp-5**
TP (mg L^{-1})	6	6	6	7	8
TN (mg L^{-1})	28	28	28	70	270
CO_2 (%)	2.5	5	0.03	0.03	0.03
I (µE m^{-2} s^{-1})	250	200	250	180	180

Growth profile data for a range of different initial nutrient concentrations was produced. Within the ranges selected (Fig. 7.4) the validation provides a reasonable fit between the experimental and model data. The base parameters identified (Table 7.2) were thus used for subsequent sensitivity analysis (Section 7.3.4) and nutrient removal profile modelling (Section 7.3.5).

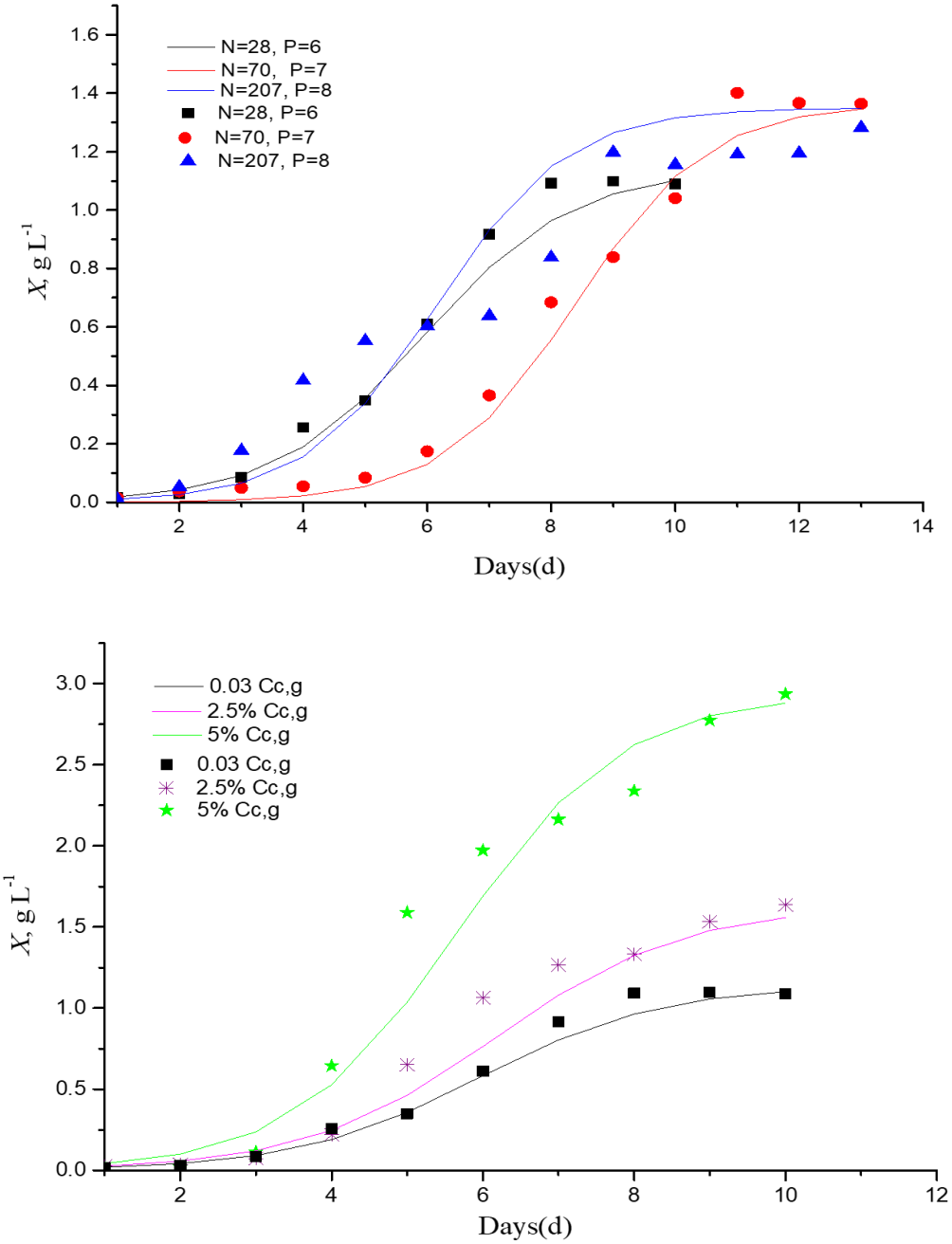

Figure 7.4 Model verification applying different cultivation conditions (a) *TN* = 28-207 and *TP* = 6-8 mg L^{-1} for an air feed ($C_{c,g}$ = 0.03% CO_2); and (b) *TN* = 28 and *TP* = 6 mg L^{-1} for CO_2-supplemented gas feed ($C_{c,g}$ = 0.03-5% CO_2) for experimental (data points) and model (continuous trend) data.

7.3.4 Sensitivity and regression analysis

The sensitivity of the growth profile to the parameters L_k, K_N, TC_K, K_p, K_d and μ_{max} was examined based on the experimental conditions of $C_{c,g}$ = 2.5%, TN= 28 mg L^{-1}, TP= 6 mg L^{-1} and I = 250 µE m^{-2} s^{-1} used for the calibration step. The pre-defined model constants (Table 7.2) were used as base values and individually varied by ± 20% and the impact on X. The mean predicted profile from four runs for each parameter is shown in Fig. 7.5 with the corresponding sensitivity coefficient estimated from Eq. (7.15), with sensitivity increasing with increasing σ_x. According to Fig. 7.5, μ_{max} (σ_x = 0.52) and the biomass loss rate (K_d, σ_x = 0.11) were the most sensitive parameters followed by considerably reduced sensitivity for the half saturation constant for carbon and light at (σ_x = 0.008 and 0.004 for K_{TC} and K_L respectively). Sensitivity to μ_{max} has been previously reported [318] and reflects the importance of this parameter on the accuracy of model prediction. The influence of remaining four parameters on biomass profile was negligible.

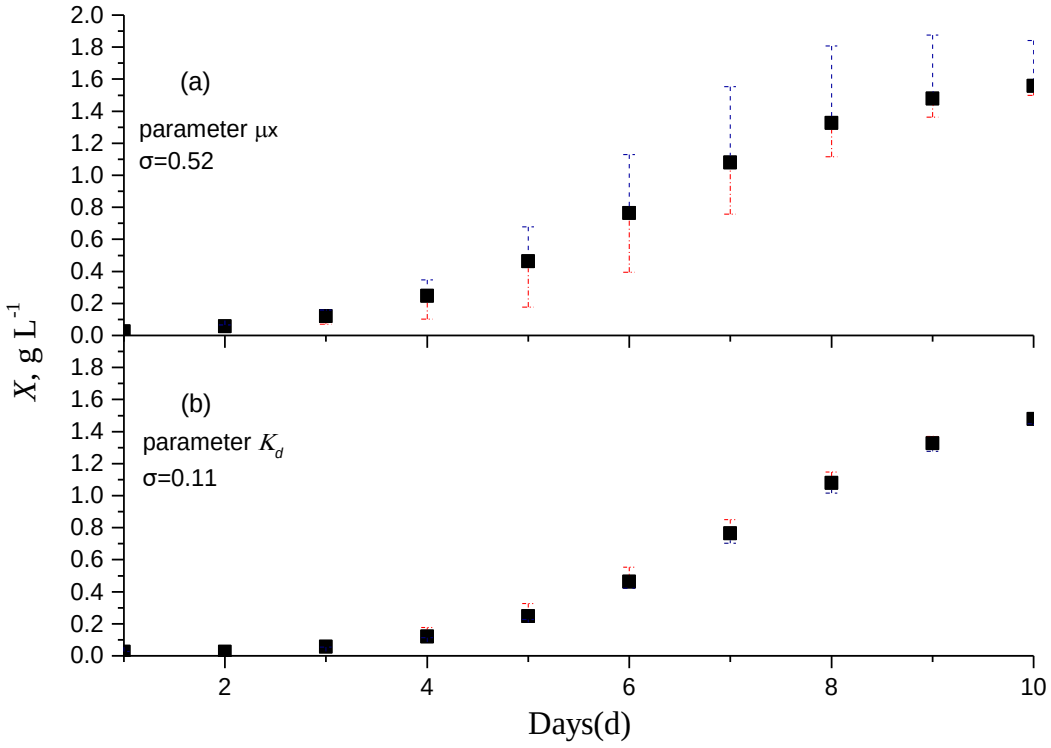

Figure 7.5 Predicted mean algal biomass concentration profile and its variation based on ±20% variation in (a) μ_X, and (b) K_d, based on four runs.

The model was further validated by applying the regression analysis for the experimental and predicted growth profiles using SAS software. Significance of the fits achieved between the

measured and predicated data (Fig. 7.6) is illustrated by R^2 values of 0.94 and *p* values below 0.0001 for the all validated points. The model appears to reflect the growth dynamics at various values of *TN*, *TP*, *I* and $C_{c,g}$ with reasonable accuracy, comparable to that reported by Wang et al. [262] who investigated the kinetics of nutrient removal and characterised the extracellular polymeric substances (EPS) generated. The specific growth rate μ_{max} calculated from Eq. (7.12) was found to be the most sensitive parameter.

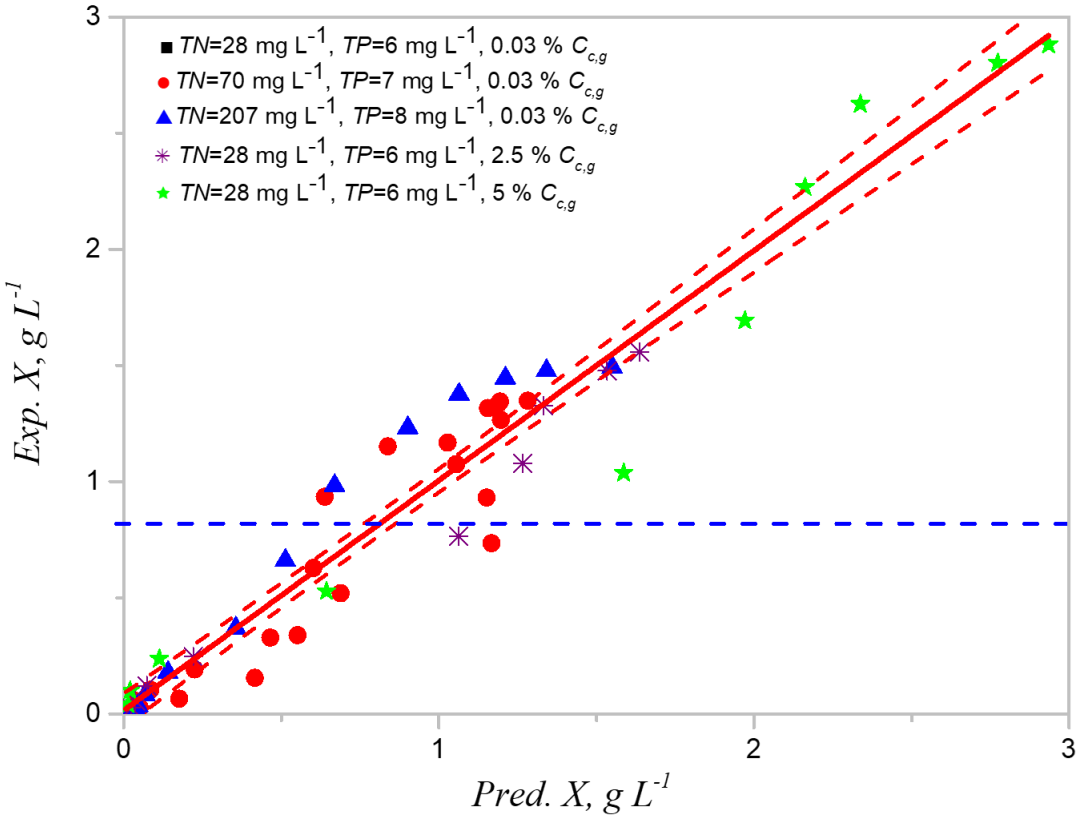

Figure 7.6 Regression analysis of fit between predicted and experimental biomass concentration R^2 = 0.94, P = 0.0001 and p>F = <0.0001 (i.e. significant). Dotted curved lines indicate >95% confidence bands; horizontal dotted lines represent mean of the Y leverage residuals (i.e. the measure of agreement with the model).

7.3.5 Nutrient removal

The evolution of nutrient uptake and algal growth kinetics as a function of TN_{init} and TP_{init} was modelled and the outputs compared with experimental data. Modelled outputs were based on Eq. (7.8) and encompassed the yield coefficient for total N or P ($Y_{N,P}$), μ_x and biomass concentration *X*, each of these parameters directly affecting the nutrient uptake rate.

Nutrient consumption transients (Fig. 7.7a-d) indicated rapid removal of P to 100% removal, such that it becomes limited by around 6 days at the lowest TP_{init} of 6 mg L^{-1} (Fig. 7.7a). Whilst the extracellular phosphorous is depleted rapidly in the cultivation medium, the cells continued to grow over the period of the experiment (Fig. 7.7a). The luxury uptake of nutrients and storage for later growth is a well-established phenomenon in phytoplankton [296], although this does not influence the P uptake rate. *TN* removal efficiencies of 80-99% were recorded after 10-13 days for TN_{init} concentrations up to 70 mg L^{-1}, whilst only 60% of the *TN* was removed after 13 days at the highest TN_{init} employed of 207 mg L^{-1} (Fig. 7.7c). The model appears to adequately predict the dynamic depletion of *TN* and *TP* in the cultivation medium, along with algal biomass production (Fig. 7.6), over the ranges of initial nutrient concentration (Figs. 7.7a,c) and feed gas CO_2 concentration (Figs. 7b,d) studied.

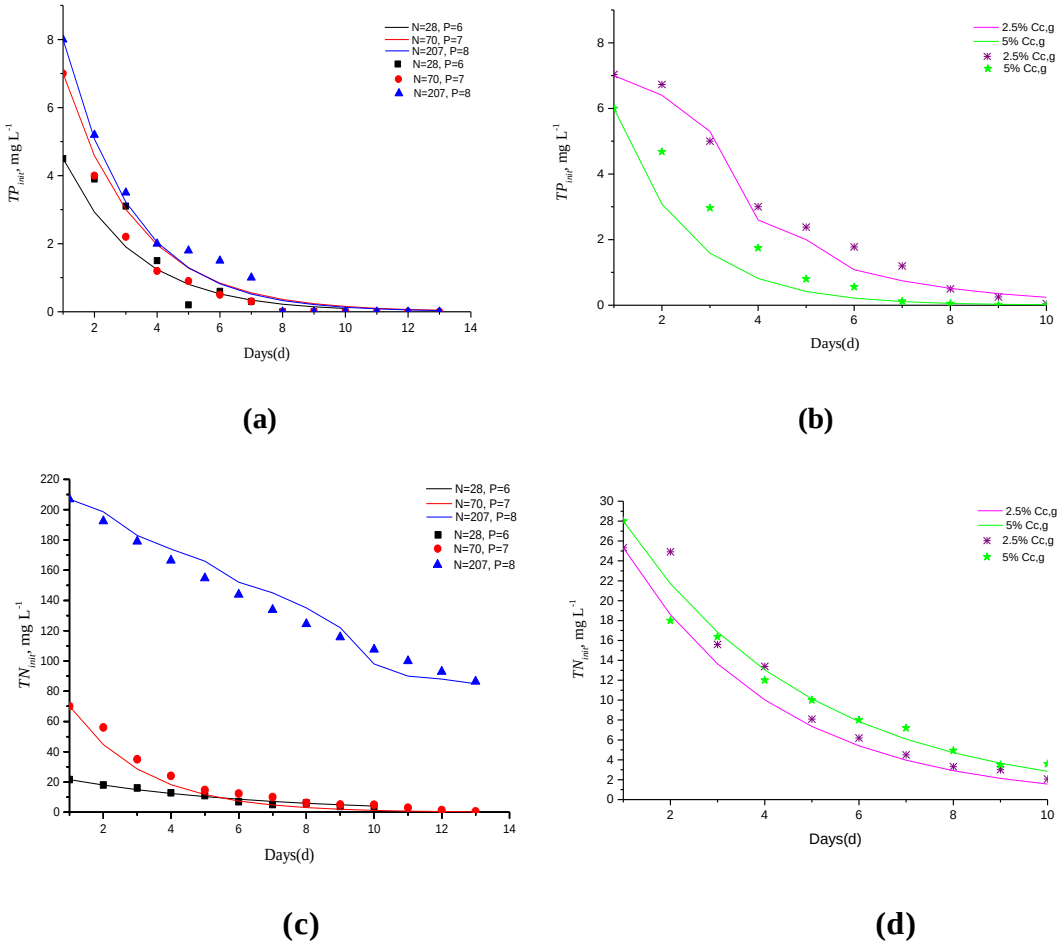

Figure 7.7 Evolution of total nutrient concentration under different conditions of initial aqueous nutrient concentration (a, c: $C_{c,g}$ = 0.03%,) and feed gas CO_2 concentration (b, d: TP_{init} and TN_{init} = 6 and 28 mg L^{-1} respectively).

7.3.6 Light attenuation profile

The predicted average irradiance I_{av} profiles over the course of the test period are shown in Fig.7.8. In all cases examined it was confirmed that the limiting step for autotrophic PBR operation was the availability of light energy: the maximum productivity is dictated by rate at which the light can be absorbed and transformed into biomass.

There was a reduction in biomass concentration (of 1.6 and 2.9 g L^{-1}) when the microalgae cells were illuminated at 200 and 250 μE m^{-2} s^{-1} and fed with 5 and 2.5% CO_2 gas respectively. Evidence therefore suggests that for irradiance values above the light saturation point photo-oxidation takes place, damaging the photosystem and inhibiting photosynthesis and microalgae growth [319]. Under such circumstances, the photo-inhibition rate (which takes place at all irradiance values) exceeds the rate of repair of the algal cells [320]. However, below the light saturation point the expected proportional increase in biomass productivity and in CO_2 uptake, from photosynthesis, with increasing light irradiance was observed. The photosynthetic rate is greater at lower biomass concentrations due to the increased light availability associated with the higher light transmission through the suspension.

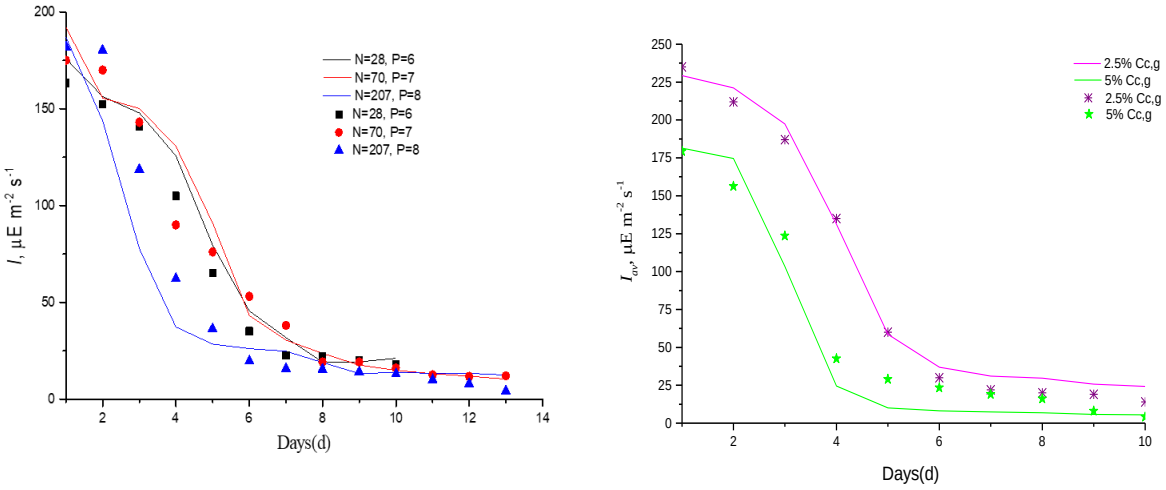

Figure 7.8 Average irradiance I_{av} profile during experiment period of 10 days in dished line and the predicated response in solid line.

7.4 Summary

A comprehensive mathematical modeling method for *chlorella vulgaris (Cv)* has been developed to assess the influence of nutrient concentration (total nitrogen *TN*= 28-207 and total phosphorus *TP*= 6-8 mg L^{-1}) and irradiation intensity (*I* = 100-250 μE) at feed gas CO_2 concentrations ($C_{c,g}$) of 0.04-5 %. The model encompasses gas-to-liquid mass transfer, algal uptake of carbon dioxide (C_d), nutrient removal efficiency (*RE* for *TN* and *TP*), and the growth biokinetics of *Cv* with reference to the specific growth rate μ in d^{-1}.

The model was validated using experimental data on the *Cv* species growth in an externally illuminated photobioreactor (PBR). The fitted parameters of the model were found to be in good agreement with experimental data obtained over the range of cultivation conditions explored. The mathematical model accurately reproduced the dynamic profiles of the algal biomass and nutrient (*TN* and *TP*) concentrations, and light attenuation at different input $C_{c,g}$ values. The proposed model may therefore be used for predicting algal growth and nutrient RE for this algal species, permitting both process ation and scale-up.

Chapter 8

Enhancement of CO_2 biofixation and lipids productivity by *chlorella vulgaris* using coloured polypropylene film for light spectral conversion

8.1 Introduction

Microalgae cultivation is strongly influenced by light irradiation conditions, these being ostensibly light intensity, wavelength and irradiation time [78-80]. Generally, reduced light intensity, or its impaired distribution, commensurately reduces algal growth whereas excessive lighting can lead to photo-oxidative damage of the cells [90-93]. There is also an impact on efficiency: low light intensities can lead to photosynthesis efficiencies (PE) of up to 80% of the theoretical maximum of 0.125 mol CO_2 fixed per mol photons absorbed [90-93]. However, light utilisation is itself dependent on algal cell concentration. For a high cell-density culture, the light energy is predominantly absorbed close to the photobioreactor (PBR) walls, since it cannot penetrate deep into the bioreactor due to dissipation by the cells. Therefore, the algal cells nearest the reactor walls may be exposed to *I* values beyond the optimum limit which can be completely utilised for biochemical energy through photosynthesis process. This oversaturation leads to light energy lost through heat dissipation [94], resulting in a reduced PE compared with that obtained at lower *I*.

The above implies that optimization may be possible through manipulating the light conditions by providing an improved balance between light capture and the photochemical process [95-97], thereby enhancing the PE. This can be achieved through minimizing the light absorption by shifting the wavelength of emitted light to the weakly absorbed green region through the use of a light filter (LF) or light emitting diode (LED), as demonstrated in recent studies on the most commonly studied *Chlorella vulgaris* (*Cv*) algal species (Table 8.1). The various pigments in green microalgae that can absorb light energy for photosynthesis at different wavelengths include chorophylls (450-475 and 630-675 nm) and carotenoids (400-500 nm) [50, 98, 321, 322].

A number of literature studies based on attenuating or adjusting the light source suggest that some efficiencies may be gained by employing a narrow range of wavelength (Table 8.1). Both light filters based on rigid acrylic sheets [323] and monochromatic light-emitting diodes (LEDs) [324] have been studied. However, the practical application of such strategies is constrained by capital cost. A potentially low-cost alternative is the use a simple light filter to apply directly to the external reactor walls. Coloured tape (CT) is a biaxial oriented (i.e. extruded in two directions) polypropylene (BOPP) film, and is used for applications as diverse as food packing, pressure sensitive tape, label printing, metallizing and decorative products [325-327]. Its use has been extended to many different applications by coating technology with solvent based acrylic adhesives [23] which make it highly transparent with excellent optical properties [23]. Since the material is produced in different colours, it can be used to filter light to provide the appropriate wavelength.

Table 8.1 Light filter and LED based algal growth studies reported in the literature for *Chlorella vulgaris* (*C. vulgaris*)

LF or LEDs used	*Process desc.*	*Wavelength λ, nm*	*Cult. Med.*	*System Confi.*	*TP_{in}, mg L^{-1}*	*TN_{in}, mg L^{-1}*	*Inlet CO_2 C_{cg}, % v/v*	*Light int, μE*	*X_{max}, g L^{-1}*	*Cd, Cells mL^{-1}*	*μ, d^{-1}*	*RE TP, %*	*RE TN, %*	*CO_2 fixn. rate RC, g L^{-1} d^{-1}*	*Lipids pr. P_{lipids} mg L^{-1} d^{-1}*	*HR T, d^{-1}*	*Ref.*
*Cell p.	Thi.	λ_B, 460	MW	M.B	4	36	0.03[a]	50	0.47	nr	nr	57	72	0.05[1]	0.008[2]	nr	[328]
	3mm	λ_R, 620							0.36	nr	nr	45	42	0.04[1]	0.007[2]		
	Btc Pr	C,620,540,430							0.27	nr	nr	37	38	0.03[1]	0.003[2]		
	LF	λ_G, 540							0.12	nr	nr	35	16	0.01[1]	0.002[2]		
*Lumi	color	λ_G	3N-	nr	31	4.1	nr	200-	nr	43×10^6	0.1	nr	nr	0.05	nr	nr	[323]
AS	dyes	λ_O, 585-620	BBM+					250	nr	42×10^6	0.13	nr	nr	0.05	nr		
	Btc Pr	λ_R, 600-700	V						nr	36×10^6	0.07	nr	nr	0.02	nr		
	LF	λ_v, 400-450							nr	43×10^6	0.11	nr	nr	0.05	nr		
*Lumi	color	λ_B	3N-	BCPBR	31	4.1	0.03[a]	250	nr	41×10^6	0.5	nr	nr	0.21	nr	90-	[329]
AS	dyes	λ_G	BBM+						nr	43×10^6	0.51	nr	nr	0.25	nr	45	
	Btc Pr	λ_Y	V						nr	41×10^6	0.36	nr	nr	0.22	nr		
	LF	λ_O							nr	40×10^6	0.37	nr	nr	0.21	nr		
		λ_R, 600-700							1.5	45×10^6	0.42	nr	nr	0.24	nr		
LED	W= 26	λ_R, 620-630	SDS	EF	5.2	43	nr	1000	0.28	nr	nr	41	55	0.0484	nr	42	[324]
	mm	λ_Y, 590-600							nr	nr	nr	nr	nr	nr	nr		
	L= 600	λ_B, 460-470							nr	nr	nr	nr	nr	nr	nr		
	mm	λ_G, 525-550							nr	nr	nr	nr	nr	nr	nr		
	Btc Pr	λ_W, 380-760							nr	nr	nr	nr	nr	nr	nr		
LED		λ_B, 460	Z8	nr	nr	nr	0.03[a]	100	0.81	nr	nr	nr	nr	0.20	0.013[2]	nr	[330]
		λ_G, 535							0.63					0.16	0.009[2]		
		λ_Y, 585							1.59					0.40	0.031[2]		
		λ_R, 620							1.26					0.31	0.021[2]		
		λ_W, 400-700							1.33					0.33	0.026[2]		
LED	Btc Pr	λ_B, 430-460	MJ	EF	nr	nr	0.03[a]	100	0.78	17.5×10^6	nr	nr	nr	0.27**	nr	nr	[331]
		λ_R, 620-665							0.84	25×10^6	nr	nr	nr	0.29**	nr		
		λ_W, 400-700							0.8	20×10^6	nr	nr	nr	0.28**	nr		

LED= light emitting diode ;* = normal external light source used, otherwise indicated; LF= light filter; Lumi AS= Luminescent acrylic sheets contains dyes; Cell p.= cellophane papers; Process desc= process description; char.=characterization; cult.med.= cultivation medium; Btc Pr = batch process; thic.=thickness; pr.=production; MW= municipal wastewater; M.B= media bottle; Btc P= batch process; λ= wavelength number, B=blue, R= Red, C= control, G= green, O=Orange, V= violate, Y= Yellow, W= white, SDS= synthetic domestic sewage; W= width; L= length; EF= Erlenmeyer flask; Z8= standard medium for green algae; MJ= standard cultivation medium; 3N-BBM+V= bold basel medium; BCPBR= bubble column photobioreactor; HRT = hydraulic residence time, [a]Atmospheric level, [1]= calculated from *Rc* = CO_2 fixation rate which estimated from Chisti ratio: $CO_{0.48}H_{1.831}N_{0.11}P_{0.01}$; *Rc* = 1.88 × P_x, P_x = biomass productivity which estimated from $\Delta X/\Delta t$,[2]= calculated from Eqs.1; Not reported= nr..

The current study employs a range of CTs to filter light to attain a specific λ_{max} and accompanying *I*. The impact of the changing light characteristics on algal growth, nutrient removal, CO_2 fixation and lipid productivity has then been evaluated, with the intention of potentially using the material as a potentially low-cost means of attenuating natural light.

8.2 Material and methods

Experimental details relating to the set-up, procedures and analysis are provided in Chapter 3, with details of the CT tests specifically given in Section 3.6. The standard deviation and mean data were analysed for significance using *JMP* statistical discovery software (SAS V11.2.1) though one way ANOVA. Results are reported as mean ± SD numerically or graphically as error bars.

8.2.1 Coloured tape light filter (CT)

To evaluate the effect of light wavelength on wastewater treatment and microalgae growth, coloured tape (CT) of different colours (red, blue, yellow, green and white) was used to filter the light. CT spectral characteristics, from spectra analysis software (Jasco *V-670*, JASCO Corporation, Japan), indicated them to produce illumination mainly in the visible range (Fig. 8.1, Table 8.2) from a Deuterium Lamp (L64081, Deuterium Lamp, Japan) source. A spherical light meter was used to measure the light intensity in three different positions around the CT-wrapped PBR (front, middle and behind). The mean and standard deviation values were then determined (Table 8.2).

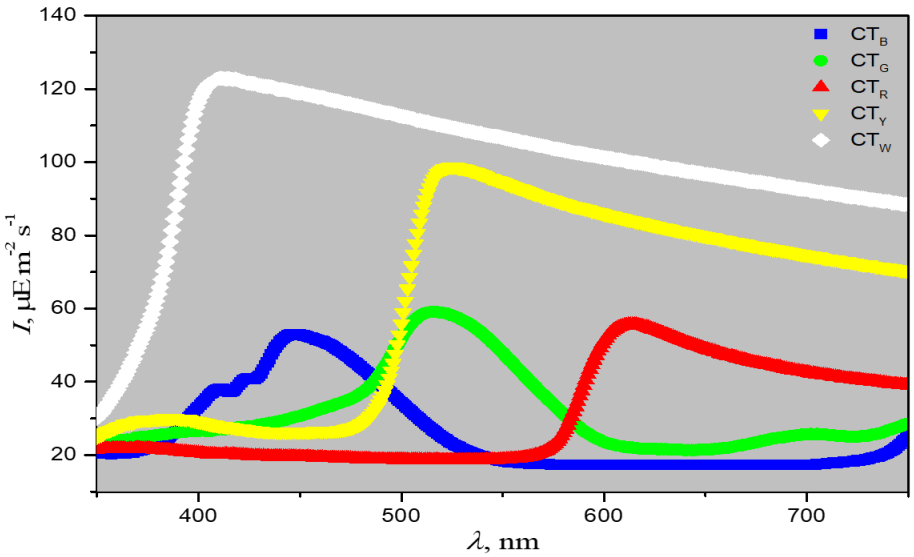

Figure 8.1 Light intensity (*I*) variation at different wavelength (λmax) CT of various colours: white (CT_W), blue (CT_B), green (CT_G), yellow (CT_Y), and red (CT_R) at fixed extrneal light intesity (I_E) of 250 µE.

The biomass concentration (X), specific gowth rate (μ) and the *Chlorella vulgaris (C. vulgaris)* cell density (C_d) were evaluated at different wavelengths using the selected filtered light (I_f) sources, namely CT_B, CT_G, CT_R, CT_Y and CT_W along with a control using the unfiltered light source (U).

Table 8.2 CT film characterization, 48 mm width, tape

Colored tape (CT_s)	*Wavelength range, nm*	*Peak wavelength λ_{peak}, nm*	*I_f^* for wrapped PBRs*	*CTs photos*
Red, CT_R	575-750	616	63± 9.0	
Yellow, CT_Y	481-750	528	100 ± 5.0	
Green, CT_G	400-600	518	64± 7.0	
Blue, CT_B	345-549	451	55 ± 4.0	
White, CT_W	350-750	413	122 ± 6.0	

*The average values of filtered light were measured at different points of wrapped PBRs, and compared with data obtained by light spectra analysis, as mean ± SD.

8.3 Results and discussion

8.3.1 Influence of *I* and λ_{max} on *Chlorella vulgaris* growth

The highest X of 2.26 g L^{-1} was obtained with CT_W along with μ and C_d values of 0.95 d^{-1} and 54×10^6 cells mL^{-1} respectively (Fig. 8.2). The corresponding values obtained with U were 1.14 g L^{-1}, 0.64 d^{-1} and 28.16 $\times10^6$ cells mL^{-1}. Against this, lower X, μ and C_d values of 0.18 g L^{-1}, 0.45 d^{-1} and 2.8 $\times10^6$ cells mL^{-1} were respectively recorded for CT_B. The values of 1.02 g L^{-1}, 0.61 and 25.9 cells mL^{-1} measured for CT_Y were comparable with those for U and CT_R, with the CT_G values being marginally lower.

CT_w provided a light wavelength range of 750-350 nm, with a peak of 413 nm, and reduced the control I (U) of 250 µE m^{-2} s^{-1} to I_f *of* 122±6 µE m^{-2} s^{-1}. Non-photochemical quenching (NPQ) is known to arise if the rate of photo-inhibition exceeds the rate of repair, resulting in a large proportion of the captured light being dissipated at high I [21]. The lower X and μ values obtained for U suggest that growth is reduced at longer random wavelengths [323]. It has been suggested that the U spectrum supplied for microalgae cells does not necessary cover

the absorption bands of microalgae pigments [332]. U may also contain the absorption bands of chlorophyll pigments of microalgae, or may comprise a combination of growth efficient and inefficient light spectra [321]. Recorded growth rates were higher than those of Kim et al [331], who reported X and C_d values of 0.78 g L^{-1} and 17.5× 10^6 cells mL^{-1} respectively using LED lighting providing a wavelength band of 400-460 nm and an I of 100 µE m^{-2} s^{-1}. Around a 78% reduction in incident I_f to approximately 55±4 µE $m^{-2}s^{-1}$ was recorded for CT_B, decreasing the level of photosynthesis active radiation (PAR) and thus photosynthesis activity accordingly. At lower I up to 80% of the theoretical maximum photosynthesis efficiency (PE) can be achieved [90-93], although a reduced I value results in a proportionally lower biomass production.

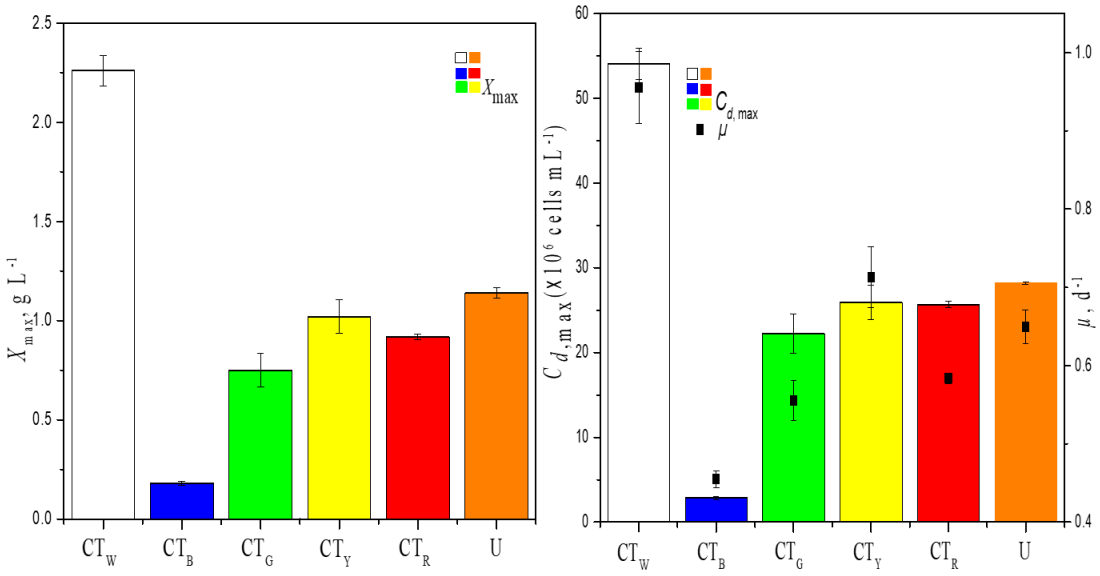

Figure 8.2 Cultivation of *C. vulgaris* in MLA under different λ_{max} and fixed *I of* $250\ \mu E\ m^{-2}\ s^{-1}$: (a) X profiles, and (b) μ and C_d as function of λ_{max}.

Similar growth patterns were obtained for CT_Y and U despite a ~60 % reduction in I for CT_Y, which has λ_{max} of 750-481 with a peak of 528 nm and I_f value of 100±5 (Table 8.2). This wavelength range has been reported as being optimal for an X_{max} of 1.5 g L^{-1} based on an initial light intensity of 250 µE m^{-2} s^{-1} [329]. The longer wavelengths/lower energies associated with CT_R have been reported to improve the algal growth in a PBR by sustaining light penetration through improving mixing within the reactor and increasing the depth of light penetration under higher light intensity [323, 329]. However, in the current study based there was no significant difference between the red light data and that of the green and yellow light, even though the irradiation intensity for CT_Y was 70-80% greater than that of CT_R or CT_G. The significant improvement using white light can thus be readily attributed to greater irradiation intensity for light wavelength encompassing the red, yellow and green ranges (Fig. 8.1).

8.3.2 Nutrients removal under different λ_{max}

The correlation of N and P removal efficiency (*RE TN* and *RE TP*) by *Chlorella vulgaris (C. vulgaris)* with wavelength (Fig. 8.3) indicates the expected maximum removal (92% *RE* for *TN*, 100% for *TP*) for CT_W in accordance with growth rate trends. Removal otherwise appeared to peak for CT_Y (65% *RE* for *TN*, 72% for *TP*), and was significantly lower (15-18% for both nutrients) for CT_B. The results show there is a significant difference in the *RE TN* obtained in CT_W and U - about 1.27 fold higher for CT_W - attributable to the lower λ_{max} of the unfiltered light source (I_f). *TP RE* for CT_W and CT_N were similar at 92% and 90% respectively.

P removal is impacted more than N removal by pH via abiotic precipitation, although assimilation by algae remains the primary P removal mechanism. The CT_W filtered spectrum contains a wide variety of wavelengths, peaking at 413 nm that can significantly enhance *C. vulgaris* growth and so nutrient uptake. CT_W thus appears to offer an optimal light wavelength band for removing both *TN* and *TP* in terms of λ_{max} at fixed external light intensity of 250 µE m^{-2} s^{-1}.

Removals overall are significantly greater than those reported by Yan et al [324] for the same algal species using LEDs with various colors. These authors reported *TN* and *TP REs* of 41% and 55% for a 620-630 nm wavelength based on a 42-day cultivation time in a batch operation with *I* of 1000 µE m^{-2} s^{-1}, compared with 122 ± 6 – 100 ± 5 µE m^{-2} s^{-1} I_f for a 413-528 nm wavelength irradiation at 10 days cultivation time in the current study (Table 8.1).

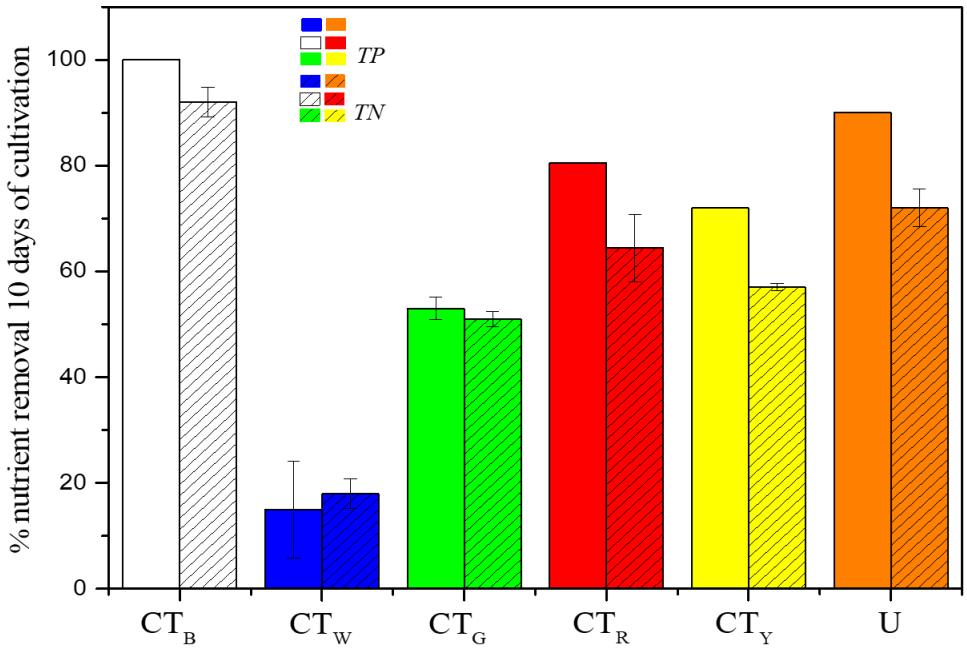

Figure 8.3 TP, TN removal efficiencies under different λ_{max}.

8.3.3 λ_{max} and *I* impacts on lipids production of *Chlorella vulgaris*

Lipid productivity (P_{lipid}) and CO_2 fixation rate (R_C) under the different light conditions follow a similar pattern to that of growth and nutrient removal, with CT_W providing the greatest lipid production and CO_2 fixation and the trend otherwise peaking for CT_Y (Fig. 8.4). According to Ruysters [333] a λ of 400-500 nm assists in the regulation of gene transcription and activation of enzymes. In the biosynthesis process of lipid, the two key components of acetyl-coA carboxylase (AAC) and nicotinamide adenine dinucleotide phosphate (NADPH) are produced by the concerted actions of ATP citrate lyase (ACL), malic enzyme (ME), and fatty acid synthase (FAS); these enzymes are effectively active only at wavelengths of 400-500 nm [334].

The results are comparable to those of Kim et al [331], based on a batch process using LED with wavelength ranges of 620-665 nm, 430-460 nm, and 400-700 nm, and a filtered light intensity of 100 µE m^{-2} s^{-1}. However, P_{lipid} reported by Hultberg et al. [330] for a batch LED process providing mean wavelengths of 460, 535, 585 and 620 nm using LED were significantly lower than that in the current study (Table 8.1). It must be acknowledged, however, that significant data scatter was evident in the current study results (Fig. 8.4) and the scope of the investigation was very limited. Nonetheless, results indicate a clear benefit from the use of light attenuated with CT_W compared with other filters and the unfiltered light source.

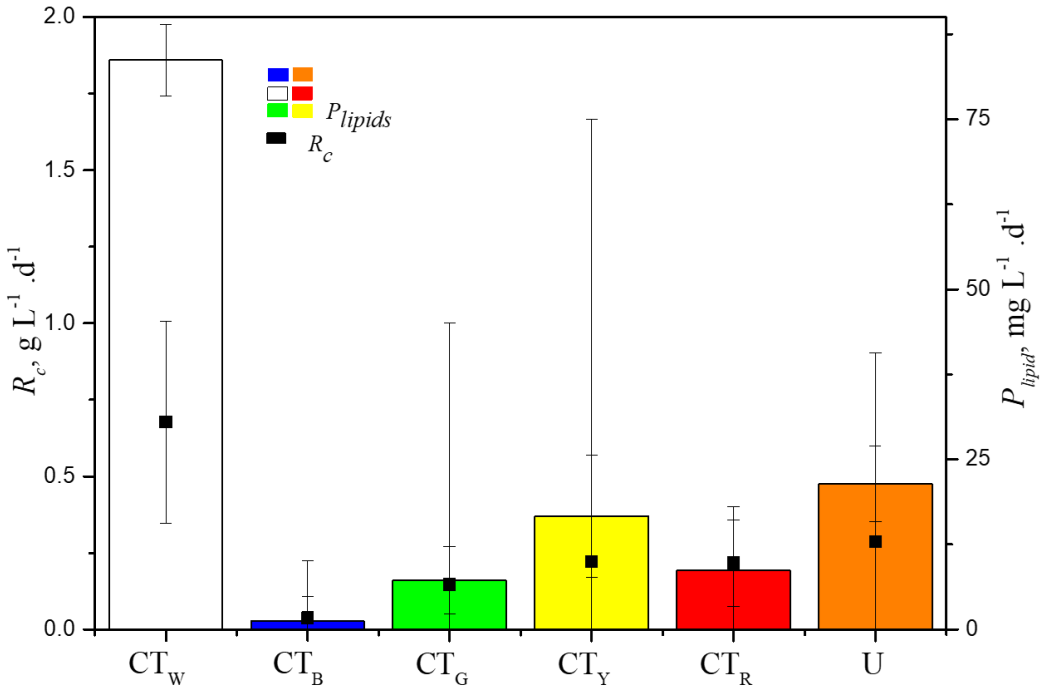

Figure 8.4 CO_2 fixation and lipids production rate at different wavelength.

8.3.4 Growth and productivity normalisation

Normalisation of key growth and lipid productivity parameters against irradiation intensity indicates significant differences between the different filtered light sources (Fig. 8.5). The Naderi et al. [225] studies based on the same algal strain using an unfiltered light (U) source at light intensities of 100 and 50 µE m^{-2} s^{-1} compared with 250 µE m^{-2} s^{-1} in the current study suggested unfiltered light to be 33-50% less effective at promoting algal growth and 75% less effective at promoting lipid productivity than filtered CT_W in the current study. Naderi indicated a similar trend of about 20-30% reduced influence in supporting algal growth compared with CT_W, although there was a slight enhancement in about 13-20% in algal growth compare with current study as a results of lower light intensity used. The optimum irradiance intensity for maximum *C. vulgaris* growth was previously reported as being 100 µE m^{-2} s^{-1} [225, 335].

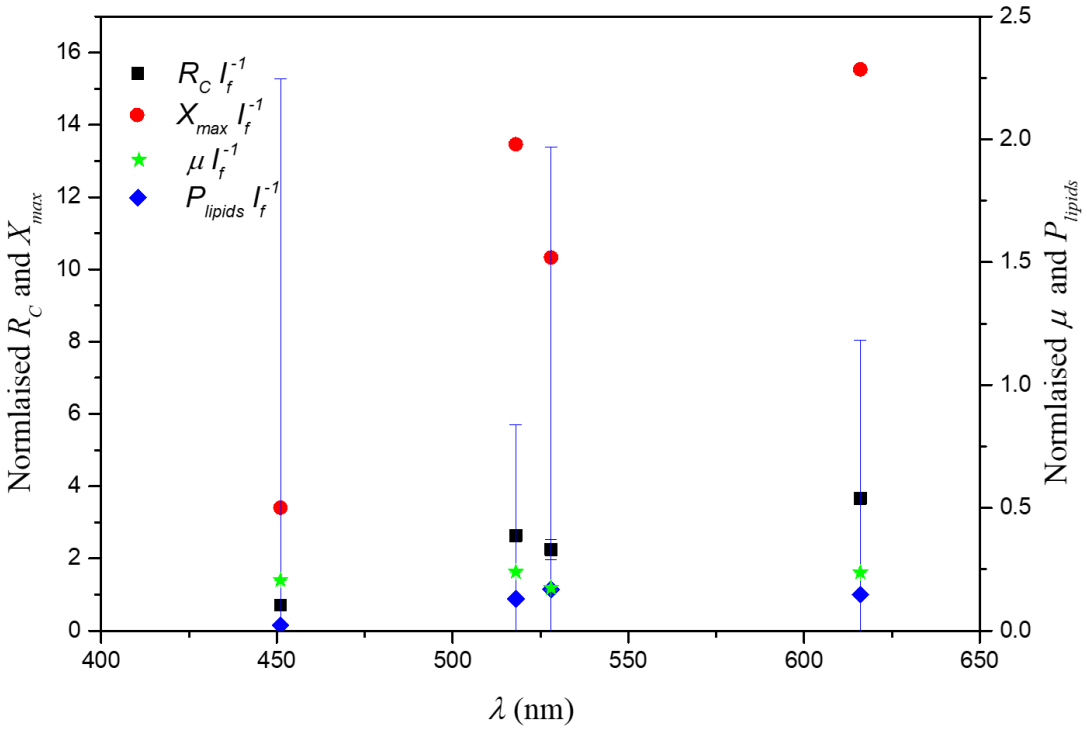

Figure 8.5 Normalised growth parameters and lipids productivity against light wavelength; normalised parameters = Vlaues of selected parameter (R_C, μ, X_{max} and P_{lipids}) / filtered light intensity (I_f).

Normalisation of algal growth parameters against light filtered (I_f) yields similar values of the specific growth rate across all I_f tests, whereas the normalised maximum algal biomass concentration was 4-5 times lower for blue light (λ_{peak} = 451 nm) than for longer light wavelengths (λ_{peak} > 518 nm). Normalised lipid productivity was similarly 85% less for blue light than for the longer light wavelengths, and <5% of the value determined for filtered white light. Excessive irradiation (250 µmol photons m^{-2} s^{-1}) appears to be detrimental to algal

growth and lipid productivity, as is light in the blue range, although reducing the light intensity to below (250 µmol photons m^{-2} s^{-1}) enhances the algal growth in [225].

8.4 Summary

The microalgae *Chlorella vulgaris* (*C. vulgaris*) was cultivated with light at different wavelengths (λ_{max}) and fixed external irradiation intensities (I) by applying coloured tape (CT) as a simple, inexpensive solar light filter. *C. vulgaris* was cultivated in a standard medium using blue (CT_B), green (CT_G), red (CT_R), yellow (CT_Y), and white (CT_W) coloured tape to filter the light, as well the unfiltered light (U). The CT-filtered light spectrum was characterized in terms of λ_{max} and filtered light intensity (I_f), and the influence of these parameters on algal growth (specific growth rate, μ), nutrient removal efficiency (% *RE* of total nitrogen, *TN*, and phosphorus, *TP*), CO_2 fixation rate (R_C) and lipid productivity (P_{lipid}) were evaluated. Growth and nutrient removal parameters were normalised against I_f for comparison.

For the un-normalised data the order of the growth and lipid productivity parameters was CT_W> unfiltered light (U) ≈ CT_Y > CT_R > CT_B. The highest biomass concentration X_{max} of 2.26 g L^{-1} was measured for CT_W of 123 µE m^{-2} s^{-1} I_f with corresponding μ, TN and *TP RE*, R_C and P_{lipid} values of 0.95 d^{-1}, 92% and 100%, 0.67 g L^{-1} d^{-1} and 83.6 mg L^{-1} d^{-1} respectively. For the normalised P_{lipids} parameters, however, the order of growth impacts CT_W > CT_Y > CT_R > CT_G > U > CT_B. The normalised algal growth and P_{lipids} parameters for U were significantly lower than in CT_W of 33-50% and 75% respectively. The corresponding non-normalised parameter values for CT_B with corresponding I_f of 53 µE m^{-2} s^{-1} were significantly lower at 0.45 d^{-1}, 0.18 g L^{-1}, 15% and 37%, 0.03 g L^{-1} d^{-1} and 1.2 mg L^{-1} d^{-1}. Results suggest a significant efficiency impact of both light intensity and wavelength, with up to a 50% increase in growth and an associated improvement in nutrient removal efficiency from optimising these two parameters.

Whilst the outcomes provide an indication of the practical viability of the low-cost light filtering method, it should be noted that the entirely heuristic approach does not lend itself to a rigorous appraisal of the individual wavelength and irradiation impacts on an individual basis. Specifically:

- a correlation of impacts against different wavelength ranges at a fixed light intensity is needed as a control
- the dynamic impacts of the above, through the recording of the impacted parameters against time

- a more comprehensive study of lipid productivity against other conditions, such as the solution chemistry (carbon and nutrient sources, pH, alkalinity, etc), so as to delineate between these effects and that of wavelength.

Chapter 9

Conclusions and Recommendations

9.1 Conclusions

The potential ability of microalgae *C. vulgaris* (*Cv*) to remove macro and micro nutrients from different wastewater quality, along with biomass production has been investigated. The influence of key cultivation process parameters of light intensity, CO_2 gas concentration, temperature and N, P have been studied. Response surface methodology (RSM) and Box Behnken Design (BBD) was used to optimise these parameters for maximizing algal biomass, nutrients removal and CO_2 fixation. A mathematical model for predicting algal growth, N, P nutrients depletions and light intensity profile has been developed and validated. Finally, the influence of light wavelength and intensity has been investigated.

1. Studies of the growth rate and bulk, macro and micro nutrient removal capability of Chlorella vulgaris (*Cv*) for three different wastewaters (primary wastewater, P_{WW}, secondary wastewater, S_{WW}, and petroleum effluent, PE) blended with MLA medium at different volume ratios revealed:
   a) The maximum biomass accumulated (X_{max}) and bulk nutrient (N and P) removal was achieved using P_{WW}, where X_{max} was 1.6 g L^{-1} after 13 days of cultivation, with 80% and 100% N and P removal respectively attained;
   b) The use of P_{WW} resulted in the highest specific growth rate (μ) of 1.21 d^{-1} as well as the highest overall removal efficiency of a range of macro and micro nutrients;
   c) On blending this water with MLA, μ progressively decreased to 0.75 d^{-1} for a 75%:25% P_{WW}:MLA blend to 0.54 d^{-1} for a 25:75 blend. The corresponding TN removal efficiency decreasing to 85% and 76% respectively; 100% removal of *TP* was recorded for all samples based on P_{WW};
   d) For S_{WW} and P_E TN removals of 79-83% TN was recorded, with corresponding X_{max} and μ values of 1.16-0.69 g L^{-1} and 0.62-0.31 d^{-1}.
   e) Whilst increasing the organic carbon (OC) concentration generally increased growth and nutrient removal, at the highest OC concentration for PE water growth was severely inhibited – presumably because of toxicity;

   The work would appear to corroborate previous observations that algal growth is promoted by wastewater carbon sources, albeit susceptible to possible toxicity for some industrial effluents, compared to synthetic ones.

2. The study of the ability of *Cv* to remove N and P at various N and P concentrations and N/P ratios (0-56 mg L^{-1} TN, 0-12 mg L^{-1} TP and 0-20 mg L^{-1} Total carbon (TC)), based on an MLA medium and using Box Behnken design (BBD) and response surface method (RSM) for process optimization revealed:

a) Unavailability of N or P in the cultivation media was found to be fatal to *Cv*;
b) A balanced N/P ratio was found to be crucial for maximizing biomass growth and nutrient removal, with the highest μ value of 0.95 d^{-1} obtained at N/P ratios of 7-10 (TN=55 mg L^{-1}, TP=7.9 mg L^{-1}) with accompanying complete nutrient removal, according to the BBD outcomes;
c) 100% removal efficiency for both N and P was recorded after 13 days of cultivation, along with a specific growth rate of 1 d^{-1} and a biomass concentration of 1.58 g L^{-1} when cultivated in MLA medium with 7 mg L^{-1} P and 70 mg L^{-1} N (N/P=10);
d) A significant decline in TN removal efficiency from 100% to 28% was recorded when the N/P ratio increased from 10 to 58; growth was impaired at lower N concentrations, although nutrient removal efficiencies were improved;
e) A synergy between TN and TP concentrations was evident for both nutrient removal and growth rate. The total carbon concentration showed no significant influence within at 0-20 mg L^{-1}; higher TC concentrations may negatively affect growth and N and P removal.
f) The regression coefficient values of 0.92, 0.95 and 0.95 for the specific growth rate, TN and TP removal efficiencies respectively indicated that the quadratic equations can adequately describe the relationship between the factors and responses: values computed by the model were in reasonable agreement with those measured experimentally.
g) The obtained results from the statistical analysis using ANOVA revealed the TN and TP concentrations to significantly influenced specific growth rate (μ) and the TN and TP removal efficiencies (p-value < 0.05). The influence of TC concentration was less significant in the within the concentration range examined, the p-values being > 0.1.
h) The TN-TC and TP-TC interactions were not significant within the experimental data range. Instead, TN removal efficiency was significantly influenced by the initial concentration values of TN and TP.
i) ~100% removal efficiency could be achieved at initial TN concentrations between 50 and 60 mg L-1 and initial TP concentrations of 6-12 mg L-1, while TC was maintained constant at its central point of 10 mg L-1.
j) The optimized TP, TN and TC concentrations in the medium that support 100% removal efficiencies of both P and N, along with a specific growth rate of 0.95 d-1, were 7 mg L-1, 54.84 mg L-1and 10 mg L-1 respectively. This equated to a balanced N/P ratio of 7.85 with higher desirability factor (d=0.94), corroborating the model outputs.

3. The assessment of CO_2 gas concentration ($C_{c,g}$), light irradiation (I), temperature (T), and aqueous nutrient concentrations (TN and TP) on the growth parameters of specific growth rate μ and CO_2 uptake rate R_c, along with nutrient removal revealed;

   Excessive $C_{c,g}$ values were deleterious to μ and R_c, as well as to nutrient removal: R_c and μ declined 2.6 and 12 fold respectively on increasing $C_{c,g}$ from 5 to 22%. This was attributed to both pH effects and impaired CO_2 mass transfer;

   a) Complete nutrient removal was observed after 10 days of cultivation, with higher μ and R_c values (of 1.17 d^{-1} and 744 mg $L^{-1}d^{-1}$ respectively) for MLA medium with a starting concentration of 6 mg L^{-1} P and 28 mg L^{-1} N.

4. BBD optimization of the cultivation parameters carried out based on a $C_{c,g}$ range of 0.03% (i.e. ambient levels) to 5%, along with a temperature range of 20-30°C and light intensity of 100-400 μE revealed:

   a) A synergy existed between $C_{c,g}$ and I for both R_c and μ, with temperature having no significant effect within the range studied;
   b) Optimum values of 5% and 100 μE were determined for $C_{c,g}$ and I respectively for maximum CO_2 fixation rate with complete nutrient removal (N and P) and a corresponding μ value of 1.53 d^{-1}, these conditions being validated through a subsequent experiment;
   c) The quadratic algorithms generated for the R_c, μ and nutrient removal trends through BBD with multiple linear regression analysis of the outputs, and ANOVA analysis confirming the relative importance of the different parameters, were found to adequately describe the system.

5. The modelling of the MCT process with reference to both biomass growth and nutrient uptake and for a determined light profile, calibrating using a base set of experimental conditions of $C_{c,g}$ = 2.5% and initial nutrient concentrations of 28 and 6 mg L^{-1} for TN and TP respectively and an irradiation intensity (I) of 250 μE m^{-2} s^{-1} revealed:,

   a) Model outputs were sensitive only to the maximum specific growth rate (μ_{max}) and the biomass loss rate K_d;
   b) There is a maximum possible ±46% deviation in the computed algal biomass concentration X associated with a ±20% variation in μ_{max};
   c) Regression analysis revealed a correlation coefficient (R^2) of 0.94 for mathematically-predicted vs experimentally-determined values of X over a wide range of input parameter values of feed gas and initial nutrient concentrations, reflecting the calibrated model predicted the X with reasonable accuracy;

d) R^2 values of 1.00 and 0.95 for the model prediction on N and P profiles were obtained, compared with a lower value of 0.91 for the average light profile;

The calibrated model obtained was successfully demonstrated for the prediction of algal growth and nutrient removal, encompassing the prediction of the average light intensity within the biomass bulk as a function of biomass concentration. The latter would be expected to inform the appropriate dilution ratio in a continuous process.

6. The influence of light wavelength (λ_{max}) and irradiation intensity (I) on μ, R_C, nutrient removal efficiency and lipids production (P_{lipid}) using coloured tape (CT), coloured blue (CT_B), green (CT_G), red (CT_R), yellow (CT_Y), white (CT_W), as a low-cost means of adjusting the wavelength, compared to unfiltered light (U) revealed:
   a) the use of CT to filter the external light reduced I_E generally benefitted the algal growth through suppressing photo-inhibition;
   b) The order the order of the growth and lipid productivity parameters was $CT_W > U \approx CT_Y > CT_R > CT_B$;
   c) Filtered white light (CT_W) was found to enhance growth, giving X_{max}, R_C, μ and P_{lipids} values of 2.26 g L^{-1}, 0.67 g L^{-1} d^{-1}, 0.95 $d^{-1}$and 83.6 mg L^{-1} d^{-1} respectively compared with 1.14 g L^{-1}, 0.28 g L^{-1} d^{-1}, 21.3 mg L^{-1} d^{-1} for U;
   d) CT_W provided significantly faster growth than colour-filtered light (CT_Y, CT_R, CT_G and CT_B), in part due to the greater I_f and λ_{max};
   e) Similarly, CT_W was also more beneficial for N and P removal, at 92% and 100% respectively. Lowest growth-related parameter values were recorded for CT_B, with μ, X_{max}, R_C and P_{lipids} of 0.45 d^{-1}, 0.18 g L^{-1}, 0.03 g L^{-1} d^{-1} and 1.2 mg L^{-1} d^{-1} respectively;
   f) Results for CT_Y were otherwise comparable with U, at 0.61 d^{-1}, 1.02 g L^{-1}, 0.22 g L^{-1} d^{-1} and 16.6 mg L^{-1} d^{-1};
   g) Slightly reduced growth for CT_R and CT_G was recorded;
   h) Normalisation of algal growth parameters against I yielded similar values of μ across all filtered light tests, but indicated a change in the order of growth impacts overall to $CT_W > CT_Y > CT_R > CT_G > U > CT_B$.

9.2 Recommendations

Based on the outcomes of the study the following recommendations can be made regarding future studies:

1. In the current study focusing on macro nutrient (mainly: nitrogen N, phosphorus P) removal was studied using the microalgae *Chlorella vulgaris* based on batch experiments. Whilst *Cv* is a reasonable algae to use, based on its widely recognised relatively high

growth rate and reasonable robustness, it is possible that other species may be more effective for nutrient removal across a wider range of N:P ratios. The work should also be extended to semi-batch and continuous systems in order to establish a minimum retention time for viable application. The results obtained could be used to inform large-scale process design for wastewater treatment and biomass production with reference to macro-nutrient demand in a PBR.

2. The work was primarily focused on nutrient and carbon dioxide abatement rather than on biofuel generation. The latter demands a study of lipid generation, this being the precursor to biofuel production. The viability of combined carbon capture from flue gases and nutrient removal from wastewaters will be dependent on the value of the biomass generated, which is critically dependent on the lipid content. The latter was only measured for the final part of the study (light wavelength influence).

3. The mathematical model presented has been successfully validated for the relatively small experimental data set generated from the study across a range of nutrient and feed CO_2 concentrations. Its validity both for other operating conditions (and in particular semi-batch and continuous) other feedwater qualities and more extended operating conditions (such as light intensity, temperature, mixing, and the impact of accumulated O_2 gas) needs to be appraised and the sensitivities established. Of particular relevance is its robustness to scaling, since algal processes must necessarily be implemented at a very large scale to be viable.

4. The work could be extended to (a) other effluents to established the system robustness to possible toxic shocks, and also examine the influence of other organic carbon sources and nutrient ratios, and (b) other key operational determinants, such as gas flow rate, mixing intensity and gas hold-up.

5. Although is only indirectly related to this work, the key aspect of cost benefit must be addressed. The most recent reviews of process cost suggest that even for mitigation of operating costs by combining flue gas with wastewater feeds in appropriate sites where the feed sources are co-located, the cost benefit offered may still be insufficient to compete with mineral fuel sources and conventional flue gas and wastewater treatment. This is clearly pivotal in the further development of MCT.

References

[1] S.-H. Ho, C.-Y. Chen, D.-J. Lee, and J.-S. Chang, "Perspectives on microalgal CO< sub> 2</sub>-emission mitigation systems—A review," *Biotechnology Advances,* vol. 29, no. 2, pp. 189-198, 2011.

[2] U. o. W. International Symposium on Eutrophication, *Eutrophication: Causes, Consequences, Correctives : Proceedings of the International Symposium, Madison, June 11-15, 1967*. National Academy of Sciences, 1970.

[3] P. b. V. P. e.V., "CO2 Capture and Storage VGB Report on the State of the Art," 25. August 2004.

[4] M. Packer, "Algal capture of carbon dioxide; biomass generation as a tool for greenhouse gas mitigation with reference to New Zealand energy strategy and policy," *Energy Policy,* vol. 37, no. 9, pp. 3428-3437, 9// 2009.

[5] M. Van Loosdrecht, C. Hooijmans, D. Brdjanovic, and J. Heijnen, "Biological phosphate removal processes," *Applied Microbiology and Biotechnology,* vol. 48, no. 3, pp. 289-296, 1997.

[6] M. Muthukumar, D. Mohan, and M. Rajendran, "Optimization of mix proportions of mineral aggregates using Box Behnken design of experiments," *Cement and Concrete Composites,* vol. 25, no. 7, pp. 751-758, 2003.

[7] C. Maher, J. Neethling, S. Murthy, and K. Pagilla, "Kinetics and capacities of phosphorus sorption to tertiary stage wastewater alum solids, and process implications for achieving low-level phosphorus effluents," *Water Research,* vol. 85, pp. 226-234, 2015.

[8] F. G. Acién Fernández, J. M. Fernández Sevilla, and E. Molina Grima, "Photobioreactors for the production of microalgae," (in English), *Reviews in Environmental Science and Bio/Technology,* vol. 12, no. 2, pp. 131-151, 2013/06/01 2013.

[9] W. Zhou *et al.*, "A hetero-photoautotrophic two-stage cultivation process to improve wastewater nutrient removal and enhance algal lipid accumulation," *Bioresource Technology,* vol. 110, no. 0, pp. 448-455, 4// 2012.

[10] R. Craggs, S. Heubeck, T. Lundquist, and J. Benemann, "Algal biofuels from wastewater treatment high rate algal ponds," *Water Science and Technology,* vol. 63, no. 4, pp. 660-665, 2011.

[11] E. J. Olguín, "Dual purpose microalgae–bacteria-based systems that treat wastewater and produce biodiesel and chemical products within a Biorefinery," *Biotechnology Advances,* vol. 30, no. 5, pp. 1031-1046, 9// 2012.

[12] P. Spolaore, C. Joannis-Cassan, E. Duran, and A. Isambert, "Commercial applications of microalgae," *Journal of Bioscience and Bioengineering,* vol. 101, no. 2, pp. 87-96, 2006.

[13] J. C. Weissman, R. P. Goebel, and J. R. Benemann, "Photobioreactor design: mixing, carbon utilization, and oxygen accumulation," *Biotechnology and Bioengineering,* vol. 31, no. 4, pp. 336-344, 1988.

[14] T. M. Mata, A. A. Martins, and N. S. Caetano, "Microalgae for biodiesel production and other applications: A review," *Renewable and Sustainable Energy Reviews,* vol. 14, no. 1, pp. 217-232, 1// 2010.

[15] F. Acién, J. Fernández, J. Magán, and E. Molina, "Production cost of a real microalgae production plant and strategies to reduce it," *Biotechnology Advances,* vol. 30, no. 6, pp. 1344-1353, 2012.

[16] J. Benemann, "Microalgae for biofuels and animal feeds," *Energies,* vol. 6, no. 11, pp. 5869-5886, 2013.

[17] I. De Godos *et al.*, "Evaluation of carbon dioxide mass transfer in raceway reactors for microalgae culture using flue gases," *Bioresource Technology,* vol. 153, pp. 307-314, 2014.

[18] S. Chinnasamy, A. Bhatnagar, R. W. Hunt, and K. C. Das, "Microalgae cultivation in a wastewater dominated by carpet mill effluents for biofuel applications," *Bioresource Technology,* vol. 101, no. 9, pp. 3097-3105, 5// 2010.
[19] I. Di Termini, A. Prassone, C. Cattaneo, and M. Rovatti, "On the nitrogen and phosphorus removal in algal photobioreactors," *Ecological Engineering,* vol. 37, no. 6, pp. 976-980, 2011.
[20] F. Ji, Y. Liu, R. Hao, G. Li, Y. Zhou, and R. Dong, "Biomass production and nutrients removal by a new microalgae strain Desmodesmus sp. in anaerobic digestion wastewater," *Bioresource Technology,* vol. 161, pp. 200-207, 2014.
[21] S. Judd, L. J. van den Broeke, M. Shurair, Y. Kuti, and H. Znad, "Algal remediation of CO 2 and nutrient discharges: A review," *Water Research,* vol. 87, pp. 356-366, 2015.
[22] S.-H. Ho, W.-M. Chen, and J.-S. Chang, "Scenedesmus obliquus CNW-N as a potential candidate for CO 2 mitigation and biodiesel production," *Bioresource Technology,* vol. 101, no. 22, pp. 8725-8730, 2010.
[23] J. E. Keffer and G. T. Kleinheinz, "Use of Chlorella vulgaris for CO2 mitigation in a photobioreactor," (in English), *Journal of Industrial Microbiology and Biotechnology,* vol. 29, no. 5, pp. 275-280, 2002/11/01 2002.
[24] L. Cheng, L. Zhang, H. Chen, and C. Gao, "Carbon dioxide removal from air by microalgae cultured in a membrane-photobioreactor," *Separation and Purification Technology,* vol. 50, no. 3, pp. 324-329, 2006.
[25] C.-L. Chiang, C.-M. Lee, and P.-C. Chen, "Utilization of the cyanobacteria Anabaena sp. CH1 in biological carbon dioxide mitigation processes," *Bioresource Technology,* vol. 102, no. 9, pp. 5400-5405, 2011.
[26] M. K. Lam and K. T. Lee, "Effect of carbon source towards the growth of Chlorella vulgaris for CO 2 bio-mitigation and biodiesel production," *International Journal of Greenhouse Gas Control,* vol. 14, pp. 169-176, 2013.
[27] S. Basu, A. S. Roy, K. Mohanty, and A. K. Ghoshal, "CO 2 biofixation and carbonic anhydrase activity in Scenedesmus obliquus SA1 cultivated in large scale open system," *Bioresource technology,* vol. 164, pp. 323-330, 2014.
[28] A. Solovchenko *et al.*, "Desmodesmus sp. 3Dp86E-1—a novel symbiotic chlorophyte capable of growth on pure CO2," *Marine Biotechnology,* vol. 16, no. 5, pp. 495-501, 2014.
[29] S. Wahal and S. Viamajala, "Maximizing algal growth in batch reactors using sequential change in light intensity," *Applied Biochemistry and Biotechnology,* vol. 161, no. 1-8, pp. 511-522, 2010.
[30] Q. Béchet, A. Shilton, and B. Guieysse, "Modeling the effects of light and temperature on algae growth: State of the art and critical assessment for productivity prediction during outdoor cultivation," *Biotechnology Advances,* vol. 31, no. 8, pp. 1648-1663, 2013.
[31] L. Giannelli, H. Yamada, T. Katsuda, and H. Yamaji, "Effects of temperature on the astaxanthin productivity and light harvesting characteristics of the green alga Haematococcus pluvialis," *Journal of Bioscience and Bioengineering,* vol. 119, no. 3, pp. 345-350, 2015.
[32] A. Parmar, N. K. Singh, A. Pandey, E. Gnansounou, and D. Madamwar, "Cyanobacteria and microalgae: a positive prospect for biofuels," *Bioresource Technology,* vol. 102, no. 22, pp. 10163-10172, 2011.
[33] Y. Kitaya, L. Xiao, A. Masuda, T. Ozawa, M. Tsuda, and K. Omasa, "Effects of temperature, photosynthetic photon flux density, photoperiod and O2 and CO2 concentrations on growth rates of the symbiotic dinoflagellate, Amphidinium sp," in *Nineteenth International Seaweed Symposium*, 2009, pp. 287-292: Springer.
[34] J. N. Rogers *et al.*, "A critical analysis of paddlewheel-driven raceway ponds for algal biofuel production at commercial scales," *Algal Research,* vol. 4, pp. 76-88, 2014.

[35] R. A. Betts, C. D. Jones, J. R. Knight, R. F. Keeling, and J. J. Kennedy, "El Nino and a record CO2 rise," *Nature Climate Change*, 2016.
[36] J. Sheehan, T. Dunahay, J. Benemann, and P. Roessler, " Biodiesel from Algae," *U.S. Department of Energy's Aquatic Species Program,* July 1998.
[37] E. Jacob-Lopes, S. Revah, S. Hernández, K. Shirai, and T. T. Franco, "Development of operational strategies to remove carbon dioxide in photobioreactors," *Chemical Engineering Journal*, vol. 153, no. 1–3, pp. 120-126, 11/1/ 2009.
[38] G. Chen, L. Zhao, and Y. Qi, "Enhancing the productivity of microalgae cultivated in wastewater toward biofuel production: A critical review," *Applied Energy*, vol. 137, pp. 282-291, 2015/01 2015.
[39] T. Freed, "Wastewater Industry Moving Toward Enhanced Nutrient Removal Standards," *WaterWorld*, 2007.
[40] A. Bhatnagar, S. Chinnasamy, M. Singh, and K. Das, "Renewable biomass production by mixotrophic algae in the presence of various carbon sources and wastewaters," *Applied Energy*, vol. 88, no. 10, pp. 3425-3431, 2011.
[41] Y. Gong and M. Jiang, "Biodiesel production with microalgae as feedstock: from strains to biodiesel," *Biotechnology Letters*, vol. 33, no. 7, pp. 1269-1284, 2011.
[42] A. Richmond, *Handbook of Microalgal Culture*. 2007.
[43] P. M. Schenk *et al.*, "Second Generation Biofuels: High-Efficiency Microalgae for Biodiesel Production," (in English), *Bioenergy Research*, vol. 1, no. 1, pp. 20-43, Mar 20082010-07-21 2008.
[44] A. Kaplan and L. Reinhold, "CO2 concentrating mechanisms in photosynthetic microorganisms," *Annual Review of Plant Biology*, vol. 50, no. 1, pp. 539-570, 1999.
[45] K. Kumar, C. N. Dasgupta, B. Nayak, P. Lindblad, and D. Das, "Development of suitable photobioreactors for CO< sub> 2</sub> sequestration addressing global warming using green algae and cyanobacteria," *Bioresource Technology*, vol. 102, no. 8, pp. 4945-4953, 2011.
[46] M. R. Badger, A. Kaplan, and J. A. Berry, "internal inorganic carbon pool of Chlamydomonas reinhardtii Evidence for a carbon dioxide-concentrating mechanism," *Plant Physiology*, vol. 66, no. 3, pp. 407-413, 1980.
[47] J. V. Moroney and R. A. Ynalvez, "Proposed carbon dioxide concentrating mechanism in Chlamydomonas reinhardtii," *Eukaryotic Cell*, vol. 6, no. 8, pp. 1251-1259, 2007.
[48] K. Chojnacka and F.-J. Marquez-Rocha, "Kinetic and stoichiometric relationships of the energy and carbon metabolism in the culture of microalgae," *Biotechnology*, vol. 3, no. 1, pp. 21-34, 2004.
[49] G. Huang, F. Chen, D. Wei, X. Zhang, and G. Chen, "Biodiesel production by microalgal biotechnology," *Applied Energy*, vol. 87, no. 1, pp. 38-46, 1// 2010.
[50] C.-Y. Chen, K.-L. Yeh, R. Aisyah, D.-J. Lee, and J.-S. Chang, "Cultivation, photobioreactor design and harvesting of microalgae for biodiesel production: a critical review," *Bioresource Technology*, vol. 102, no. 1, pp. 71-81, 2011.
[51] S.-Y. Chiu, C.-Y. Kao, M.-T. Tsai, S.-C. Ong, C.-H. Chen, and C.-S. Lin, "Lipid accumulation and CO2 utilization of Nannochloropsis oculata in response to CO2 aeration," *Bioresource Technology*, vol. 100, no. 2, pp. 833-838, 1// 2009.
[52] H. Xu, X. Miao, and Q. Wu, "High quality biodiesel production from a microalga Chlorella protothecoides by heterotrophic growth in fermenters," *Journal of Biotechnology*, vol. 126, no. 4, pp. 499-507, 12/1/ 2006.
[53] K. Chojnacka, "Kinetic and stoichiometric relationships of the energy and carbonmetabolism in the culture of microalgae," *Biotechnology*, vol. 3, 2004.
[54] W. Xiong, X. Li, J. Xiang, and Q. Wu, "High-density fermentation of microalga Chlorella protothecoides in bioreactor for microbio-diesel production," *Applied Microbiology and Biotechnology*, vol. 78, no. 1, pp. 29-36, 2008.

[55] J. C. Ogbonna and H. Tanaka, "Cyclic autotrophic/heterotrophic cultivation of photosynthetic cells: a method of achieving continuous cell growth under light/dark cycles," *Bioresource Technology,* vol. 65, no. 1, pp. 65-72, 1998.
[56] M. G. De Morais and J. A. V. Costa, "Biofixation of carbon dioxide by< i> Spirulina</i> sp. and< i> Scenedesmus obliquus</i> cultivated in a three-stage serial tubular photobioreactor," *Journal of Biotechnology,* vol. 129, no. 3, pp. 439-445, 2007.
[57] L. Brennan and P. Owende, "Biofuels from microalgae—A review of technologies for production, processing, and extractions of biofuels and co-products," *Renewable and Sustainable Energy Reviews,* vol. 14, no. 2, pp. 557-577, 2// 2010.
[58] Y. Chisti, "Biodiesel from microalgae," *Biotechnology Advances,* vol. 25, no. 3, pp. 294-306, 2007.
[59] S. S. Ahluwalia and D. Goyal, "Microbial and plant derived biomass for removal of heavy metals from wastewater," *Bioresource Technology,* vol. 98, no. 12, pp. 2243-2257, 2007.
[60] L. H. Fan, Y. T. Zhang, L. H. Cheng, L. Zhang, D. S. Tang, and H. L. Chen, "Optimization of Carbon Dioxide Fixation by Chlorella vulgaris Cultivated in a Membrane-Photobioreactor," *Chemical Engineering & Technology,* vol. 30, no. 8, pp. 1094-1099, 2007.
[61] A. A. G. Kommareddy, "Mixing and Eddie Currents in a Modified Bubble Column Reactor. ," *Paper Number: RRV03-0043 aN asae Meeting Presentation. Written for presentation at the 2003 CSAE/ASAE Annual Intersectional Meeting Sponsored by the Red River Section of ASAE Quality Inn& Suites 301 3 rd Avenue North Fargo, North Dakota, USA October 3-4,2003* 2003
[62] B. R. Poulsen and J. J. L. Iversen, "Characterization of gas transfer and mixing in a bubble column equipped with a rubber membrane diffuser," *Biotechnology and Bioengineering,* vol. 58, no. 6, pp. 633-641, 1998.
[63] A. S. C. Miron, F. G; Gomez, A. C.; Grima, E. M. & Chisti, Y., "Bubble -column and airlift photobioreactors for algal culture," *American Institute of Chemical Engineering Journal* vol. 46(2), pp. 1872-1887, 2000.
[64] A. Sánchez Mirón, F. Garcia Camacho, A. Contreras Gomez, E. M. Grima, and Y. Chisti, "Bubble-column and airlift photobioreactors for algal culture," *AIChE Journal,* vol. 46, no. 9, pp. 1872-1887, 2000.
[65] S. A. Razzak, M. M. Hossain, R. A. Lucky, A. S. Bassi, and H. de Lasa, "Integrated CO2 capture, wastewater treatment and biofuel production by microalgae culturing—A review," *Renewable and Sustainable Energy Reviews,* vol. 27, no. 0, pp. 622-653, 11// 2013.
[66] S. Y. Chiu, M. T. Tsai, C. Y. Kao, S. C. Ong, and C. S. Lin, "The air-lift photobioreactors with flow patterning for high-density cultures of microalgae and carbon dioxide removal," *Engineering in Life Sciences,* Article vol. 9, no. 3, pp. 254-260, 2009.
[67] G. Markou and D. Georgakakis, "Cultivation of filamentous cyanobacteria (blue-green algae) in agro-industrial wastes and wastewaters: a review," *Applied Energy,* vol. 88, no. 10, pp. 3389-3401, 2011.
[68] C.-Y. Chen, G. D. Saratale, C.-M. Lee, P.-C. Chen, and J.-S. Chang, "Phototrophic hydrogen production in photobioreactors coupled with solar-energy-excited optical fibers," *International Journal of Hydrogen Energy,* vol. 33, no. 23, pp. 6886-6895, 2008.
[69] F. Ma and M. A. Hanna, "Biodiesel production: a review," *Bioresource technology,* vol. 70, no. 1, pp. 1-15, 1999.
[70] M. Janssen, J. Tramper, L. R. Mur, and R. H. Wijffels, "Enclosed outdoor photobioreactors: Light regime, photosynthetic efficiency, scale-up, and future prospects," *Biotechnology and Bioengineering,* vol. 81, no. 2, pp. 193-210, 2003.

[71] R. M. El-Shishtawy, S. Kawasaki, and M. Morimoto, "Biological H 2 production using a novel light-induced and diffused photoreactor," *Biotechnology Techniques*, vol. 11, no. 6, pp. 403-407, 1997.
[72] A. A. Tsygankov, T. V. Laurinavichene, and I. N. Gogotov, "Laboratory scale photobioreactor," *Biotechnology Techniques*, vol. 8, no. 8, pp. 575-578, 1994.
[73] K. Issarapayup, S. Powtongsook, and P. Pavasant, "Flat panel airlift photobioreactors for cultivation of vegetative cells of microalga Haematococcus pluvialis," *Journal of Biotechnology*, vol. 142, no. 3, pp. 227-232, 2009.
[74] F. J. Sánchez, C. González-López, F. F. Acién, S. J. Fernández, and G. E. Molina, "Utilization of Anabaena sp. in CO_2 removal processes: modelling of biomass, exopolysaccharides productivities and CO_2 fixation rate," *Applied Microbiology and Biotechnology*, vol. 94, no. 3, pp. 613-624, 2012.
[75] A. Gonçalves, M. Simões, and J. Pires, "The effect of light supply on microalgal growth, CO 2 uptake and nutrient removal from wastewater," *Energy Conversion and Management*, vol. 85, pp. 530-536, 2014.
[76] J. Pires, A. Gonçalves, F. Martins, M. Alvim-Ferraz, and M. Simões, "Effect of light supply on CO2 capture from atmosphere by Chlorella vulgaris and Pseudokirchneriella subcapitata," *Mitigation and Adaptation Strategies for Global Change*, vol. 19, no. 7, pp. 1109-1117, 2014.
[77] F. G. A. Fernández, C. González-López, J. F. Sevilla, and E. M. Grima, "Conversion of CO2 into biomass by microalgae: how realistic a contribution may it be to significant CO2 removal?," *Applied Microbiology and Biotechnology*, vol. 96, no. 3, pp. 577-586, 2012.
[78] H. L. MacIntyre, T. M. Kana, and R. J. Geider, "The effect of water motion on short-term rates of photosynthesis by marine phytoplankton," *Trends in Plant Science*, vol. 5, no. 1, pp. 12-17, 2000.
[79] J. A. Raven and R. J. Geider, "Adaptation, acclimation and regulation in algal photosynthesis," in *Photosynthesis in Algae*: Springer, 2003, pp. 385-412.
[80] Z. Dubinsky and O. Schofield, "From the light to the darkness: thriving at the light extremes in the oceans," *Hydrobiologia*, vol. 639, no. 1, pp. 153-171, 2010.
[81] E. B. Sydney *et al.*, "Potential carbon dioxide fixation by industrially important microalgae," *Bioresource Technology*, vol. 101, no. 15, pp. 5892-5896, 2010.
[82] S. Ruangsomboon, "Effect of light, nutrient, cultivation time and salinity on lipid production of newly isolated strain of the green microalga, Botryococcus braunii KMITL 2," *Bioresource Technology*, vol. 109, no. 0, pp. 261-265, 4// 2012.
[83] R. Honda, J. Boonnorat, C. Chiemchaisri, W. Chiemchaisri, and K. Yamamoto, "Carbon dioxide capture and nutrients removal utilizing treated sewage by concentrated microalgae cultivation in a membrane photobioreactor," *Bioresource Technology*, vol. 125, pp. 59-64, 2012.
[84] D. Tang, W. Han, P. Li, X. Miao, and J. Zhong, "CO 2 biofixation and fatty acid composition of Scenedesmus obliquus and Chlorella pyrenoidosa in response to different CO 2 levels," *Bioresource Technology*, vol. 102, no. 3, pp. 3071-3076, 2011.
[85] A. Ruiz-Marin, L. G. Mendoza-Espinosa, and T. Stephenson, "Growth and nutrient removal in free and immobilized green algae in batch and semi-continuous cultures treating real wastewater," *Bioresource Technology*, vol. 101, no. 1, pp. 58-64, 2010.
[86] M.-K. Ji *et al.*, "Cultivation of microalgae species in tertiary municipal wastewater supplemented with CO2 for nutrient removal and biomass production," *Ecological Engineering*, vol. 58, no. 0, pp. 142-148, 9// 2013.
[87] R. A. I. Abou-Shanab, M.-K. Ji, H.-C. Kim, K.-J. Paeng, and B.-H. Jeon, "Microalgal species growing on piggery wastewater as a valuable candidate for nutrient removal and biodiesel production," *Journal of Environmental Management*, vol. 115, no. 0, pp. 257-264, 1/30/ 2013.

[88] C. G. López, F. A. Fernández, J. F. Sevilla, J. S. Fernández, M. C. García, and E. M. Grima, "Utilization of the cyanobacteria Anabaena sp. ATCC 33047 in CO 2 removal processes," *Bioresource Technology,* vol. 100, no. 23, pp. 5904-5910, 2009.
[89] F. Gao, Z.-H. Yang, C. Li, G.-M. Zeng, D.-H. Ma, and L. Zhou, "A novel algal biofilm membrane photobioreactor for attached microalgae growth and nutrients removal from secondary effluent," *Bioresource Technology,* vol. 179, pp. 8-12, 2015.
[90] O. Björkman and B. Demmig, "Photon yield of O2 evolution and chlorophyll fluorescence characteristics at 77 K among vascular plants of diverse origins," *Planta,* vol. 170, no. 4, pp. 489-504, 1987.
[91] R. Emerson and C. M. Lewis, "The dependence of the quantum yield of Chlorella photosynthesis on wave lenghth of light," *American Journal of Botany,* pp. 165-178, 1943.
[92] J. Evans, "The dependence of quantum yield on wavelength and growth irradiance," *Functional Plant Biology,* vol. 14, no. 1, pp. 69-79, 1987.
[93] S. Malkin and D. C. Fork, "Bill Arnold and calorimetric measurements of the quantum requirement of photosynthesis—once again ahead of his time," *Photosynthesis Research,* vol. 48, no. 1-2, pp. 41-46, 1996.
[94] B. Demmig-Adams, J. J. Stewart, T. A. Burch, and W. W. Adams III, "Insights from placing photosynthetic light harvesting into context," *The journal of Physical chemistry Letters,* vol. 5, no. 16, pp. 2880-2889, 2014.
[95] L. Pilon, H. Berberoğlu, and R. Kandilian, "Radiation transfer in photobiological carbon dioxide fixation and fuel production by microalgae," *Journal of Quantitative Spectroscopy and Radiative Transfer,* vol. 112, no. 17, pp. 2639-2660, 2011.
[96] Z. Perrine, S. Negi, and R. T. Sayre, "Optimization of photosynthetic light energy utilization by microalgae," *Algal Research,* vol. 1, no. 2, pp. 134-142, 2012.
[97] G. Peers, "Increasing algal photosynthetic productivity by integrating ecophysiology with systems biology," *Trends in Biotechnology,* vol. 32, no. 11, pp. 551-555, 2014.
[98] P. Das, W. Lei, S. S. Aziz, and J. P. Obbard, "Enhanced algae growth in both phototrophic and mixotrophic culture under blue light," *Bioresource Technology,* vol. 102, no. 4, pp. 3883-3887, 2011.
[99] C. L. Teo, M. Atta, A. Bukhari, M. Taisir, A. M. Yusuf, and A. Idris, "Enhancing growth and lipid production of marine microalgae for biodiesel production via the use of different LED wavelengths," *Bioresource Technology,* vol. 162, pp. 38-44, 2014.
[100] Y. H. Seo, C. Cho, J.-Y. Lee, and J.-I. Han, "Enhancement of growth and lipid production from microalgae using fluorescent paint under the solar radiation," *Bioresource Technology,* vol. 173, pp. 193-197, 2014.
[101] R. B. Levine, T. Pinnarat, and P. E. Savage, "Biodiesel Production from Wet Algal Biomass through in Situ Lipid Hydrolysis and Supercritical Transesterification," *Energy & Fuels,* vol. 24, no. 9, pp. 5235-5243, 2010/09/16 2010.
[102] H. Tang, N. Abunasser, M. Garcia, M. Chen, K. Simon Ng, and S. O. Salley, "Potential of microalgae oil from< i> Dunaliella tertiolecta</i> as a feedstock for biodiesel," *Applied Energy,* vol. 88, no. 10, pp. 3324-3330, 2011.
[103] J. Yang, M. Xu, X. Zhang, Q. Hu, M. Sommerfeld, and Y. Chen, "Life-cycle analysis on biodiesel production from microalgae: Water footprint and nutrients balance," *Bioresource Technology,* vol. 102, no. 1, pp. 159-165, 1// 2011.
[104] G. E. Fogg and B. Thake, *Algal Cultures and Phytoplankton Ecology*. Univ of Wisconsin Press, 1987.
[105] A. a. Q. Thronson, A, "Trace Elements," *Ecological Stoichiometry in the Encyclopedia of Ecology,* vol. 5, pp. 3564-3573, 2008.
[106] A. P. Abreu, B. Fernandes, A. A. Vicente, J. Teixeira, and G. Dragone, "Mixotrophic cultivation of Chlorella vulgaris using industrial dairy waste as organic carbon source," *Bioresource Technology,* vol. 118, pp. 61-66, 2012.

[107] A. Ruiz-Martinez, N. Martin Garcia, I. Romero, A. Seco, and J. Ferrer, "Microalgae cultivation in wastewater: Nutrient removal from anaerobic membrane bioreactor effluent," *Bioresource Technology,* vol. 126, no. 0, pp. 247-253, 12// 2012.
[108] L. Marbelia *et al.*, "Membrane photobioreactors for integrated microalgae cultivation and nutrient remediation of membrane bioreactors effluent," *Bioresource Technology,* vol. 163, pp. 228-235, 2014.
[109] F. Gao *et al.*, "Continuous microalgae cultivation in aquaculture wastewater by a membrane photobioreactor for biomass production and nutrients removal," *Ecological Engineering,* vol. 92, pp. 55-61, 2016.
[110] I.-S. Yang *et al.*, "Cultivation and harvesting of microalgae in photobioreactor for biodiesel production and simultaneous nutrient removal," *Energy Conversion and Management,* vol. 117, pp. 54-62, 2016.
[111] E. Sydney *et al.*, "Screening of microalgae with potential for biodiesel production and nutrient removal from treated domestic sewage," *Applied Energy,* vol. 88, no. 10, pp. 3291-3294, 2011.
[112] F. A. AlMomani and B. Örmeci, "Performance Of Chlorella Vulgaris, Neochloris Oleoabundans, and mixed indigenous microalgae for treatment of primary effluent, secondary effluent and centrate," *Ecological Engineering,* vol. 95, pp. 280-289, 2016.
[113] Y. Canedo-López, A. Ruiz-Marín, and J. d. C. Zavala-Loría, "A two-stage culture process using Chlorella vulgaris for urban wastewater nutrient removal and enhanced algal lipid accumulation under photoautotrophic and mixotrophic conditions," *Journal of Renewable and Sustainable Energy,* vol. 8, no. 3, p. 033102, 2016.
[114] H. Takahashi, S. Kopriva, M. Giordano, K. Saito, and R. Hell, "Sulfur assimilation in photosynthetic organisms: molecular functions and regulations of transporters and assimilatory enzymes," *Annual Review of Plant Biology,* vol. 62, pp. 157-184, 2011.
[115] P. Brownell and D. Nicholas, "Some effects of sodium on nitrate assimilation and N2 fixation in Anabaena cylindrica," *Plant Physiology,* vol. 42, no. 7, pp. 915-921, 1967.
[116] A. Pirson, "u. SSA Badour: Kennzeichnung von Mineralsalzmangelzuständen bei Grünalgen mit analytisch-chemischer Methodik. Kohlenhydratspiegel, organischer Stickstoff und Chlorophyll bei Kalimangel im Vergleich mit Magnesium-und Manganmangel," *Planta (Berl.),* vol. 150, pp. 243-258, 1961.
[117] H. C. Utkilen, "Magnesium-limited growth of the cyanobacterium Anacystis nidulans," *Microbiology,* vol. 128, no. 8, pp. 1849-1862, 1982.
[118] D. F. Goldspink, "Development and specialization of skeletal muscle " *Society for Experimental Biology,* 1980.
[119] H.-B. Jiang, H.-M. Cheng, K.-S. Gao, and B.-S. Qiu, "Inactivation of Ca2+/H+ exchanger in Synechocystis sp. strain PCC 6803 promotes cyanobacterial calcification by upregulating CO2-concentrating mechanisms," *Applied and Environmental Microbiology,* vol. 79, no. 13, pp. 4048-4055, 2013.
[120] O'Kelley, "Inorganic nutrients," *Algal Physiology and Biochemistry,* pp. 610–635, 1974.
[121] J. F. Da Silva and R. J. P. Williams, *The biological chemistry of the elements: the inorganic chemistry of life*. Oxford University Press, 2001.
[122] W. G. Sunda, "Feedback interactions between trace metal nutrients and phytoplankton in the ocean," *Front. Microbiol,* vol. 3, no. 204, p. 10.3389, 2012.
[123] S. La Fontaine *et al.*, "Copper-dependent iron assimilation pathway in the model photosynthetic eukaryote Chlamydomonas reinhardtii," *Eukaryotic Cell,* vol. 1, no. 5, pp. 736-757, 2002.
[124] R. Maldonado, O. Valverde, and F. Berrendero, "Involvement of the endocannabinoid system in drug addiction," *Trends in Neurosciences,* vol. 29, no. 4, pp. 225-232, 2006.

[125] C. L. Dupont, K. Barbeau, and B. Palenik, "Ni uptake and limitation in marine Synechococcus strains," *Applied and Environmental Microbiology*, vol. 74, no. 1, pp. 23-31, 2008.
[126] H. Araie and Y. Shiraiwa, "Selenium utilization strategy by microalgae," *Molecules*, vol. 14, no. 12, pp. 4880-4891, 2009.
[127] P. J. Harrison, F. A. Whitney, A. Tsuda, H. Saito, and K. Tadokoro, "Nutrient and plankton dynamics in the NE and NW gyres of the subarctic Pacific Ocean," *Journal of Oceanography*, vol. 60, no. 1, pp. 93-117, 2004.
[128] K. H. Coale, "Effects of iron, manganese, copper, and zinc enrichments on productivity and biomass in the subarctic Pacific," *Limnology and Oceanography*, vol. 36, no. 8, pp. 1851-1864, 1991.
[129] J. L. Levy, J. L. Stauber, M. S. Adams, W. A. Maher, J. K. Kirby, and D. F. Jolley, "Toxicity, biotransformation, and mode of action of arsenic in two freshwater Microalgae (Chlorella sp. and Monoraphidium arcuatum)," *Environmental Toxicology and Chemistry*, vol. 24, no. 10, pp. 2630-2639, 2005.
[130] M. G. de Morais and J. A. V. Costa, "Isolation and selection of microalgae from coal fired thermoelectric power plant for biofixation of carbon dioxide," *Energy Conversion and Management*, vol. 48, no. 7, pp. 2169-2173, 2007.
[131] M. G. De Morais and J. A. V. Costa, "Biofixation of carbon dioxide by Spirulina sp. and Scenedesmus obliquus cultivated in a three-stage serial tubular photobioreactor," *Journal of Biotechnology*, vol. 129, no. 3, pp. 439-445, 2007.
[132] S. Kajiwara, H. Yamada, N. Ohkuni, and K. Ohtaguchi, "Design of the bioreactor for carbon dioxide fixation by Synechococcus PCC7942," *Energy Conversion and Management*, vol. 38, pp. S529-S532, 1997.
[133] K. D. Sung, J. Lee, C. Shin, and S. Park, "Isolation of a new highly CO2 tolerant fresh water microalga Chlorella sp. KR-1," *Renewable Energy*, vol. 16, no. 1-4, pp. 1019-1022, 1999.
[134] N. Xu and X. Zhang, "Effect of temperature, light intensity and pH on the growth and fatty acid compositions of Ellipsoidion sp," *Journal of Ocean University of Qingdao*, vol. 31, no. 4, pp. 541-547, 2000.
[135] A. Kumar *et al.*, "Enhanced CO 2 fixation and biofuel production via microalgae: recent developments and future directions," *Trends in Biotechnology*, vol. 28, no. 7, pp. 371-380, 2010.
[136] K. Maeda, M. Owada, N. Kimura, K. Omata, and I. Karube, "CO 2 fixation from the flue gas on coal-fired thermal power plant by microalgae," *Energy Conversion and Management*, vol. 36, no. 6, pp. 717-720, 1995.
[137] L. Yue and W. Chen, "Isolation and determination of cultural characteristics of a new highly CO 2 tolerant fresh water microalgae," *Energy Conversion and Management*, vol. 46, no. 11, pp. 1868-1876, 2005.
[138] B. Wang, Y. Li, N. Wu, and C. Q. Lan, "CO2 bio-mitigation using microalgae," *Applied Microbiology and Biotechnology*, vol. 79, no. 5, pp. 707-718, 2008.
[139] Y. Chisti, "Biodiesel from microalgae beats bioethanol," *Trends in biotechnology*, vol. 26, no. 3, pp. 126-131, 2008.
[140] L. Christenson and R. Sims, "Production and harvesting of microalgae for wastewater treatment, biofuels, and bioproducts," *Biotechnology Advances*, vol. 29, no. 6, pp. 686-702, 2011.
[141] J. Park, R. Craggs, and A. Shilton, "Wastewater treatment high rate algal ponds for biofuel production," *Bioresource technology*, vol. 102, no. 1, pp. 35-42, 2011.
[142] Y. Zhang, X. Liu, M. A. White, and L. M. Colosi, "Economic evaluation of algae biodiesel based on meta-analyses," *International Journal of Sustainable Energy*, pp. 1-13, 2015/09/23 2015.
[143] C. Yoo, S.-Y. Jun, J.-Y. Lee, C.-Y. Ahn, and H.-M. Oh, "Selection of microalgae for lipid production under high levels carbon dioxide," *Bioresource Technology*, vol. 101, no. 1, pp. S71-S74, 2010.

[144] D. J. Farrelly, L. Brennan, C. D. Everard, and K. P. McDonnell, "Carbon dioxide utilisation of Dunaliella tertiolecta for carbon bio-mitigation in a semicontinuous photobioreactor," *Applied Microbiology and Biotechnology,* vol. 98, no. 7, pp. 3157-3164, 2014.
[145] S. K. Singh, A. Rahman, K. Dixit, A. Nath, and S. Sundaram, "Evaluation of promising algal strains for sustainable exploitation coupled with CO2 fixation," *Environmental Technology,* vol. 37, no. 5, pp. 613-622, 2016.
[146] O. Pulz and W. Gross, "Valuable products from biotechnology of microalgae," *Applied Microbiology and Biotechnology,* vol. 65, no. 6, pp. 635-648, 2004.
[147] K. Skjånes, P. Lindblad, and J. Muller, "BioCO 2–a multidisciplinary, biological approach using solar energy to capture CO 2 while producing H 2 and high value products," *Biomolecular Engineering,* vol. 24, no. 4, pp. 405-413, 2007.
[148] M. M. Abu-Khader, "Recent progress in CO2 capture/sequestration: a review," *Energy Sources, Part A,* vol. 28, no. 14, pp. 1261-1279, 2006.
[149] D. Bilanovic, A. Andargatchew, T. Kroeger, and G. Shelef, "Freshwater and marine microalgae sequestering of CO< sub> 2</sub> at different C and N concentrations–Response surface methodology analysis," *Energy conversion and Management,* vol. 50, no. 2, pp. 262-267, 2009.
[150] O. Pulz, "Photobioreactors: production systems for phototrophic microorganisms," (in English), *Applied Microbiology and Biotechnology,* vol. 57, no. 3, pp. 287-293, 2001/10/01 2001.
[151] A. N. G. G. Inventory, "National Greenhouse Gas Inventory Total, Carbon Dioxide Equivalent Emissions, 2011, Kyoto Accounting " 2013.
[152] H. J. Herzog, "Peer Reviewed: What Future for Carbon Capture and Sequestration?," *Environmental Science & Technology,* vol. 35, no. 7, pp. 148A-153A, 2001.
[153] H. Herzog and O. Falk-Pedersen, "The Kvaerner membrane contactor: lessons from a case study in how to reduce capture costs."
[154] W. Leitner, "Supercritical carbon dioxide as a green reaction medium for catalysis," *Accounts of Chemical Research,* vol. 35, no. 9, pp. 746-756, 2002.
[155] M. Ishibashi *et al.*, "Technology for removing carbon dioxide from power plant flue gas by the physical adsorption method," *Energy Conversion and Management,* vol. 37, no. 6, pp. 929-933, 1996.
[156] J. Barnard, "Third International Conference on Chemical Structures," *Journal of Chemical Information and Computer Sciences,* vol. 34, no. 1, pp. 1-2, 1994/01/01 1994.
[157] T. D. B. Roddie R. Judkins, "CO2 Removal From Gas Streams Using a Carbon Fiber Composite Molecular Sieve," 2001.
[158] L. Marcel, *Enhanced Oil Recovery*. Editions OPHRYS, 1980.
[159] D. J. Beecy and V. A. Kuuskraa, "Status of U.S. Geologic Carbon Sequestration Research and Technology," *Environmental Geosciences,* vol. 8, no. 3, pp. 152-159, 2001.
[160] F. Gao, Z.-H. Yang, C. Li, Y.-j. Wang, W.-h. Jin, and Y.-b. Deng, "Concentrated microalgae cultivation in treated sewage by membrane photobioreactor operated in batch flow mode," *Bioresource Technology,* vol. 167, pp. 441-446, 2014.
[161] M. del Mar Morales-Amaral, C. Gómez-Serrano, F. G. Acién, J. M. Fernández-Sevilla, and E. Molina-Grima, "Production of microalgae using centrate from anaerobic digestion as the nutrient source," *Algal Research,* vol. 9, pp. 297-305, 2015.
[162] C. Sepúlveda, F. Acién, C. Gómez, N. Jiménez-Ruíz, C. Riquelme, and E. Molina-Grima, "Utilization of centrate for the production of the marine microalgae Nannochloropsis gaditana," *Algal Research,* vol. 9, pp. 107-116, 2015.
[163] M. S. de Alva, V. M. Luna-Pabello, E. Cadena, and E. Ortíz, "Green microalga Scenedesmus acutus grown on municipal wastewater to couple nutrient removal with lipid accumulation for biodiesel production," *Bioresource Technology,* vol. 146, pp. 744-748, 2013.

[164] M. Suplee, P. Hartman, and J. Cleland, "Wastewater treatment perforamnce and cost data to support an affordable analysis for water quaility standardes",2007.
[165] N. J. Horan, *Biological Wastewater Treatment Systems: Theory and Operation*. John Wiley & Sons Ltd., 1989.
[166] D. I. E. S. E. v. Beelen, "Municipal Waste Water Treatment Plant (WWTP) Effluents," *RTWA riJnwaterbedrijern*, 2007.
[167] K. Mosse, A. Patti, E. Christen, and T. Cavagnaro, "Review: winery wastewater quality and treatment options in Australia," *Australian Journal of Grape and Wine Research*, vol. 17, no. 2, pp. 111-122, 2011.
[168] B. D. Burks and M. M. Minnis, *Onsite wastewater treatment systems*. Hogarth House Madison, 1994.
[169] M. d. M. Morales-Amaral, C. Gómez-Serrano, F. G. Acién, J. M. Fernández-Sevilla, and E. Molina-Grima, "Production of microalgae using centrate from anaerobic digestion as the nutrient source," *Algal Research*, vol. 9, pp. 297-305, 2015/05 2015.
[170] A. Bhatnagar, M. Bhatnagar, S. Chinnasamy, and K. Das, "Chlorella minutissima—a promising fuel alga for cultivation in municipal wastewaters," *Applied Biochemistry and Biotechnology*, vol. 161, no. 1-8, pp. 523-536, 2010.
[171] C. Li *et al.*, "High efficient treatment of citric acid effluent by Chlorella vulgaris and potential biomass utilization," *Bioresource Technology*, vol. 127, pp. 248-255, 2013.
[172] R. Kothari, V. V. Pathak, V. Kumar, and D. Singh, "Experimental study for growth potential of unicellular alga Chlorella pyrenoidosa on dairy waste water: an integrated approach for treatment and biofuel production," *Bioresource Technology*, vol. 116, pp. 466-470, 2012.
[173] N. Mallick, "Biotechnological potential of immobilized algae for wastewater N, P and metal removal: a review," *Biometals*, vol. 15, no. 4, pp. 377-390, 2002.
[174] L. E. de-Bashan and Y. Bashan, "Immobilized microalgae for removing pollutants: review of practical aspects," *Bioresource Technology*, vol. 101, no. 6, pp. 1611-1627, 2010.
[175] C. Vílchez, I. Garbayo, M. V. Lobato, and J. Vega, "Microalgae-mediated chemicals production and wastes removal," *Enzyme and Microbial Technology*, vol. 20, no. 8, pp. 562-572, 1997.
[176] N. Srivastava and C. Majumder, "Novel biofiltration methods for the treatment of heavy metals from industrial wastewater," *Journal of Hazardous Materials*, vol. 151, no. 1, pp. 1-8, 2008.
[177] J. Perdigón-Melón, J. Carbajo, A. Petre, R. Rosal, and E. García-Calvo, "Coagulation–Fenton coupled treatment for ecotoxicity reduction in highly polluted industrial wastewater," *Journal of Hazardous Materials*, vol. 181, no. 1, pp. 127-132, 2010.
[178] X. Ma and X. Wang, "Ecotoxicity comparison of organic contaminants and heavy metals using Vibrio-qinghaiensis sp.-Q67," *Water Science and Technology*, vol. 67, no. 10, pp. 2221-2227, 2013.
[179] J. Ma, R. Zheng, L. Xu, and S. Wang, "Differential sensitivity of two green algae, Scenedesmus obliqnus and Chlorella pyrenoidosa, to 12 pesticides," *Ecotoxicology and Environmental Safety*, vol. 52, no. 1, pp. 57-61, 2002.
[180] R. L. Knight, R. H. Kadlec, and H. M. Ohlendorf, "The use of treatment wetlands for petroleum industry effluents," *Environmental Science & Technology*, vol. 33, no. 7, pp. 973-980, 1999.
[181] W. J. Oswald, "Advanced integrated wastewater pond systems," in *ASCE Convention EE Div/ASCE, San Francisco, CA*, 1990, pp. 5-8.
[182] F. M. Bosch, Lootens, H., Van -Vaerenbergh, E, "The elimination of phosphates and nitrates of waste water by algal cultures," *Natuurwetensch T*, 1974.
[183] Y. S. Yun, S. B. Lee, J. M. Park, C. I. Lee, and J. W. Yang, "Carbon dioxide fixation by algal cultivation using wastewater nutrients," *Journal of Chemical Technology and Biotechnology*, vol. 69, no. 4, pp. 451-455, 1997.

[184] M. Gavrilescu and Y. Chisti, "Biotechnology—a sustainable alternative for chemical industry," *Biotechnology Advances,* vol. 23, no. 7, pp. 471-499, 2005.
[185] Z. Liang *et al.*, "Efficiency assessment and pH effect in removing nitrogen and phosphorus by algae-bacteria combined system of Chlorella vulgaris and Bacillus licheniformis," *Chemosphere,* vol. 92, no. 10, pp. 1383-1389, 2013.
[186] J. de la Noue and N. de Pauw, "The potential of microalgal biotechnology: a review of production and uses of microalgae," *Biotechnology Advances,* vol. 6, no. 4, pp. 725-770, 1988.
[187] J. Sheehan, T. Dunahay, J. Benemann, and P. Roessler, "Look Back at the U.S. Department of Energy's Aquatic Species Program: Biodiesel from Algae; Close-Out Report," Office of Scientific and Technical Information (OSTI)1998/07/01 1998, Available: http://dx.doi.org/10.2172/15003040.
[188] N. C. Boelee, H. Temmink, M. Janssen, C. J. Buisman, and R. H. Wijffels, "Scenario analysis of nutrient removal from municipal wastewater by microalgal biofilms," *Water,* vol. 4, no. 2, pp. 460-473, 2012.
[189] B. S. Sturm and S. L. Lamer, "An energy evaluation of coupling nutrient removal from wastewater with algal biomass production," *Applied Energy,* vol. 88, no. 10, pp. 3499-3506, 2011.
[190] Y. Li *et al.*, "Characterization of a microalga Chlorella sp. well adapted to highly concentrated municipal wastewater for nutrient removal and biodiesel production," *Bioresource Technology,* vol. 102, no. 8, pp. 5138-5144, 4// 2011.
[191] Z. Chi, Y. Zheng, A. Jiang, and S. Chen, "Lipid production by culturing oleaginous yeast and algae with food waste and municipal wastewater in an integrated process," *Applied Biochemistry and Biotechnology,* vol. 165, no. 2, pp. 442-453, 2011.
[192] W. Mulbry, S. Kondrad, C. Pizarro, and E. Kebede-Westhead, "Treatment of dairy manure effluent using freshwater algae: algal productivity and recovery of manure nutrients using pilot-scale algal turf scrubbers," *Bioresource Technology,* vol. 99, no. 17, pp. 8137-8142, 2008.
[193] E. P. Tang, W. F. Vincent, D. Proulx, P. Lessard, and J. De La Noüe, "Polar cyanobacteria versus green algae for tertiary waste-water treatment in cool climates," *Journal of Applied Phycology,* vol. 9, no. 4, pp. 371-381, 1997.
[194] E. W. Wilde and J. R. Benemann, "Bioremoval of heavy metals by the use of microalgae," *Biotechnology Advances,* vol. 11, no. 4, pp. 781-812, // 1993.
[195] R. Slade and A. Bauen, "Micro-algae cultivation for biofuels: Cost, energy balance, environmental impacts and future prospects," *Biomass and Bioenergy,* vol. 53, pp. 29-38, 2013/06 2013.
[196] F. Delrue *et al.*, "Comparison of various microalgae liquid biofuel production pathways based on energetic, economic and environmental criteria," *Bioresource Technology,* vol. 136, pp. 205-212, 2013/05 2013.
[197] L. Gouveia *et al.*, "Microalgae biomass production using wastewater: Treatment and costs," *Algal Research,* vol. 16, pp. 167-176, 2016/06 2016.
[198] D. Batten *et al.*, "Using wastewater and high-rate algal ponds for nutrient removal and the production of bioenergy and biofuels," *Water Science & Technology,* vol. 67, no. 4, p. 915, 2013/01 2013.
[199] N. D. Orfield, G. A. Keoleian, and N. G. Love, "A GIS based national assessment of algal bio-oil production potential through flue gas and wastewater co-utilization," *Biomass and Bioenergy,* vol. 63, pp. 76-85, 2014/04 2014.
[200] S. O. Lourenço, E. Barbarino, J. Mancini-Filho, K. P. Schinke, and E. Aidar, "Effects of different nitrogen sources on the growth and biochemical profile of 10 marine microalgae in batch culture: an evaluation for aquaculture," *Phycologia,* vol. 41, no. 2, pp. 158-168, 2002.
[201] B. Wang, Y. Li, N. Wu, and C. Lan, "CO2 bio-mitigation using microalgae," (in English), *Applied Microbiology and Biotechnology,* vol. 79, no. 5, pp. 707-718, 2008/07/01 2008.

[202] K. I. Reitan, J. R. Rainuzzo, and Y. Olsen, "Effect of nutrient limitation on fatty acid and lipid content of marine microalgaei" *Journal of Phycology,* vol. 30, no. 6, pp. 972-979, 1994.
[203] K. Yamaberi, M. Takagi, and T. Yoshida, "Nitrogen depletion for intracellular triglyceride accumulation to enhance liquefaction yield of marine microalgal cells into a fuel oil," *Journal of Marine Biotechnology,* vol. 6, pp. 44-48, 1998.
[204] C. Ratledge, "Regulation of lipid accumulation in oleaginous micro-organisms," *Biochemical Society Transactions,* vol. 30, no. 6, pp. 1047-1049, 2002.
[205] T. Cai, S. Y. Park, and Y. Li, "Nutrient recovery from wastewater streams by microalgae: Status and prospects," *Renewable and Sustainable Energy Reviews,* vol. 19, no. 0, pp. 360-369, 3// 2013.
[206] G. Charnley and J. Doull, "Human exposure to dioxins from food, 1999–2002," *Food and Chemical Toxicology,* vol. 43, no. 5, pp. 671-679, 2005.
[207] G. I. Ågren, "The C: N: P stoichiometry of autotrophs–theory and observations," *Ecology Letters,* vol. 7, no. 3, pp. 185-191, 2004.
[208] M. Martinez, J. Jimenez, and F. El Yousfi, "Influence of phosphorus concentration and temperature on growth and phosphorus uptake by the microalga< i> Scenedesmus obliquus</i>," *Bioresource Technology,* vol. 67, no. 3, pp. 233-240, 1999.
[209] D. Gauthier and D. Turpin, "Interactions between inorganic phosphate (Pi) assimilation, photosynthesis and respiration in the Pi-limited green alga Selenastrum minutum," *Plant, Cell & Environment,* vol. 20, no. 1, pp. 12-24, 1997.
[210] J.-S. Lee and J.-P. Lee, "Review of advances in biological CO2 mitigation technology," (in English), *Biotechnology and Bioprocess Engineering,* vol. 8, no. 6, pp. 354-359, 2003/12/01 2003.
[211] D. L. Sutherland, M. H. Turnbull, P. A. Broady, and R. J. Craggs, "Effects of two different nutrient loads on microalgal production, nutrient removal and photosynthetic efficiency in pilot-scale wastewater high rate algal ponds," *Water Research,* vol. 66, pp. 53-62, 2014.
[212] S. H. Lee, B. H. Jo, J. Y. Park, and H. M. Oh, "Increased microalgae growth and nutrient removal using balanced N: P ratio in wastewater," *Journal of Microbiology and Biotechnology,* vol. 23, no. 1, pp. 92-98, 2013.
[213] R. Boonchai, G. T. Seo, and C. Y. Seong, "Microalgae photobioreactor for nitrogen and phosphorus removal from wastewater of sewage treatment plant," *International Journal of Bioscience, Biochemistry and Bioinformatics,* vol. 2, no. 6, p. 407, 2012.
[214] H. J. Choi and S. M. Lee, "Effect of the N/P ratio on biomass productivity and nutrient removal from municipal wastewater," *Bioprocess and Biosystems Engineering,* vol. 38, no. 4, pp. 761-766, 2015.
[215] I. Karapinar Kapdan and S. Aslan, "Application of the Stover–Kincannon kinetic model to nitrogen removal by Chlorella vulgaris in a continuously operated immobilized photobioreactor system," *Journal of chemical Technology and Biotechnology,* vol. 83, no. 7, pp. 998-1005, 2008.
[216] P. Lau, N. Tam, and Y. Wong, "Wastewater nutrients removal by Chlorella vulgaris: optimization through acclimation," *Environmental Technology,* vol. 17, no. 2, pp. 183-189, 1996.
[217] A. M. Silva-Benavides and G. Torzillo, "Nitrogen and phosphorus removal through laboratory batch cultures of microalga Chlorella vulgaris and cyanobacterium Planktothrix isothrix grown as monoalgal and as co-cultures," *Journal of Applied Phycology,* vol. 24, no. 2, pp. 267-276, 2012.
[218] Y. Feng, C. Li, and D. Zhang, "Lipid production of< i> Chlorella vulgaris</i> cultured in artificial wastewater medium," *Bioresource Technology,* vol. 102, no. 1, pp. 101-105, 2011.
[219] L. Xin, H. Hong-ying, G. Ke, and S. Ying-xue, "Effects of different nitrogen and phosphorus concentrations on the growth, nutrient uptake, and lipid accumulation of

a freshwater microalga Scenedesmus sp," *Bioresource Technology,* vol. 101, no. 14, pp. 5494-5500, 7// 2010.
[220] S. Aslan and I. K. Kapdan, "Batch kinetics of nitrogen and phosphorus removal from synthetic wastewater by algae," *Ecological Engineering,* vol. 28, no. 1, pp. 64-70, 2006.
[221] P. Lau, N. Tam, and Y. Wong, "Wastewater nutrients (N and P) removal by carrageenan and alginate immobilized Chlorella vulgaris," *Environmental Technology,* vol. 18, no. 9, pp. 945-951, 1997.
[222] S. Judd, L. J. P. van den Broeke, M. Shurair, Y. Kuti, and H. Znad, "Algal remediation of CO2 and nutrient discharges: A review," *Water Research,* vol. 87, pp. 356-366, 2015/12 2015.
[223] J. A. Berges, D. O. Charlebois, D. C. Mauzerall, and P. G. Falkowski, "Differential effects of nitrogen limitation on photosynthetic efficiency of photosystems I and II in microalgae," *Plant Physiology,* vol. 110, no. 2, pp. 689-696, 1996.
[224] S. A. Scott *et al.*, "Biodiesel from algae: challenges and prospects," *Current opinion in Biotechnology,* vol. 21, no. 3, pp. 277-286, 2010.
[225] G. Naderi, M. O. Tade, and H. Znad, "Modified Photobioreactor for Biofixation of Carbon Dioxide by Chlorella vulgaris at Different Light Intensities," *Chemical Engineering & Technology,* vol. 38, no. 8, pp. 1371-1379, 2015.
[226] A. Toledo-Cervantes, M. Morales, E. Novelo, and S. Revah, "Carbon dioxide fixation and lipid storage by Scenedesmus obtusiusculus," *Bioresource Technology,* vol. 130, pp. 652-658, 2013.
[227] L.-H. Fan, Y.-T. Zhang, L. Zhang, and H.-L. Chen, "Evaluation of a membrane-sparged helical tubular photobioreactor for carbon dioxide biofixation by Chlorella vulgaris," *Journal of Membrane Science,* vol. 325, no. 1, pp. 336-345, 2008.
[228] G. E. Box and D. W. Behnken, "Some new three level designs for the study of quantitative variables," *Technometrics,* vol. 2, no. 4, pp. 455-475, 1960.
[229] S. Kasiri, S. Abdulsalam, A. Ulrich, and V. Prasad, "Optimization of CO 2 fixation by Chlorella kessleri using response surface methodology," *Chemical Engineering Science,* vol. 127, pp. 31-39, 2015.
[230] S. Ghosh, S. Roy, and D. Das, "Improvement of Biomass Production by Chlorella sp. MJ 11/11 for Use as a Feedstock for Biodiesel," *Applied Biochemistry and Biotechnology,* vol. 175, no. 7, pp. 3322-3335, 2015.
[231] V. Skorupskaite, V. Makareviciene, and D. Levisauskas, "Optimization of mixotrophic cultivation of microalgae Chlorella sp. for biofuel production using response surface methodology," *Algal Research,* vol. 7, pp. 45-50, 2015.
[232] D. C. Montgomery, *Design and analysis of experiments*. John Wiley & Sons, 2008.
[233] S. C. Ferreira *et al.*, "Box-Behnken design: An alternative for the optimization of analytical methods," *Analytica chimica acta,* vol. 597, no. 2, pp. 179-186, 2007.
[234] N. Porcelli and S. Judd, "Chemical Cleaning of Potable Water Membranes: a review," *Separation and Purification Technology,* vol. 71, no. 2, pp. 137-143, 2010.
[235] M. Raffin, E. Germain, and S. Judd, "Optimising operation of an integrated membrane system (IMS)—A Box–Behnken approach," *Desalination,* vol. 273, no. 1, pp. 136-141, 2011.
[236] P. Gorham, J. McLachlan, U. Hammer, and W. Kim, "Isolation and cultutre of toxic strains of anabaena flos-aquae(LYNGB)DE BREB," 1964.
[237] M. Petrovich *et al.*, "Near-IR absorption of Ga: La: S and Ga: La: S: O glasses by free-electron laser-based laser calorimetry," *Journal of Non-Ccrystalline Solids,* vol. 326, pp. 93-97, 2003.
[238] E. G. Bligh and W. J. Dyer, "A rapid method of total lipid extraction and purification," *Canadian Journal of Biochemistry and Physiology,* vol. 37, no. 8, pp. 911-917, 1959.
[239] J. Folch, M. Lees, and G. Sloane-Stanley, "A simple method for the isolation and purification of total lipids from animal tissues," *J biol Chem,* vol. 226, no. 1, pp. 497-509, 1957.

[240] S.-H. Seo *et al.*, "Light intensity as major factor to maximize biomass and lipid productivity of Ettlia sp. in CO 2-controlled photoautotrophic chemostat," *Bioresource Technology*, 2017.
[241] F. Dautant, K. Simancas, A. Sandoval, and A. Müller, "Effect of temperature, moisture and lipid content on the rheological properties of rice flour," *Journal of Food Engineering*, vol. 78, no. 4, pp. 1159-1166, 2007.
[242] E. W. Rice, L. Bridgewater, A. American Public Health, A. American Water Works, and F. Water Environment, *Standard methods for the examination of water and wastewater / prepared and published jointly by American Public Health Association, American Water Works Association, Water Environment Federation ; joint editorial board, Eugene W. Rice ... [and others] ; managing editor, Laura Bridgewater*, Twenty-second edition.. ed. Washington, D.C.: Washington, D.C. : American Public Health Association, 2012.
[243] A. P. H. Association, "Standard methods for the examination of water and wastewater / prepared and published jointly by American Public Health Association, American Water Works Association and Water Environment Federation," *Washington, D. C. : APHA-AWWA-WEF* 2005.
[244] E. Harrington, "The desirability function," *Industrial Quality Control*, vol. 21, no. 10, pp. 494-498, 1965.
[245] I. Rawat, R. Ranjith Kumar, T. Mutanda, and F. Bux, "Dual role of microalgae: Phycoremediation of domestic wastewater and biomass production for sustainable biofuels production," *Applied Energy*, vol. 88, no. 10, pp. 3411-3424, 10// 2011.
[246] B. A. Whitton, *Ecology of Cyanobacteria II: their diversity in space and time*. Springer Science & Business Media, 2012.
[247] P. Choudhary, S. K. Prajapati, P. Kumar, A. Malik, and K. K. Pant, "Development and performance evaluation of an algal biofilm reactor for treatment of multiple wastewaters and characterization of biomass for diverse applications," *Bioresource Technology*, vol. 224, pp. 276-284, 2017.
[248] P. Choudhary, S. K. Prajapati, and A. Malik, "Screening native microalgal consortia for biomass production and nutrient removal from rural wastewaters for bioenergy applications," *Ecological Engineering*, vol. 91, pp. 221-230, 2016.
[249] S. K. Prajapati, P. Choudhary, A. Malik, and V. K. Vijay, "Algae mediated treatment and bioenergy generation process for handling liquid and solid waste from dairy cattle farm," *Bioresource Technology*, vol. 167, pp. 260-268, 2014.
[250] C. Gómez-Serrano, M. Morales-Amaral, F. Acién, R. Escudero, J. Fernández-Sevilla, and E. Molina-Grima, "Utilization of secondary-treated wastewater for the production of freshwater microalgae," *Applied Microbiology and Biotechnology*, vol. 99, no. 16, pp. 6931-6944, 2015.
[251] H. B. A.-B. Ayed, B. Taidi, H. Ayadi, D. Pareau, and M. Stambouli, "Effect of magnesium ion concentration in autotrophic cultures of Chlorella vulgaris," *Algal Research*, vol. 9, pp. 291-296, 2015.
[252] G. Markou, D. Iconomou, T. Sotiroudis, C. Israilides, and K. Muylaert, "Exploration of using stripped ammonia and ash from poultry litter for the cultivation of the cyanobacterium Arthrospira platensis and the green microalga Chlorella vulgaris," *Bioresource Technology*, vol. 196, pp. 459-468, 2015.
[253] G.-J. Zhou, G.-G. Ying, S. Liu, L.-J. Zhou, Z.-F. Chen, and F.-Q. Peng, "Simultaneous removal of inorganic and organic compounds in wastewater by freshwater green microalgae," *Environmental Science: Processes & Impacts*, vol. 16, no. 8, pp. 2018-2027, 2014.
[254] F. Gao *et al.*, "Removal of nutrients, organic matter, and metal from domestic secondary effluent through microalgae cultivation in a membrane photobioreactor," *Journal of Chemical Technology and Biotechnology*, 2016.
[255] R. Khanal, H. Furumai, and F. Nakajima, "Characterization of toxicants in urban road dust by Toxicity Identification Evaluation using ostracod Heterocypris

incongruens direct contact test," *Science of The Total Environment,* vol. 530, pp. 96-102, 2015.
[256] S.-X. Li, F.-J. Liu, F.-Y. Zheng, Y.-G. Zuo, and X.-G. Huang, "Effects of nitrate addition and iron speciation on trace element transfer in coastal food webs under phosphate and iron enrichment," *Chemosphere,* vol. 91, no. 11, pp. 1486-1494, 2013.
[257] I. Woertz, A. Feffer, T. Lundquist, and Y. Nelson, "Algae grown on dairy and municipal wastewater for simultaneous nutrient removal and lipid production for biofuel feedstock," *Journal of Environmental Engineering,* 2009.
[258] J. Lalucat, J. Imperial, and R. Pares, "Utilization of light for the assimilation of organic matter in Chlorella sp. VJ79," *Biotechnology and Bioengineering,* vol. 26, no. 7, pp. 677-681, 1984.
[259] K. Larsdotter, "Wastewater treatment with microalgae-a literature review," *Vatten,* vol. 62, no. 1, p. 31, 2006.
[260] O. Perez-Garcia, L. E. De-Bashan, J. P. Hernandez, and Y. Bashan, "Efficiency of growth and nutrient uptake from wastewater by heterotrophic, autotrophic, and mixotrophic cultivation of Chlorella vulgaris immobilized with Azospirillum brasilense," *Journal of Phycology,* vol. 46, no. 4, pp. 800-812, 2010.
[261] W. Kong, H. Song, Y. Cao, H. Yang, S. Hua, and C. Xia, "The characteristics of biomass production, lipid accumulation and chlorophyll biosynthesis of Chlorella vulgaris under mixotrophic cultivation," *African Journal of Biotechnology,* vol. 10, no. 55, pp. 11620-11630, 2011.
[262] M. Wang, W. C. Kuo-Dahab, S. Dolan, and C. Park, "Kinetics of nutrient removal and expression of extracellular polymeric substances of the microalgae, Chlorella sp. and Micractinium sp., in wastewater treatment," *Bioresource Technology,* vol. 154, pp. 131-137, 2014.
[263] A. Chavan and S. Mukherji, "Effect of co-contaminant phenol on performance of a laboratory-scale RBC with algal-bacterial biofilm treating petroleum hydrocarbon-rich wastewater," *Journal of Chemical Technology and Biotechnology,* vol. 85, no. 6, pp. 851-859, 2010.
[264] P. Bohutskyi *et al.*, "Mineral and non-carbon nutrient utilization and recovery during sequential phototrophic-heterotrophic growth of lipid-rich algae," *Applied Microbiology and Biotechnology,* vol. 98, no. 11, pp. 5261-5273, 2014.
[265] M. Chen, H. Tang, H. Ma, T. C. Holland, K. S. Ng, and S. O. Salley, "Effect of nutrients on growth and lipid accumulation in the green algae Dunaliella tertiolecta," *Bioresource Technology,* vol. 102, no. 2, pp. 1649-1655, 2011.
[266] L. E. de-Bashan and Y. Bashan, "Recent advances in removing phosphorus from wastewater and its future use as fertilizer (1997–2003)," *Water Research,* vol. 38, no. 19, pp. 4222-4246, 11// 2004.
[267] A. F. Clarens, E. P. Resurreccion, M. A. White, and L. M. Colosi, "Environmental life cycle comparison of algae to other bioenergy feedstocks," *Environmental Science & Technology,* vol. 44, no. 5, pp. 1813-1819, 2010.
[268] D. C. Montgomery, D. C. Montgomery, and D. C. Montgomery, *Design and Analysis of Experiments*. Wiley New York, 1984.
[269] T. M. Mata, R. Almeidab, and N. Caetanoa, "Effect of the culture nutrients on the biomass and lipid productivities of microalgae Dunaliella tertiolecta," *Chem Eng,* vol. 32, p. 973, 2013.
[270] H.-X. Chang, Y. Huang, Q. Fu, Q. Liao, and X. Zhu, "Kinetic characteristics and modeling of microalgae Chlorella vulgaris growth and CO 2 biofixation considering the coupled effects of light intensity and dissolved inorganic carbon," *Bioresource Technology,* vol. 206, pp. 231-238, 2016.
[271] H. J. Silva and S. J. Pirt, "Carbon dioxide inhibition of photosynthetic growth of Chlorella," *Journal of General Microbiology,* vol. 130, no. 11, pp. 2833-2838, 1984.

[272] K.-D. Sung, J.-S. Lee, C.-S. Shin, S.-C. Park, and M.-J. Choi, "CO 2 fixation by Chlorella sp. KR-1 and its cultural characteristics," *Bioresource Technology,* vol. 68, no. 3, pp. 269-273, 1999.
[273] W. Fu, O. Gudmundsson, A. M. Feist, G. Herjolfsson, S. Brynjolfsson, and B. Ø. Palsson, "Maximizing biomass productivity and cell density of Chlorella vulgaris by using light-emitting diode-based photobioreactor," *Journal of Biotechnology,* vol. 161, no. 3, pp. 242-249, 2012.
[274] T. E. Purba, "CO2 reduction and production of algal oil using microalgae Nannochloropsis oculata and Tetraselmis chuii," *Chem. Eng. Trans.21 (2010), pp. 397–402,* 2010.
[275] J. A. Raven and R. J. Geider, "Temperature and algal growth," *New phytologist,* pp. 441-461, 1988.
[276] J. C. M. Pires, M. C. M. Alvim-Ferraz, F. G. Martins, and M. Simões, "Carbon dioxide capture from flue gases using microalgae: Engineering aspects and biorefinery concept," *Renewable and Sustainable Energy Reviews,* vol. 16, no. 5, pp. 3043-3053, 2012.
[277] J. Seckbach and R. Ikan, "Sterols and chloroplast structure of Cyanidium caldarium," *Sterols and chloroplast structure of Cyanidium caldarium,* vol. Mar, no. 3, pp. 457-459, 1972.
[278] S. Miyairi, "CO 2 assimilation in a thermophilic cyanobacterium," *Energy Conversion and Management,* vol. 36, no. 6, pp. 763-766, 1995.
[279] J. Taucher *et al.*, "Combined effects of CO2 and temperature on carbon uptake and partitioning by the marine diatoms Thalassiosira weissflogii and Dactyliosolen fragilissimus," *Limnology and Oceanography,* vol. 60, no. 3, pp. 901-919, 2015.
[280] C. Vílchez and J. M. Vega, "Nitrite uptake by Chlamydomonas reinhardtii cells immobilized in calcium alginate," *Applied microbiology and biotechnology,* vol. 41, no. 1, pp. 137-141, 1994.
[281] A. C. Redfield, "The influence of organisms on the composition of sea-water," *The sea,* pp. 26-77, 1963.
[282] A. Widjaja, C.-C. Chien, and Y.-H. Ju, "Study of increasing lipid production from fresh water microalgae Chlorella vulgaris," *Journal of the Taiwan Institute of Chemical Engineers,* vol. 40, no. 1, pp. 13-20, 2009.
[283] C. Sacasa Castellanos, "Batch and continuous studies of Chlorella vulgaris in photo-bioreactors," 2013.
[284] C. Wilhelm and T. Jakob, "From photons to biomass and biofuels: evaluation of different strategies for the improvement of algal biotechnology based on comparative energy balances," *Applied Microbiology and Biotechnology,* vol. 92, no. 5, pp. 909-919, 2011.
[285] Y. Su, A. Mennerich, and B. Urban, "Coupled nutrient removal and biomass production with mixed algal culture: Impact of biotic and abiotic factors," *Bioresource Technology,* vol. 118, no. 0, pp. 469-476, 8// 2012.
[286] J. C. Rooke, A. Léonard, C. F. Meunier, and B. L. Su, "Designing photobioreactors based on living cells immobilized in silica gel for carbon dioxide mitigation," *ChemSusChem,* vol. 4, no. 9, pp. 1249-1257, 2011.
[287] A. Kumar *et al.*, "Enhanced CO< sub> 2</sub> fixation and biofuel production via microalgae: recent developments and future directions," *Trends in Biotechnology,* vol. 28, no. 7, pp. 371-380, 2010.
[288] I. Douskova *et al.*, "Simultaneous flue gas bioremediation and reduction of microalgal biomass production costs," *Applied Microbiology and Biotechnology,* vol. 82, no. 1, pp. 179-185, 2009.
[289] C. Posten and G. Schaub, "Microalgae and terrestrial biomass as source for fuels—a process view," *Journal of Biotechnology,* vol. 142, no. 1, pp. 64-69, 2009.
[290] F. Z. Mennaa, Z. Arbib, and J. A. Perales, "Urban wastewater treatment by seven species of microalgae and an algal bloom: Biomass production, N and P removal kinetics and harvestability," *Water Research,* vol. 83, pp. 42-51, 2015.

[291] P. Dechatiwongse, S. Srisamai, G. Maitland, and K. Hellgardt, "Effects of light and temperature on the photoautotrophic growth and photoinhibition of nitrogen-fixing cyanobacterium Cyanothece sp. ATCC 51142," *Algal Research*, vol. 5, pp. 103-111, 2014.
[292] B. Decostere, J. De Craene, S. Van Hoey, H. Vervaeren, I. Nopens, and S. W. Van Hulle, "Validation of a microalgal growth model accounting with inorganic carbon and nutrient kinetics for wastewater treatment," *Chemical Engineering Journal*, vol. 285, pp. 189-197, 2016.
[293] J. Quinn, L. De Winter, and T. Bradley, "Microalgae bulk growth model with application to industrial scale systems," *Bioresource Technology*, vol. 102, no. 8, pp. 5083-5092, 2011.
[294] J. Ruiz, P. Álvarez-Díaz, Z. Arbib, C. Garrido-Pérez, J. Barragán, and J. Perales, "Performance of a flat panel reactor in the continuous culture of microalgae in urban wastewater: prediction from a batch experiment," *Bioresource Technology*, vol. 127, pp. 456-463, 2013.
[295] M. Droop, "Vitamin B12 and marine ecology. IV. The kinetics of uptake, growth and inhibition in Monochrysis lutheri," *J. Mar. Biol. Assoc. UK*, vol. 48, no. 3, pp. 689-733, 1968.
[296] M. Droop, "25 Years of Algal Growth Kinetics A Personal View," *Botanica marina*, vol. 26, no. 3, pp. 99-112, 1983.
[297] A. Packer, Y. Li, T. Andersen, Q. Hu, Y. Kuang, and M. Sommerfeld, "Growth and neutral lipid synthesis in green microalgae: a mathematical model," *Bioresource Technology*, vol. 102, no. 1, pp. 111-117, 2011.
[298] N. Powell, A. N. Shilton, S. Pratt, and Y. Chisti, "Factors influencing luxury uptake of phosphorus by microalgae in waste stabilization ponds," *Environmental Science & Technology*, vol. 42, no. 16, pp. 5958-5962, 2008.
[299] E. Sforza, M. Enzo, and A. Bertucco, "Design of microalgal biomass production in a continuous photobioreactor: an integrated experimental and modeling approach," *Chemical Engineering Research and Design*, vol. 92, no. 6, pp. 1153-1162, 2014.
[300] F. García-Camacho, A. Sánchez-Mirón, E. Molina-Grima, F. Camacho-Rubio, and J. Merchuck, "A mechanistic model of photosynthesis in microalgae including photoacclimation dynamics," *Journal of Theoretical Biology*, vol. 304, pp. 1-15, 2012.
[301] B. Decostere *et al.*, "A combined respirometer–titrimeter for the determination of microalgae kinetics: Experimental data collection and modelling," *Chemical Engineering Journal*, vol. 222, pp. 85-93, 2013.
[302] A. Concas, M. Pisu, and G. Cao, "Novel simulation model of the solar collector of BIOCOIL photobioreactors for CO 2 sequestration with microalgae," *Chemical Engineering Journal*, vol. 157, no. 2, pp. 297-303, 2010.
[303] S. J. Yoo, J. H. Kim, and J. M. Lee, "Dynamic modelling of mixotrophic microalgal photobioreactor systems with time-varying yield coefficient for the lipid consumption," *Bioresource Technology*, vol. 162, pp. 228-235, 2014.
[304] S. Jensen and G. Knutsen, "Influence of light and temperature on photoinhibition of photosynthesis inSpirulina platensis," *Journal of Applied Phycology*, vol. 5, no. 5, pp. 495-504, 1993.
[305] A. Vonshak and R. Guy, "Photoadaptation, photoinhibition and productivity in the blue-green alga, Spirulina platensis grown outdoors," *Plant, Cell & Environment*, vol. 15, no. 5, pp. 613-616, 1992.
[306] J. Cabello, M. Morales, and S. Revah, "Dynamic photosynthetic response of the microalga Scenedesmus obtusiusculus to light intensity perturbations," *Chemical Engineering Journal*, vol. 252, pp. 104-111, 2014.
[307] Y. Shah, B. G. Kelkar, S. Godbole, and W. D. Deckwer, "Design parameters estimations for bubble column reactors," *AIChE Journal*, vol. 28, no. 3, pp. 353-379, 1982.

[308] O. Bernard, Z. Hadj-Sadok, D. Dochain, A. Genovesi, and J. P. Steyer, "Dynamical model development and parameter identification for an anaerobic wastewater treatment process," *Biotechnology and Bioengineering,* vol. 75, no. 4, pp. 424-438, 2001.
[309] O. Bernard, "Hurdles and challenges for modelling and control of microalgae for CO 2 mitigation and biofuel production," *Journal of Process Control,* vol. 21, no. 10, pp. 1378-1389, 2011.
[310] E. Sada, H. Kumazawa, C. H. Lee, and H. Narukawa, "Gas-liquid interfacial area and liquid-side mass-transfer coefficient in a slurry bubble column," *Industrial & Engineering Chemistry Research,* vol. 26, no. 1, pp. 112-116, 1987.
[311] V. O. Adesanya, M. P. Davey, S. A. Scott, and A. G. Smith, "Kinetic modelling of growth and storage molecule production in microalgae under mixotrophic and autotrophic conditions," *Bioresource Technology,* vol. 157, pp. 293-304, 2014.
[312] T. Bannister, "Comparison of Kiefer-Mitchell and Bannister-Laws algal models," *Limnology and Oceanography,* vol. 35, no. 4, pp. 972-979, 1990.
[313] E. M. Grima, F. G. Camacho, J. S. Pérez, F. A. Fernandez, and J. F. Sevilla, "Evaluation of photosynthetic efficiency in microalgal cultures using averaged irradiance," *Enzyme and Microbial Technology,* vol. 21, no. 5, pp. 375-381, 1997.
[314] R. H. P. a. D. Green., "Perry's chemical engineer's handbook," *New York : McGraw Hill* 2008.
[315] J. Li, N. S. Xu, and W. W. Su, "Online estimation of stirred-tank microalgal photobioreactor cultures based on dissolved oxygen measurement," *Biochemical Engineering Journal,* vol. 14, no. 1, pp. 51-65, 2003.
[316] C. Paille, J. Albiol, R. Curwy, C. Lasseur, and F. Godia, "FEMME: a precursor experiment for the evaluation of bioregenerative life support systems," *Planetary and Space Science,* vol. 48, no. 5, pp. 515-521, 2000.
[317] A. Sciandra, "Study and modelling of a simple planktonic system reconstituted in an experimental microcosm," *Ecological Modelling,* vol. 34, no. 1-2, pp. 61-82, 1986.
[318] S. R. Ronda *et al.,* "A growth inhibitory model with SOx influenced effective growth rate for estimation of algal biomass concentration under flue gas atmosphere," *Bioresource Technology,* vol. 152, pp. 283-291, 2014.
[319] I. S. Suh and C.-G. Lee, "Photobioreactor engineering: design and performance," *Biotechnology and Bioprocess Engineering,* vol. 8, no. 6, pp. 313-321, 2003.
[320] E. Molina, J. Fernández, F. Acién, and Y. Chisti, "Tubular photobioreactor design for algal cultures," *Journal of Biotechnology,* vol. 92, no. 2, pp. 113-131, 2001.
[321] B. Cheirsilp and S. Torpee, "Enhanced growth and lipid production of microalgae under mixotrophic culture condition: effect of light intensity, glucose concentration and fed-batch cultivation," *Bioresource Technology,* vol. 110, pp. 510-516, 2012.
[322] B. Wang and C. Q. Lan, "Biomass production and nitrogen and phosphorus removal by the green alga Neochloris oleoabundans in simulated wastewater and secondary municipal wastewater effluent," *Bioresource Technology,* vol. 102, no. 10, pp. 5639-5644, 2011.
[323] S. F. Mohsenpour, B. Richards, and N. Willoughby, "Spectral conversion of light for enhanced microalgae growth rates and photosynthetic pigment production," *Bioresource Technology,* vol. 125, pp. 75-81, 2012.
[324] C. Yan, L. Zhang, X. Luo, and Z. Zheng, "Effects of various LED light wavelengths and intensities on the performance of purifying synthetic domestic sewage by microalgae at different influent C/N ratios," *Ecological Engineering,* vol. 51, pp. 24-32, 2013.
[325] D. L. Cho, K. H. Shin, W.-J. Lee, and D.-H. Kim, "Improvement of paint adhesion to a polypropylene bumper by plasma treatment," *Journal of Adhesion Science and Technology,* vol. 15, no. 6, pp. 653-664, 2001.
[326] Y. Wu, C. Han, J. Yang, S. Jia, and S. Wang, "Polypropylene films modified by air plasma and feather keratin graft," *Surface and Coatings Technology,* vol. 206, no. 2, pp. 506-510, 2011.

[327] R. Aiyengar and J. Divecha, "Experimental and statistical analysis of the effects of the processing parameters on the seal strength of heat sealed, biaxially oriented polypropylene film for flexible food packaging applications," *Journal of Plastic Film and Sheeting*, vol. 28, no. 3, pp. 244-256, 2012.

[328] Z. Kang *et al.*, "A cost analysis of microalgal biomass and biodiesel production in open raceways treating municipal wastewater and under optimum light wavelength," *J Microbiol Biotechnol*, vol. 25, pp. 109-118, 2015.

[329] S. F. Mohsenpour and N. Willoughby, "Luminescent photobioreactor design for improved algal growth and photosynthetic pigment production through spectral conversion of light," *Bioresource Technology*, vol. 142, pp. 147-153, 2013.

[330] M. Hultberg, H. L. Jönsson, K.-J. Bergstrand, and A. S. Carlsson, "Impact of light quality on biomass production and fatty acid content in the microalga Chlorella vulgaris," *Bioresource Technology*, vol. 159, pp. 465-467, 2014.

[331] D. G. Kim, C. Lee, S.-M. Park, and Y.-E. Choi, "Manipulation of light wavelength at appropriate growth stage to enhance biomass productivity and fatty acid methyl ester yield using Chlorella vulgaris," *Bioresource Technology*, vol. 159, pp. 240-248, 5// 2014.

[332] Y. J. Zhao *et al.*, "Efficiency of two-stage combinations of subsurface vertical down-flow and up-flow constructed wetland systems for treating variation in influent C/N ratios of domestic wastewater," *Ecological Engineering*, vol. 37, no. 10, pp. 1546-1554, 2011.

[333] G. Ruyters, "Effects of blue light on enzymes," in *Blue light effects in biological systems*: Springer, 1984, pp. 283-301.

[334] A. A. Hamid, N. F. Mokhtar, E. M. Taha, O. Omar, and W. M. W. Yusoff, "The role of ATP citrate lyase, malic enzyme and fatty acid synthase in the regulation of lipid accumulation in Cunninghamella sp. 2A1," *Annals of Microbiology*, vol. 61, no. 3, pp. 463-468, 2011.

[335] Znad, H. T., A. Alketife, S. Judd, F. AlMomani, and H. Vuthaluru. 2018. "Bioremediation and nutrient removal from wastewater by Chlorella vulgaris." *ECOLOGICAL ENGINEERING* 110: 1-7.

[336] Al Ketife, A., S. Judd, and H. Znad. 2017. “Synergistic effects and optimization of nitrogen and phosphorus concentrations on the growth and nutrient uptake of a freshwater *Chlorella vulgaris”*. *Environmental Technology* 38: 94-102.

[337] AL KETIFE, A., JUDD, S. & ZNAD, H. 2017. Optimization of cultivation conditions for combined nutrient removal and CO_2 fixation in a batch photobioreactor. *Journal of Chemical Technology and Biotechnology*. 92(5): 1085-1093.

[338] AL KETIFE, A. M., JUDD, S. & ZNAD, H. 2016. A mathematical model for carbon fixation and nutrient removal by an algal photobioreactor. *Chemical Engineering Science*, 153, 354-362.

Appendix A Articles copyright

Copyright of Bioremediation and nutrient removal from wastewater by *Chlorella Vulgaris*

Copyright Clearance Center RightsLink®

Home | Account Info | Help

Title: Bioremediation and nutrient removal from wastewater by Chlorella vulgaris

Author: Hussein Znad,Ahmed M.D Al Ketife,Simon Judd,Fares AlMomani,Hari Babu Vuthaluru

Publication: Ecological Engineering

Publisher: Elsevier

Date: January 2018

Logged in as:
Ahmed M.D. Al ketife
Account #:
3001068835

LOGOUT

Copyright of Synergistic effects and optimzation of nitreogen and phosphrous concetration on the growth and nutrient updtake of freshwater *chlorella vulgaris*

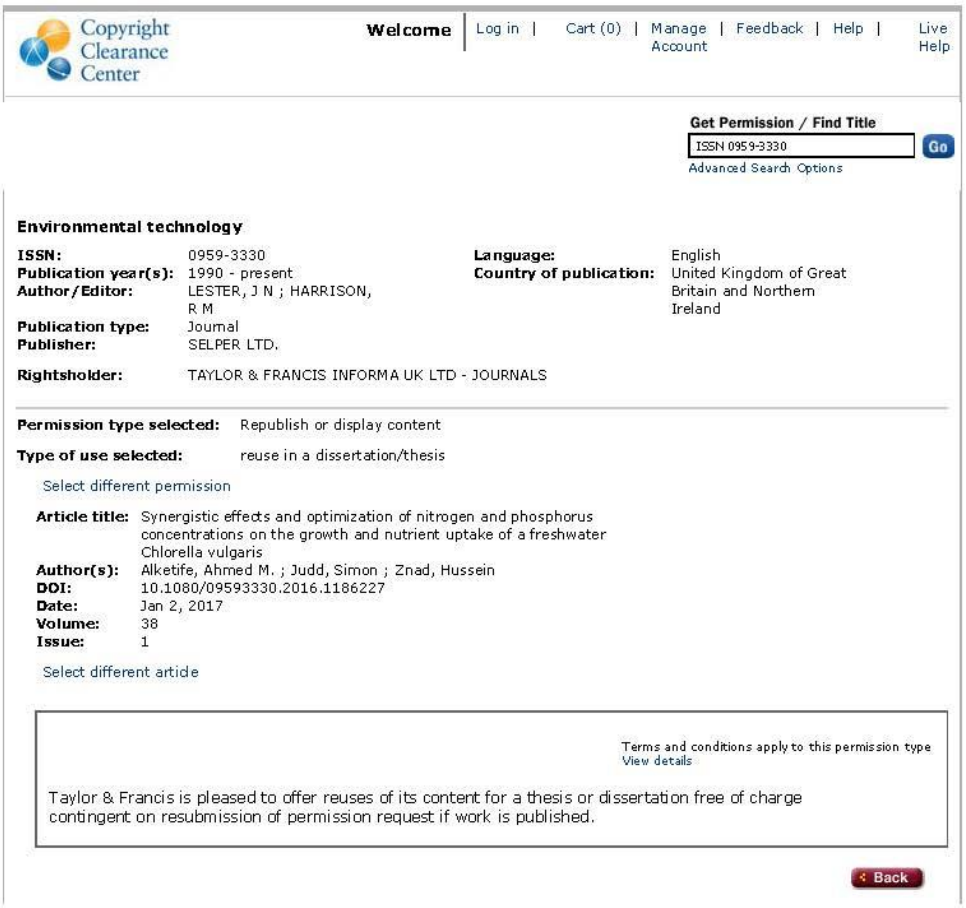

Copyright Clearance Center

Welcome | Log in | Cart (0) | Manage Account | Feedback | Help | Live Help

Get Permission / Find Title

ISSN 0959-3330 Go

Advanced Search Options

Environmental technology

ISSN:	0959-3330	**Language:**	English
Publication year(s):	1990 - present	**Country of publication:**	United Kingdom of Great Britain and Northern Ireland
Author/Editor:	LESTER, J N ; HARRISON, R M		
Publication type:	Journal		
Publisher:	SELPER LTD.		
Rightsholder:	TAYLOR & FRANCIS INFORMA UK LTD - JOURNALS		

Permission type selected: Republish or display content

Type of use selected: reuse in a dissertation/thesis

Select different permission

Article title: Synergistic effects and optimization of nitrogen and phosphorus concentrations on the growth and nutrient uptake of a freshwater Chlorella vulgaris
Author(s): Alketife, Ahmed M. ; Judd, Simon ; Znad, Hussein
DOI: 10.1080/09593330.2016.1186227
Date: Jan 2, 2017
Volume: 38
Issue: 1

Select different artide

Terms and conditions apply to this permission type
View details

Taylor & Francis is pleased to offer reuses of its content for a thesis or dissertation free of charge contingent on resubmission of permission request if work is published.

Back

About Us | Privacy Policy | Terms & Conditions | Pay an Invoice

Copyright of Optimzation of cultivation conditions fro combine nutreitn removal and CO2 fixation in a batch photobioreactor

JOHN WILEY AND SONS LICENSE TERMS AND CONDITIONS

Oct 03, 2016

This Agreement between Ahmed M.D. Al ketife ("You") and John Wiley and Sons ("John Wiley and Sons") consists of your license details and the terms and conditions provided by John Wiley and Sons and Copyright Clearance Center.

License Number	3961250918958
License date	Oct 03, 2016
Licensed Content Publisher	John Wiley and Sons
Licensed Content Publication	Journal of Chemical Technology & Biotechnology
Licensed Content Title	Optimization of cultivation conditions for combined nutrient removal and CO2 fixation in a batch photobioreactor
Licensed Content Author	Ahmed MD Al Ketife,Simon Judd,Hussein Znad
Licensed Content Date	Oct 3, 2016
Licensed Content Pages	1
Type of use	Dissertation/Thesis
Requestor type	Author of this Wiley article
Format	Print and electronic
Portion	Full article
Will you be translating?	No
Title of your thesis / dissertation	1- Coupling the wastewater treatment with CO2 bio-mitigation and microalgae biomass production in a solar filter photo-bioreactor.
Expected completion date	Feb 2017
Expected size (number of pages)	180
Requestor Location	Ahmed M.D. Al ketife Kent St, Bently GPO Box U1987 Perth WA 6845 Westren Australia, 6102 Australia Attn: Ahmed M.D. Al ketife
Publisher Tax ID	EU826007151
Billing Type	Invoice
Billing Address	Ahmed M.D. Al ketife Kent St, Bently GPO Box U1987 Perth WA 6845 Westren Australia, Australia 6102 Attn: Ahmed M.D. Al ketife
Total	0.00 USD
Terms and Conditions	

TERMS AND CONDITIONS

This copyrighted material is owned by or exclusively licensed to John Wiley & Sons, Inc. or one of its group companies (each a"Wiley Company") or handled on behalf of a society with which a Wiley Company has exclusive publishing rights in relation to a particular work (collectively "WILEY"). By clicking "accept" in connection with completing this licensing transaction, you agree that the following terms and conditions apply to this transaction

Copyright of A mathematical model for carbon fixation and nutrient removal by an algal phototbioreactor

ELSEVIER LICENSE
TERMS AND CONDITIONS

Oct 03, 2016

This Agreement between Ahmed M.D. Al ketife ("You") and Elsevier ("Elsevier") consists of your license details and the terms and conditions provided by Elsevier and Copyright Clearance Center.

License Number	3961160162205
License date	Oct 03, 2016
Licensed Content Publisher	Elsevier
Licensed Content Publication	Chemical Engineering Science
Licensed Content Title	A mathematical model for carbon fixation and nutrient removal by an algal photobioreactor
Licensed Content Author	Ahmed M.D. Al Ketife,Simon Judd,Hussein Znad
Licensed Content Date	22 October 2016
Licensed Content Volume Number	153
Licensed Content Issue Number	n/a
Licensed Content Pages	9
Start Page	354
End Page	362
Type of Use	reuse in a thesis/dissertation
Portion	full article
Format	both print and electronic
Are you the author of this Elsevier article?	Yes
Will you be translating?	No
Order reference number	
Title of your thesis/dissertation	1- Coupling the wastewater treatment with CO2 bio-mitigation and microalgae biomass production in a solar filter photo-bioreactor.
Expected completion date	Feb 2017
Estimated size (number of pages)	180
Elsevier VAT number	GB 494 6272 12
Requestor Location	Ahmed M.D. Al ketife Kent St, Bently GPO Box U1987 Perth WA 6845 Westren Australia, 6102 Australia Attn: Ahmed M.D. Al ketife
Total	0.00 AUD
Terms and Conditions	

INTRODUCTION

1. The publisher for this copyrighted material is Elsevier. By clicking "accept" in connection with completing this licensing transaction, you agree that the following terms and conditions apply to this transaction (along with the Billing and Payment terms and conditions